

University of Alberta
Department of Civil Engineering



Structural Engineering Report No. 54

**A Monte Carlo Study of the
Strength Variability of
Reinforced Concrete Columns**

by
L.H. Grant
and
J.G. MacGregor

January, 1976

THE UNIVERSITY OF ALBERTA

RELEASE FORM

NAME OF AUTHOR Leon Hadsley Grant
TITLE OF THESIS A MONTE CARLO STUDY OF THE STRENGTH
VARIABILITY OF RECTANGULAR TIED
REINFORCED CONCRETE COLUMNS
DEGREE FOR WHICH THESIS WAS PRESENTED M. Sc.
YEAR THIS DEGREE GRANTED 1976

Permission is hereby granted to THE UNIVERSITY OF ALBERTA LIBRARY to reproduce single copies of this thesis and to lend or sell such copies for private, scholarly or scientific research purposes only.

The author reserves other publication rights, and neither the thesis nor extensive extracts from it may be printed or otherwise reproduced without the author's permission.

(Signed)

Leon H. Grant
.....

PERMANENT ADDRESS:

231 Connell Street

Woodstock

New Brunswick

DATED *January 15* 1976

THE UNIVERSITY OF ALBERTA

A MONTE CARLO STUDY OF THE STRENGTH VARIABILITY OF
RECTANGULAR TIED REINFORCED CONCRETE COLUMNS

by

Leon Hadsley Grant

A THESIS

SUBMITTED TO THE FACULTY OF GRADUATE STUDIES AND RESEARCH
IN PARTIAL FULFILMENT OF THE REQUIREMENTS FOR THE DEGREE
OF MASTER OF SCIENCE

DEPARTMENT OF CIVIL ENGINEERING

EDMONTON, ALBERTA

SPRING, 1976

ABSTRACT

The safety provisions proposed for use in Canada for limit states design involve load factors to account for possible overloads and resistance or performance factors to account for possible understrength of structural members. The purpose of this study was to evaluate the understrength or ϕ factor applicable to rectangular tied reinforced column cross sections based on a probabilistic analysis of the results of a Monte Carlo Study.

Probability models were described for the major variables affecting the cross sectional strength. A Monte Carlo procedure was used to develop a sample of cross section strengths from which the understrength factor was calculated. This study showed that the concrete strength variability and the steel strength variability were the major contributing factors to the variability in cross sectional strength.

The understrength factors calculated from the results of this study were found to be in close agreement with the understrength factors used in the ACI 318-71 Building Code.

ACKNOWLEDGEMENTS

This investigation was made possible by a grant provided by the National Research Council of Canada (Grant A1673).

The author wishes to express his sincere appreciation to Dr. J.G. MacGregor under whose direction this study was performed.

The assistance of Dr. S. Ali Mirza in describing the variability of steel strength as contained in Appendix A is gratefully acknowledged.

TABLE OF CONTENTS

CHAPTER	PAGE
I INTRODUCTION	1
1.1 General	1
1.2 The Monte Carlo Technique	3
1.3 Development of the Understrength Factor ϕ	5
II THEORETICAL BEHAVIOUR OF REINFORCED CONCRETE SECTIONS	9
2.1 The Basic Assumptions for Analysis	9
2.2 The Stress-Strain Relationship for Concrete	10
2.3 The Stress-Strain Relationship for Steel	19
2.4 Numerical Method for Developing the Interaction Diagram	19
III COMPUTER PROGRAM FOR ANALYSIS	27
3.1 Description of The Monte Carlo Technique	27
3.2 Description of The Computer Program	28
3.3 Comparison of Theory With Test Results	43
IV PROBABILITY MODELS OF VARIABLES AFFECTING SECTION STRENGTH	48
4.1 Concrete Variability	48
4.1.1 Introduction	48
4.1.2 Distribution of Concrete Strength	50
4.1.3 Statistical Description of Concrete Strength Variation	53
4.1.4 Cylinder Strength vs. Design Strength	56
4.1.5 In-situ Strength of Concrete	58

TABLE OF CONTENTS CONTINUED

CHAPTER	PAGE
4.1.6 Probability Model for Concrete Strength	61
4.2 Reinforcing Steel Variability	62
4.3 Cross Section Dimensional Variability	62
4.3.1 Introduction	62
4.3.2 Probability Model for Cross Section Dimensions	63
4.4 Reinforcing Steel Placement Variability	67
V THE MONTE CARLO STUDY	71
5.1 Size of Columns and Reinforcement Studied	71
5.2 Size of Sample Studied	77
5.3 Results of The Monte Carlo Simulation	87
5.3.1 General	87
5.3.2 The Effect of Steel Strength Distribution Used	87
5.3.3 The Effect of the Concrete Strength Variation	93
5.3.4 The Effect of the Variables Studied	97
5.4 Cross Section Strength	100
5.5 Calculation of ϕ Factors	110
5.5.1 Based on 1 in 100 Understrength	110
5.5.2 Based on Cornell-Lind Procedure	114
VI SUMMARY AND CONCLUSIONS	118
REFERENCES	120

TABLE OF CONTENTS CONTINUED

CHAPTER	PAGE
APPENDIX A VARIABILITY IN REINFORCING STEEL	127
APPENDIX B COLUMNS STUDIED	145
APPENDIX C FLOW DIAGRAMS OF THE MONTE CARLO PROGRAM	150
APPENDIX D LISTING OF THE MONTE CARLO PROGRAM	185
APPENDIX E DESCRIPTION OF INPUT DATA	204
APPENDIX F NOMENCLATURE	207

LIST OF TABLES

Table	Description	Page
3.1	Comparison of Ptest/Ptheory With the Value of k_3	45
3.2	Theory Comparison With Hognestad's Tests II	46
3.3	Theory Comparison With Hognestad's Tests III	47
4.1	Concrete Strength Variability	52
4.2	Concrete Strength in Structures vs. Cylinder Strength	60
5.1	Comparison of the Mean Value of the Ratio Ptheory/PACI for Sample Sizes of 200, 500 and 1000	83
5.2	Comparison of the Coefficient of Variation of the Ratio Ptheory/PACI for Sample Sizes of 200, 500 and 1000	84
5.3	Comparison of the Coefficient of Skewness of the Ratio Ptheory/PACI for Sample Sizes of 200, 500 and 1000	85
5.4	Comparison of the Measure of Kurtosis of the Ratio Ptheory/PACI for Sample Sizes of 200, 500 and 1000	86
5.5	Comparison of the Mean Value of the Ratio Ptheory/PACI for a Normal and a Modified Log-normal Steel Strength Distribution	89
5.6	Comparison of the Coefficient of Variation of the Ratio Ptheory/PACI for a Normal and a Modified Log-normal Steel Strength Distribution	90

LIST OF TABLES CONTINUED

Table	Description	Page
5.7	Comparison of the Coefficient of Skewness of the Ratio P_{theory}/P_{ACI} for a Normal and a Modified Log-normal Steel Strength Distribution	91
5.8	Comparison of the Measure of Kurtosis of the Ratio P_{theory}/P_{ACI} for a Normal and a Modified Log-normal Steel Strength Distribution	92
5.9	Comparison of the Mean Value of the Ratio P_{theory}/P_{ACI} for Concrete Cylinder Strength Coefficients of Variation of 10%, 15% and 20%	94
5.10	Comparison of the Coefficient of Variation of the Ratio P_{theory}/P_{ACI} for Concrete Cylinder Strength Coefficients of Variation of 10%, 15% and 20%	95
5.11	Comparison of the Coefficient of Skewness of the Ratio P_{theory}/P_{ACI} for Concrete Cylinder Strength Coefficients of Variation of 10%, 15% and 20%	96
5.12	Comparison of the Mean Value of the Ratio P_{theory}/P_{ACI} for the 12 in. and 24 in. Columns	109
5.13	The Understrength Factor for the 12 in. by 12 in. Column Based on a Probability of Understrength of 1 in 100	111
5.14	The Understrength Factor for the 24 in. by 24 in. Column Based on a Probability of Understrength of 1 in 100	112
5.15	The Understrength Factor for the 12 in. by 12 in.	

LIST OF TABLES CONTINUED

Table	Description	Page
	Column Based on $\phi = \gamma_R e^{-\beta\alpha V_R}$	116
5.16	The Understrength Factor for the 24 in. by 24 in.	
	Column Based on $\phi = \gamma_R e^{-\beta\alpha V_R}$	117
A-1	Summary of Selected Studies on Steel Strength	130
B-1	Properties of the 12 in. Column Assumed in the Calculations	146
B-2	Properties of the 24 in. Column Assumed in the Calculations	147

LIST OF FIGURES

Figure	Description	Page
2.1	Compression Block Parameters	11
2.2	Some Suggested Stress-Strain Curves for Confined Concrete	13
2.3	The Kent and Park Stress-Strain Curve for Concrete	15
2.4	The Stress-Strain Curve for Concrete Used in This Study	20
2.5	The Stress-Strain Curve for Steel Used in This Study	21
2.6	Typical Moment Curvature Diagram	23
2.7	Basic Notation Used in the Flexural Analysis of Reinforced Concrete Sections	24
3.1	The Monte Carlo Technique	29
3.2	Condensed Flow Diagram of the Monte Carlo Program	31
3.3	Condensed Flow Diagram of the Subroutines ACI and ASTEEL	33
3.4	The ACI Interaction Diagram	34
3.5	Condensed Flow Diagram of the Subroutine CURVE	36
3.6	Condensed Flow Diagram of the Subroutine THMEAN	37
3.7	Condensed Flow Diagram of the Subroutine THEORY	39
3.8	Condensed Flow Diagram of the Subroutine AXIAL	40
3.9	Condensed Flow Diagram of the Subroutine FSTEEL	41
3.10	Condensed Flow Diagram of the Subroutine STAT	42
4.1	Relationship Between Standard Deviation and Mean	

LIST OF FIGURES CONTINUED

Figure	Description	Page
	Strength of Concrete	54
4.2	Histogram of Cross Section Dimensional Variation Reported by Tso and Zelman	64
4.3	Histograms of Cross Section Dimensional Variation Reported by Hernandez and Martinez	66
4.4	Histogram of Variation in Concrete Cover Reported by Hernandez and Martinez	70
5.1	Histogram of the Frequency of Column Sizes vs. Column Size	72
5.2	Histogram of the Percentage of Reinforcing Steel in All Columns	73
5.3	Histogram of the Percentage of Reinforcing Steel in Columns Less Than 16 in.	74
5.4	Histogram of the Percentage of Reinforcing Steel in Columns 16 in. to 24 in.	75
5.5	Histogram of the Percentage of Reinforcing Steel in Columns 24 in. to 36 in.	76
5.6	Final Column Cross sections Studied	78
5.7	Mean Value of the Ratio P_{theory}/P_{ACI} vs. e/h for Sample Sizes of 200, 500 and 1000 for a 12 in. Square Column and Modified Log-normal Steel Strength Distribution	80
5.8	Coefficient of Variation of the Ratio P_{theory}/P_{ACI} vs. e/h for Sample Sizes of 200, 500	

LIST OF FIGURES CONTINUED

Figure	Description	Page
	and 1000 for a 12 in. Square Column and Modified Log-normal Steel Strength Distribution	81
5.9	Coefficient of Skewness of the Ratio P_{theory}/P_{ACI} vs. e/h for Sample Sizes of 200, 500 and 1000 for a 12 in. Square Column and Modified Log-normal Steel Strength Distribution	82
5.10	Standard Deviation Squared of the Ratio P_{theory}/P_{ACI} vs. e/h for the Variables Affecting Column Strength for a 12 in. Square Column and Modified Log-normal Steel Strength Distribution	99
5.11	Dispersion of Strengths of an Eccentrically Loaded 12 in. Square Column	101
5.12	Dispersion of Strengths of an Eccentrically Loaded 24 in. Square Column	102
5.13	Normal Cumulative Frequency Plot of the Ratio P_{theory}/P_{ACI} for the 12 in. Column, $e/h = 0.10$	105
5.14	Log-normal Cumulative Frequency Plot of the Ratio P_{theory}/P_{ACI} for the 12 in. Column, $e/h = 0.10$	106
5.15	Normal Cumulative Frequency Plot of the Ratio P_{theory}/P_{ACI} for the 24 in. Column, Pure Moment	107
5.16	Log-normal Cumulative Frequency Plot of the Ratio P_{theory}/P_{ACI} for the 24 in. Column, Pure Moment	108
5.17	The Understrength Factor ϕ vs. e/h Based on a Probability of Understrength of 1 in 100 for the	

LIST OF FIGURES CONTINUED

Figure	Description	Page
	12 in. and 24 in. Columns	113
A-1	Steel Strength Distribution for Grade 40 Reinforcing Bars	132
A-2	Probability Density Function for Grade 40 Bars	134
A-3	Steel Strength Distribution for Grade 60 Reinforcing Bars	135
A-4	Probability Density Function for Grade 60 Bars	136
A-5	Effect of Bar Diameter on Steel Strength, Grade 40	140
A-6	Effect of Bar Diameter on Steel Strength, Grade 60	141
B-1	Nominal or Designer's Properties of the 12 in. and 24 in. Columns	148
B-2	Mean Values of the Properties of the 12 in. and 24 in. Columns	149

CHAPTER I
INTRODUCTION

1.1 General

It is generally recognized that there is some degree of uncertainty in the design equations used to calculate the resistance of a reinforced concrete section. The strength of a reinforced concrete section is calculated by the designer as a constant nominal value but it is recognized that the ultimate strength of a reinforced column is affected by variations in:

- Concrete strength
- Steel strength
- Cross section dimensions
- Location of steel reinforcement
- Eccentricity of load
- Rate of loading
- Amount of creep and plastic flow

The three most common approaches that have been used to estimate the variability of the ultimate strength of a reinforced concrete section are:

The technique of error statistics or regression analysis applied to the results of full scale or laboratory tests.

Direct statistical evaluation of means and

standard deviations from the means and standard deviations of the individual parameters involved.

The Monte Carlo Technique in which the variables affecting the cross section strength are treated as random variables and are randomly chosen and used to calculate a population of ultimate strengths based on structural theory.

The method of error statistics has been applied to sets of test results in various fields and has been accepted as a method of analyzing test data. This method of using test data has the disadvantage of requiring many tests to produce reliable results. More important, however, the sample may never be representative of the population due to testing procedures and systematic errors. Construction tolerances may not be adequately modeled, for example.

When the cross sectional strength can be calculated with relatively simple analytical expressions, standard statistical techniques can be used to calculate the mean error and coefficient of variation of the cross sectional strength based on the descriptions of the distributions of the individual variables. This procedure becomes awkward if the strength expressions become complex.

The Monte Carlo Technique has been used to model a population of values in various fields. This method has the disadvantage of requiring a statistical description of each

individual variable which affects the final variable being studied. The Monte Carlo Technique has the advantage of being able to generate a large size sample using computer simulations rather than actual test data.

Since the error statistics method of predicting strength has been considered insufficient and too costly for developing probability models of cross section strength and the equations used to calculate the strength of reinforced concrete cross sections are relatively complex, the Monte Carlo Technique has become popular.

1.2 The Monte Carlo Technique

The Monte Carlo Technique is a method of obtaining information about the total system performance from the individual component characteristics. It consists of generating many total systems from the component data and analyzing the sample of total systems.

This procedure has been used by various researchers to model the variability of structure strength and loading conditions. Housner and Jennings³⁰ have used this procedure to develop "Artificial Earthquakes" from which the various effects of earthquakes could be measured. Using the data generated with the Monte Carlo Technique close agreement was found with actual measured values.

Warner and Kabalia⁷² have described a method of

developing the strength and serviceability of a real structure using the Monte Carlo Technique. The strength of an idealized axially loaded reinforced concrete column was calculated including the effects of variations in the material and geometric properties.

Allen⁵ has presented a probability distribution of the ultimate moment and ductility ratio for reinforced concrete in bending. The ultimate moment and ductility ratio were obtained using prediction equations and probability distributions of the parameters. The computations were based on the method of using the Monte Carlo Technique described by Warner and Kabalia⁷². The results showed that the probability distributions of the ultimate moment and ductility ratio are affected by material properties, duration of loading, steel percentage and geometric properties.

In this study the Monte Carlo Technique was used to develop a probability model of the strength of a rectangular tied reinforced concrete column. The actual probability distribution developed was that for the ratio of the theoretical load capacity to that computed in accordance with the ACI design equations, P_{theory}/P_{ACI} , for specific values of e/h or eccentricity of axial load. This study shows the effect of variations in the concrete strength, steel strength, cross section dimensions, location of reinforcing steel and steel percentage on the probability

distribution of the strength of a reinforced concrete section under axial load and bending moment.

1.3 Development of the Understrength Factor ϕ

The ACI 318-71 Building Code Requirements for Reinforced Concrete³ requires that the design equation follow the format of:

$$\phi R \geq \gamma_D D + \gamma_L L \quad (1.1)$$

Where ϕ is an understrength factor, R is the nominal calculated resistance or strength, L and D are the live and dead loads respectively and γ_L and γ_D are the load factors to account for uncertainties in the loads.

Generally the procedure used for determining the values of ϕ , γ_L , and γ_D has been to rely on "common sense and experience" along with a semi-mathematical approach. These factors may also be determined using a logical mathematical approach using the probabilistic concepts.

The first consistent proposal for design based on the concept of probability appears to have been made by Torroja⁶⁸. This proposal was based on the concept of limit states in which the design loads and resistance have a specified probability of being exceeded.

Basler¹⁰ has suggested that the coefficient of variation may be used as a probabilistic but distribution

that:

$$M_{(R-S)} \geq \beta \sigma_{(R-S)} \quad (1.2)$$

Lind³⁹ has extended Cornell's approach to code formats of higher order and demonstrated a method of calibrating a partial safety factor format to Cornell's as well as Ang and Amin's format. Since it is possible to choose β by calibrating probabilistic code formats to existing codes, the parameters may be adjusted to yield designs comparable to existing code designs. This leads to a more acceptable implementation of probabilistic code concepts initially.

Siu et al.⁶³ have presented a method of code calibration which may be used to calibrate probabilistic code formats with existing code formats as well as to compare various probabilistic code formats.

In this study understrength factors for rectangular tied reinforced concrete columns were calculated directly from the distribution of column strength and a probability of understrength of 1 in 100 and have been compared with the understrength factors calculated on the basis of the first order second moment format.

The form of the second moment format used was that developed by Cornell, Lind and ACI Committee 348:

$$\phi = \gamma_R e^{-\beta \alpha V_R} \quad (1.3)$$

The derivation of this equation has been reviewed by
Mac Gregor⁴⁰.

CHAPTER II

THEORETICAL BEHAVIOUR OF REINFORCED CONCRETE SECTIONS

2.1 The Basic Assumptions for Analysis

If an analytical expression is to be used to determine the ultimate strength of a reinforced concrete cross section a number of assumptions must first be made. The following basic assumptions were made for the analysis:

(a) Plane sections remain plane, that is, the strain in the concrete or steel is directly proportional to the distance from the fibre to the neutral axis.

(b) The concrete stress is a function of the strain as expressed by the modified Kent and Park stress strain curve for concrete for the theoretical calculations.

(c) The steel stress is a function of the strain as expressed by an elastic plastic stress strain curve.

(d) There is no slip between the concrete and steel reinforcing.

(e) Bending in one plane is assumed and biaxial bending is neglected.

(f) Stability failure of the member is not included.

(g) The stiffness in bending of the individual layers of steel reinforcement is neglected.

(h) The effect of duration of loading is neglected.

2.2 The Stress-Strain Relationship for Concrete

The properties of the compressive stress block of a concrete flexural member may be defined by the parameters k_1 , k_2 , and k_3 as shown in Figure 2.1. These parameters depend on the shape of the stress-strain curve for concrete.

In North America the most widely accepted stress-strain curve for concrete is that proposed by Hognestad²⁹ which consists of a second order parabola up to a maximum stress f'_c at a strain ϵ_0 and then a linear falling branch. Hognestad's²⁸ curve was obtained from results of tests on eccentrically loaded short columns in which he found that $f''_c = 0.85f'_c$.

There is controversy as to whether the shape of the stress-strain curve for concrete is affected by a strain gradient. Sturman, Shah and Winter⁶⁷ concluded that the peak occurred at a 20% higher stress and a 50% higher strain for eccentrically loaded prisms compared to concentrically loaded prisms. In Hognestad's tests this was not observed. There may be no significant effect of the presence of a strain gradient but its presence, if anything, will improve the properties of the compression block. There is no doubt, however, that the presence of a strain gradient delays the appearance of longitudinal cracking in the compression zone.

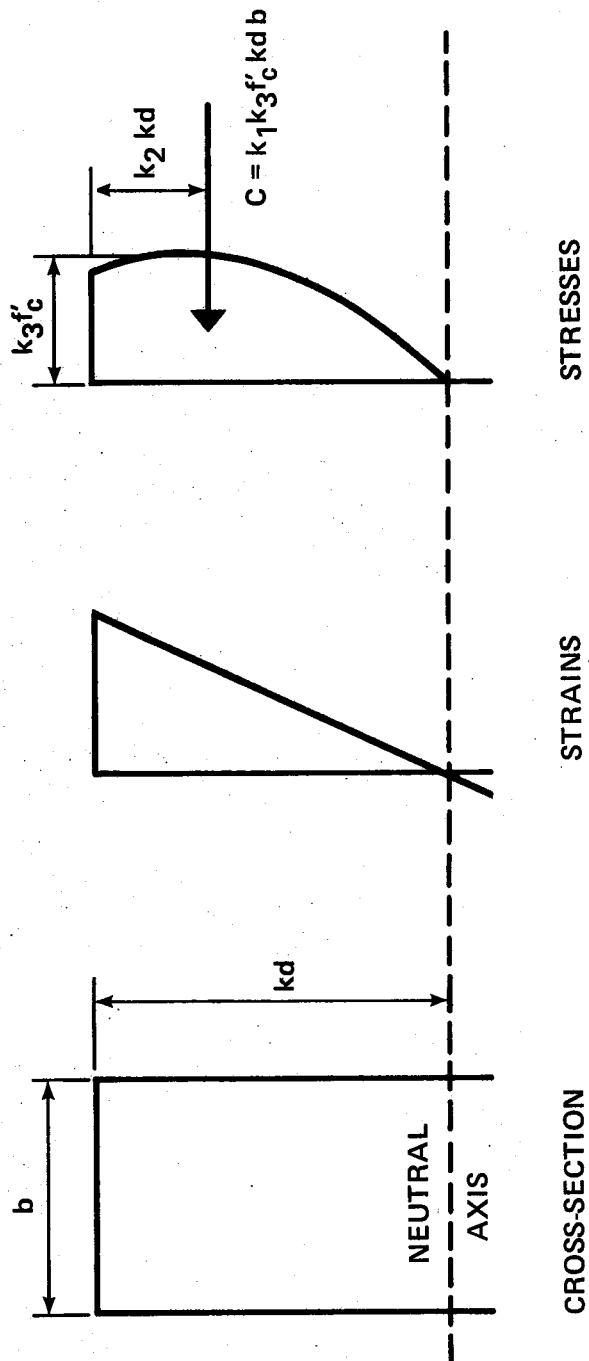


Figure 2.1 Compression Block Parameters

In columns the concrete is confined by the ties to some extent, depending on the type of ties used. The confinement due to the ties does not affect the concrete strength until there has been some yielding of the concrete to cause a load in the ties. At low levels of stress the ties will not be stressed and therefore the concrete will act as unconfined concrete. Tests have shown that when the stress in the concrete approaches the maximum uniaxial strength, deterioration of the concrete causes an outward expansion perpendicular to the load causing a stress in the ties which in turn causes a confining pressure. In this case spiral ties are more effective than rectangular ties since the spiral is able to exert pressure for its entire length whereas the rectangular ties tend to exert pressure at the corners and not along their entire length. This is due to the relatively flexible bar between the corner points. As a result the concrete is confined at the corners and in the centroidal core of the member. Even though the rectangular ties are not as effective as the spiral ties, they do produce a significant increase in ductility of the core as a whole.

Some stress-strain curves proposed for concrete confined by rectangular ties are shown in Figure 2.2. In Chan's¹⁷ trilinear curve the range OAB approximates the curve for unconfined concrete and the slope BC depends on the lateral confinement. Soliman and Yu's⁶⁴ curve consists

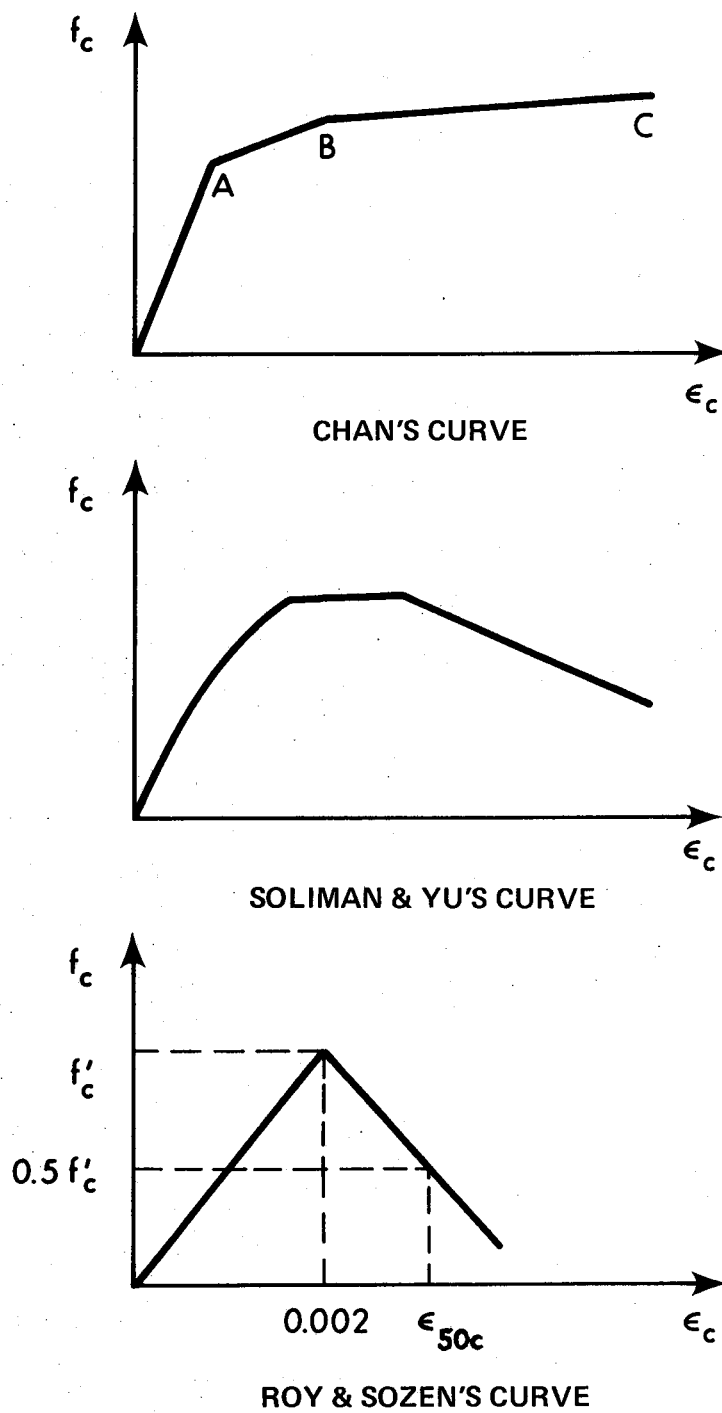


Figure 2.2 Some Suggested Stress-Strain Curves for Confined Concrete

of a parabola and two straight lines. Values for the critical points are related to the properties found from tests on eccentrically loaded prisms. Roy and Sozen⁵⁷ conducted tests on axially loaded prisms and suggested that the descending branch of the stress-strain curve could be replaced by a straight line. The strain at 50% of the maximum stress on the falling branch ϵ_{50c} was related to the volumetric ratio of the transverse steel.

Roy and Sozen⁵⁷ concluded that rectangular hoops did not increase the concrete strength. Other investigators such as Chan¹⁷, Soliman and Yu⁶⁴, Bertero and Felippa¹¹, and Rusch and Stockl⁵⁹ have observed an increase in strength due to closely spaced rectangular ties.

Kent and Park³⁶, on the basis of experimental evidence have proposed the stress-strain curve shown in Figure 2.3 for confined and unconfined concrete. This curve combines many of the features of the previously described curves. The ascending region AB is represented by a second order parabola in common with the Hognestad²⁹ curve. The confining steel is assumed to have no effect on the stress strain relationship before the maximum stress. Kent and Park³⁵ used a maximum stress in bending equal to f'_c , that is, $k_3=1.0$ in Figure 2.1. Sturman, Shah and Winter's⁶⁷ work suggests that the value of $k_3=1.0$ is conservative where there is a strain gradient. Kent and Park³⁶ assume the strain, ϵ_o , at maximum stress to be 0.002 which is in the range commonly accepted

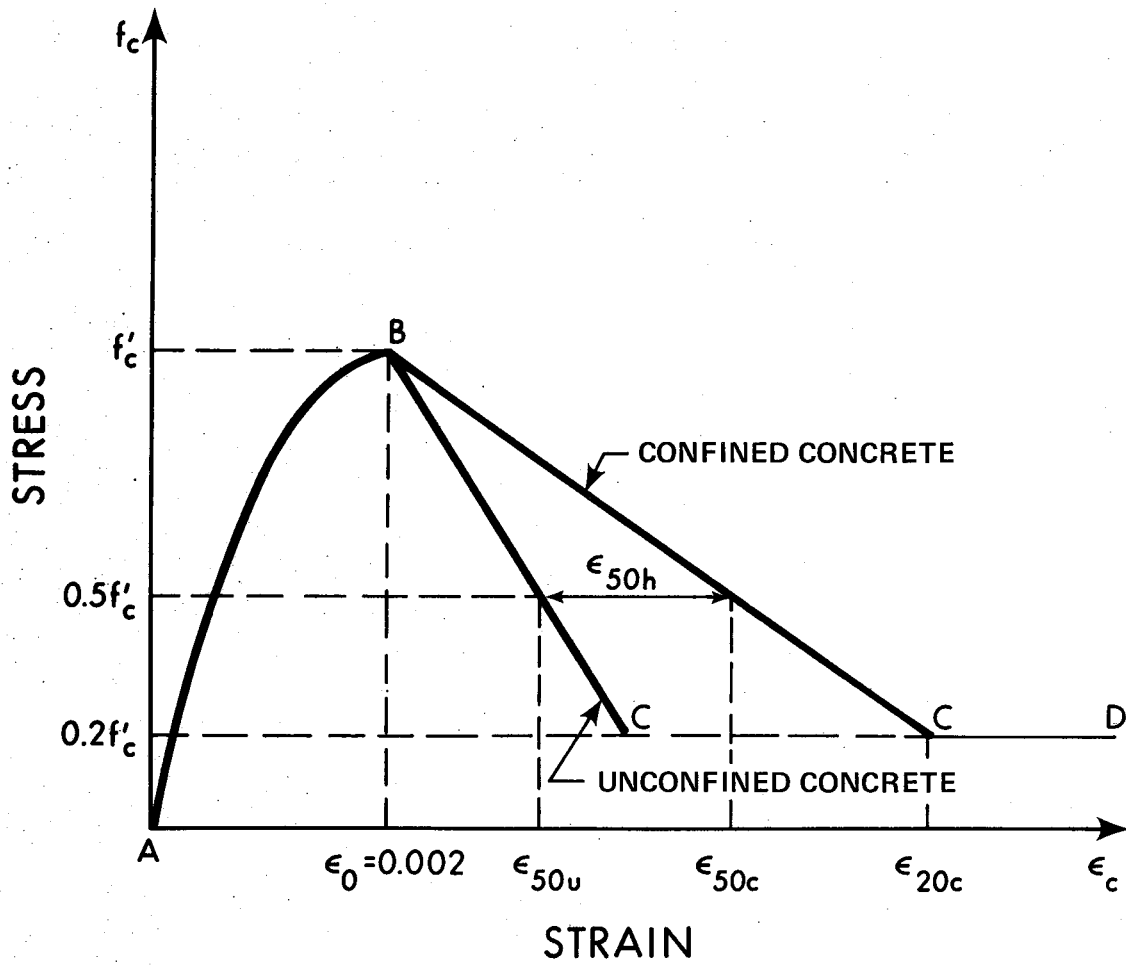


Figure 2.3 The Kent and Park Stress-Strain Curve for Concrete

for unconfined concrete. Confinement may increase the maximum strain but this will occur after the maximum stress is reached. Region AB for the Kent and Park³⁶ curve is expressed using:

$$f_c = f'_c \left[\frac{2\epsilon_c}{\epsilon_0} - \left(\frac{\epsilon_c}{\epsilon_0} \right)^2 \right] \quad (2.1)$$

In this study the value for k_3 was taken as 0.85 based on comparison with Hognestad's²⁹ test results, (See Section 3.3). To allow compatibility between the ACI equation for modulus of elasticity and the strain at about $0.4f'_c$, the strain ϵ_0 at a maximum stress of $k_3 f'_c$, was taken as:

$$\epsilon_0 = \frac{1.8 f'_c}{E_c} \quad (2.2)$$

The region of the curve after the maximum stress is linear from ϵ_0 and $f_{c \max}$ and is described by the strain in the concrete at 50% of the maximum stress as suggested by Roy and Sozen. The slope of the falling branch increases rapidly with an increase in concrete strength. This suggests that ϵ_{50u} is dependent on f'_c . This can easily be observed by the fact that high strength concrete is more brittle than low strength concrete. For concrete that is not laterally restrained, Kent and Park suggest that the strain ϵ_{50u} at 50% of f'_c is:

$$\epsilon_{50u} = \frac{3.0 + 0.002f'_c}{f'_c - 1000} \quad (2.3)$$

For concrete confined by rectangular ties the slope of

the falling branch is reduced. This is due mainly to the restraint supplied by the ties. Kent and Park³⁵ expressed this in terms of the ratio of the volume of the ties to the volume of the concrete core within the ties. Kent and Park³⁶ expressed the volumetric ratio as:

$$\rho'' = \frac{2.0 (b''+d'') A''_s}{b''d''s} \quad (2.4)$$

Corley¹⁸ suggested that the compression steel should be included in the volumetric ratio. In this study the compression steel was included in the volumetric ratio which was expressed as:

$$\rho'' = \frac{2.0 (b''+d'') A''_s + A'_s S}{b''d''s} \quad (2.5)$$

The descending branch of Kent and Park's³⁶ curve for confined concrete may be described by:

$$f_c = f'_c \left[1.0 - Z (\epsilon_c - \epsilon_o) \right] \quad (2.6)$$

where:

$$Z = \frac{0.5}{\epsilon_{50h} + \epsilon_{50u} - \epsilon_o} \quad (2.7)$$

and:

$$\epsilon_{50h} = 3/4 \rho'' \sqrt{\frac{b''}{s}} \quad (2.8)$$

Kent and Park³⁶ assumed that confined concrete could sustain a stress of $0.20f'_c$ at an infinite strain as shown by the dashed line in Figure 2.3. In this study the descending

region was assumed to continue to zero.

The tensile strength of concrete is usually neglected in most flexural theories as well as codes of practice. It is reasoned that it may be unsafe to take into account the tensile strength of the concrete since the concrete may be cracked due to shrinkage or other reasons even before any load is applied. While the tensile strength of concrete is small compared to its compressive strength it has a sizeable effect on the resistance and deformation of the uncracked section. After the appearance of the first cracks this influence becomes smaller and smaller as the load increases. This is due to the fact that with the advancement of cracking the tensile block becomes closer to the neutral axis resulting in a smaller lever arm and a negligible addition to the moment capacity.

In view of the above it was assumed that for the purposes of this study an elastic brittle stress-strain relationship can represent fairly well the behaviour of concrete in tension. An elastic brittle stress-strain relationship can be expressed as follows:

$$\sigma_t = E_{ct} \epsilon_t \quad \text{for } \epsilon_t \leq \epsilon_{tr} \quad (2.9)$$

and:

$$\sigma_t = 0 \quad \text{for } \epsilon_t > \epsilon_{tr} \quad (2.10)$$

The modulus of elasticity of concrete in tension was

taken as the accepted value in compression:

$$E_c = 57000 \sqrt{f'_c} \quad (2.11)$$

The modulus of rupture was taken as the accepted value:

$$\sigma_{tr} = 7.5 \sqrt{f'_c} \quad (2.12)$$

The complete stress-strain curve for concrete used in this study is shown in Figure 2.4.

2.3 The Stress-Strain Relationship for Steel

In this study an elastic purely plastic stress-strain relationship was assumed for steel as shown in Figure 2.5. The modulus of elasticity of steel was taken as 29,000 ksi. in tension as well as in compression. The steel stress was assumed to increase to the yield point and remain at the yield stress for any further strain. This is a conservative representation of the steel strength since the effect of strain hardening is neglected.

2.4 Numerical Method for Developing the Interaction Diagram

The inter-relationship between the effects of the axial load and applied moment on a reinforced concrete section are best shown by an interaction diagram. These diagrams are a graphical representation of the envelope of the maximum capacities of a reinforced concrete section under various

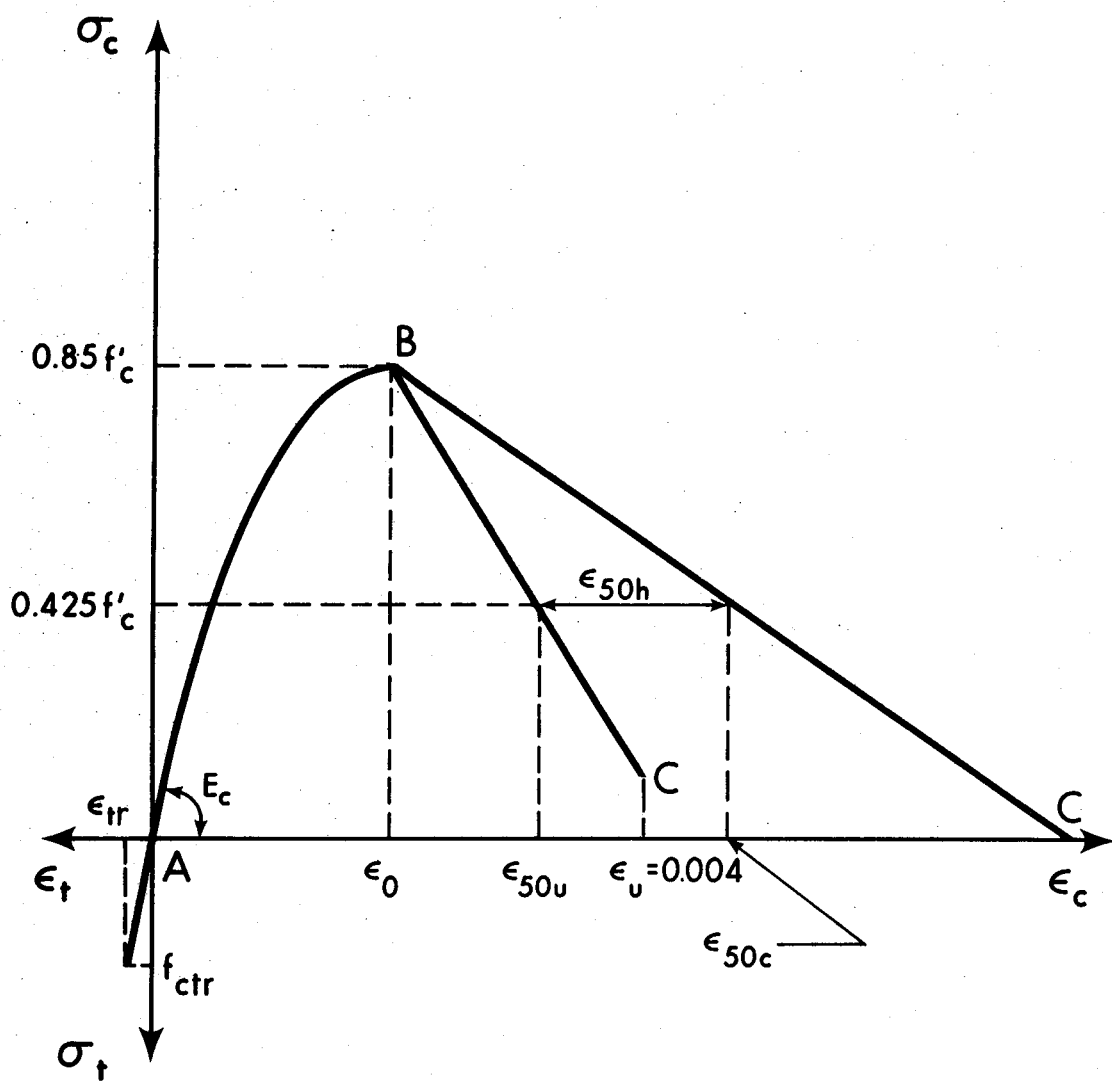


Figure 2.4 The Stress-Strain Curve for Concrete Used in This Study

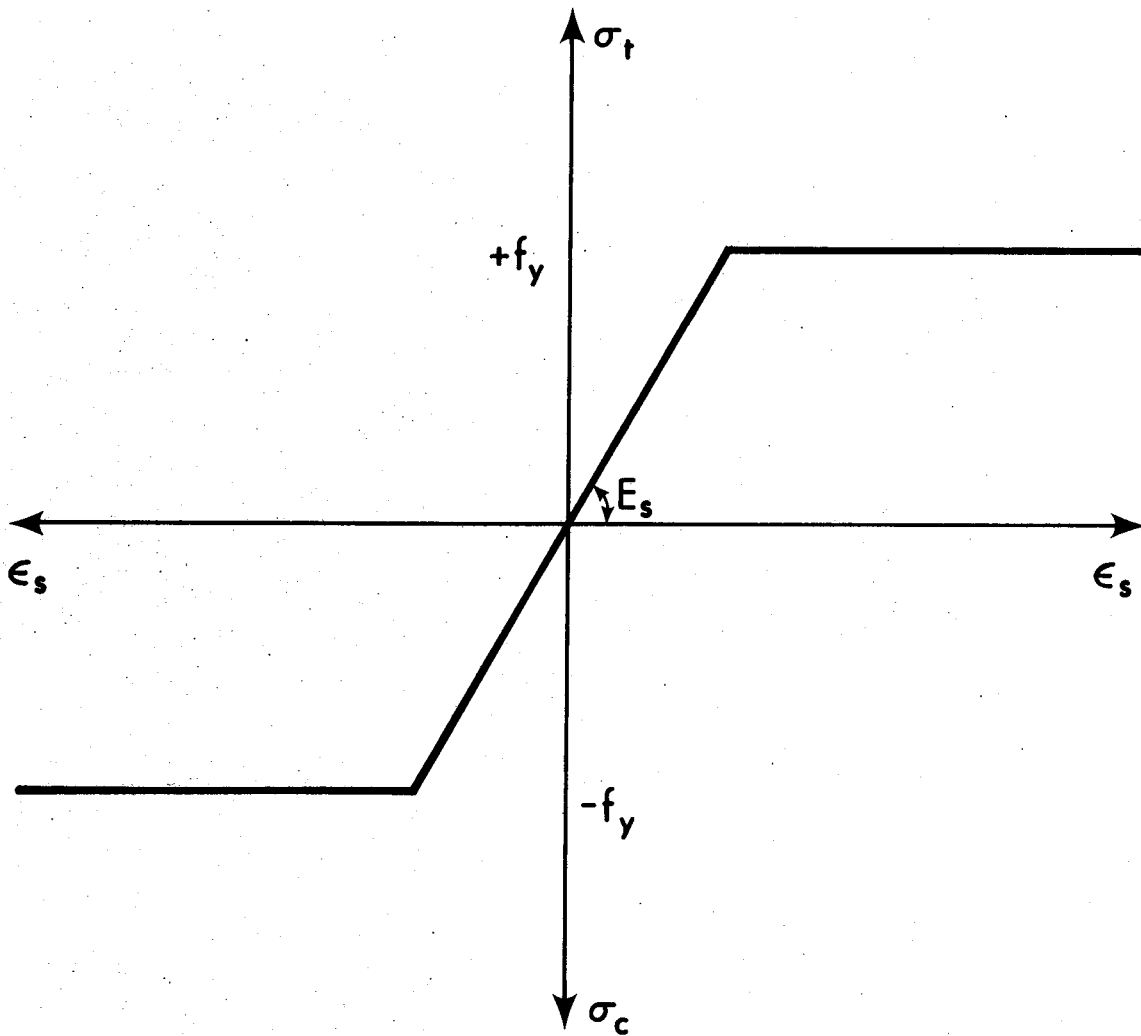


Figure 2.5 The Stress-Strain Curve for Steel Used in This Study

axial load and moment combinations.

Using strain compatibility, the moment curvature relationships were derived for the section for a number of axial load levels using the procedure described in the next few paragraphs. The moment curvature relationship developed is similar to that shown in Figure 2.6. The maximum moment in the moment curvature diagram was taken as the ultimate moment for that given load. The various values of load and ultimate moment were plotted as an interaction diagram.

The calculation of the moment curvature diagram was started by assuming a strain distribution across the cross section and determining the location of the neutral axis and the point at which the tensile strains exceeded ϵ_{tr} . The compression region was then divided into sections with equal widths measured perpendicular to the neutral axis, (See Figure 2.7). Using the concept of linear strains in the cross section the strain at the centroid of each section may be determined. By assuming the strain is constant over each section the resulting stress and total force over the area was determined with the aid of the stress-strain curve for concrete. The total compressive force supplied by the concrete may be expressed as:

$$F_c = \sum_{i=1}^{ns} f_{ci} b dx \quad (2.13)$$

Assuming the maximum tensile stress in concrete occurs at a strain of ϵ_{tr} and assuming a linear stress-strain curve

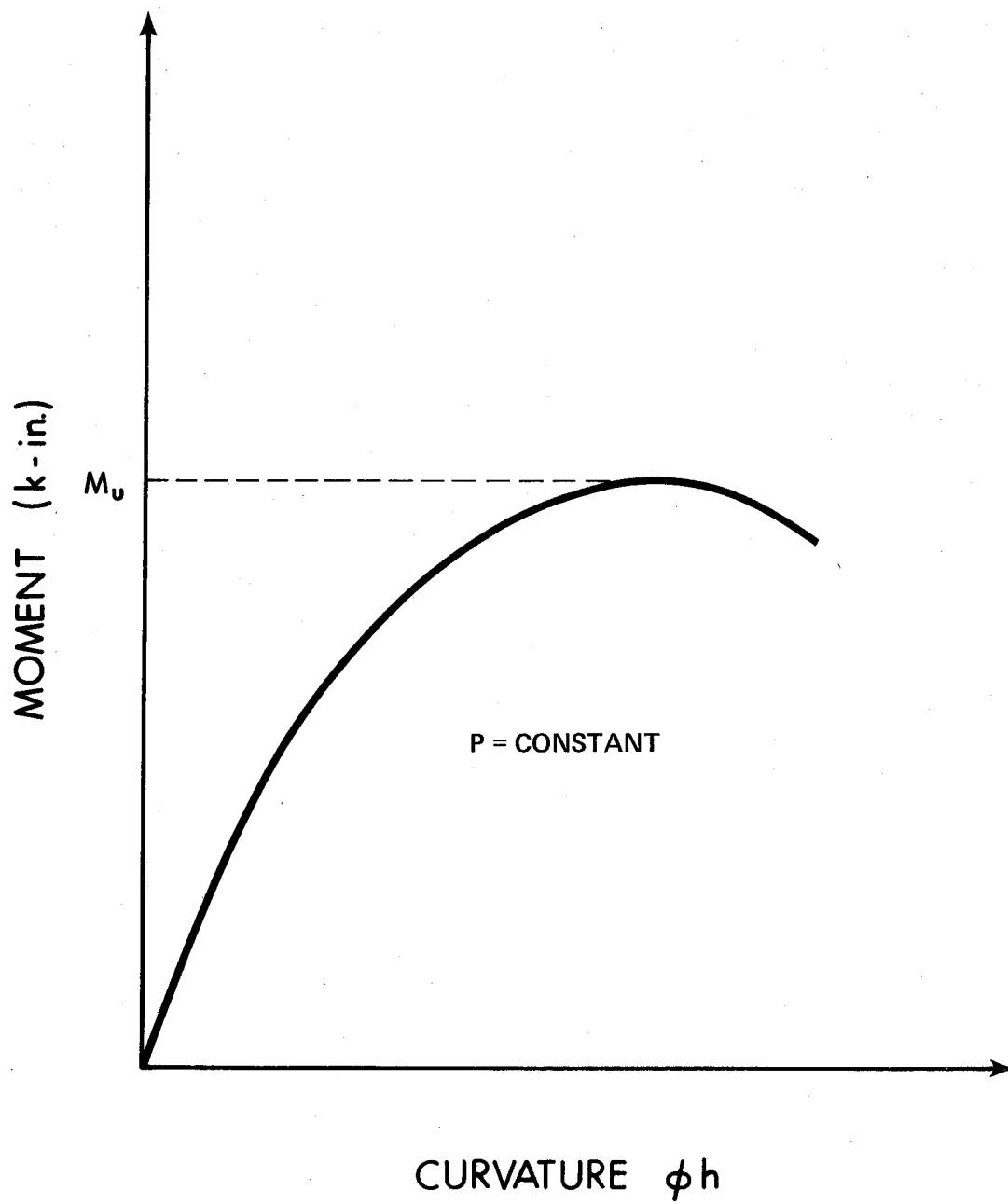


Figure 2.6 Typical Moment Curvature Diagram

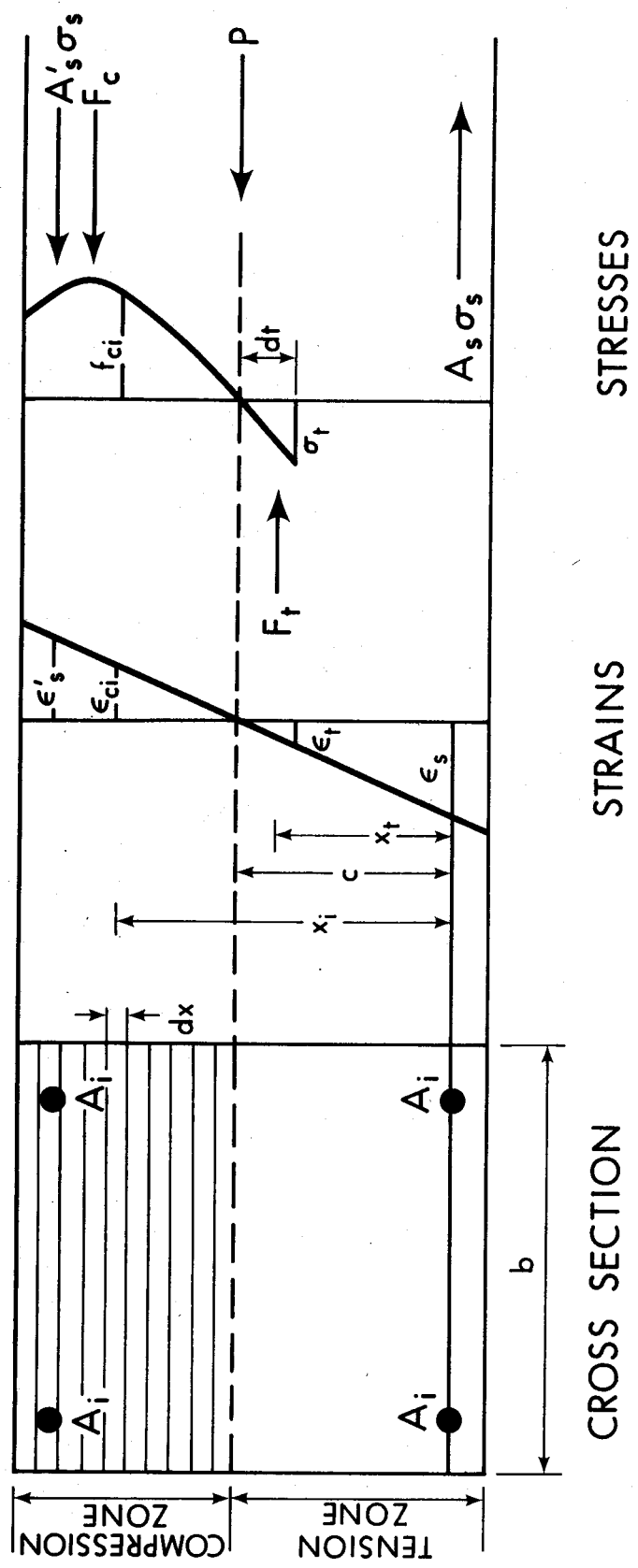


Figure 2.7 Basic Notation Used in the Flexural Analysis of Reinforced Concrete Sections

for concrete in tension, the total tensile force may be calculated using a triangular stress block. The total concrete tensile force may be expressed as:

$$F_t = \sigma_t b \frac{dt}{2} \quad (2.14)$$

From the strain distribution the strain in each steel bar may be determined. Using the stress-strain curve for steel the stress in each bar may be calculated. The total steel force may be expressed as:

$$F_{st} = \sum_{i=1}^{nb} f_{si} A_i \quad (2.15)$$

The total axial force resisted by the cross section is the algebraic sum of the concrete compressive force, the concrete tensile force and the steel force. The total moment that the section is subjected to may be determined by summing the moments of the above forces about the centroidal axis. The moment may be expressed as:

$$m = \sum_{i=1}^{ns} F_{ci} x_i + \sum_{i=1}^{nb} F_{st} x_{si} + F_t x_t - Pc \quad (2.16)$$

where c = the distance from the tension steel to the centroid of the cross section.

The first three terms are the moments of the internal forces about the tension steel and the last term, Pc , is to convert the moment to a moment about the centroid of the cross section.

The required points on the axial load-moment interaction curve were developed by selecting specific axial load levels at which the ultimate moment was calculated. At each axial load level an initial strain at the extreme compression fibre and initial curvature was assumed. For the initial curvature the edge strain was incremented until the sum of the internal forces and the external specified load were balanced within a specified tolerance. After balancing the axial loads the moment required to provide equilibrium was calculated. The curvature was then incremented and the axial load again balanced and the moment calculated. This procedure was repeated until the maximum moment on the moment curvature curve was calculated.

The subroutine THEORY and flow diagram in Section 3.2 gives a further description of the above procedure. The accuracy of this procedure is discussed in Section 3.3.

CHAPTER III
COMPUTER PROGRAM FOR ANALYSIS

3.1 Description of The Monte Carlo Technique

The Monte Carlo Technique is a method for obtaining information about system performance from the performance data of the individual components. This method may be called a synthetic or empirical method of sampling. It consists of simulating many systems by computer calculation and then evaluating the performance of the overall system by evaluating the performance of the population of synthesized systems.

If a system consists of many components each with a number of values, a number of systems could be built to measure the performance of the system using each component value. Although this would give an indication of the variability of the system, it would generally be impractical or uneconomical. If there is a relationship between the total system performance and each component variable, a measurement of the total system performance may be calculated without actually building the system. By knowing the statistical properties of the distribution of each variable and drawing a value from this distribution rather than using measured values, it is possible to calculate the performance of a specified number of synthetic systems to get the variability of the system.

This procedure is called the Monte Carlo Technique and is shown graphically in the form of a flow diagram in Figure 3.1. The availability of high speed computers has led to the popularity of this technique.

In this study the Monte Carlo Technique was used to generate a family of theoretical axial load-moment interaction curves for rectangular column cross sections using random values of the variables affecting the cross section strength. The random value of each variable was based on the statistical properties of each individual variable. Each theoretical curve was then compared to the ACI axial load-moment interaction curve to obtain a sample of ratios of the random theoretical capacity to that based on the ACI Code, P_{theory}/P_{ACI} . These ratios were eventually used to calculate ϕ or understrength factors for rectangular tied column cross sections.

3.2 Description of The Computer Program

The computer program used in this study is capable of developing the axial load-moment interaction diagram for rectangular tied column cross sections with the longitudinal steel at any location in the cross section. The program is capable of developing the interaction diagram using the ACI method and assumptions as well as the theoretical interaction diagram using a theoretical calculation of strength based on material and cross section properties.

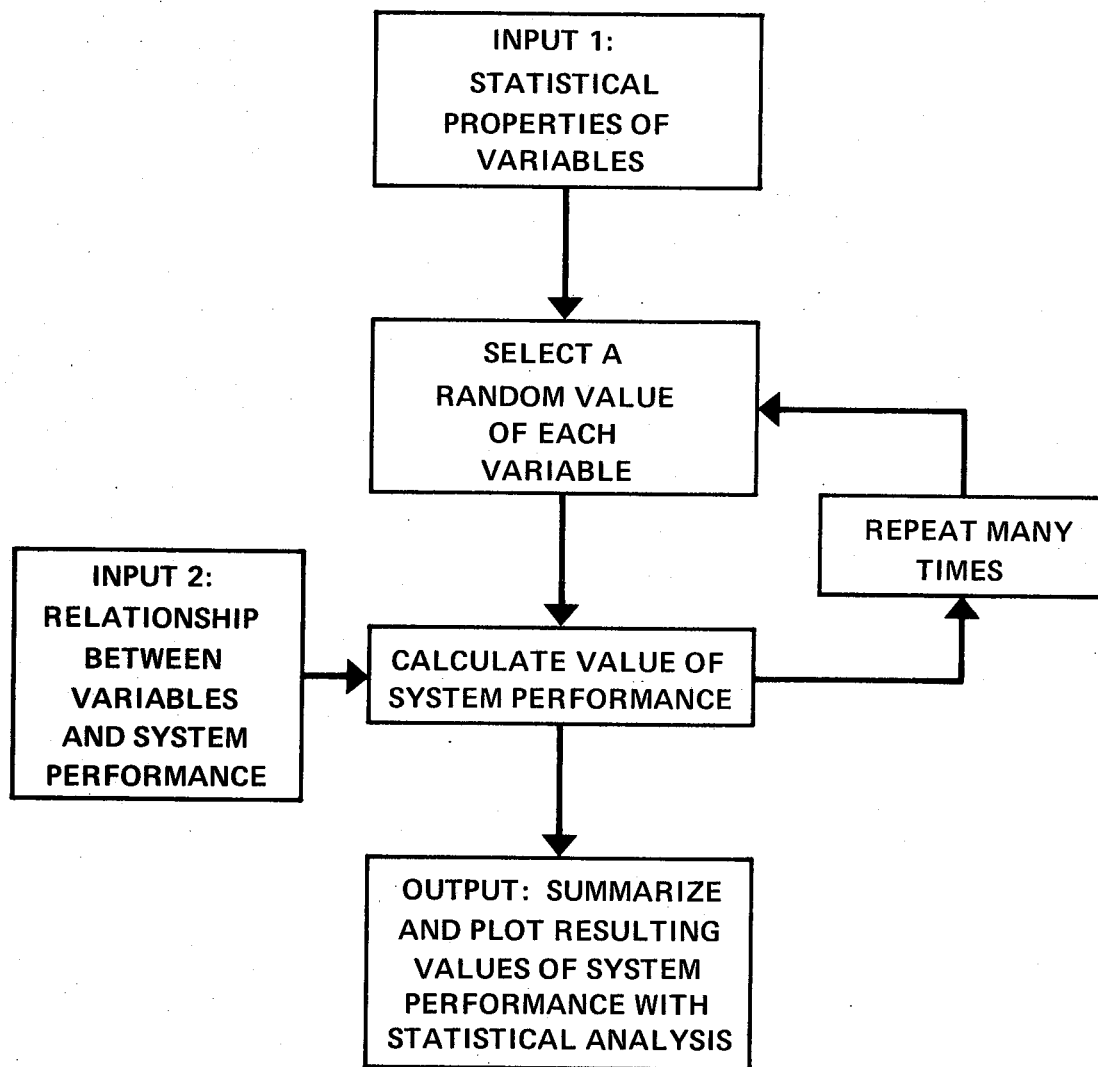


Figure 3.1 The Monte Carlo Technique

Figure 3.2 is a condensed flow diagram of the Monte Carlo program. The main program consists of the subroutines PROP, ACI, CURVE, THMEAN, RANDOM, THEORY and STAT. A complete listing of the program with its subroutines may be found in Appendix D. Detailed flow diagrams of the subroutines are given in Appendix C.

The subroutine PROP is used to read and write the nominal cross section properties. The statistical properties of the variables are read and written in the main program. A complete description and format of input data is given in Appendix E.

The subroutine ACI is used to calculate the ACI axial load-moment interaction diagram using the nominal or designer's values of section and material properties. The subroutine ACI uses the subroutine ASTEEL to calculate the forces in the steel reinforcement in the cross section. The capacity under pure axial load, balanced conditions and pure moment are first calculated. Using the concept of linear strain across the cross section the axial load and associated moment are calculated for various strain distributions using equations based on Sections 10.2.1 to 10.2.5 and 10.2.7 of ACI 318-71³. Tension or compression failures are classified by comparing the axial load with the axial load at balanced conditions. The value of e/h for each load level considered is calculated for use in fitting a curve to the interaction diagram. Finally the ACI axial

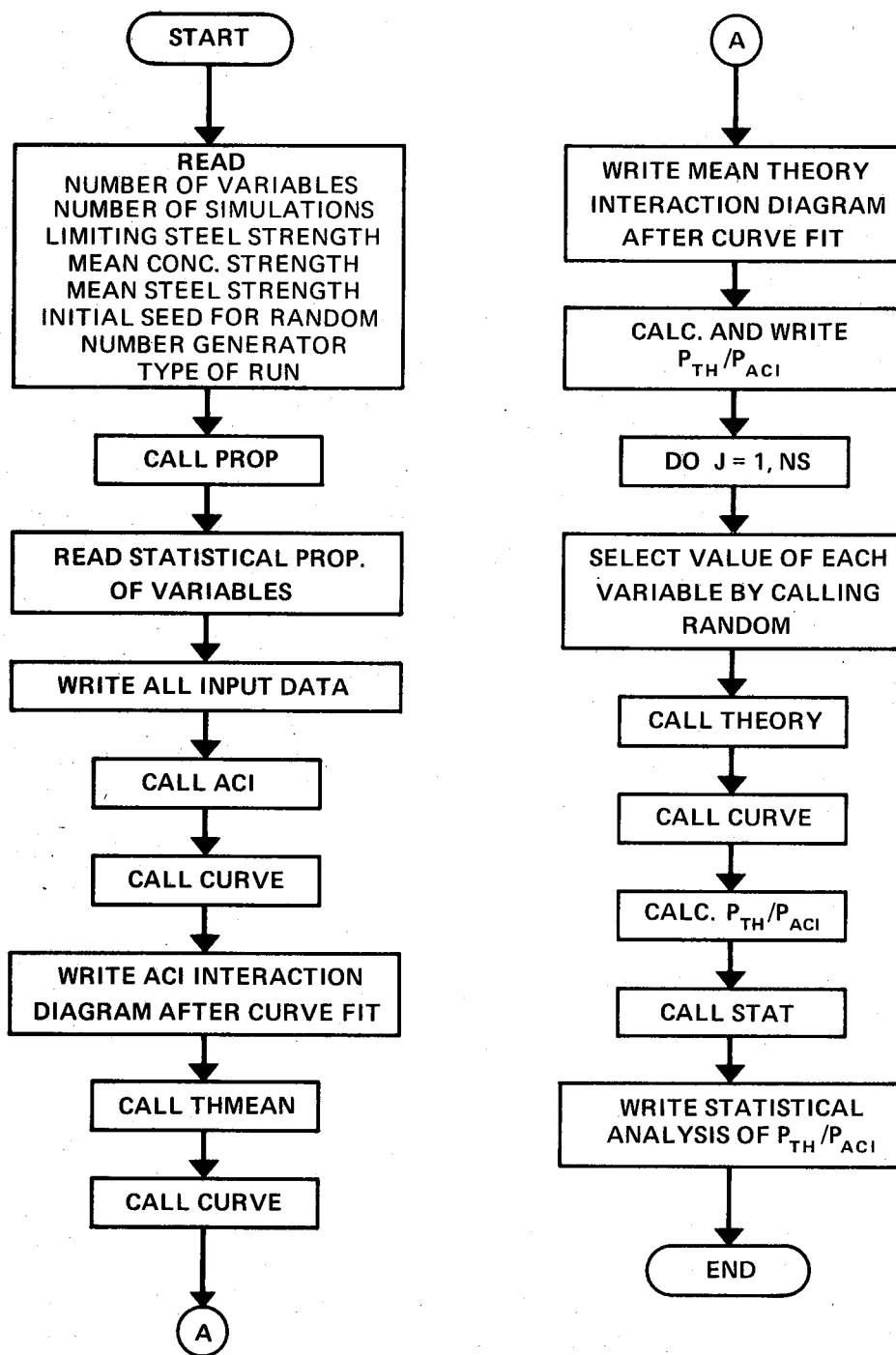


Figure 3.2 Condensed Flow Diagram of the Monte Carlo Program

load-moment interaction diagram is written. A condensed flow diagram of the subroutines ACI and ASTEEL is shown in Figure 3.3.

The subroutine CURVE is called a number of times to fit a polynomial curve to the interaction diagram developed. The interaction diagram is transformed into a curve of axial load vs. e/h for axial loads above the balance point or compression failures and a curve of moment vs. h/e for axial loads below the balance point or tension failures. The two part curve fit was used to achieve greater accuracy in fitting the curve near the balance point. The use of moment rather than the axial load was used for the tension region to achieve greater accuracy since e/h approaches infinity as P approaches zero. There was no attempt made to force the two curves to coincide at the balance point but the last point used for fitting the curve above the balance point was used as the first point for fitting the curve below the balance point. By using the same point in both curve fits a close agreement was achieved at the balance point. When the subroutine CURVE is used to fit a polynomial to the interaction diagram the calculated points with an associated value of e/h greater than 3.0 are eliminated from the curve fit since these points may cause large errors. Figure 3.4 is a plot of the ACI interaction diagram plotted from the ACI calculated values and the ACI interaction diagram plotted from values from the curve fit. Figure 3.4 is the transformed diagram with axial load vs. e/h and moment vs.

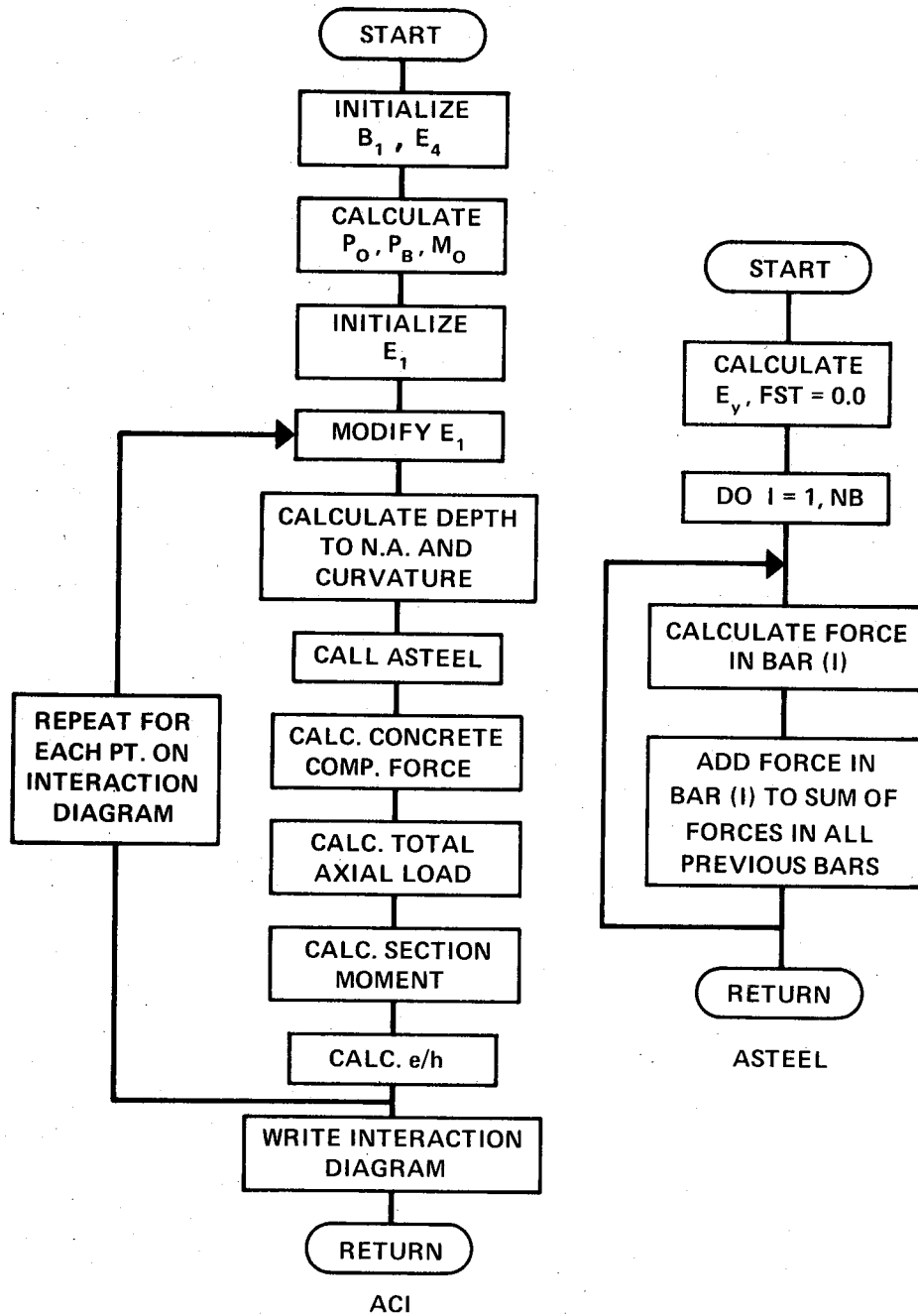


Figure 3.3 Condensed Flow Diagram of the Subroutines ACI and ASTEEL

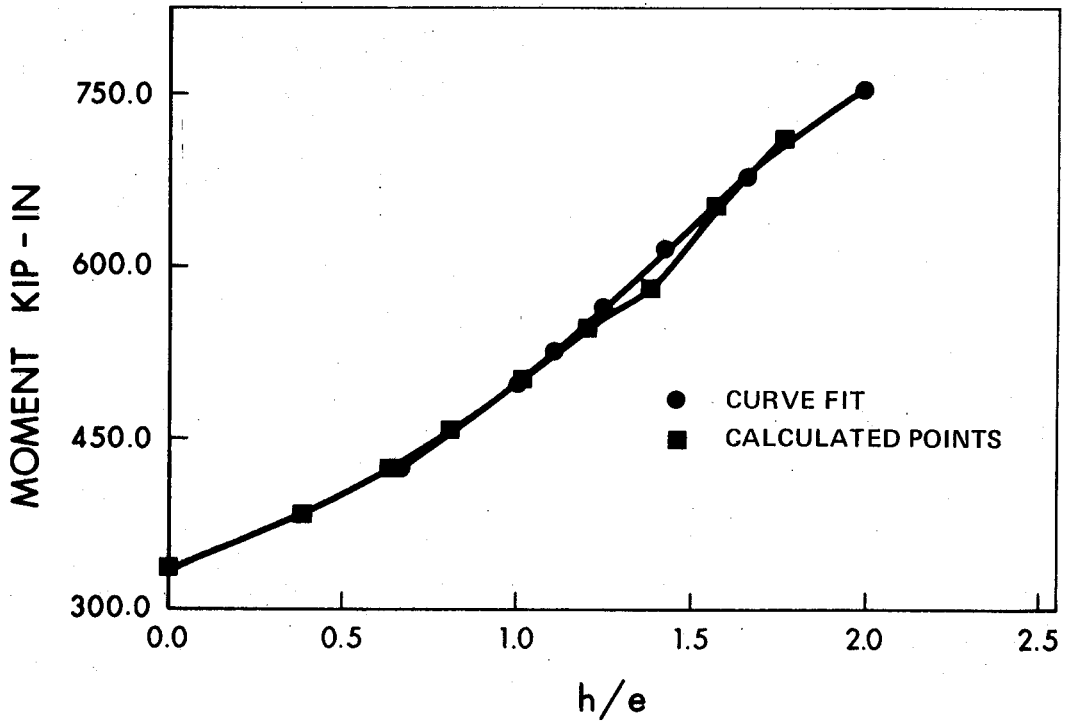
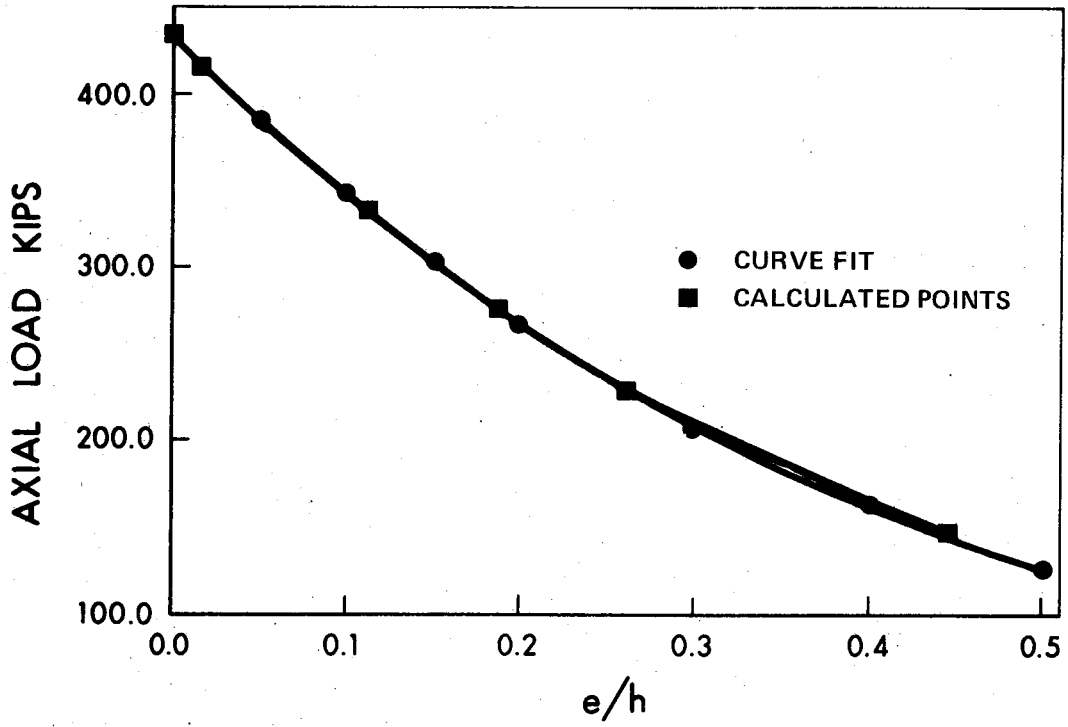


Figure 3.4 The ACI Interaction Diagram

h/e plotted.

The curve fit used for the interaction diagram required a minimum of two points above the balance point and a minimum of two points between the balance point and an e/h value of 3.0. This resulted in a curve fit for three points above and below the balance point. It was determined that a curve fit using a minimum of six points resulted in a curve fit with virtually no error above the balance point and a maximum error of about 2.5% below the balance point with the general error below the balance point in the range of 1% or less. On this basis twenty points on the interaction diagram were considered sufficient to achieve a satisfactory curve fit.

The subroutine CURVE uses the IBM subroutines GDATA, ORDER, MINV and the modified IBM subroutine MULTR to TMULTR. These subroutines are described in Reference 31. A condensed flow diagram of the subroutine CURVE is shown in Figure 3.5.

The subroutine THMEAN uses the subroutine THEORY to calculate the theoretical axial load-moment interaction diagram using the mean value of the individual variables. This subroutine also writes the interaction diagram calculated. A condensed flow diagram of the subroutine THMEAN is shown in Figure 3.6.

The subroutine RANDOM is a subroutine which combines the IBM subroutine GAUSS and RANDU to calculate random

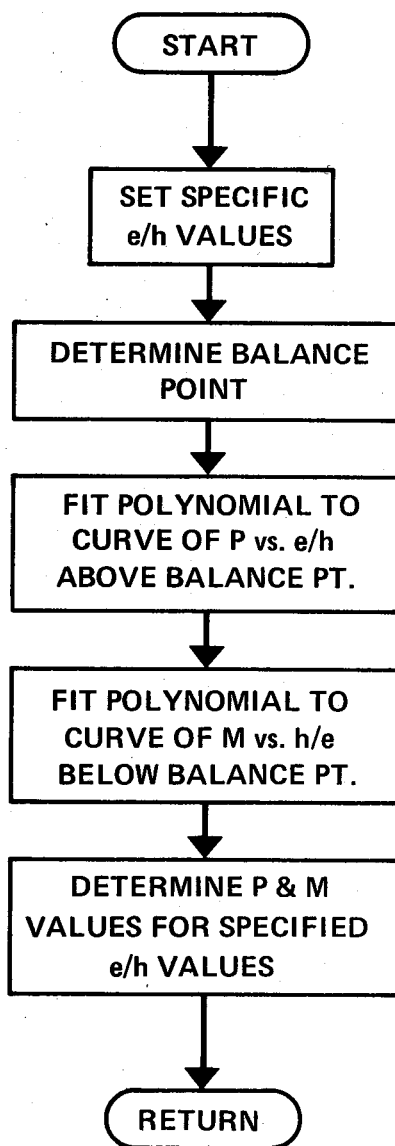


Figure 3.5 Condensed Flow Diagram of the Subroutine CURVE

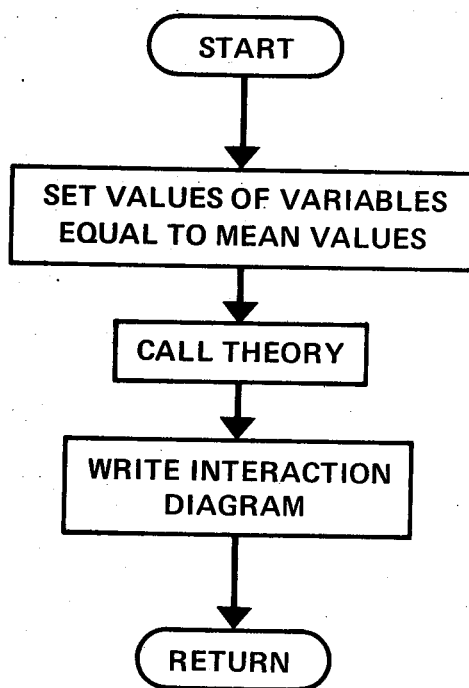


Figure 3.6 Condensed Flow Diagram of the Subroutine THMEAN

values of each variable based on the statistical properties of each variable. These IBM subroutines are also described in Reference 31.

The subroutine THEORY was developed to calculate the theoretical axial load-moment interaction diagram using the subroutines AXIAL and FSTEEL. A specific axial load level is chosen in THEORY which in turn calls AXIAL. Using the axial load level selected, a strain distribution is determined at a given curvature for which the external load and internal forces balance. For this curvature the moment required to develop the curvature is determined. The above procedure is repeated with increasing curvature until the moment capacity is determined at each load level. This method produces a moment curvature diagram similar to the one shown in Figure 2.6. The subroutine FSTEEL is used by AXIAL to calculate the forces in the reinforcing steel. Figures 3.7 through 3.10 are condensed flow diagrams of the subroutines THEORY, AXIAL and FSTEEL. The theoretical interaction diagram was obtained as the locus of the values of M_u for each value of P for which a moment curvature diagram had been computed as explained in Section 2.4. All comparisons of the theoretical strength with the ACI strength or Hognestad's tests were done using values of the theoretical strength after the interaction diagram was subjected to a curve fit.

The subroutine STAT is a subroutine used to perform a statistical analysis on the ratio P_{theory}/P_{ACI} for the

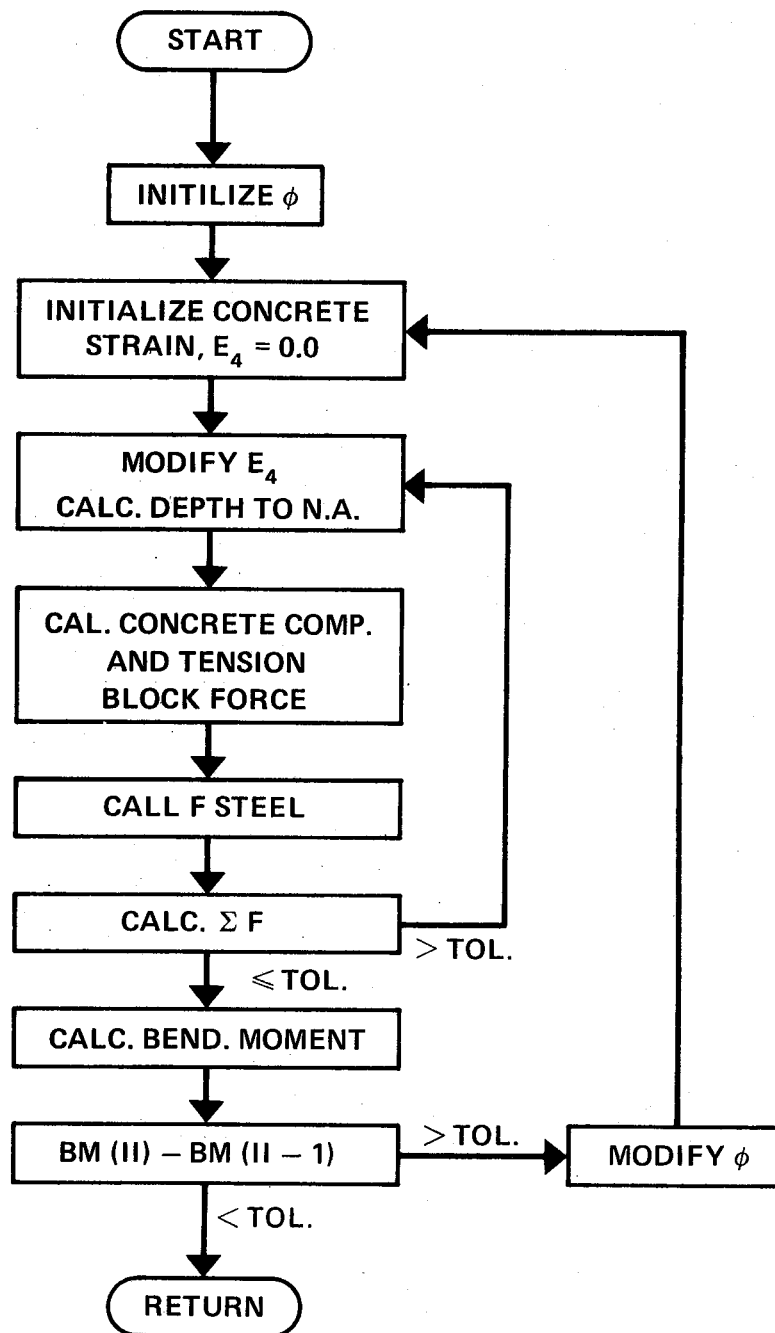


Figure 3.8 Condensed Flow Diagram of the Subroutine AXIAL

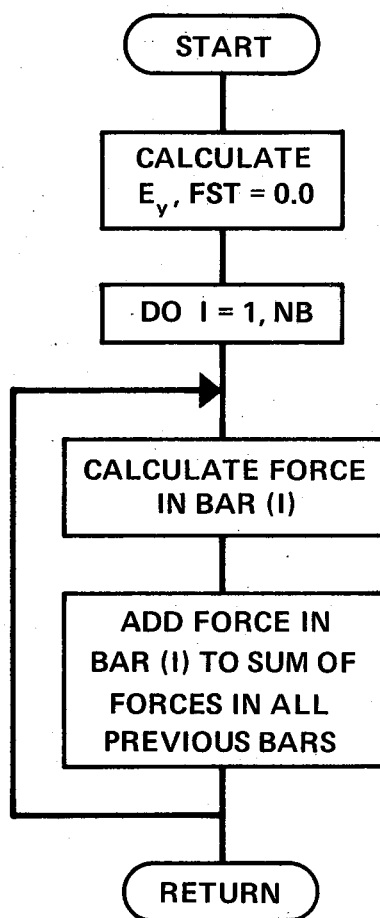


Figure 3.9 Condensed Flow Diagram of the Subroutine FSTEEL

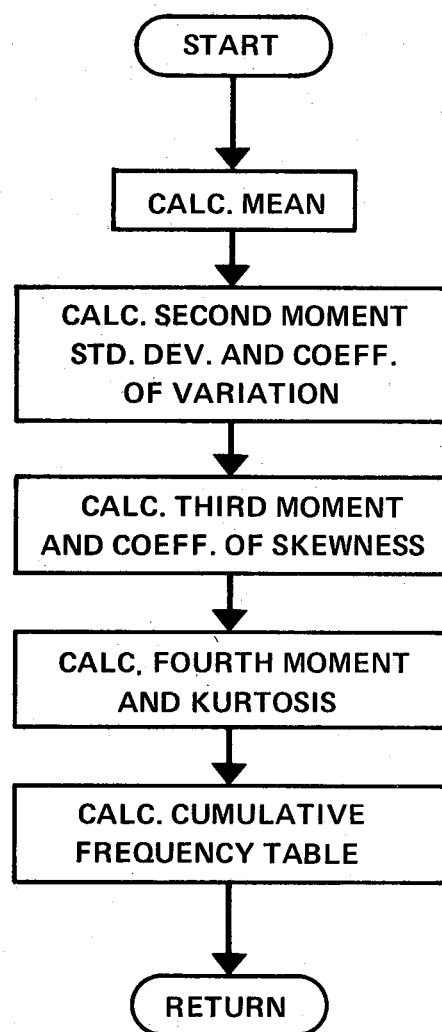


Figure 3.10 Condensed Flow Diagram of the Subroutine STAT

various values of e/h specified. The output from the subroutine STAT includes the mean, standard deviation, coefficient of variation, coefficient of skewness, kurtosis, minimum and maximum value, median and cumulative frequency table of the ratio P_{theory}/P_{ACI} . A condensed flow diagram of the subroutine STAT is shown in Figure 3.10.

3.3 Comparison of Theory With Test Results

The subroutine used to calculate the theoretical axial load-moment interaction diagram was compared with the results of tests on rectangular tied columns reported by Hognestad. Using Hognestad's column properties and the total eccentricity of the reported failure loads the mean ratio of P_{test}/P_{theory} was calculated to be 1.0068 with a standard deviation of 0.064 when k_3 used to define the maximum compressive stress, $k_3 f'_c$, was taken equal to 0.85. Table 3.1 is a summary of the values of the ratio P_{test}/P_{theory} and standard deviation for various values of k_3 . Tables 3.2 and 3.3 are the results of a comparison of the theoretical calculations with Hognestad's²⁹ test results using a value of $k_3=0.85$. Although the lowest standard deviation was obtained for $k_3=0.87$, any increased accuracy did not warrant abandoning the traditional value of $k_3=0.85$.

In this study the compression block was divided into ten equal segments between the extreme compressive fibre and the neutral axis with the strain averaged over the segment

depth. A comparison of the analysis with an analysis using twenty segments showed no significant difference in the ratio of P_{test}/P_{theory} . The mean value of P_{test}/P_{theory} for ten segments was 1.0068 compared with 1.005 for calculations using twenty segments.

In view of the above the calculations in the subroutine THEORY were based on ten segments with a value of $k_3=0.85$ resulting in a mean value of P_{test}/P_{theory} of 1.0068 with a standard deviation of 0.064. Any inaccuracies due to the use of the curve fitting subroutine CURVE are included in these statistics.

TABLE 3.1Comparison of P_{test}/P_{theory} with the value of k_3

k_3	P_{test}/P_{theory}	Std. Deviation
0.70	1.0810	0.080
0.80	1.0300	0.066
0.85	1.0068	0.064
0.86	1.0020	0.062
0.87	0.9980	0.060
0.90	0.9850	0.062
1.00	0.9470	0.067

Table 3.2

Theory Comparison With Hognestad's Tests II

Concrete Strength Psi.	e/h	Ptest Kips	Ptheory Kips	Ptest/Ptheory
5810	0.276	284.0	290.1	0.978
5810	0.540	152.0	167.7	0.906
5520	0.534	162.0	166.6	0.972
5240	0.344	274.0	233.0	1.176
5170	0.789	91.2	93.7	0.973
5170	1.275	44.0	45.9	0.959
5100	1.278	46.1	45.9	1.004
5100	0.787	89.0	93.7	0.950
4700	0.785	94.0	91.7	1.025
4700	0.535	156.0	159.8	0.977
4370	1.279	44.0	45.0	0.977
4370	0.782	89.5	90.9	0.985
4260	0.532	146.0	150.6	0.970
4260	1.278	43.5	44.8	0.971
4080	0.007	456.0	427.6	1.066
4080	0.275	256.0	227.8	1.124
4040	0.006	420.0	429.8	0.977
4040	0.274	248.0	227.9	1.088
2300	1.285	44.5	42.9	1.038
2020	0.010	225.0	263.8	0.853
1970	0.278	141.0	143.0	0.981
1880	0.788	73.0	73.2	0.998
1820	0.532	99.0	99.7	0.993
1820	0.539	99.0	98.9	1.001
1770	1.288	45.0	42.0	1.071
1730	0.785	65.5	71.7	0.914
1520	0.018	202.0	221.5	0.912
1520	0.277	126.8	130.5	0.971

Table 3.3

Theory Comparison With Hognestad's Tests III

Concrete Strength Psi.	e/h	Ptest Kips	Ptheory Kips	Ptest/Ptheory
5350	0.536	220.0	218.1	1.009
5350	0.787	142.0	151.0	0.940
5100	1.292	88.0	79.7	1.105
5100	0.793	153.0	147.2	1.040
5050	0.272	326.0	325.6	1.001
4850	0.534	210.0	208.2	1.008
4850	1.285	79.0	79.8	0.991
4630	1.292	84.5	78.0	1.083
4300	0.272	303.0	293.8	1.031
4290	0.534	206.0	194.3	1.060
4150	0.270	315.0	287.7	1.095
4070	0.010	485.0	514.5	0.943
4010	0.276	284.0	279.8	1.015
3870	0.008	500.0	501.7	0.997
3800	1.291	74.0	77.9	0.950
3580	0.535	180.0	179.8	1.001
3580	0.789	138.8	135.0	1.028
2300	0.276	252.0	215.3	1.171
2300	0.533	151.0	145.5	1.038
2200	0.272	230.0	217.9	1.055
2070	0.000	353.0	376.8	0.937
2070	0.528	137.0	141.4	0.969
2070	0.787	104.0	112.0	0.928
2070	1.291	74.5	72.0	1.035
1950	1.289	72.5	69.0	1.051
1950	0.784	115.5	107.1	1.078

17 with e/h < 0.3
 $\bar{x} = 1.012$
 $s = 0.085$
 $v = 0.082$

CHAPTER IV

PROBABILITY MODELS OF VARIABLES AFFECTING SECTION STRENGTH

4.1 Concrete Variability

4.1.1 Introduction

Concrete, like all other construction materials, is variable. This variability is influenced by design, production and testing procedures. Research data shows that under current design and construction techniques concrete which differs from the specified strength is placed in structures. These structures have performed satisfactorily due to redistribution of stresses, mixing of the under strength concrete with over strength concrete within the forms, and the fact that the concrete strength increases with age after the time at which tests are made. In some cases experience has lead to design equations which result in conservative designs even though the assumptions used are not entirely correct.

The two broad causes of variations in concrete strength are variations in material properties and variations in the testing procedures. Since concrete is a heterogeneous mixture of cement, water, coarse and fine aggregate, entrained air, and in some cases admixtures, variations in the final concrete strength are inevitable. Variations in any one of the ingredients or a combination of variations in

more than one ingredient will result in a variation in the final concrete strength. Variation in the water-cement ratio will cause significant strength variation. The water-cement ratio may be altered due to poor control of water content, variation in moisture content or nonuniformity of the aggregate. Variations in the properties or proportioning of any of the materials will cause strength variation. The methods of transporting, placing and curing will also affect the final concrete strength.

Variations in the testing methods will lead to apparent variations in the concrete strength. Variations in testing may be due to inconsistent sampling, nonuniform fabrication of test samples or poor handling and care of fresh samples and variations in temperature and moisture conditions. Also the preparation of the samples for testing and the procedure used in testing may cause variations in the test strength.

The control strength is affected by material properties and test procedures whereas the structure concrete strength will be affected by the material properties and placing procedures. This results in different concrete strengths in the test specimen and in the structure. The concrete strength will differ from place to place in the structure due to different placing procedures, curing conditions, and the location in the structure.

4.1.2 Distribution of Concrete Strength

Generally the distribution of concrete strength has been assumed to be a Gaussian or normal distribution. ACI Committee 214² found that for practical concrete control the normal distribution adequately describes the variation in concrete strength. Rusch and Rackwitz have presented data from an international study of cube and cylinder tests which also follows a normal distribution in most cases.

In establishing understrength factors for members to reflect the probability of the material strength being lower than the specified strength, the low strength tail ends of the curve are important. Because little data is available for these tail areas, the tail of the curve must be extrapolated from the central area of the curve. The normal distribution fits the data very well for the majority of the data in the central portion of the curve. Some researchers have shown however, that the normal curve does not always give the best fit in the tail areas.

Freudenthal²⁴, Julian³³, and Shalon and Reintz⁶¹ have shown that the log-normal distribution gives a better fit for concrete strength in which the control is poorer than average and should be used where extreme values are important. Shalon and Reintz⁶¹ have shown that the normal curve as a general assumption is valid but in almost every case a skew towards the higher strengths was observed, especially for cases of high coefficient of variation. Using

the x^2 test as a measure of discrepancy, a discrepancy was observed between the actual distribution and the normal distribution at the 5% level of significance for a coefficient of variation of 23% whereas for a coefficient of variation of 14.2% practically no skew was observed. Freudenthal²⁴ suggests the use of the log-normal or the extreme distribution to better describe the tail area but the extreme distribution has the disadvantage of mathematical complexity.

Table 4.1 is a collection of data from a number of statistical studies of concrete strength. The majority of researchers have used a normal distribution due to its simplicity and the fact that in concrete control it is the central area of the curve that is important. Due to this, studies in concrete control are generally not concerned with the tail areas of the distribution.

For concrete strengths with a coefficient of variation of 15% or lower the normal curve describes the variation in the concrete strength as well as any other distribution. For cases where the coefficient of variation is greater than 15% a skewed distribution is observed for which a log-normal transformation becomes valid to increase the accuracy in the tail areas of the curve.

Table 4.1
Concrete Strength Variability

Source	Test		Type of Distribution	Coefficient of Variation %	
	Type	No.			
Julian	1950	cyl.	861	Normal	10.4
Cummings	1953	cyl.	208	Normal	9.3
Shalon	1955	cube	---	Normal	14.2
"	"	cube	---	Log-normal	23.6
Bloem	1955	cyl.	1429	Normal	11.4
"	"	cyl.	354	Normal	16.4
Wagner	1955	cyl.	613	Normal	11.8
Erntroy	1960	cube	4000	-----	20.0
Malhotra	1962	cyl.	68	-----	13.5
Wagner	1963	cyl.	688	Normal	12.4
"	"	cyl.	688	Normal	15.2
BPR	1963	cyl.	975	Normal	12.4
"	1964	cyl.	200	Normal	10.9
Virginia Hwy.	1965	cyl.	210	Normal	7.2
Soroka	1968	cyl.	68	Normal	15.2
Riley	1971	cyl.	50,000	Normal	13.6

4.1.3 Statistical Description of Concrete Strength Variation

The average strength and variation in strength of concrete cylinder tests may be described by the mean, standard deviation and coefficient of variation. The coefficient of variation has become the accepted measure of concrete strength variation.

Depending on the control of the concrete operations the coefficient of variation may range from 5% for laboratory conditions to as high as 30% for uncontrolled conditions. The 30% value is unacceptable under present construction techniques and the 5% value is not practical for field conditions. On the Skylon Tower³⁷ at Niagara Falls, Ontario coefficients of variation ranging from 6.8% to 9.8% were achieved using exceptional control methods. This suggests a minimum value for site conditions. The Bureau of Reclamation² consistently achieves a coefficient of variation of about 15% which suggests a value for better than average control or good control. Table 4.1 indicates that the coefficient of variation in many cases is between 15% and 20% which suggests that 20% is a reasonable maximum value.

An ASTM² task force working on the question of concrete strength suggested a coefficient of variation of 20% when no control data is available for the average job. Figure 4.1 illustrates that the coefficient of variation varies but, on

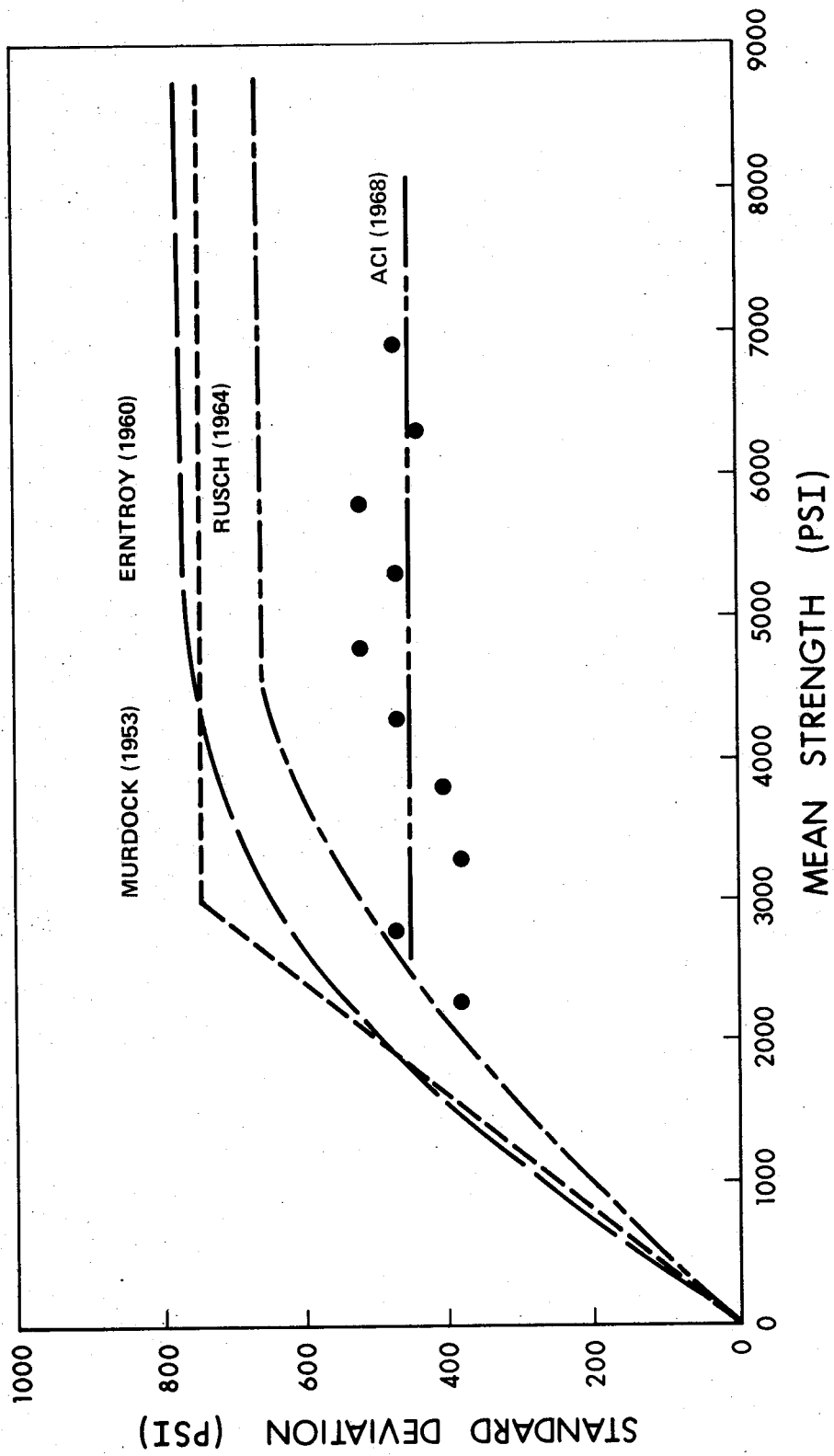


Figure 4.1 Relationship Between Standard Deviation and Mean Strength of Concrete

the average, is less than 20%. In this study the levels of control were divided into three classes with corresponding coefficients of variation as follows:

Excellent Control	10%
Average Control	15%
Poor Control	20%

The total variation in concrete strength must include the variation in concrete strength within a single batch. This in batch test variation may be considered as a variation in testing procedures or a variation in the actual concrete strength. The variation in concrete strength in a single batch will include the effects of mixer inefficiencies. Comparison of samples taken from different locations in the mixer may be used to evaluate the variation within a single batch. In this study the levels of control for within batch tests were divided into three classes with corresponding coefficients of variation as follows:

Excellent Control	4%
Average Control	5%
Poor Control	6%

Figure 4.1 illustrates that the standard deviation and the coefficient of variation are not a constant for different strength levels. Due to this the mean strength along with the coefficient of variation is required to adequately describe the strength variation. The relationship between the mean strength and the standard deviation shown

in Figure 4.1 was developed using the data from several continents. The relationships shown by Murdock, Erntroy and Rusch⁴⁷ indicate that above a certain value of mean strength the standard deviation remains constant while below this value the coefficient of variation remains constant. The ACI data indicates a constant standard deviation for all strength levels.

The differences in values reported by the different sources may be partially explained by the type of data used. The specimens of Erntroy and Murdock⁴⁷ were 6 in. cubes while the ACI specimens were standard cylinders. The data reported by Rusch⁴⁷ contains test specimens of both types. Neville⁴⁶ notes that cube tests tend to be more variable than cylinder tests. The relationship reported by Erntroy and Murdock were based on individual test values whereas the ACI values were based on two specimens per test. The Rusch data again contains both types of data.

On the basis of test data available and reported it appears that the standard deviation remains constant for concrete strengths above a value of 3500 to 4000 psi. and the coefficient of variation is constant for strength levels below 3500 psi.

4.1.4 Cylinder Strength vs. Design Strength

The average concrete strength required by the ACI

Building Code³ must exceed the value of the design strength, f'_c , by at least:

400 psi. if the standard deviation is ≤ 300 psi.

550 psi. if the standard deviation is 300 to 400 psi.

700 psi. if the standard deviation is 400 to 500 psi.

900 psi. if the standard deviation is 500 to 600 psi.

If the standard deviation of the test cylinders exceeds 600 psi. or if a suitable record of test results is not available proportions shall be used which provide an average strength 1200 psi. greater than the design strength. After test data becomes available the amount by which the average must exceed the design strength may be reduced such that the probability of a test being 500 psi. below the design strength is 1 in 100 and the probability of the average of three consecutive tests being below the design strength is 1 in 100.

The amounts by which the average strength must exceed the design strength in the ACI Code are based on the following criteria:

1. The probability of less than 1 in 10 that a random individual strength test will be below f'_c .

$$f_{cr} = f'_c + 1.282\sigma \quad (4.1)$$

2. The probability of 1 in 100 that an average of three consecutive strength tests will be below f'_c .

$$f_{cr} = f'_c + 1.343\sigma \quad (4.2)$$

3. The probability of 1 in 100 that an individual strength test will be more than 500 psi. below f'_c .

$$f_{cr} = f'_c + 2.326\sigma - 500 \quad (4.3)$$

where:

f'_c = the design concrete strength

f_{cr} = the average cylinder strength

σ = the standard deviation individual tests

4.1.5 In-situ Strength of Concrete

The concrete strength in a structure is not clearly defined as some specific multiple of the standard cured cylinder strength. Most researchers agree that the strength of the concrete in the structure is somewhat lower than the standard test cylinder strength.

Tests by Petersons⁴⁸ on columns under well controlled laboratory conditions suggest that the strength of the concrete in the structure ranges from 90% to 70% of the standard cylinder strength. Bloem¹² suggests the strength of the concrete in columns is 80% of the standard cylinder

strength for all but the top 10 in. of the column. Allen's⁵ study of beams failing in flexure suggests the strength of concrete in the cases of compression failure to be 90% of the cylinder strength. Table 4.2 gives the average ratios of core strengths to cylinder strengths from various researchers.

Petersons^{4,6} reviewed the data available on core strength as compared to standard cylinder strength and concluded that the three most important factors affecting the strength of the concrete in the structure are:

1. The strength level of the concrete- The ratio between the strength of the concrete in the structure and the standard cylinder strength decreases as the strength level increases.

2. The curing of the concrete- The difference between the minimum curing acceptable and good curing can be approximated by a factor of 0.9.

3. The location of the concrete in the structure- Tests by several researchers have indicated that the concrete in the top foot of columns is weaker than the concrete in the remainder of the column. This may be explained by the increased water cement ratio at the top due to water migration after the concrete is placed. The reduction in strength is of the order of 15% of the strength of the remainder of the column.

Table 4.2

Concrete Strength in Structure vs. Cylinder Strength

Researcher	Ratio $\frac{\text{Core Strength}}{\text{Cylinder Strength}}$
Kaplan	0.74
	0.96
	0.90
Petersons	0.90
	0.88
Bloem	0.83
Campbell and Tobin	0.87

The reduction in the concrete strength in the structure is partially offset by the requirement that the average cylinder strength must be from 700 to 900 psi. greater than the design strength to meet existing design codes. Based on this observation and on the equations from Allen and Bloem⁴⁰ the mean strength for minimum acceptable curing may be expressed as:

$$f_{c(\text{structure})} = (0.675f'_c + 1.1) \text{ ksi} \quad (4.4)$$

4.1.6 Probability Model for Concrete Strength

The variation in concrete strength was described with a normal distribution and a mean value of:

$$\bar{f}_c = \left(\frac{0.78f'_c + 670}{f'_c} \right) \left(\frac{f'_c \text{ real}}{f'_c \text{ test}} \right) (f'_{\text{cyl}}) \quad (4.5)$$

with a coefficient of variation:

$$v = \sqrt{v_1^2 - v_2^2 + v_3^2} \quad (4.6)$$

where:

v_1 = the variation in test cylinder strengths

v_2 = the variation between real strength of cylinders and measured cylinder strengths, "in-test variation"

v_3 = the variation of in-situ strength relative to cylinder strength

The basic cylinder strength variation was taken as 0.15 with a basic in-test variation of 0.04 and a variation of 0.10 for differences between in-situ and test cylinder strengths. Checks were also made with test cylinder variation of 0.10 and 0.20.

4.2 Reinforcing Steel Variability

The variability of the strength of the reinforcing steel was described with a normal distribution as well as a modified log-normal distribution. The complete description of the reinforcing steel strength distribution used is given in Appendix A.

4.3 Cross Section Dimensional Variability

4.3.1 Introduction

Geometric imperfections are the variations in the dimensions, shape, lines, grades and surfaces of as-built structures compared to the specified values. Variations in cross section dimensions, verticality of columns, misalignment and initial curvature of columns are inevitable in structures. Geometric imperfections arise during each phase of the construction process. Variations in the size and shape are particularly dependent on the size, shape and quality of the forms used for manufacture. Setting out and assembly affect the geometry of the overall structure and

are dependent on construction techniques and construction and inspection personnel.

Data from field measurements of imperfections is needed for various purposes such as for the evaluation of specified tolerances, construction performance and theoretical probability models. It is important that data be collected which is complete and uniform. Unfortunately at present there is not a uniform method of collecting and reporting this data. Without some degree of standardization it is difficult to compare the results of measurements made by various investigators with any degree of reliability.

4.3.2 Probability Model for Cross Section Dimensions

The variation in column cross section dimensions has been reported by Tso and Zelman⁶⁹. Their results are summarized in the histogram in Figure 4.2. The dimensional measurements were made to the nearest 1/4 in. in conjunction with a study of the strength variation in concrete. The data is based on 299 columns from 8 buildings. The nominal dimensions ranged from 12 in. to 30 in.. Usually two measurements were made at each of five levels over the storey height of the column. The mean variation was found to be + 0.06 in., that is, the width or thickness averaged 0.06 in. larger than the specified value with a standard deviation of 0.28 in.. Tso and Zelman's⁶⁹ measurements indicate the distribution of dimensional variations to be

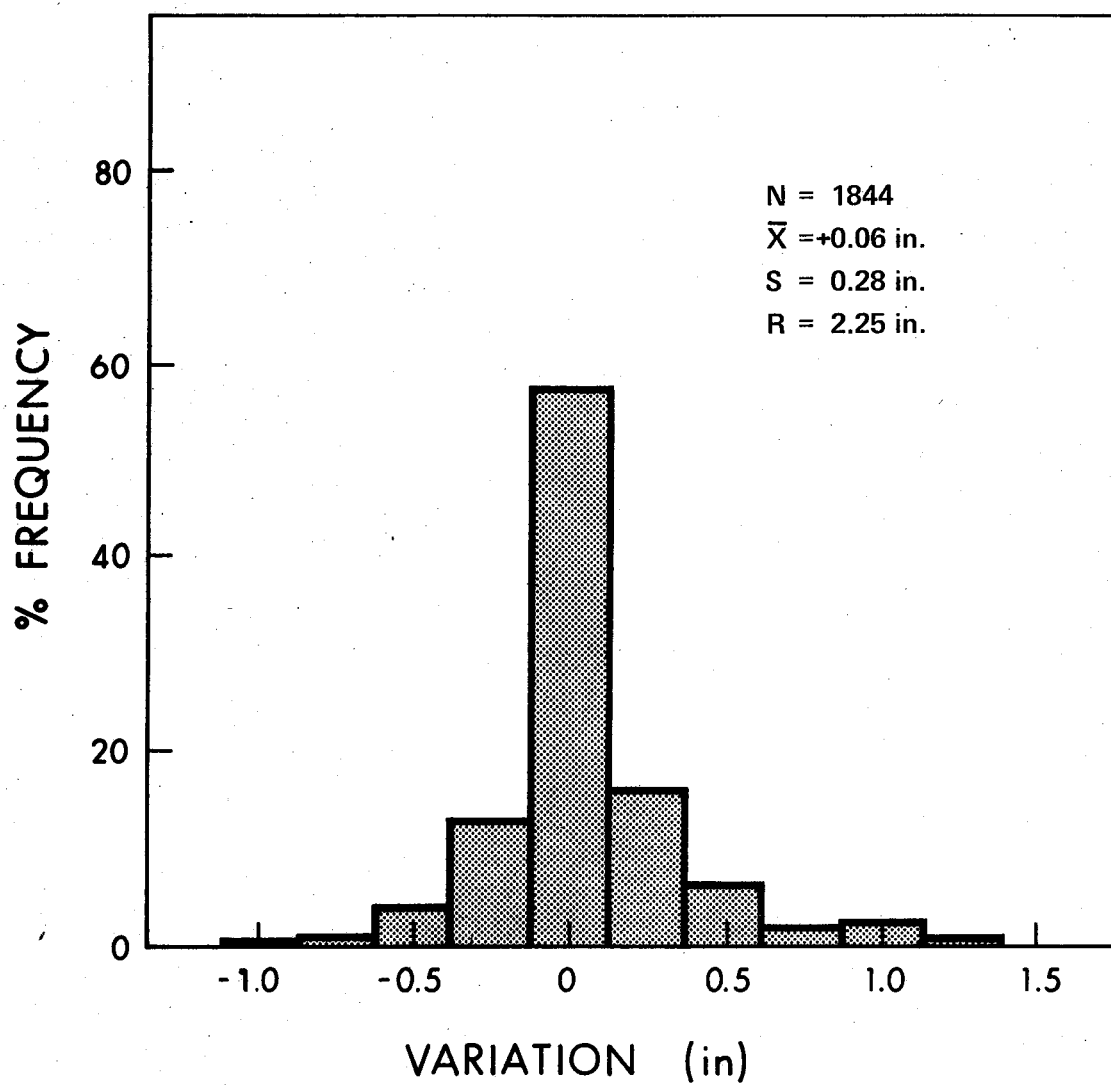


Figure 4.2 Histogram of Cross Section Dimensional Variation Reported by Tso and Zelman

normal.

The variation in the dimensions of one size of column has been reported by Hernandez and Martinez²⁸. Their results are summarized in the histogram in Figure 4.3. The measurements were made at five levels over the storey height of the column. At each level the width and thickness were measured at each face and at the centre line of the column. Seventeen columns were studied with a nominal cross section of 11.811 in. (30 cm.) by 19.685 in. (50 cm.). A mean variation was found to be + 0.15 in., that is, the width or thickness averaged 0.15 in. larger than the specified value with a standard deviation of 0.157 in.. A normal distribution also describes the variation in column dimensions reported by Hernandez and Martinez²⁸.

Fiorato²³ has reported a mean deviation of 0.0118 in. (0.3 mm.) to 0.276 in. (7.0 mm.) with a standard deviation ranging from 0.063 in. (1.6 mm.) to 0.154 in. (3.9 mm.) for precast beams and columns ranging in size from 7.87 in. (200 mm.) to 23.62 in. (600 mm.). These values are based on a collection and comparison of published data from field measurements, primarily from Sweden. These values may not be considered comprehensive but do give an indication of the variations which may occur in prefabricated structures.

As stated earlier, due to inconsistencies in measuring and reporting techniques, comparison of data on column dimensions from various researchers is difficult. The

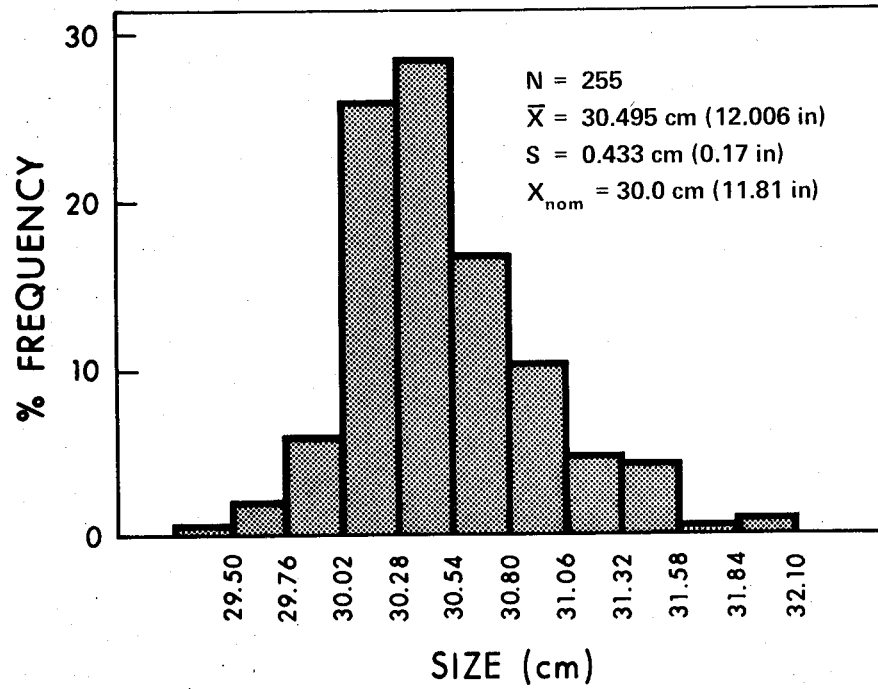
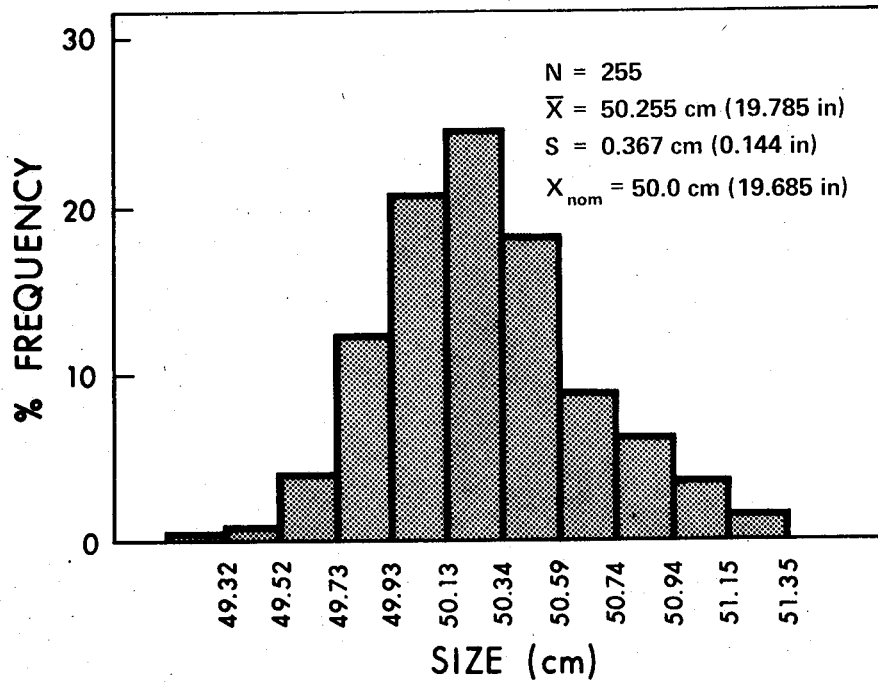


Figure 4.3 Histograms of Cross Section Dimensional Variation Reported by Hernandez and Martinez

majority of researchers are interested in actual construction tolerances in which a maximum and minimum tolerance is reported rather than a mean value and its standard deviation.

In this study a normal distribution was used to describe the variation in column dimensions with a mean value of + 0.06 in. and a standard deviation of 0.28 in.. Tso and Zelman's⁶⁹ results were used since they are based on North American data and are based on a larger sample size than that obtained by Hernandez and Martinez²⁸.

4.4 Reinforcing Steel Placement Variability

Redkop⁵³ has developed models describing the error in placing reinforcing steel in rectangular tied columns based on test data from measurements on several columns in several buildings. He describes the variation in steel placement with respect to the specified cover for the steel in the exterior layers and the specified position for the interior steel. The error in steel placement may be described by the normal probability distribution. Redkop⁵³ observed that the placement error was a function of the column size as well as construction practices. Since statistical data available does not suggest a complicated relationship, a linear relationship between column size and placement error was assumed with a normal distribution of scatter.

Based on Redkop's⁵³ data the error in placement of the

interior steel may be described with:

$$e_n = 0.04 \text{ in.}$$

$$\sigma = 0.2035 + 0.0329 h \quad (4.7)$$

The placement of the steel in the exterior layers may be described with:

$$c_a = c_{sp} + 0.250 + 0.0039 h \quad (4.8)$$

$$\sigma = 0.166$$

where:

e_n = placement error of interior steel in inches.

σ = standard deviation in inches.

h = column dimension perpendicular to the neutral axis.

c_a = actual cover of exterior steel in inches.

c_{sp} = specified cover of exterior steel in inches.

Based on Redkop's⁵³ data the mean variation in concrete cover of the exterior steel is + 0.315 in., that is, the actual cover on the average is 0.315 in. larger than the specified cover, with a standard deviation of 0.166 in.. Hernandez and Martinez report a mean variation of + 0.473 in. with a standard deviation of 0.13 in.. The smaller standard deviation of the Mexican data is due to measurements being taken only from one size of column whereas the measurements

reported by Redkop⁵³ were taken from various sizes of columns. Figure 4.4 is a histogram summarizing the results of concrete cover reported by Hernandez and Martinez¹⁷. The normal distribution may be used to describe the variation in the concrete cover for both sets of measurements.

In this study the error in steel placement was described by Equations 4.7 and 4.8 with a normal distribution. Negative cover is not a problem since with 1 1/2 in. nominal cover negative cover does not occur before the value of cover is the mean value minus 10.54 standard deviations. The probability of the value of cover being the mean value minus eight standard deviations is approximately 6.22×10^{-6} .

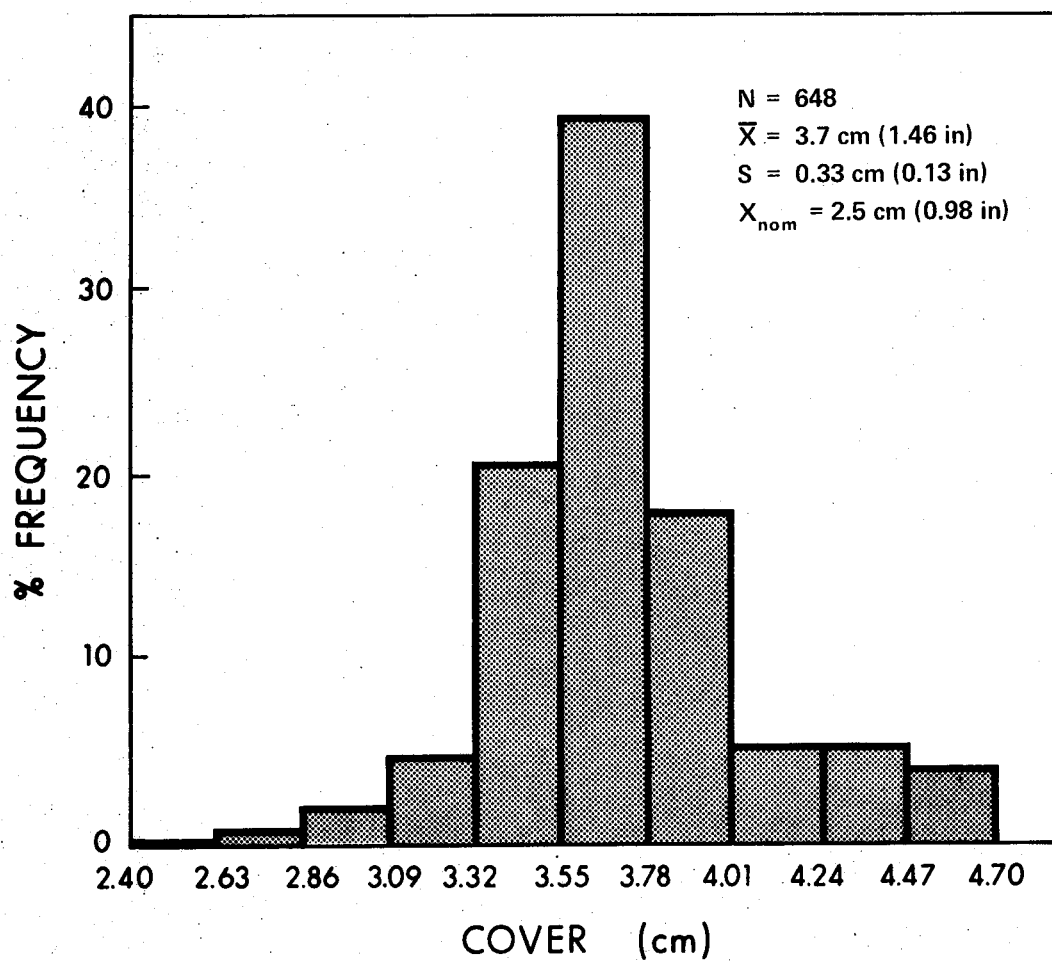


Figure 4.4 Histogram of Variation in Concrete Cover Reported by Hernandez and Martinez

CHAPTER V
THE MONTE CARLO STUDY

5.1 Size of Columns and Reinforcement Studied

For this study the size of columns and reinforcement selected was based on a limited study of columns in existing structures. A column take-off was done on five buildings including a high rise office building, a parking garage, a university building, a hospital and an industrial type building.

Figure 5.1 is a histogram of the frequency of column size vs. column size. This histogram indicates that the majority of columns are 24 in. or smaller. The high percentage of columns in the 52 in. to 56 in. range is due to the small number of buildings studied in which one was a high rise with large columns throughout. From the histogram of column sizes the 12 in. column and the 24 in. column were taken as representative of the smaller and larger sizes of columns.

Representative reinforcing steel percentages were chosen in the same manner as the column sizes. Figure 5.2 is a histogram of the reinforcing steel percentage used in all columns. Figures 5.3 through 5.5 are histograms of steel percentages used in the various sizes of columns. From these histograms it can be seen that the most commonly used steel percentage ranges from 1% to 3%. Based on these histograms a

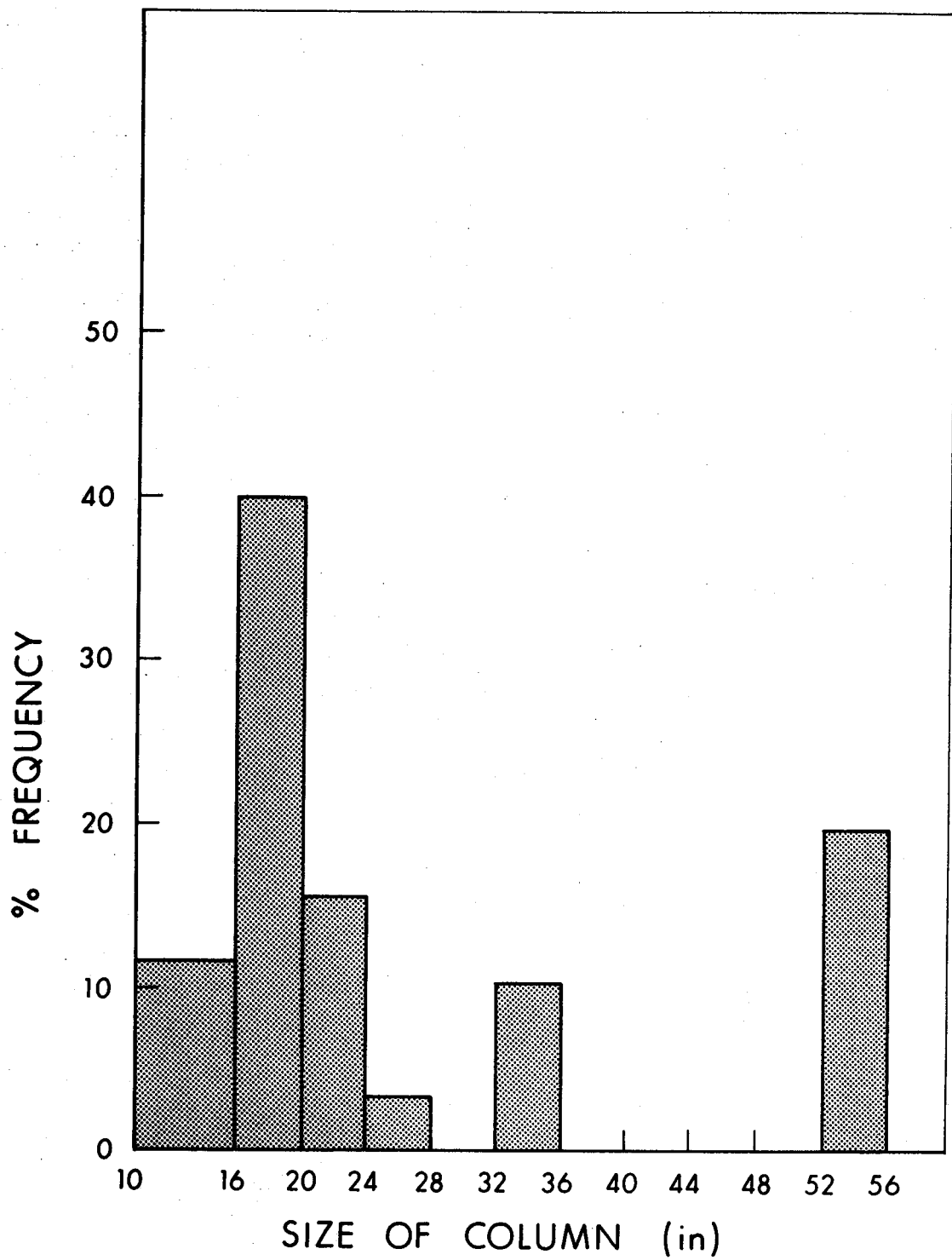


Figure 5.1 Histogram of the Frequency of Column Sizes vs. Column Size

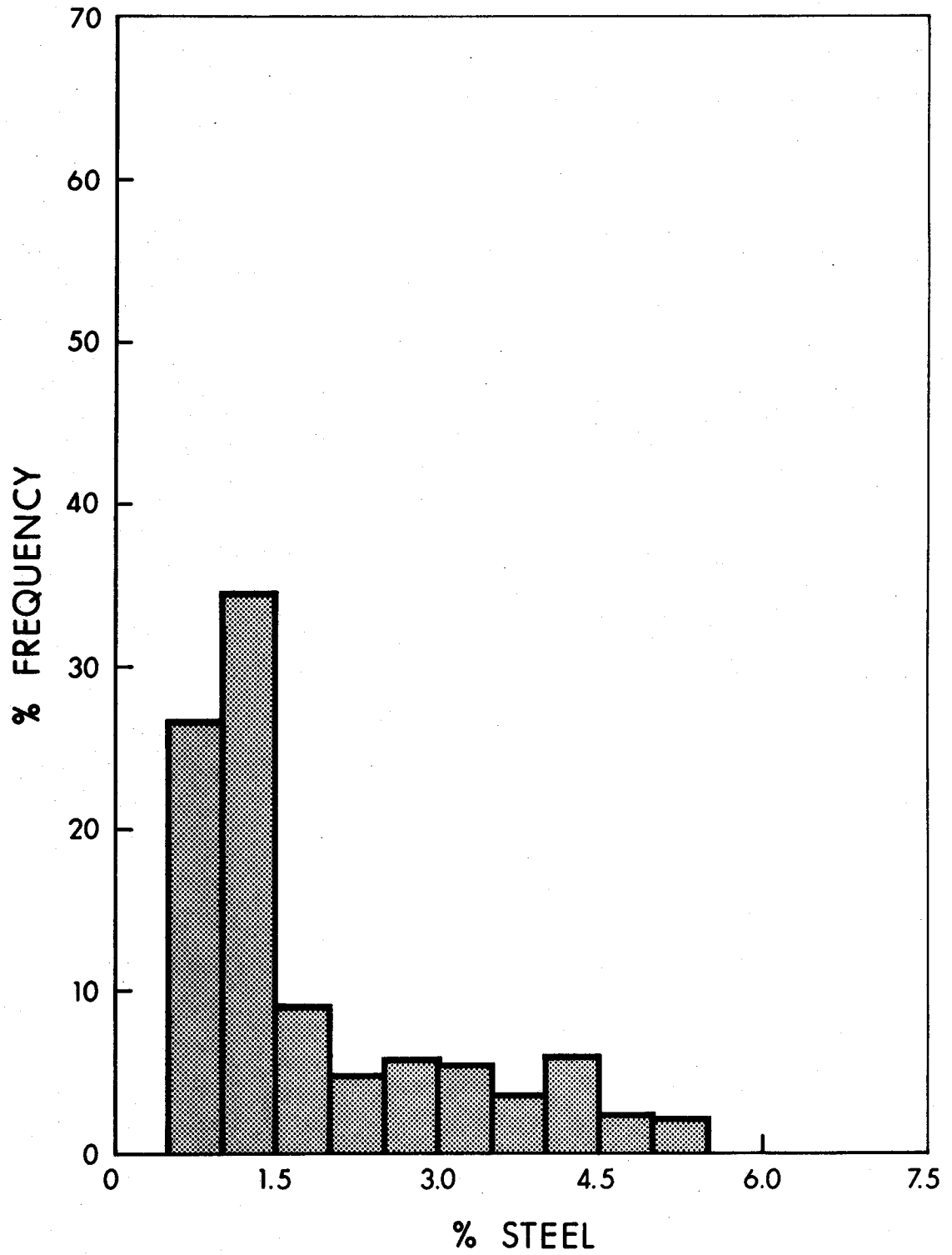


Figure 5.2 Histogram of the Percentage of Reinforcing Steel in All Columns

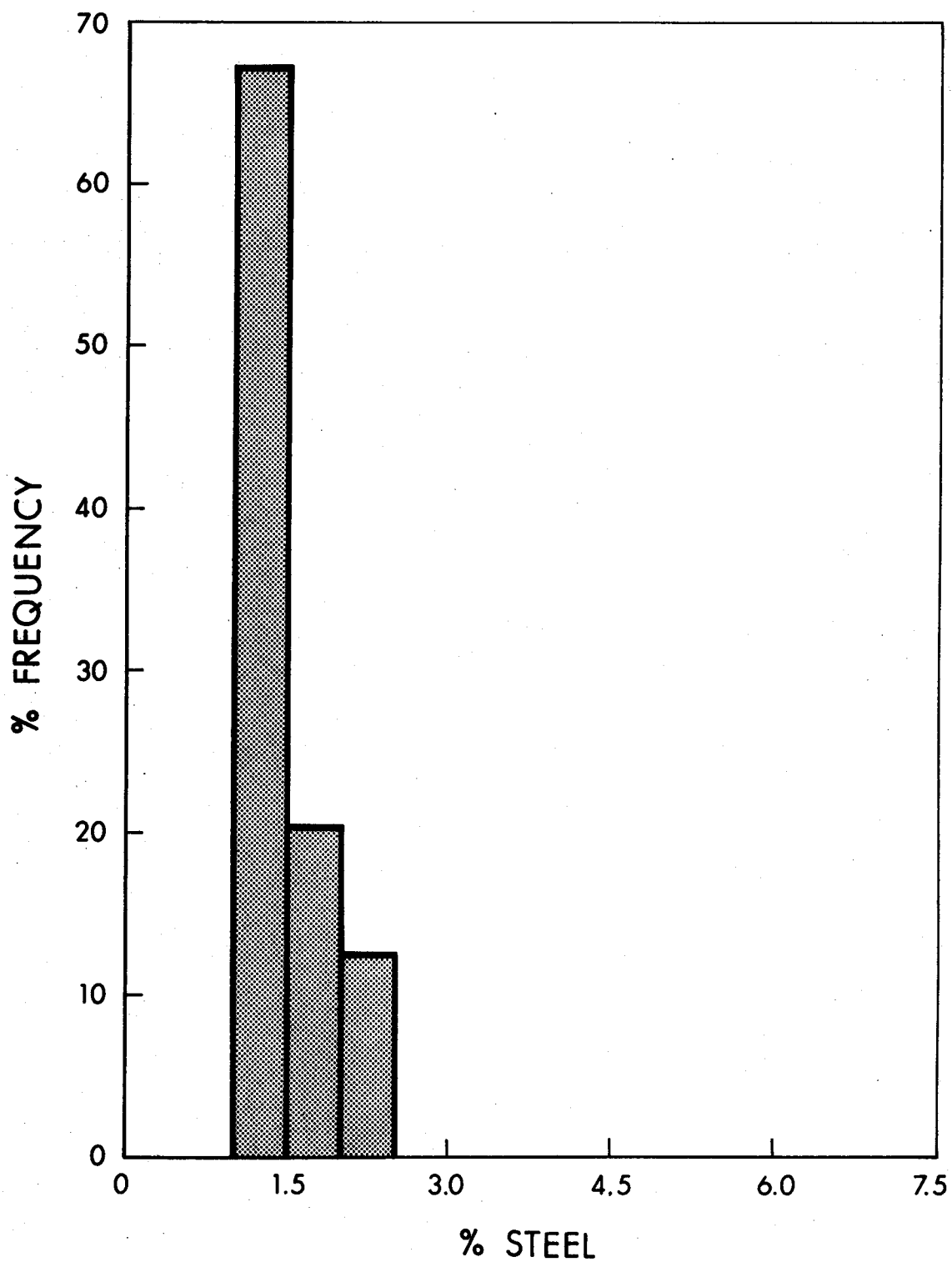


Figure 5.3 Histogram of the Percentage of Reinforcing Steel in Columns Less Than 16 in.

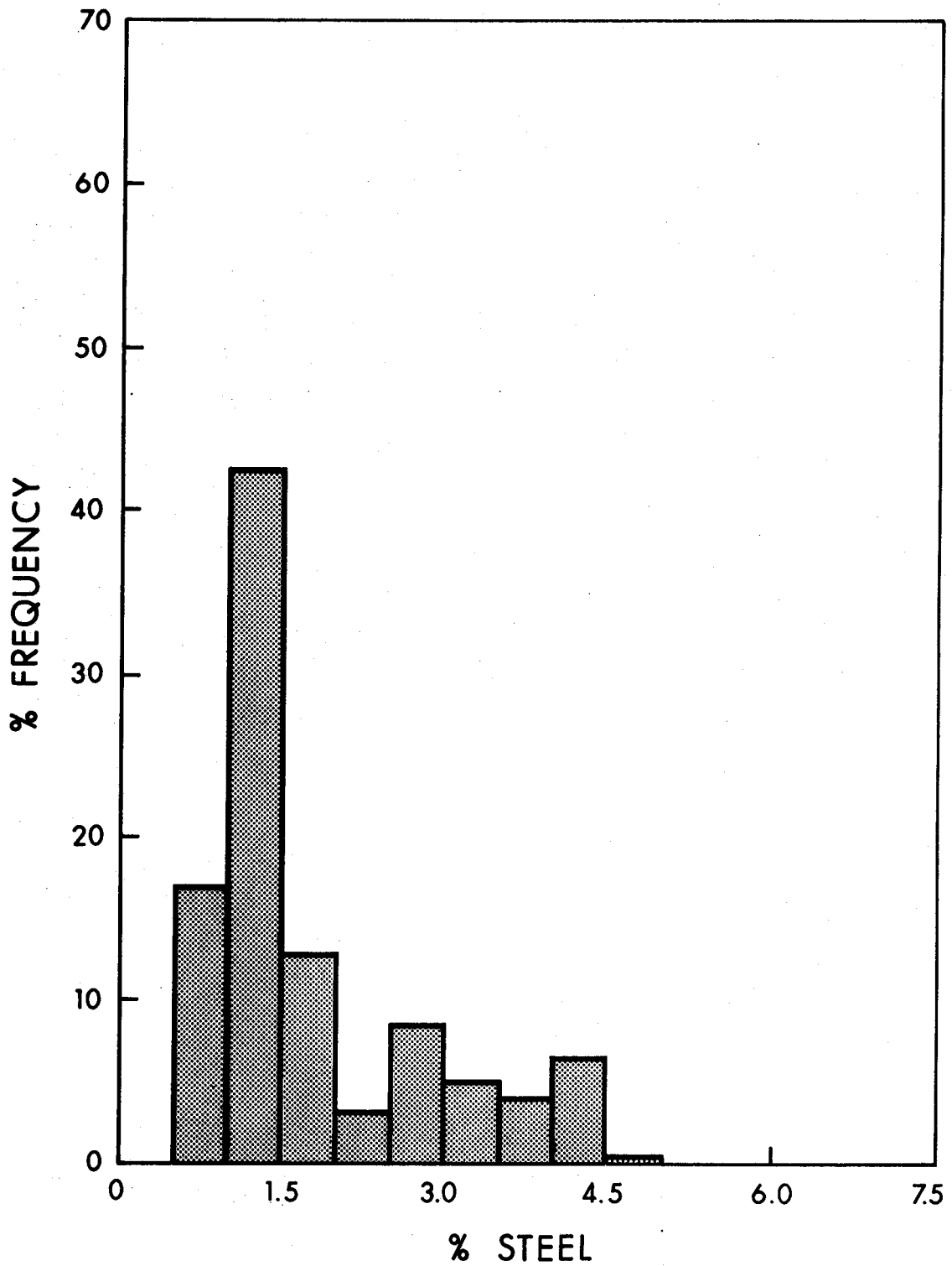


Figure 5.4 Histogram of the Percentage of Reinforcing Steel in Columns 16 in. to 24 in.

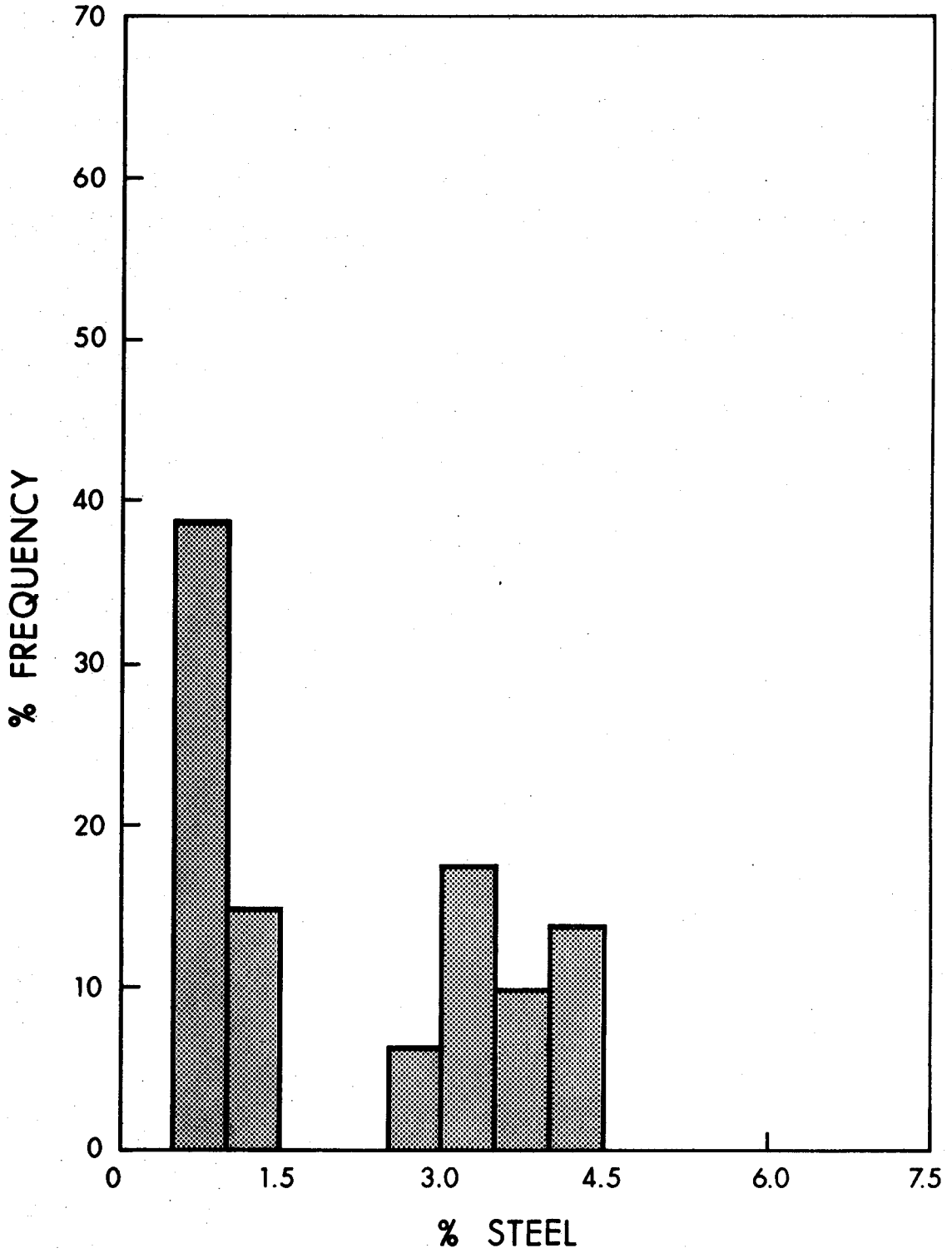


Figure 5.5 Histogram of the Percentage of Reinforcing Steel in Columns 24 in. to 36 in.

steel percentage of 1% was chosen for a lower limit and a steel percentage of 3% was chosen for an upper limit.

The final column cross sections chosen are shown in Figure 5.6. The basic column was 12 in. by 12 in. with a nominal steel percentage of 1%. A 24 in. by 24 in. column was chosen to have a low variability of strength with a nominal steel percentage of 3%. The nominal or designer's concrete and steel strengths were 3000 psi. and 40000 psi. respectively. These strengths and properties were chosen to get an estimate of the upper and lower bounds of the variabilities.

Interaction diagrams for the two sections are presented in Figures 5.11 and 5.12 and will be discussed more fully in Section 5.4. The balanced eccentricity, e_b/h , was 0.4 for the 12 in. column and 0.5 for the 24 in. column. The columns are fully described in Appendix B with their nominal properties and the mean values and standard deviations of the variables affecting column strength.

5.2 Size of Sample Studied

For this study a sample size was required which would give reasonable results compared to a large sample size without using an excessive amount of computer time. Sample sizes of 1000, 500 and 200 were used to determine the smallest practical sample size.

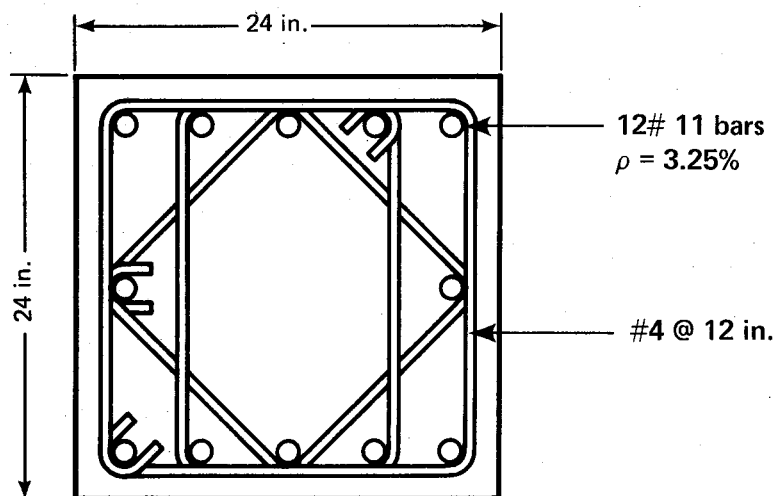
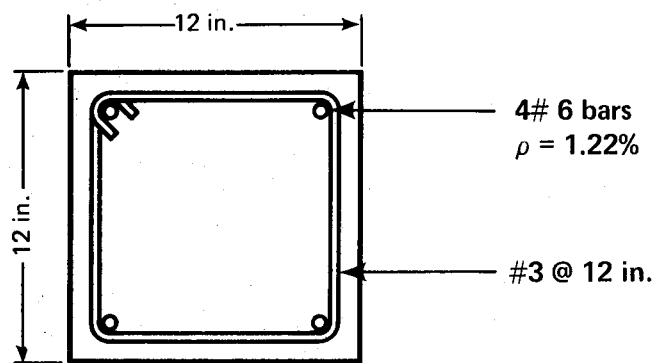


Figure 5.6 Final Column Cross Sections Studied

Figure 5.7 is a plot of the mean value of $P_{theory}/PACI$ vs. e/h for each sample size. The mean value is practically independent of the sample size so that any of the sample sizes could be used to determine the mean value of $P_{theory}/PACI$.

Figure 5.8 is a plot of coefficient of variation of the ratio $P_{theory}/PACI$ vs. e/h for the three sample sizes. The coefficient of variation for the sample size of 500 is practically the same as the coefficient of variation for a sample size of 1000 over the range of e/h less than 1.0. Since a good correlation was found between the sample size of 500 and the sample size of 1000 below an e/h value of 1.0 the sample size of 500 was acceptable when the mean and coefficient of variation were needed as output.

Figure 5.9 is a plot of the coefficient of skewness of the ratio of $P_{theory}/PACI$ vs. e/h for the three sample sizes. The coefficient of skewness for a sample size of 500 is not significantly different from the coefficient of skewness for a sample size of 1000.

Tables 5.1 through 5.4 are tables of comparison of the mean values, coefficients of variation, coefficients of skewness and kurtosis of the ratio of $P_{theory}/PACI$ for sample sizes of 200, 500 and 1000.

All the tables and graphs of comparison indicate no meaningful increase in accuracy in using a sample size of

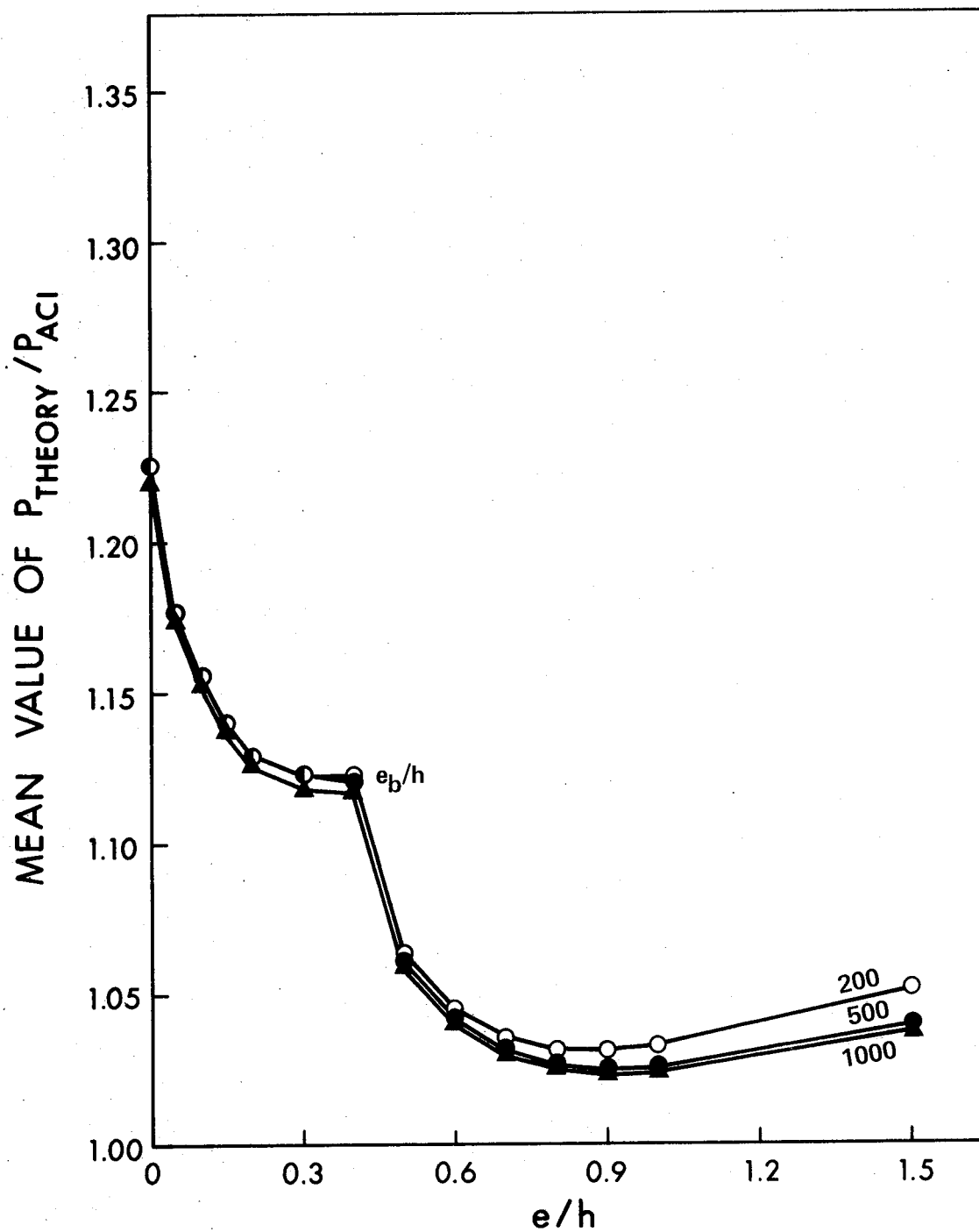


Figure 5.7 Mean Value of the Ratio P_{theory}/P_{ACI} vs. e/h for Sample Sizes of 200, 500 and 1000 for a 12 in. Square Column and Modified Log-normal Steel Strength Distribution

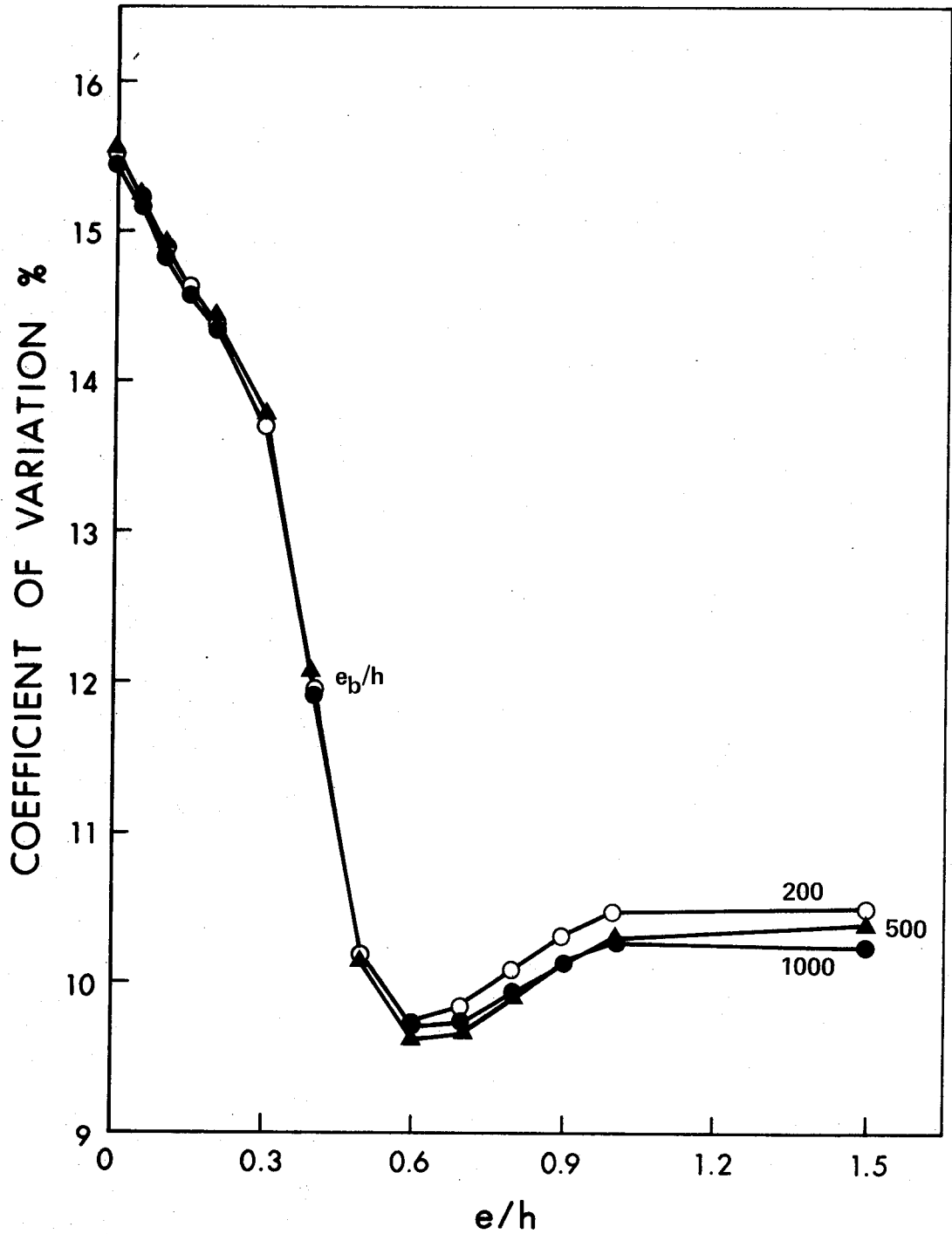


Figure 5.8 Coefficient of Variation of the Ratio P_{theory}/P_{ACI} vs. e/h for Sample Sizes of 200, 500 and 1000 for a 12 in. Square Column and Modified Log-normal Steel Strength Distribution

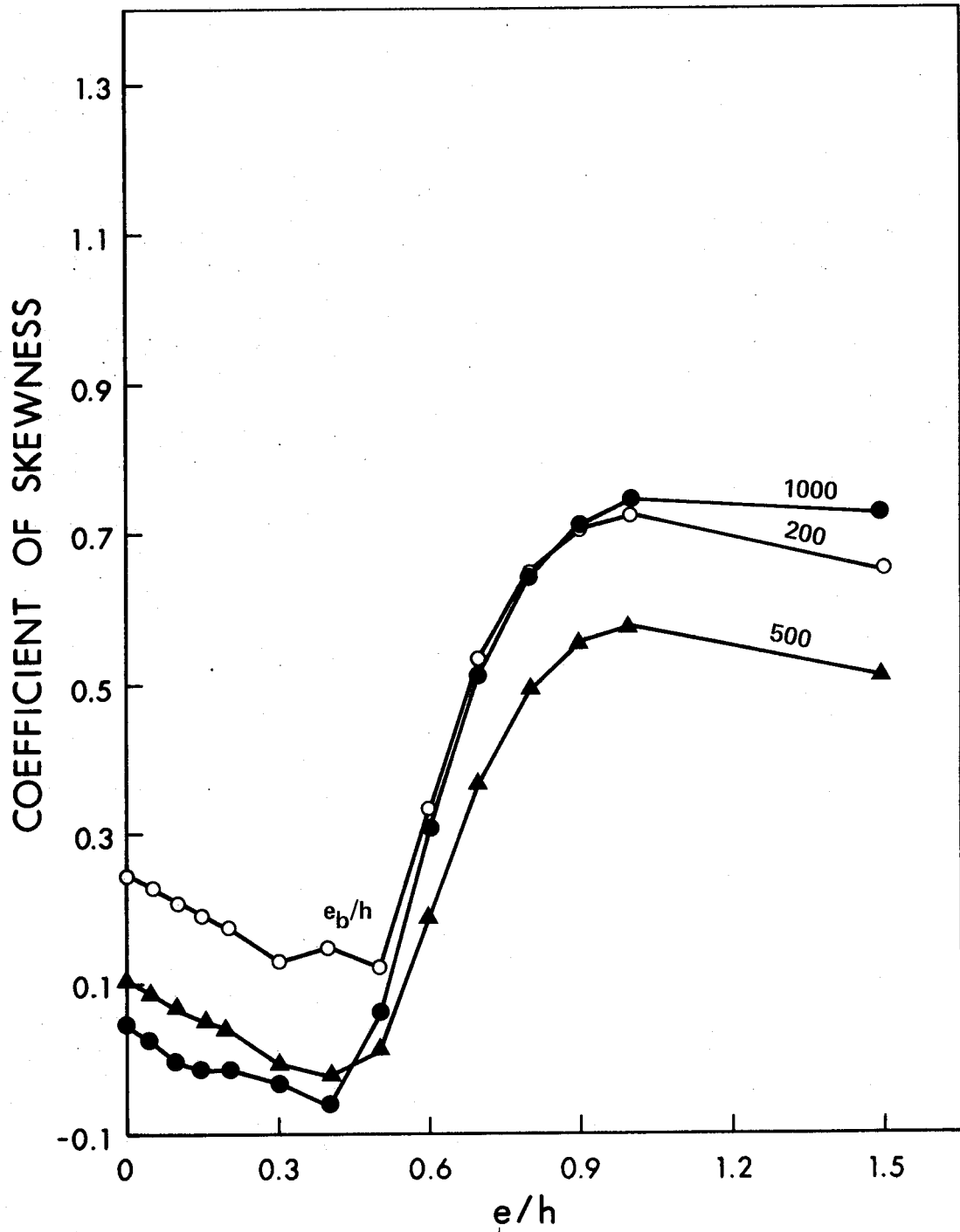


Figure 5.9 Coefficient of Skewness of the Ratio P_{theory}/P_{ACI} vs. e/h for Sample Sizes of 200, 500 and 1000 for a 12 in. Square Column and Modified Log-normal Steel Strength Distribution

Table 5.1

Comparison of the Mean Value of the Ratio P_{theory}/P_{ACI} for
Sample Sizes of 200, 500 and 1000

Sample Size e/h	200	500	1000
0.0	1.22535	1.22497	1.22010
0.05	1.17705	1.17698	1.17245
0.10	1.15581	1.15575	1.15143
0.15	1.13981	1.13985	1.13559
0.20	1.12921	1.12937	1.12505
0.30	1.12255	1.12239	1.11790
0.40	1.12228	1.12039	1.11645
0.50	1.06353	1.06030	1.05756
0.60	1.04519	1.04139	1.03926
0.70	1.03560	1.03100	1.02921
0.80	1.03162	1.02598	1.02434
0.90	1.03116	1.02439	1.02278
1.00	1.03285	1.02498	1.02334
1.50	1.05147	1.03976	1.03766
∞	1.02563	1.01598	1.01551

Table 5.2

Comparison of the Coefficient of Variation of the Ratio
 P_{theory}/P_{ACI} for Sample Sizes of 200, 500 and 1000

Sample Size e/h	200	500	1000
0.0	0.15521	0.15491	0.15549
0.05	0.15230	0.15159	0.15234
0.10	0.14802	0.14802	0.14871
0.15	0.14625	0.14549	0.14619
0.20	0.14394	0.14352	0.14428
0.30	0.13696	0.13693	0.13798
0.40	0.11955	0.11908	0.12018
0.50	0.10186	0.10190	0.10117
0.60	0.09741	0.09705	0.09620
0.70	0.0840	0.0733	0.09661
0.80	0.10085	0.09929	0.09889
0.90	0.10313	0.10127	0.10124
1.00	0.10470	0.10266	0.10295
1.50	0.10497	0.10241	0.10396
∞	0.10744	0.10590	0.10441

Table 5.3

Comparison of the Coefficient of Skewness of the Ratio
 P_{theory}/P_{ACI} for Sample Sizes of 200, 500 and 1000

Sample Size e/h	200	500	1000
0.0	0.24511	0.10136	0.04325
0.05	0.22741	0.08661	0.02044
0.10	0.20932	0.06424	-0.00657
0.15	0.19112	0.04905	-0.01670
0.20	0.17406	0.03912	-0.01357
0.30	0.13074	-0.00716	-0.03286
0.40	0.14910	-0.02379	-0.06445
0.50	0.12192	-0.00978	0.05817
0.60	0.33447	0.18334	0.30627
0.70	0.53488	0.36708	0.51101
0.80	0.65065	0.49013	0.64057
0.90	0.70518	0.55422	0.71160
1.00	0.72474	0.57855	0.74623
1.50	0.65006	0.50968	0.72784
∞	0.82210	0.68282	0.81786

Normal and log-normal distributions have coefficients of skewness of 0.0 and 0.5 to 1.5 respectively.

Table 5.4

Comparison of the Measure of Kurtosis of the Ratio
 P_{theory}/P_{ACI} for Sample Sizes of 200, 500 and 1000

Sample Size e/h	200	500	1000
0.0	3.43756	3.09968	3.05566
0.05	3.49080	3.11334	3.07339
0.10	3.49196	3.11702	3.08846
0.15	3.46624	3.10238	3.08172
0.20	3.42402	3.07604	3.05890
0.30	3.41098	3.03726	3.03096
0.40	3.39169	3.13717	3.16894
0.50	3.45578	3.18934	3.30727
0.60	3.28053	3.10547	3.50337
0.70	3.15174	3.11376	3.72044
0.80	3.10245	3.15105	3.88468
0.90	3.09217	3.16791	3.99297
1.00	3.09422	3.15747	4.06460
1.50	3.07980	2.96226	4.01951
∞	3.19293	3.09842	4.08547

A normal distribution has a Kurtosis of 3.0.

1000 over a sample size of 500. On this basis sample size of 500 was used for all subsequent calculations.

5.3 Results of The Monte Carlo Simulation

5.3.1 General

In this Monte Carlo study the relationship between the theoretical axial load-moment interaction diagram and the ACI axial load-moment interaction diagram was determined. This relationship was calculated using the Monte Carlo Technique to give the mean ratio of the theoretical strength divided by the ACI strength along with its standard deviation at various e/h values. From the mean ratio, the standard deviation and the type of distribution an understrength or ϕ factor was calculated.

To aid in the development of an understrength factor the effect of the variation in concrete strength, steel strength, cross section dimensions and location of the reinforcing steel was studied. In addition the effect of the type of distribution of steel strength used was studied using a normal distribution and a modified log-normal distribution.

5.3.2. The Effect of Steel Strength Distribution Used

The effect on the strength of the column cross section

of the type of distribution of steel strength was studied using a normal and a log-normal distribution of steel strength. Both types of distribution can be fitted to the data on steel strength as shown in Appendix A. Tables 5.5 through 5.8 are tables of comparison of the mean values, coefficients of variation, coefficients of skewness and measure of kurtosis of the ratio P_{theory}/P_{ACI} for calculations based on steel strength normally distributed and steel strength which follows a modified log-normal distribution.

The distribution assumed for the variation in the steel strength did not significantly affect the mean ratio of the theoretical strength to the ACI strength as shown in Table 5.5 but did affect the distribution of the ratio in the tension failure region of the interaction diagram. When the modified log-normal steel strength distribution was used, the distribution of the ratio of theoretical strength to the ACI strength approached a log-normal distribution for values of axial loads below the balance point. If a normal distribution of the steel strength were used, this ratio was normally distributed. This is shown by the coefficient of skewness given in Table 5.7. For normally distributed steel yield strengths the coefficient of skewness remained close to zero throughout corresponding to a normal distribution. With the log-normal assumption the coefficient of skewness approaches 1.0 for tension failures corresponding to a log-normal distribution, (See also Figure 5.9). The use of the

Table 5.5

Comparison of the Mean Value of the Ratio P_{theory}/P_{ACI} for a Normal and a Modified Log-normal Steel Strength Distribution

Distribution Type e/h	Normal	Mod. Log-normal
0.0	1.22495	1.22497
0.05	1.17712	1.17698
0.10	1.15605	1.15575
0.15	1.14012	1.13985
0.20	1.12946	1.12937
0.30	1.12212	1.12239
0.40	1.12012	1.12039
0.50	1.05996	1.06030
0.60	1.04163	1.04139
0.70	1.03157	1.03100
0.80	1.02663	1.02598
0.90	1.02495	1.02439
1.00	1.02535	1.02498
1.50	1.03889	1.03976
∞	1.01677	1.01598

Table 5.6

Comparison of the Coefficient of Variation of the Ratio P_{theory}/P_{ACI} for a Normal and a Modified Log-normal Steel Strength Distribution

Distribution Type e/h	Normal	Mod. Log-normal
0.0	0.15464	0.15441
0.05	0.15189	0.15159
0.10	0.14831	0.14802
0.15	0.14576	0.14549
0.20	0.14378	0.14352
0.30	0.13729	0.13693
0.40	0.12078	0.11908
0.50	0.10391	0.10190
0.60	0.10051	0.09705
0.70	0.10183	0.09733
0.80	0.10437	0.09929
0.90	0.10658	0.10127
1.00	0.10798	0.10266
1.50	0.10689	0.10241
∞	0.10807	0.10590

Table 5.7

Comparison of the Coefficient of Skewness of the Ratio P_{theory}/P_{ACI} for a Normal and a Modified Log-normal Steel Strength Distribution

Distribution Type e/h	Normal	Mod. Log-normal
0.0	0.09843	0.10136
0.05	0.08254	0.08661
0.10	0.05519	0.06424
0.15	0.03722	0.04905
0.20	0.02797	0.03912
0.30	-0.00223	-0.00716
0.40	-0.04916	-0.02379
0.50	-0.10565	0.00978
0.60	-0.08048	0.18334
0.70	-0.03075	0.36708
0.80	0.00709	0.49013
0.90	0.02321	0.55422
1.00	0.02142	0.57855
1.50	-0.03508	0.50968
∞	0.04325	0.68282

Table 5.8

Comparison of the Measure of Kurtosis of the Ratio P_{theory}/P_{ACI} for a Normal and a Modified Log-normal Distribution of Steel Strength

Distribution Type e/h	Normal	Mod. Log-normal
0.0	3.10221	3.09968
0.05	3.11561	3.11334
0.10	3.12425	3.11702
0.15	3.10326	3.10238
0.20	3.06481	3.07604
0.30	3.04098	3.03726
0.40	3.13422	2.13717
0.50	3.18301	3.18934
0.60	2.95718	3.10547
0.70	2.81651	3.11376
0.80	2.76677	3.15105
0.90	2.74429	3.16791
1.00	2.72148	3.15747
1.50	2.65068	2.96226
∞	2.69439	3.09842

modified log-normal steel strength distribution resulted in a larger ϕ factor at the 1% level of probability of failure than that for the normal distribution of steel strength in the tension region of the interaction diagram. The calculation of this term is discussed in Section 5.5.

The type of steel strength distribution used did not significantly affect the calculated value of the ϕ factor at the 1% level of probability of failure in the compression failure region of the interaction diagram. The distribution of the ratio of the theoretical strength to the ACI strength in the compression failure region followed a normal distribution for both types of steel strength distribution. This may be explained by the failure in the compression region being dependent on the concrete strength rather than the steel strength.

5.3.3 The Effect of The Concrete Strength Variation

The effect of the coefficient of variation of the concrete cylinder strength was studied by keeping all other variables at their mean values and using a cylinder strength variation of 10%, 15% and 20%. The overall coefficients of variation of in-situ strength were 13.6%, 17.6% and 22% as computed per Eqn. 4.6 in Section 4.1.6. Tables 5.9 through 5.11 are tables of comparison the mean values, coefficients of variation and skewness of the ratio P_{theory}/P_{ACI} for various values of e/h and cylinder strength coefficients of

Table 5.9

Comparison of the Mean Value of the Ratio P_{theory}/P_{ACI} for Concrete Cylinder Strength Coefficients of Variation of 10%, 15% and 20%

Coefficient of Variation e/h	10%	15%	20%
0.0	1.18146	1.22622	1.28386
0.05	1.13652	1.17774	1.23088
0.10	1.11642	1.15546	1.20598
0.15	1.10207	1.14005	1.18897
0.20	1.09345	1.13111	1.17910
0.30	1.09010	1.12616	1.17157
0.40	1.08946	1.11784	1.15384
0.50	1.04264	1.06022	1.08408
0.60	1.03276	1.04554	1.06304
0.70	1.02775	1.03794	1.05140
0.80	1.02602	1.03474	1.04549
0.90	1.02646	1.03426	1.04316
1.00	1.02829	1.03544	1.04310
1.50	1.04443	1.04915	1.05515
∞	1.01756	1.02138	1.02887

Table 5.10

Comparison of the Coefficient of Variation of the Ratio of P_{theory}/P_{ACI} for Concrete Cylinder Strength Coefficients of Variation of 10%, 15% and 20%

Coefficient of Variation e/h	10%	15%	20%
0.0	0.11363	0.14790	0.18607
0.05	0.11066	0.14377	0.18100
0.10	0.10804	0.14022	0.17669
0.15	0.10695	0.13842	0.17369
0.20	0.10667	0.13762	0.17215
0.30	0.10229	0.13189	0.16487
0.40	0.08303	0.10936	0.13953
0.50	0.05665	0.07589	0.10000
0.60	0.04427	0.05873	0.07803
0.70	0.03672	0.04840	0.06355
0.80	0.03191	0.04191	0.05381
0.90	0.02881	0.03789	0.04742
1.00	0.02679	0.03551	0.04337
1.50	0.02844	0.03400	0.03872
∞	0.02689	0.03184	0.03738

Table 5.11

Comparison of the Coefficient of Skewness of the Ratio of P_{theory}/P_{ACI} for Concrete Cylinder Strength Coefficients of Variation of 10%, 15% and 20%

Coefficient of Variation e/h	10%	15%	20%
0.0	0.02523	0.02478	0.02786
0.05	-0.01578	-0.01428	0.00366
0.10	-0.04927	-0.03626	-0.00627
0.15	-0.05004	-0.04489	-0.02282
0.20	-0.02722	-0.04231	-0.04249
0.30	-0.01351	-0.05370	-0.07949
0.40	-0.17206	-0.15911	-0.17109
0.50	-0.21277	-0.22505	-0.23879
0.60	-0.38463	-0.30449	-0.35791
0.70	-0.50581	-0.38219	-0.50237
0.80	-0.56889	-0.43285	-0.62403
0.90	-0.55617	-0.41673	-0.67631
1.00	-0.47411	-0.32853	-0.65730
1.50	0.09033	-0.05914	-0.51679
∞	0.26793	0.41395	0.39448

variation.

The mean value of the ratio P_{theory}/P_{ACI} increased in the compression failure region of the interaction diagram with increasing cylinder strength coefficient of variation. This increase may be explained by the increased mean concrete strength required by ACI 318-71 Section 4.2 to account for the increased coefficient of variation. There was no significant increase in the theoretical strength in the tension region due to the increased mean concrete strength. Again this may be explained by the compression failures depending on the concrete strength and the tension failures depending on the steel strength.

As the coefficient of variation of the concrete cylinder strength was increased the overall coefficient of variation of the ratio P_{theory}/P_{ACI} increased. Again the increase in overall coefficient of variation was greater in the compression region of the interaction diagram where the concrete strength has more effect on the cross section strength than in the tension failure region.

5.3.4 The Effect of The Variables Studied

The effect of the variation in concrete strength, steel strength, cross section dimensions and location of the reinforcing steel was determined for the 12 in. by 12 in. cross section with a nominal steel percentage of 1%. A

coefficient of variation of concrete cylinder strength of 15% was used for this study. Each variables effect was studied with all other variables at their mean value.

Figure 5.10 gives a graphical representation of the overall variation in cross section strength for various e/h values for each of the variables and for all the variables combined. The plot of standard deviation squared vs. e/h indicates the major component causing variation in cross section strength in the compression region of the interaction diagram is the variability in the concrete strength. The effect of the variability in the concrete strength becomes minimal in the tension failure region. This may be explained by the fact that the full strength of the concrete is not utilized in the tension failure region such that the high concrete strengths have no effect on the variability of the cross section strength.

The effect of the variability in the steel strength on the overall cross section strength variability is greater in the tension region where the steel strength controls the cross section capacity. The effect of the steel strength variability in the compression failure region is again minimal due to the concrete strength being the controlling factor.

The effect of the variability of the concrete strength and the steel strength are about the same at the balance point. This is to be expected since the failures in a

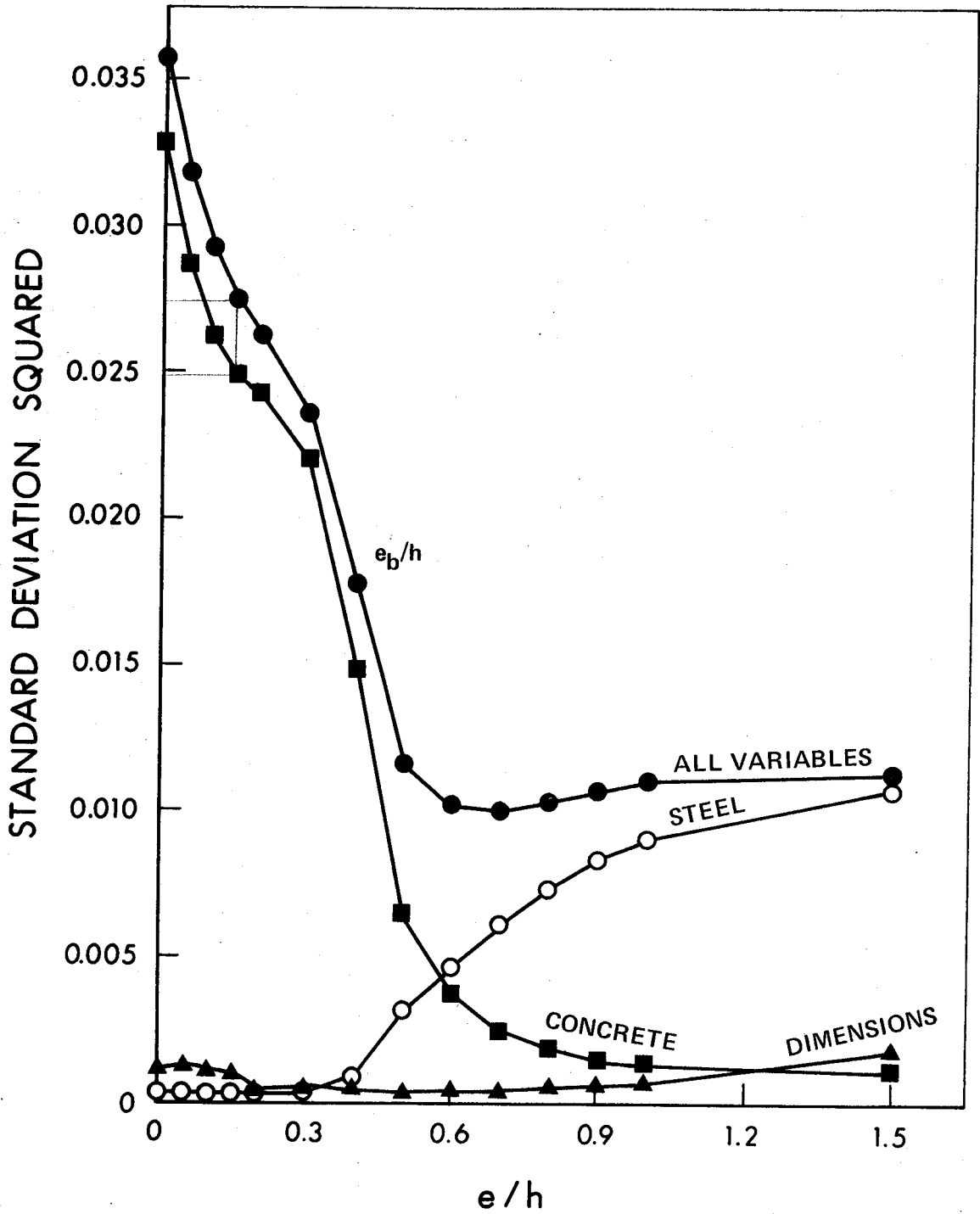


Figure 5.10 Standard Deviation Squared of the Ratio P_{theory}/P_{ACI} vs. e/h for the Variables Affecting Column Strength for a 12 in. Square Column and Modified Log-normal Steel Strength Distribution

randomly selected sample would depend on the concrete and steel strength equally at the balance point.

The effect of the variability in the cross section dimensions and the location of the steel was very small for both compression and tension failures. The most significant effect occurred for the cases of pure axial load and pure moment.

The total variability in the cross section strength may be closely approximated by the expression:

$$V_t^2 = V_{tc}^2 + V_{ts}^2 + V_{td}^2 \quad (5.1)$$

where V_t may be the total standard deviation or coefficient of variation and V_{tc} , V_{ts} and V_{td} are the standard deviation or coefficient of variation of the cross sectional strength if only the concrete strength, steel strength or the dimensions are varied separately.

5.4 Cross Section Strength

Figures 5.11 and 5.12 are plots of the interaction curves for the 12 in. and 24 in. columns based on a modified log-normal distribution of steel strength. The mean strength indicated is the mean strength calculated from a sample size of 500 using the Monte Carlo Technique and the theoretical calculation of cross section strength. The maximum and minimum strength curves are also calculated from the Monte Carlo calculations. The ACI ultimate strength is the cross

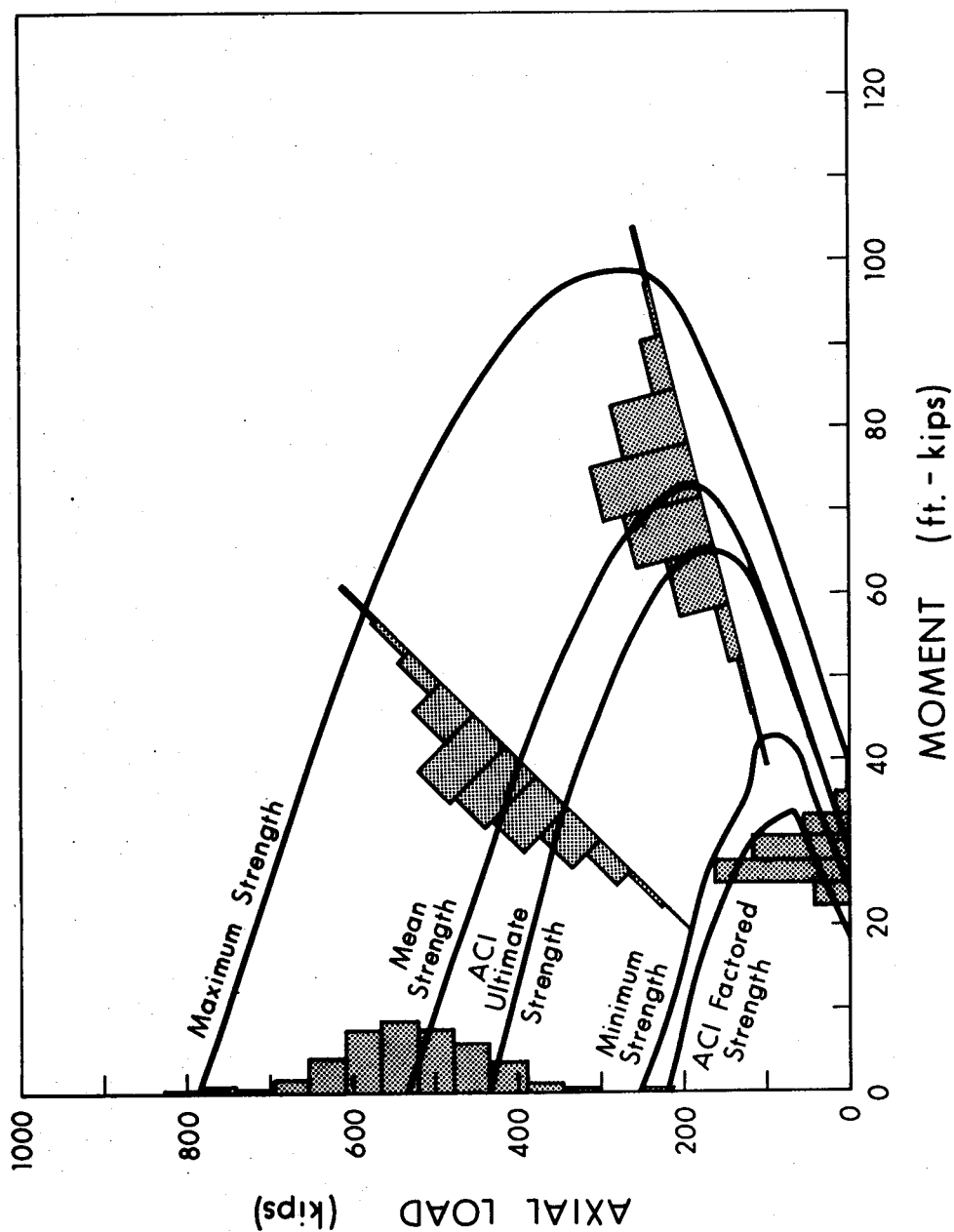


Figure 5.11 Dispersion of Strengths of an Eccentrically Loaded 12 in. Square Column

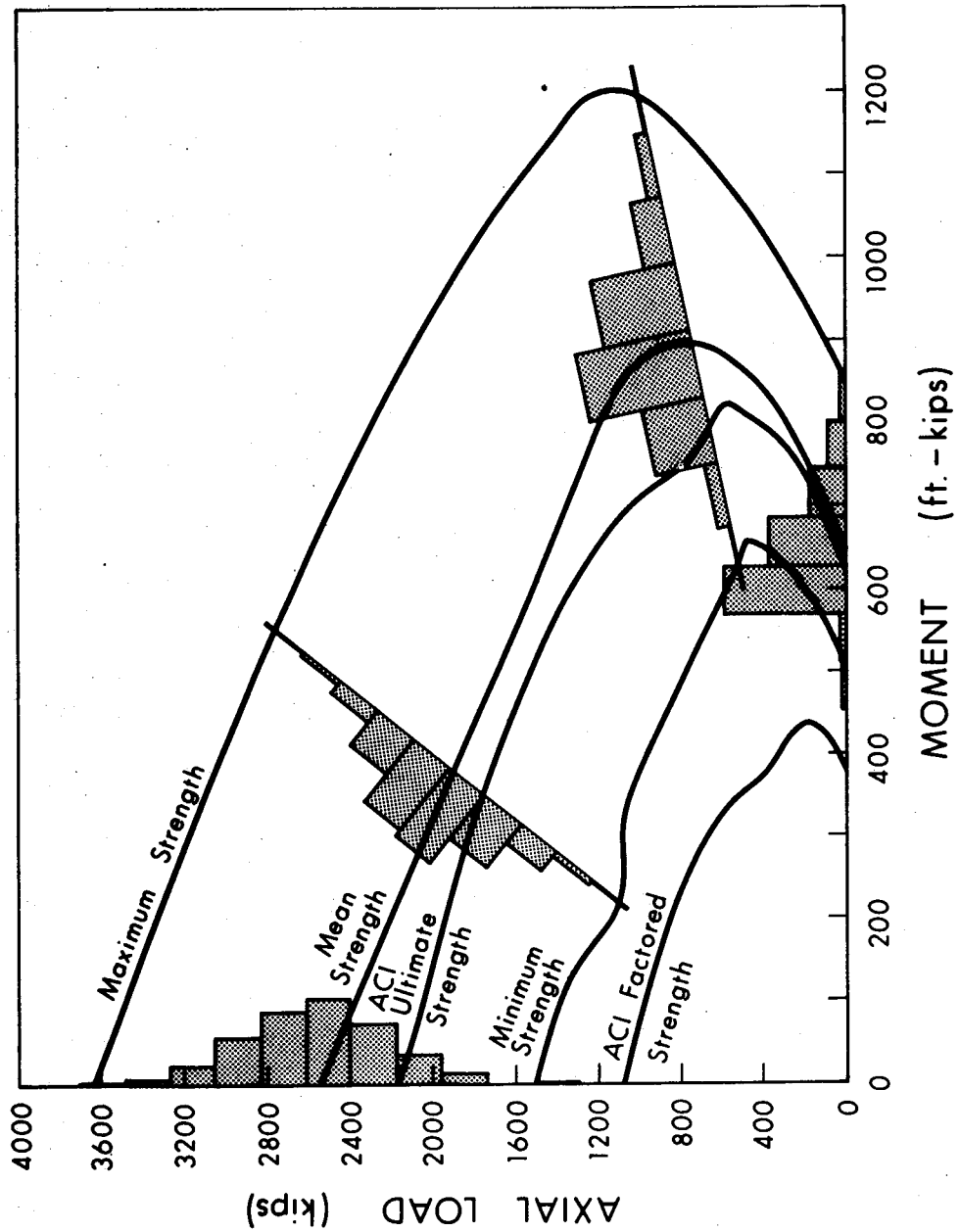


Figure 5.12 Dispersion of Strengths of an Eccentrically Loaded 24 in. Square Column

section capacity calculated using the ACI 318-71 Building Code. The ACI factored strength is the ACI ultimate strength divided by $1.4/0.7$ corresponding to the lowest possible load factor. The ACI factored strength corresponds to the normal service load conditions. The discrepancy in the mean strength of the 24 in. column immediately above the balance point is due to the reinforcing steel placement in the column cross section. As a result of the reinforcing steel at the centre of the cross section shifting from compression to tension steel the capacity of the section appears to increase to a second balance point but the first downturn of the curve is not a true representation of the capacity of the cross section.

The dispersion of cross section strength is plotted at selected values of e/h . In each case the dispersion of the cross section strength is a normal distribution for the compression failure region and a log-normal distribution for the tension failure region. At the balance point the dispersion of cross section strength may be represented equally well with either a normal or log-normal distribution.

Table 5.12 is a comparison of the mean value and coefficient of variation of P_{theory}/P_{ACI} for a sample size of 500 for the cross sections of 12 in. by 12 in. with 1% steel and 24 in. by 24 in. with 3% steel.

In the compression failure region the variation in the

strength of the 12 in. and the 24 in. columns are similar but the mean value of P_{theory}/P_{ACI} is larger for the 12 in. column. This is due to the higher dependence on the concrete strength. Since the ratio of the mean concrete strength to the nominal concrete strength is higher than the ratio of the mean steel strength to the nominal steel strength the capacity in the compression region increases for decreasing steel percentages relative to the ACI capacity.

The variability of the theoretical strength of the 24 in. by 24 in. column is greater than that of the 12 in. by 12 in. column in the tension region. This may be due to the increase in steel percentage from 1% to 3%. Also the mean value of the ratio P_{theory}/P_{ACI} is larger in the 24 in. column in the tension region due to the increased steel percentage.

Figures 5.13 through 5.16 are cumulative frequency plots of the ratio P_{theory}/P_{ACI} for the 12 in. and 24 in. columns at selected e/h values. A comparison of these and similar cumulative frequency plots for a normal and a log-normal dispersion of the ratio P_{theory}/P_{ACI} and the data in Tables 5.1 to 5.4 and 5.9 to 5.11 suggest that for compression failures the dispersion may be represented by the normal distribution and for tension failures the dispersion may be represented with a log-normal distribution.

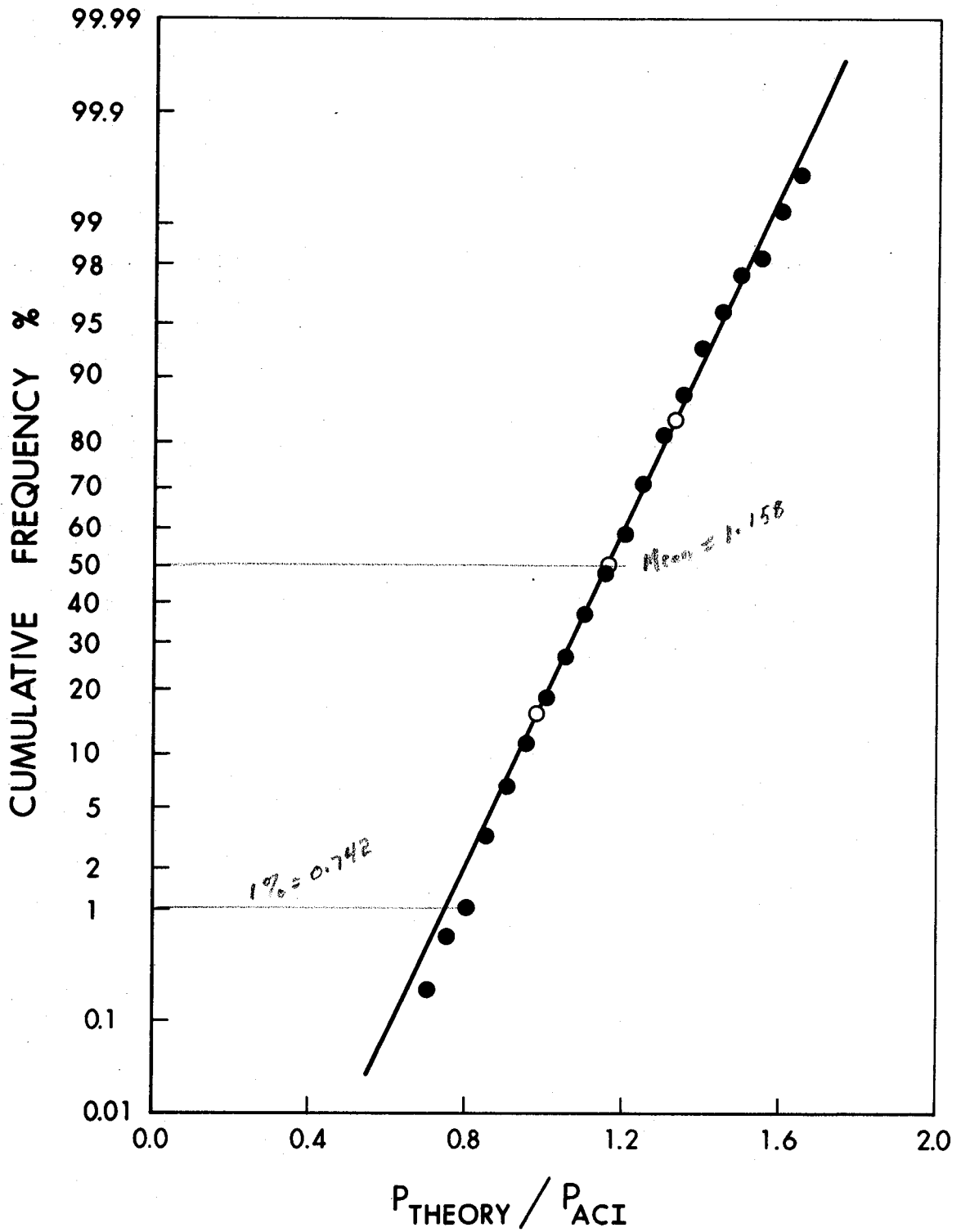


Figure 5.13 Normal Cumulative Frequency Plot of the Ratio P_{theory}/P_{ACI} for the 12 in. Column, $e/h = 0.10$

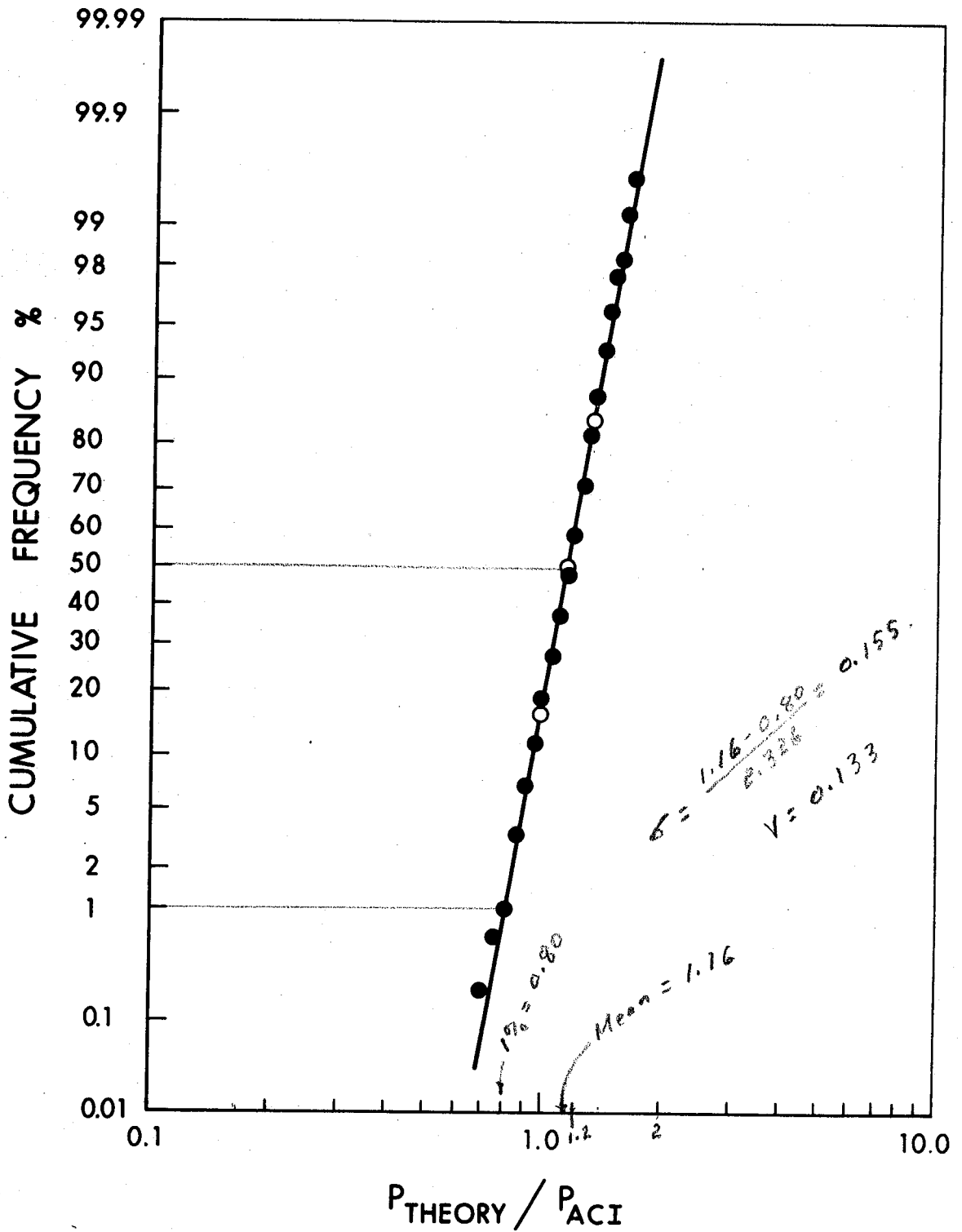


Figure 5.14 Log-normal Cumulative Frequency Plot of the Ratio P_{theory}/P_{ACI} for the 12 in. Column, $e/h = 0.10$

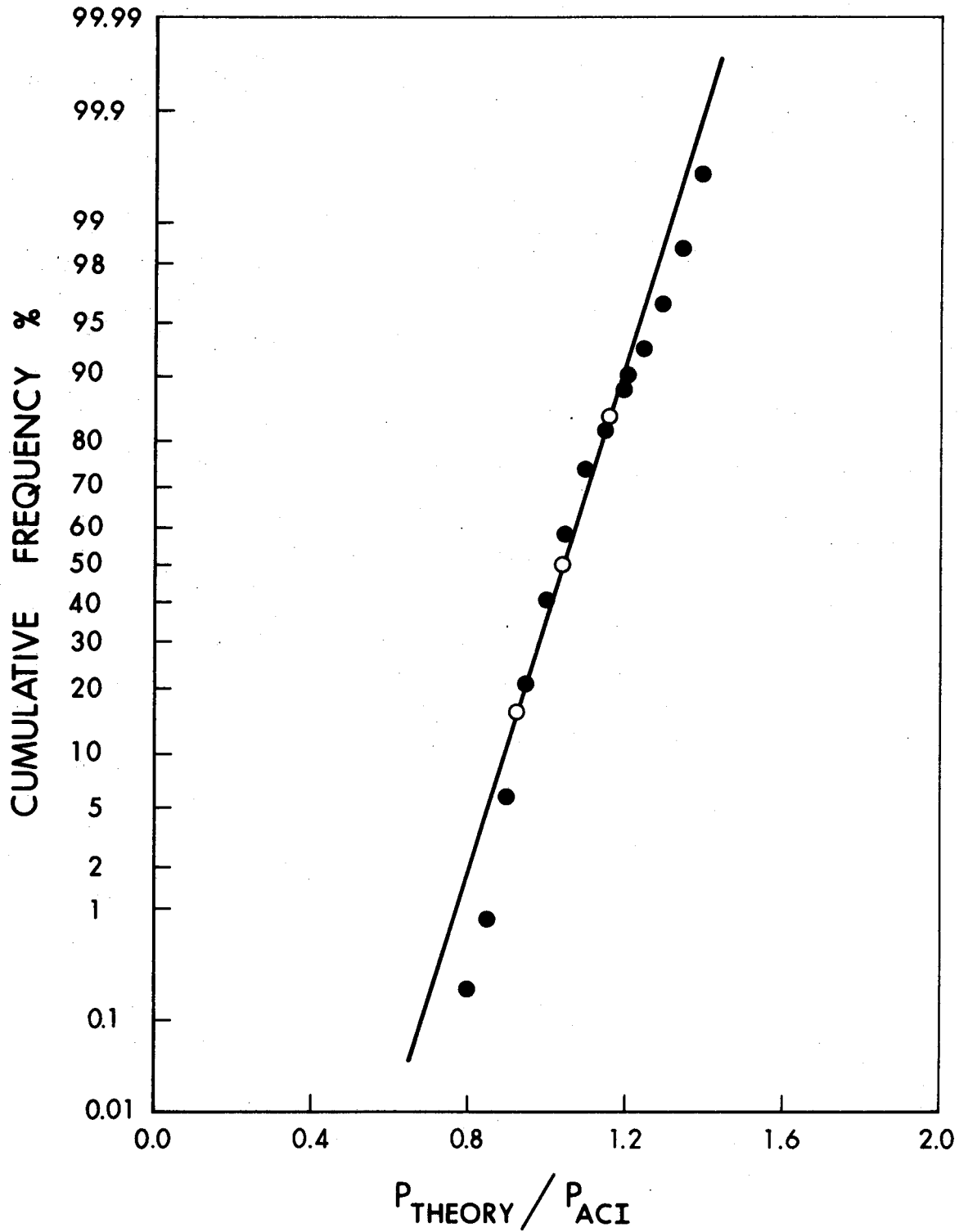


Figure 5.15 Normal Cumulative Frequency Plot of the Ratio P_{theory}/P_{ACI} for the 24 in. Column, Pure Moment

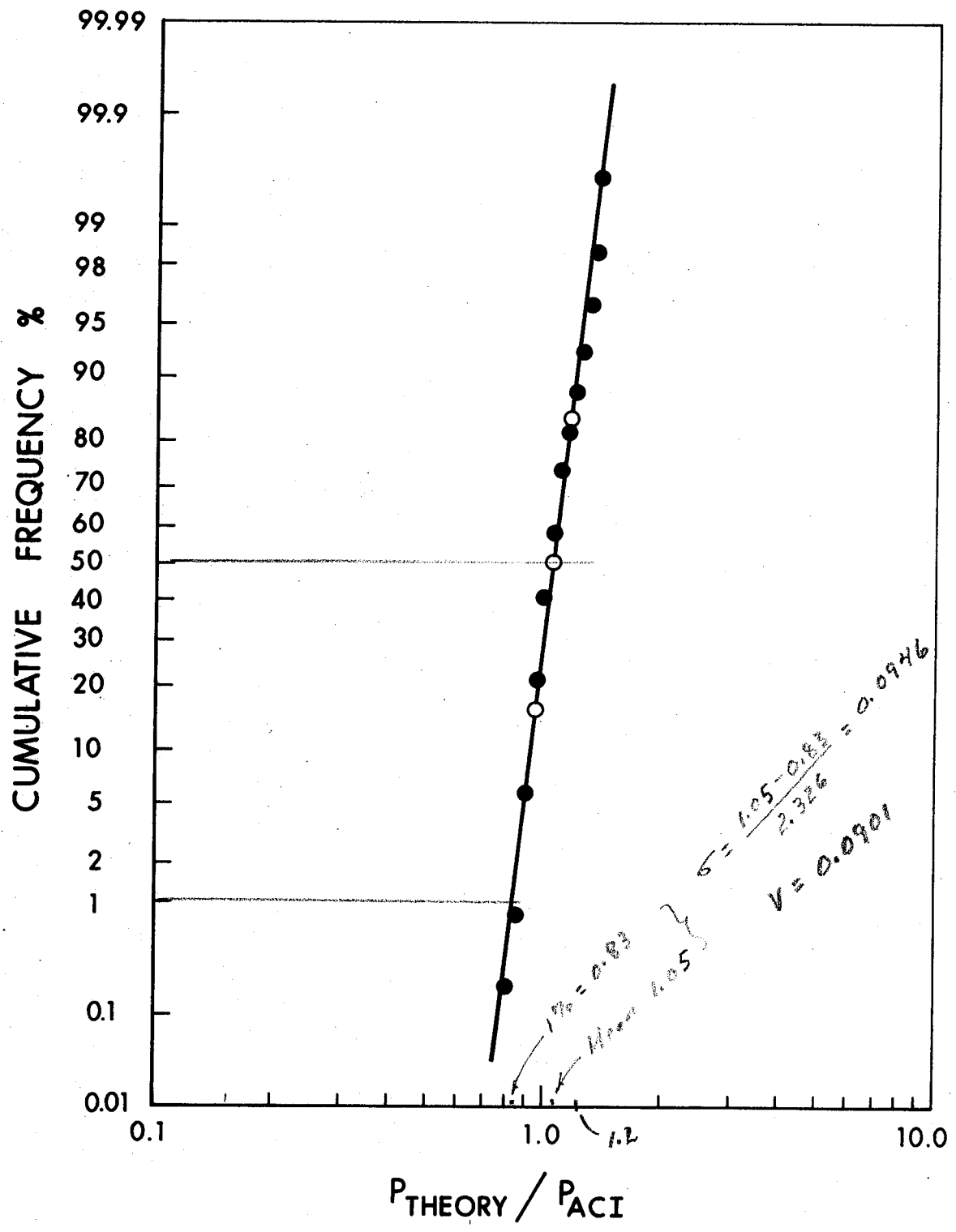


Figure 5.16 Log-normal Cumulative Frequency Plot of the Ratio P_{theory}/P_{ACI} for the 24 in. Column, Pure Moment

Table 5.12

Comparison of the Mean Value of the Ratio P_{theory}/P_{ACI} for the 12 in. and 24 in. Columns

e/h	12 in. x 12 in. Column		24 in. x 24 in. Column	
	Mean Value	C.O.V.	Mean Value	C.O.V.
0.0	1.22497	0.15441	1.17160	0.13031
0.05	1.17698	0.15159	1.11903	0.13367
0.10	1.15575	0.14802	1.08382	0.14170
0.15	1.13985	0.14549	1.06790	0.14099
0.20	1.12937	0.14352	1.07079	0.13601
0.30	1.12239	0.13693	1.12003	0.11802
0.40	1.12039	0.11908	1.17984	0.11500
0.50	1.06030	0.10190	1.19744	0.10429
0.60	1.04139	0.09705	1.13196	0.10118
0.70	1.03100	0.09733	1.07567	0.10021
0.80	1.02598	0.09929	1.07338	0.09812
0.90	1.02439	0.10127	1.06804	0.09731
1.00	1.02498	0.10266	1.06246	0.09703
1.50	1.03976	0.10241	1.04738	0.09961
∞	1.01598	0.10590	1.04568	0.10978

5.5 Calculation of ϕ Factors

5.5.1 Based on 1 in 100 Understrength

Tables 5.13 and 5.14 are tables of the calculated ϕ factor based on a probability of understrength of 1 in 100 and a normal dispersion of cross section strength in the compression failure region and a log-normal dispersion of cross section strength in the tension failure region. Figure 5.17 is a plot of the ϕ factor for the 12 in. and the 24 in. columns vs. e/h based on a probability of understrength of 1 in 100. The ϕ factors in the ACI Code are related to a probability of understrength of 1 in 100*0.

Table 5.13

The Understrength Factor for the 12 in. by 12 in. Column
Based on a Probability of Understrength of 1 in 100

e/h	Mean Value	Std. Dev.	ϕ Factor
0.0	1.22497	0.18915	0.78
0.05	1.17698	0.17842	0.76
0.10	1.15575	0.17108	0.76
0.15	1.13985	0.16583	0.75
0.20	1.12937	0.16208	0.75
0.30	1.12239	0.15369	0.76
0.40	1.12039	0.13342	0.81
0.50	1.06030	0.10804	0.83
0.60	1.04139	0.10107	0.83
0.70	1.03100	0.10035	0.82
0.80	1.02598	0.10187	0.81
0.90	1.02439	0.10374	0.81
1.00	1.02498	0.10522	0.80
1.50	1.03976	0.10649	0.82
∞	1.01598	0.10759	0.79

Table 5.14

The Understrength Factor for the 24 in. by 24 in. Column
Based on a Probability of Understrength of 1 in 100

e/h	Mean Value	Std. Dev.	ϕ Factor
0.0	1.17160	0.15267	0.82
0.05	1.11903	0.14958	0.77
0.10	1.08382	0.15358	0.73
0.15	1.06790	0.15057	0.72
0.20	1.07079	0.14564	0.73
0.30	1.12003	0.13218	0.81
0.40	1.17984	0.13568	0.86
0.50	1.19744	0.12489	0.91
0.60	1.13196	0.11453	0.87
0.70	1.07567	0.10779	0.85
0.80	1.07338	0.10532	0.85
0.90	1.06804	0.10393	0.85
1.00	1.06246	0.10309	0.84
1.50	1.04738	0.10433	0.83
∞	1.04568	0.11479	0.82

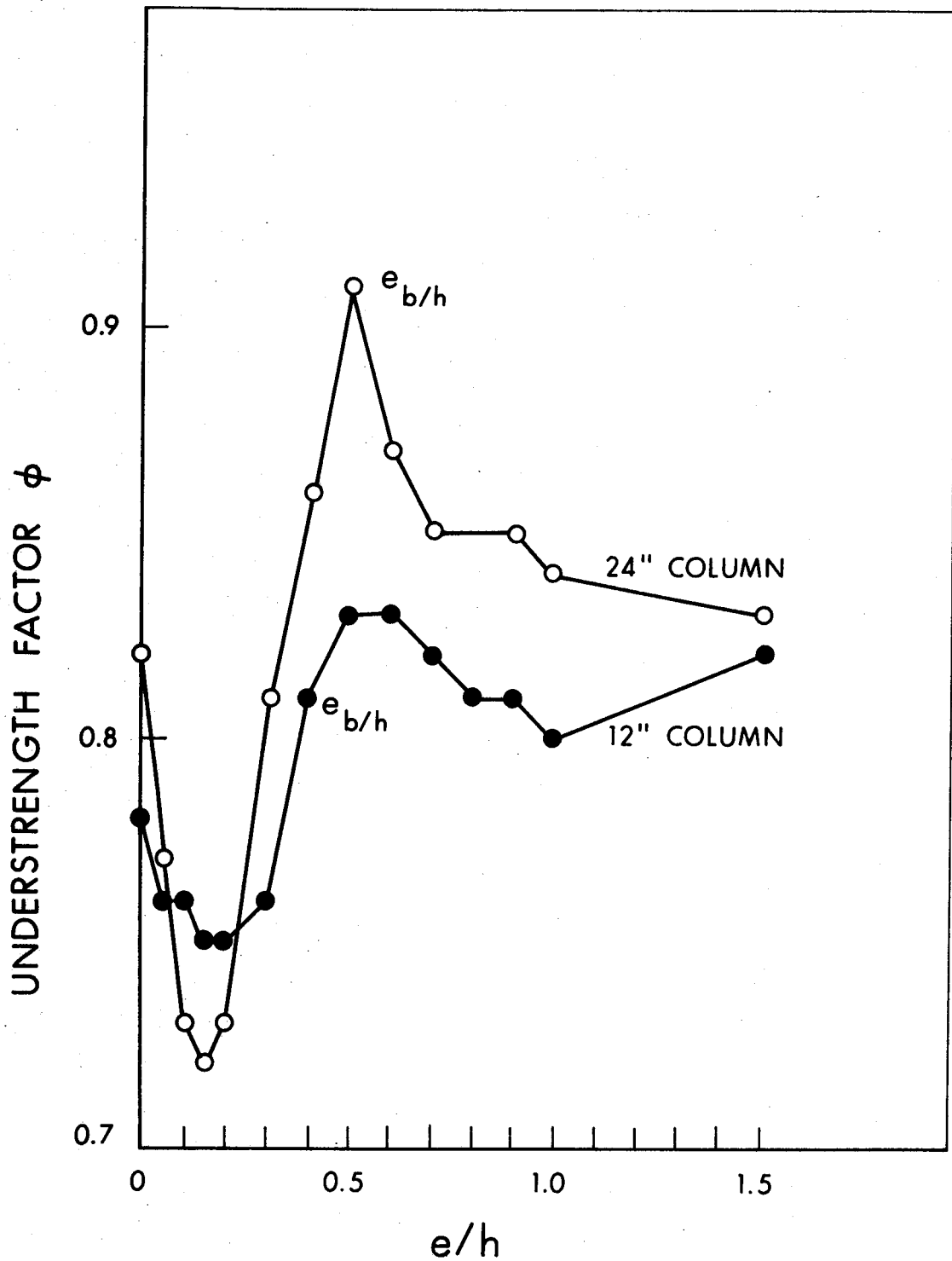


Figure 5.17 The Understrength Factor ϕ vs. e/h Based on a Probability of Understrength of 1 in 100 for the 12 in. and 24 in. Columns

5.5.2 Based on Cornell-Lind Procedure

It has been proposed that future code revisions have factors based on the equation:

$$R \gamma_R e^{-\beta \alpha V_R} \geq U \gamma_u e^{\beta \alpha V_u} \quad (5.2)$$

or:

$$\phi R \geq \lambda U$$

where:

$$\phi = \gamma_R e^{-\beta \alpha V_R}$$

= the understrength factor

$$\lambda = \gamma_u e^{\beta \alpha V_u}$$

= the overload factor

$$\gamma_R = P_{\text{theory}}/P_{\text{ACI}}$$

β = safety index

= 3.5 for probability of failure of 1.1×10^{-4}

= 4.0 for probability of failure of 3.2×10^{-5}

V_R = the variability of the strength or resistance

V_u = the variability of the loads

$\alpha = 0.75$

The α value is used to allow the separation of the effects of the variability of the member strength and the variability of the member loading.

Tables 5.15 and 5.16 are tables of the ϕ factor for the 12 in. and 24 in. columns based on the above equation. In these tables the ϕ factors are based on values of β of 4.0 for compression failures and 3.5 for tension failures. The lower probability was used for the compression failures due to the sudden brittle mode of failure.

The 12 in. square column cross section was chosen to display a large variability. For this column, ϕ was 0.78 ± 0.03 throughout the entire range of e/h studied. The 24 in. column was chosen to have a low variability. For this column, ϕ was 0.79 ± 0.09 . The large variability in the 24 in. column was due to the discrepancy in the theoretical strength discussed in Section 5.4.

Table 5.15

The Understrength Factor for the 12 in. by 12 in. Column
 Based on $\phi = \gamma_R e^{-\beta\alpha V_R}$

e/h	Mean	C.O.V.	ϕ Factor
0.0	1.22497	0.15441	0.77
0.05	1.17698	0.15159	0.75
0.10	1.15575	0.14802	0.74
0.15	1.13985	0.14549	0.74
0.20	1.12937	0.14352	0.78
0.30	1.12239	0.13693	0.78
0.40	1.12039	0.11908	0.78
0.50	1.06030	0.10190	0.81
0.60	1.04139	0.09705	0.81
0.70	1.03100	0.09733	0.80
0.80	1.02598	0.09929	0.79
0.90	1.02439	0.10127	0.79
1.00	1.02498	0.10266	0.78
1.50	1.03976	0.10241	0.80
∞	1.01598	0.10590	0.77

Avg = 0.779

Table 5.16

The Understrength Factor for the 24 in. by 24 in. Column

Based on $\phi = \gamma_R e^{-\beta \alpha V_R}$

e/h	Mean	C.O.V.	ϕ Factor
0.0	1.17160	0.13031	0.79
0.05	1.11903	0.13367	0.75
0.10	1.08382	0.14170	0.71
0.15	1.06790	0.14099	0.70
0.20	1.07079	0.13601	0.71
0.30	1.12003	0.11802	0.79
0.40	1.17984	0.11500	0.84
0.50	1.19744	0.10429	0.88
0.60	1.13196	0.10118	0.84
0.70	1.07567	0.10021	0.83
0.80	1.07338	0.09812	0.83
0.90	1.06804	0.09731	0.83
1.00	1.06246	0.09703	0.82
1.50	1.04738	0.09961	0.81
∞	1.04568	0.10978	0.78

Avg = 0.794

CHAPTER VI
SUMMARY AND CONCLUSIONS

In this study probability models were developed to describe the variability of the major variables affecting the strength of a reinforced concrete section. Based on data from a literature search the concrete strength, cross sectional dimensions and location of reinforcing steel were described with a normal distribution as described in Chapter IV. The steel was described with a normal and modified log-normal distribution of yield strength as discussed in Appendix A.

A Monte Carlo study was performed using the probability models developed to determine the variability in the cross sectional strength of a 12 in. square and a 24 in. square tied reinforced concrete column. The results of this study show that the variability of the concrete strength is the major contributing factor to cross sectional strength variability in the compression failure region and the variability in the steel strength is the major contributing factor to cross sectional strength variability in the tension failure region. The effect on the overall strength variability of the dimensional variability and the variability in the location of the steel strength were found to be minor compared to the effects of the concrete and steel strength variability. The type of distribution assumed

for the steel strength variability was found to significantly affect the overall strength variability in the tension failure region only.

The ϕ or understrength factors were calculated based on a probability of understrength of 1 in 100 and based on the first order second moment procedure developed by Cornell and Lind. The calculated values of ϕ were in close agreement with those used in the ACI 318-71 Code for column cross sections but significantly different for the case of pure bending. This suggests that the ϕ factors used in the ACI Code are adequate and may be conservative for rectangular tied column cross sections but seem to be unconservative for bending tension failures.

REFERENCES

1. ACI Committee 318, " Commentary on Building Code Requirements for Reinforced Concrete (ACI 318-71) ", American Concrete Institute, Detroit, 1971.
2. ACI Committee 214, " Realism in the Application of Standard 214-65 ", American Concrete Institute, Publication SP-37, 1973.
3. ACI Standard 318-71, " Building Code Requirements for Reinforced Concrete (ACI 318-71) ", American Concrete Institute, Detroit, 1971.
4. Allen, D.E., " Statistical Study of the Mechanical Properties of Reinforcing Bars ", Building Research Note No. 85, Division of Building Research, National Research Council, Ottawa, April 1972.
5. Allen, D.E., " Probabilistic Study of Reinforced Concrete in Bending ", Technical Paper NRC 11139, National Research Council of Canada, Ottawa, 1970.
6. Ang, A.H-S. and Cornell C.S., " Realibility Bases of Structural Safety and Design ", American Society of Civil Engineers, Journal of the Structural Division, Vol. 100, No. ST9, September 1974, pp. 1755-1769.
7. ASCE Committee on Structural Safety, " Structural Safety - A Literature Review ", American Society of Civil Engineers, Journal of the Structural Division, Vol. 98, No. ST4, April 1972, pp. 845-863.
8. Baker, M.J., " The Evaluation of Safety Factors in Structures: Variation in the Strength of Structural Materials and Their effect on Structural Safety ", Report, Department of Civil Engineering, Imperial College, London, July 1970.
9. Bannister, J.L., " Steel Reinforcement and Tendons for Structural Concrete, Part 1: Steel for Reinforced Concrete ", Concrete, Vol. 2, No. 7, July 1968, pp. 295-306.
10. Basler, E., " Analysis of Structural Safety ", ASCE Annual Convention, Boston, Massachusetts, 1960.
11. Bertero, V.V. and Felippa, C., " Discussion of Ductility of Concrete ", Proceedings of the International Symposium on Flexural Mechanics of Reinforced Concrete, ASCE-ACI, Miami, November 1964, pp. 227-234.

12. Bloem, D.L., " Concrete Strength in Structures ", Journal of the American Concrete Institute, Proceedings, Vol 65, No. 3, March 1968, pp. 176-187.
13. Bloem, D.L., " Concrete Strength Measurement-Cores Versus Cylinders ", American Society for Testing and Materials, Proceedings, Vol. 65, 1965, pp. 668-686.
14. Bloem, D.L., " Studies of Uniformity of Compression Strength Tests of Ready Mixed Concrete ", American Society for Testing and Materials, Bulletin No. 206, May 1955, pp. 65-70.
15. Cady, P.D., " Statistical Evaluation of Concrete Tests ", American Society of Civil Engineers, Journal of the Construction Division, Vol. 89, No. C01, March 1963, pp. 19-31.
16. Campbell, R.H. and Tobin, R.E., " Core and Cylinder Strengths of Natural and Lightweight Concrete ", Journal of the American Concrete Institute, Proceedings, Vol. 64, No. 4, April 1967, pp. 190-195.
17. Chan, W.L., " The Ultimate Strength and Deformation of Plastic Hinges in Reinforced Concrete Frameworks ", Magazine of Concrete Research, Vol. 7, No. 21, November 1955, pp. 121-132.
18. Corley, W.G., " Rotational Capacity of Reinforced Concrete Beams ", American Society of Civil Engineers, Journal of the Structural Division, Vol. 92, No. ST5, October 1966, pp. 121-146.
19. Cornell, C.A., " A Probability Based Structural Code ", Journal of the American Concrete Institute, Vol. 66, No. 12, December 1969, pp. 974-985.
20. Costello, J.F. and Chu, K., " Failure Probabilities of Reinforced Concrete Beams ", American Society of Civil Engineers, Journal of the Structural Division, Vol. 95, No. ST10, October 1969, pp. 2281-2304.
21. Cummings, A.E., " Strength Variations in Ready Mixed Concrete ", Journal of the American Concrete Institute, Vol. 51, No. 4, April 1955, pp. 765-772.
22. Drysdale, R.G., " Variation of Concrete Strength in Existing Buildings ", Magazine of Concrete Research, Vol. 25, No. 85, December 1973, pp. 201-207.

23. Fiorato, A.E., " Geometric Imperfections in Concrete Structures ", Chalmers University of Technology, Gothenberg, Sweden, National Swedish Building Research Document Number 5, 1973.
24. Freudenthal, A.M., " Safety and the Probability of Structural Failure ", American Society of Civil Engineers, Transactions, Vol. 121, 1956, pp. 1337-1375.
25. Gamble, W.L., " Some Observations of the Strength of Large Reinforcing Bars ", Journal of the American Concrete Institute, Vol. 70, No. 1, Januray 1973, pp. 31-35.
26. Hahn, G.J. and Shapiro, S.S., " Statistical Models in Engineering ", John Wiley and Sons, Inc, New York, 1967.
27. Haris, A., " Minimum Eccentricity Requirements in the Design of Reinforced Concrete Columns ", The University of Texas at Austin, Ph. D. Disertation, 1972, Engineering, Civil.
28. Hernandez, A.A. and Martinez, F.V., " Variaciones de las Demensiones y de la Posicion del Acero de Refuerzo en las Estructuras de Concreto ", Universidad Nacional Autonoma de Mexico, Facultad de Ingenieria, 1974.
29. Hognestad, E., " A Study of Combined Bending and Axial Load in Reinforced Concrete Members ", Bulletin No. 399, Engineering Experiment Station, University of Illinois, Urbana, November 1951.
30. Housner, G.W. and Jennings, P.C., " Generation of Artificial Earthquakes ", American Society of Civil Engineers, Journal of the Engineering Mechanics Division, Vol. 90, No. EM1, February 1964, pp. 113-150.
31. IBM Application Program GH20-0205-4, " System/360 Scientific Subroutine Package, Version III Programers Manual ", Fifth Edition (1970), International Business Machines Corporation 1968.
32. Johnson, A.I., " The Determination of the Design Factor for Reinforced Concrete Structures ", Symposium on the Strength of Concrete Structures ", Institution of Civil Engineers - Cement and Concrete Association, London, May 1956.
33. Julian, O.G., " Discussion of Reference 21 ", Journal of the American Concrete Institute, Vol. 51, No. 12,

44. Narayanaswamy, V.P. and Gadh, A.D., " Characteristic Strength of Reinforcing Steel ", Journal of the Institute of Engineers (India), Civil Engineering Division, Vol. 53, Part CI2, November 1972, pp. 85-88.
45. National Academy of Sciences-National Research Council, " The AASHO Road Test, Report 2, Materials and Construction ", Highway Research Board of the NAS-NRC division of Engineering and Industrial Research, Special Report 61B, Publication No. 951, Washington, D.C., 1962.
46. Neville, A.M., " The Relation Between Standard Deviation and Mean Strength of Concrete Test Cubes ", Magazine of Concrete Research, Vol. 11, No. 32, July 1959, pp. 75-84.
47. Newlon, H.H., " Variability of Portland Cement Concrete ", National Conference on Statistical Quality Control Methodology in Highway and Airfield Construction ", Proceedings, University of Virginia, Charlottesville, Virginia, 1966, pp. 259-289.
48. Petersons, N., " Should Standard Cube Test Specimens Be Replaced by Test Specimens Taken From Structures ", Materiaux et Constructions, RILEM, Paris, Vol. 1, No. 5, 1968, pp. 425-435.
49. Plowman, J.M., Smith, W.F., and Sheriff, T., " Cores, Cubes and the Specified Strength of Concrete ", The Structural Engineer, Vol. 52, No. 11, November 1974, pp. 421-426.
50. Plum, N.M., " Quality Control of Concrete Its Rational Bases and Economic Aspects ", Institution of Civil Engineers, Proceedings, Vol. 2, Part 1, London, 1953, pp. 311-333.
51. Rackwitz, R., " Statistical Control in Concrete Structures ", C-4, CEB International Course on Structural Concrete, Laboratorio Nacional de Engenharia Civil, Lisbon, 1973.
52. Rao, N.R.N., Lohrmann, M. and Tall, L., " The Effect of Strain on the Yield Stress of Structural Steels ", American Society for Testing and Materials, Journal of Materials, Vol. 1, No. 1, March 1966, pp. 241-262.
53. Redekop, D., " A Study of Reinforced Concrete Columns in Existing Buildings ", Master of Engineering Thesis, Mc Master University, August 1971.

54. Riley, O. and Cooper, S.B., " Concrete Control on a Major Project ", Journal of the American Concrete Institute Proceedings, Vol. 68, No. 2, February 1971, pp. 107-114.
55. Roberts, N.P., " The Characteristic Strength of Steel for Reinforcing and Prestressing Concrete ", Concrete, Vol. 1, No. 8 August 1967, pp. 273-275.
56. Robles, F., " Strength Factors: Material and Geometrical Aspects ", ASCE-IABSE International Conference on Tall Buildings, Lehigh University, Proceedings, Vol. III, 1972, pp. 907-921.
57. Roy, H.E.H. and Sozen, M.A., " Ductility of Concrete ", Proceedings of the International Symposium on Flexural Mechanics of Reinforced Concrete, ASCE-ACI, Miami, November 1964, pp. 213-224.
58. Rusch, H., " Die Streuung der Eigenschaften von Schwerbeton ", Symposium on Concepts of Safety of Structures and Methods of Design, International Association for Bridge and Structural Engineering, London, 1969, pp. 63-74.
59. Rusch, H. and Stokl, S., " Der Einfluss von Bugelin and Druckstaben auf das Verhalten der Biegedruckzone von Stahlbetonbalken ", Bulletin No. 148, Deutscher Ausschuss Fur Stahlbetonbau, Berlin, 1963, p. 75.
60. Sargin, M., " Stress-Strain Relationships for Concrete and the Analysis of Structural Concrete Sections ", SM Study No. 4, Solid Mechanics Division, University of Waterloo, 1971.
61. Shalon, R. and Reintz, R.C., " Interpretation of Strengths Distribution As a Factor in Quality Control of Concrete ", RILEM Symposium on the Observation of Structures, Vol. 2, Lisbon Laboratorio Nacional de Engenharia Civil, 1955, pp. 100-116.
62. Sexsmith, R.G. and Nelson, M.F., " Limitations in Applications of Probabilistic Concepts ", Journal of the American Concrete Institute, Proceedings, Vol. 66, No. 10, October 1969, pp. 823-828.
63. Siu, W.W.C., Parimi, S.R. and Lind, N.C., " Practical Approach to Code Calibration ", American Society of Civil Engineers, Journal of the Structural Division, Vol. 101, No. ST7, July 1975, pp. 1469-1480.

64. Soliman, M.T.M. and Yu, C.W., " The Flexural Stress-Strain Relationship of Concrete Confined by Rectangular Transverse Reinforcement ", Magazine of Concrete Research, Vol. 19, No. 61, December 1967, pp. 223-238.
65. Soroka, I., " An Application of Statistical Procedures to Quality Control of Concrete ", Materiaux et Constructions, RILEM, Paris, Vol. 1, No. 5, 1968, pp. 437-441.
66. Soroka, I., " On Compressive Strength Variation in Concrete ", Materiaux et Constructions, RILEM, Vol. 4, No. 21, 1971, pp. 155-161.
67. Sturman, G.M., Shah, S.P. and Winter, G., " Effect of Flexural Strain Gradients on Microcracking and Stress-Strain Behaviour of Concrete ", Journal of the American Concrete Institute, Proceedings, Vol. 62, No. 7, July 1965, pp. 805-822.
68. Torroja, E., " Philosophy of Structures ", University of California Press, Berkley, California, 1958.
69. Tso, W.K. and Zelman, I.M., " Concrete Strength Variation in Actual Structures ", Journal of the American Concrete Institute, Proceedings, Vol. 67, No. 12, December 1970, pp. 981-988.
70. Wagner, W.K., " Discussion of Reference 21 ", Journal of the American Concrete Institute, Proceedings, Vol. 51, No. 12, December 1955, pp. 772-14, 772-16.
71. Wagner, W.K., " Effect of Sampling and Job Curing Procedures on Compressive Strength of Concrete ", Materials and Research Standards, August 1973.
72. Warner, R.F. and Kabaila, " Monte Carlo Study of Structural Safety ", American Society of Civil Engineers, Journal of the Structural Division, Vol. 94, No. ST12, December 1968, pp. 2847-2859.

APPENDIX A
VARIABILITY IN REINFORCING STEEL

Introduction

The three main sources of variation in steel strength are:

- (1) variation in the strength of material,
- (2) variation in area of the cross-section of the bar, and
- (3) variation in the rate of loading.

The variability of yield strength depends on the source and the nature of the population. The variation in strength within a single bar is relatively small, while the in-batch variations are slightly larger. However, variability of samples derived from different batches and sources may be high. This is expected since rolling practices and quality measures vary for different countries, different manufacturers and different bar sizes. Furthermore, the cross-sectional areas vary due to differences in the setting of the rolls, and this adds to the variation. Mill tests are generally carried out at a rapid rate of loading (ASTM corresponds to 1040 micro-in/in/sec) and have the tendency of reporting the unstable high yield point rather than the stable low yield point. Since the strains in the structure are induced at a much lower rate than the mill tests, mill tests tend to overestimate the strength of reinforcement,

hence another source of variation.

An examination of the test data revealed that the bars of large diameter tended to develop less strength (4, 24, 55) than #3 to #11 bars. Thus, for the purpose of statistical evaluation, the #14 and #18 bars were studied separately from the other sizes. Also the #2 bars were not included in this study because of their rare use for structural concrete.

In this study the terms Grade 40, Grade 50 and Grade 60 refer to reinforcing bars with minimum specified yield strength of 40, 50 and 60 ksi, respectively, even though the bars in question may not have been produced according to ASTM or CSA specifications. Only data for deformed bars has been included. In some cases data for cold-worked bars has been considered but most of the data is for hot-rolled bars.

Variation in Steel Strength

Different values for the yield strength of steel may be obtained depending on how it is defined. The static yield strength based on nominal area seems to be desirable because the strain rate is similar to what is expected in a structure and designers use the nominal areas in their calculations. Most mill tests, however, are conducted with a rapid rate of loading, and the strength is generally referred to actual areas. For these reasons the yield strength corresponding to rapid strain rate and measured

area is discussed in this section, the effects on this strength of variations in cross-sectional area and rate of loading are dealt with in the succeeding sections.

A review of literature on steel strength showed that the coefficient of variation was in general in the order of 1% to 4% for individual bar sizes and 4% to 7% overall for data derived from any one source. When data was taken from many sources the coefficient of variation increased to 5% to 8% for individual sizes and 10% to 12% overall. A summary of selected studies from literature (4,8,9,33,43) is shown in Table A-1.

The data reported by Allen⁴ and Julian³³ on Grade 40 and 60 steel bars showed close agreement with a normal distribution (with respective mean and standard deviation) in the range approximately 5 to 95 percentile but differ from the normal distribution outside this range. Some authors have suggested other types of distributions such as skewed distribution (9,54), truncated normal (31) and Beta distribution (20). These suggestions were, however, based on a particular set of data and only approximated the distribution of the population from which the data was drawn. Nonetheless, they suggest that the yield strength is a phenomenon that can be described by a particular theoretical distribution with certain limitations. The normal distribution seems to correlate very well in the vicinity of the mean values for different populations of yield strength,

Table A-1
Summary of Selected Studies on Steel Strength

Study Number	Grade	Size	Total Number of Samples	Number of Sources	Testing House	Manufacturing Country	Reported By
1	40	#3, #5, #8, #11	78	one	Lab	Canada	Allen
2	40	#5, #8, #11	---	one	Mill	Canada	Allen
3	60	#5 to #14	132	one	Mill	Canada	Allen
4	40	#3 to #10	171	---	---	---	Julian
5	50	#8	35	one	Lab	India	Narayanaswamy
6	60	#8	34	one	Lab	India	Narayanaswamy
7	60	#3 to #10	1173	---	---	England	Bannister
8	50	#4 to #10	656	---	Lab	England	Baker
9	60	#3 to #10	381	---	Lab	England	Baker

Study Number	Yield Strength		Overall Mean (ksi)	Overall C.O.V. (%)	Individual Bar Sizes		Overall Mean (ksi)	Overall C.O.V. (%)
	Individual Mean (ksi)	C.O.V. (%)			Individual Mean (ksi)	C.O.V. (%)		
1	49.0 to 54.0	0.5 to 3.0	51.2	4.1	0.958 to 0.985	0.2 to 1.5	0.967	1.4
2	48.4 to 58.4	---	52.4	---	0.962 to 1.016	---	0.987	---
3	---	---	71.5	7.7	---	---	1.000	1.9
4	---	---	47.7	12.4	---	---	---	---
5	---	---	60.8	1.2	---	---	0.986	0.5
6	---	---	73.4	2.5	---	---	0.992	1.6
7	64.9 to 70.2	2.8 to 4.5	67.0	---	---	---	---	---
8	62.1 to 69.1	5.6 to 11.9	66.7	---	0.988 to 1.008	1.0 to 3.1	1.000	---
9	64.0 to 68.2	5.1 to 7.7	66.1	---	1.115 to 1.212	4.8 to 9.0	1.169	---

but it is a crude approximation at low and high levels of probability where the steel strength distribution curves tend to have certain minimum and maximum values rather than following the theoretical tails. This is expected since there are always some quality controls that are used to attain a certain minimum yield strength with the result that the manufacturing of steel is not truly a random process. Furthermore, certain data indicated a positive skewness, particularly when derived from different sources and mixed together. Theoretically a log-normal distribution should be a better fit for this case than a normal distribution since it takes into account the skew nature of the data. However the logarithmically distributed values of yield strength at low and high levels of probability did not show a significant improvement over normally distributed values of available data. Therefore, it was decided to empirically establish a "modified" log-normal distribution that would yield correlate with the North American data on yield strength.

Values of $(f_y - 34 \text{ ksi})$ are plotted on log-normal probability paper in Figure A-1 for the data from Julian³³ and Allen⁴ for Grade 40 reinforcing bars grouped together. The values were found to be in good agreement with a log-normal distribution in the range from the 0.01 percentile to the 99th percentile. The modification constant of 34 ksi was established by trial and error. The corresponding frequency curve, the histogram of the grouped data and the

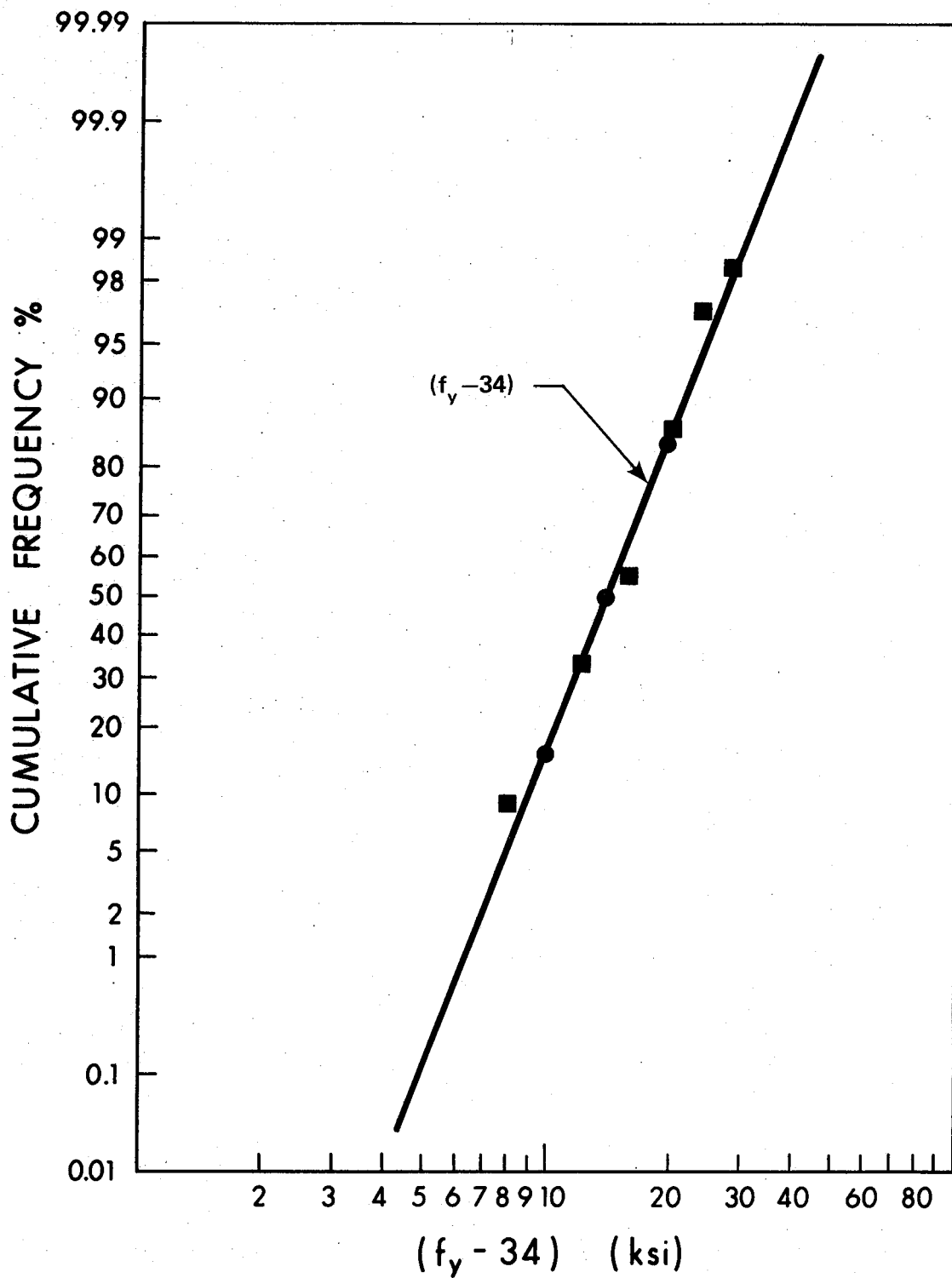


Figure A-1 Steel Strength Distribution for Grade 40 Reinforcing Bars

corresponding normal frequency distribution curve are shown in Figure A-2 for the purpose of comparison. The mean value of the data was found to be 48.8 ksi with a maximum value of 66 ksi and a coefficient of variation of 10.7%.

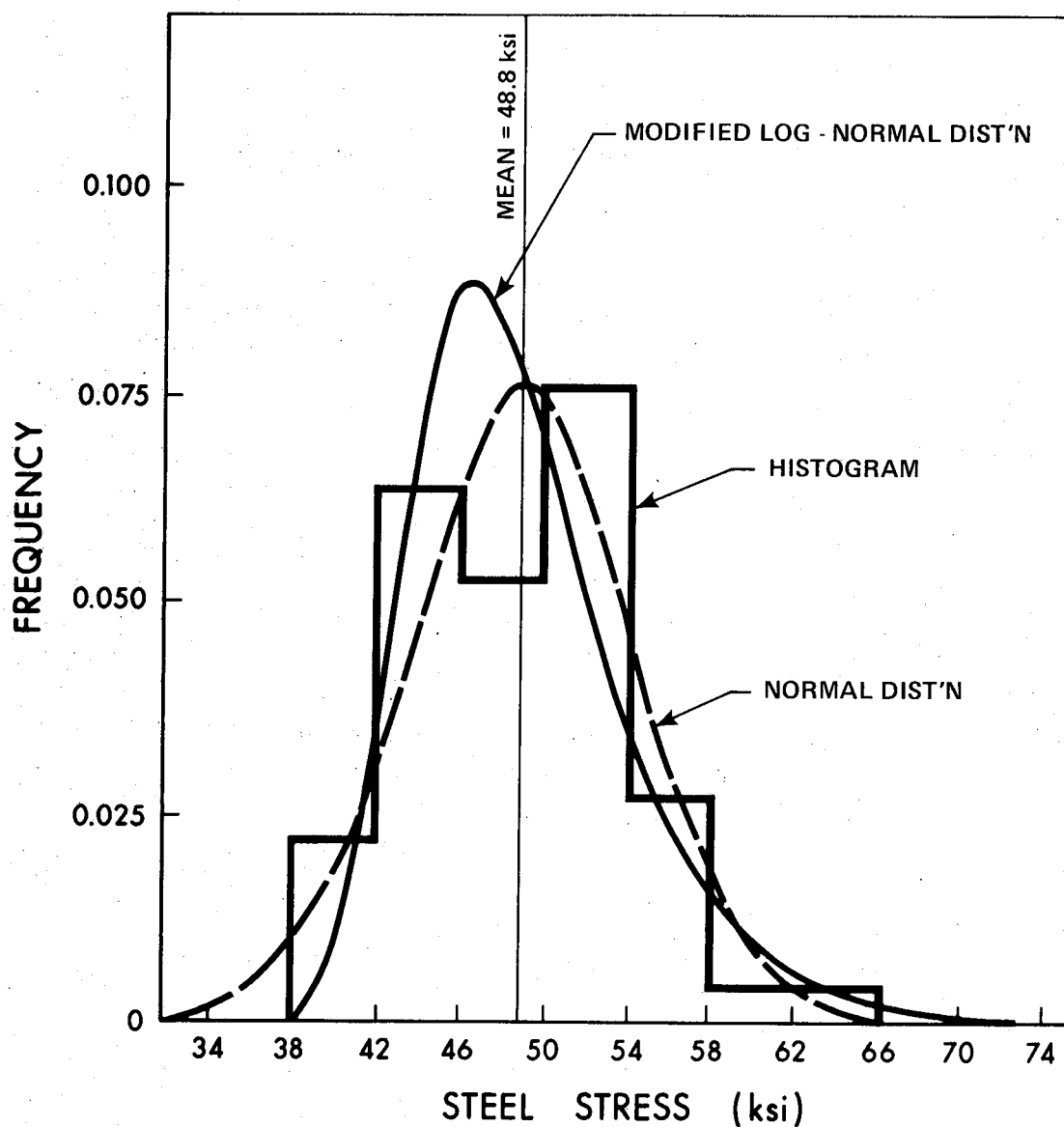
Similarly, values of (f_y -55ksi) for Grade 60 reinforcing bars from mill tests reported by Allen⁴ were found to be log-normally distributed in the range from the 0.01 percentile to the 99th percentile as shown in Figure A-3. The frequency curves and histogram for Grade 60 steel are shown in Figure A-4. The mean value for the data was 71.5 ksi with a maximum value of 90 ksi and a coefficient of variation of 7.7%.

In both cases the modified log-normal curve is a better approximation at the lower end of the curve while the normal curve is better at the high end of the curve.

Variation in Steel Cross-Sectional Area

The actual areas of reinforcing bars tends to deviate from the nominal areas due to the rolling process. The designers do not have this information readily available to them, and hence use the nominal areas in their calculations. For this reason this variation should be incorporated in the strength of steel.

This variation in the ratio of measured to nominal areas (A_e/A_n) was studied as a measure of the variation in



MODIFIED LOG-NORMAL DISTRIBUTION

$$\text{PDF} = \frac{C}{y\sigma_x\sqrt{2\pi}} * \exp \left[-\frac{1}{2} \left(\frac{x-\bar{x}}{\sigma_x} \right)^2 \right]$$

$$\bar{x} = 1.19456, \sigma_x = 0.14112$$

$$c = 0.43429$$

$$y = (f_y - 34 \text{ ksi}), \quad x = \text{LOG}_{10} y$$

NORMAL DISTRIBUTION

$$\bar{x} = 48.8 \text{ ksi}, \sigma_x = 5.506 \text{ ksi}$$

$$x = f_y \text{ ksi}$$

Figure A-2 Probability Density Function for Grade 40 Bars

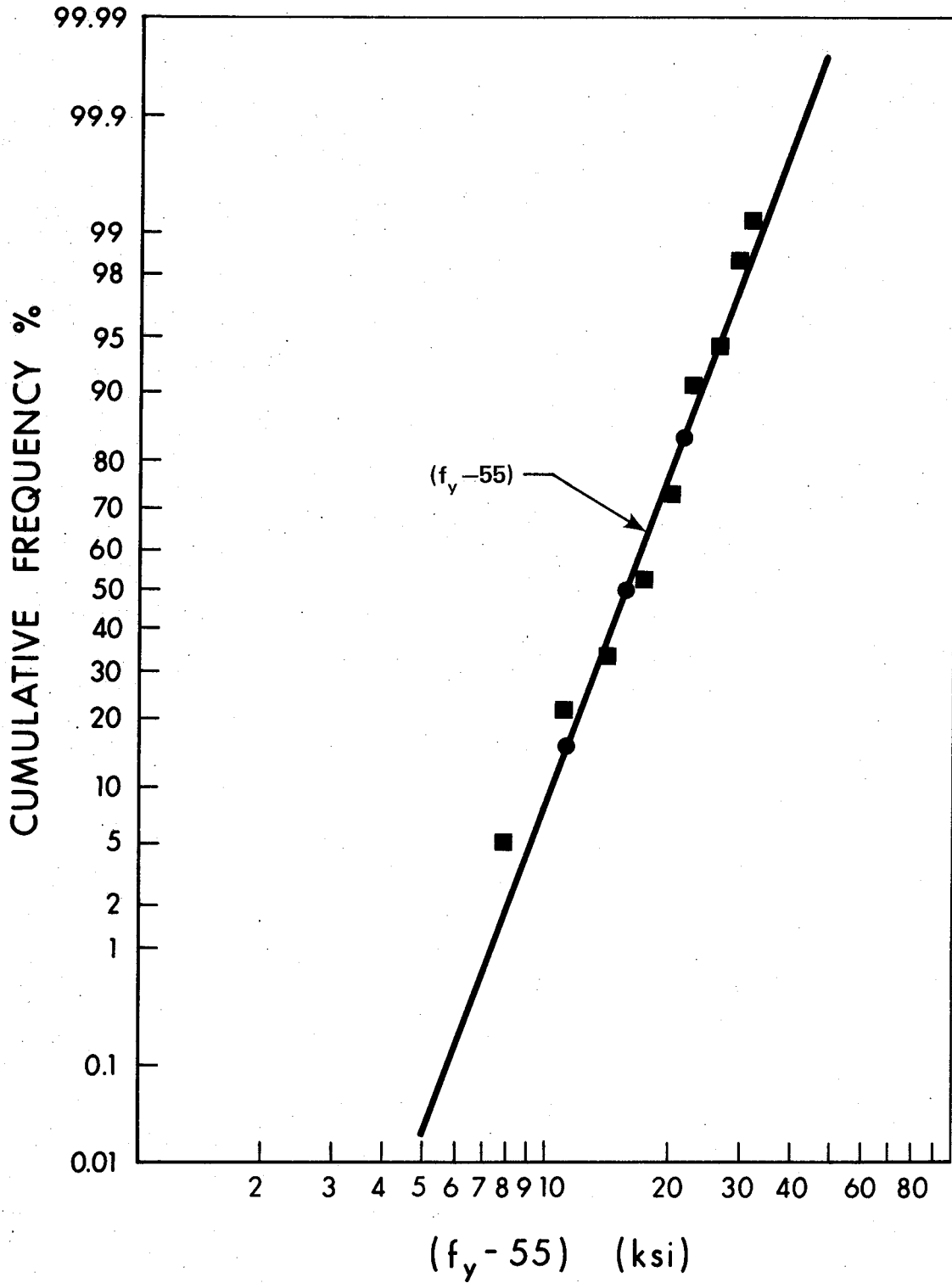
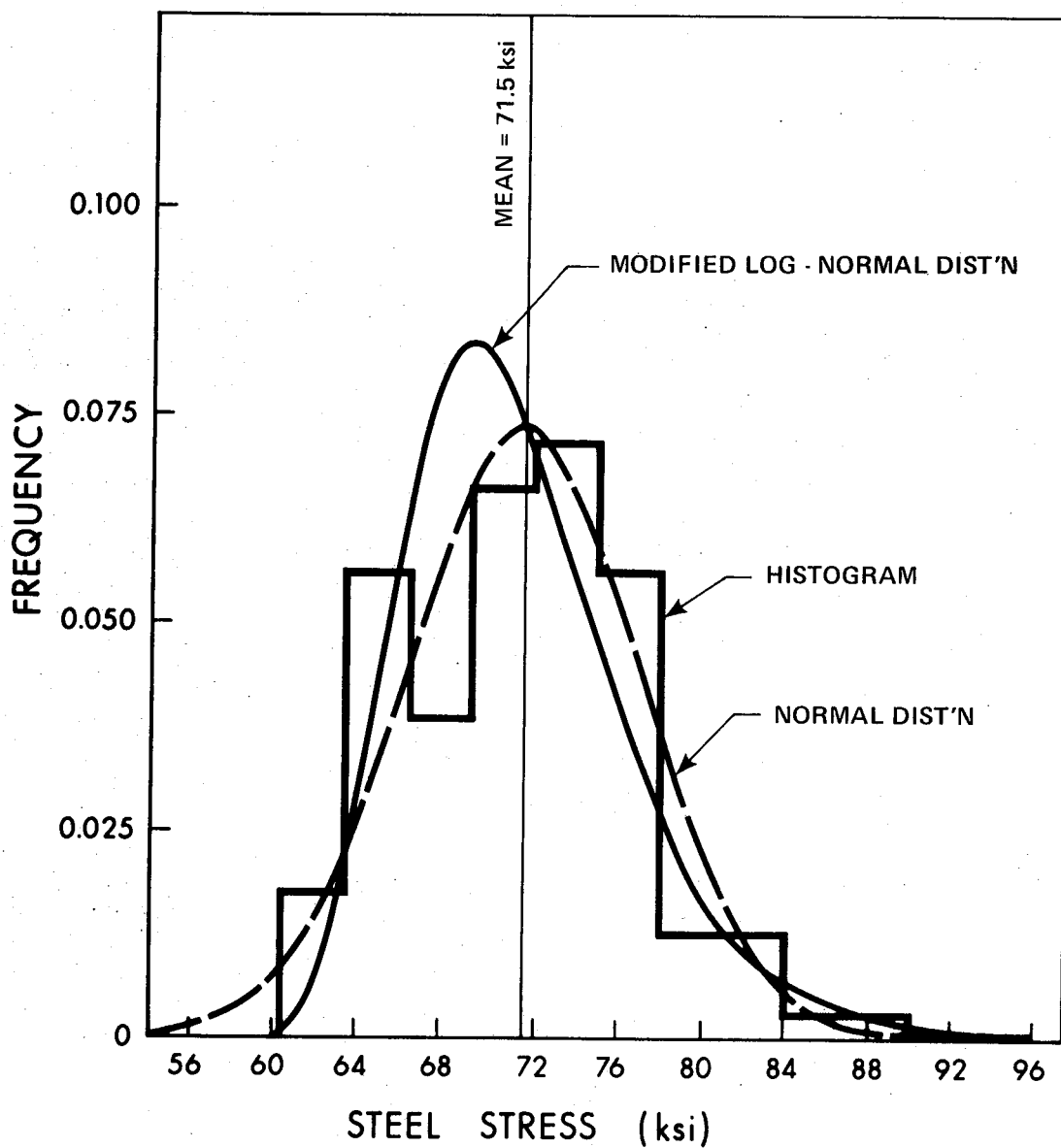


Figure A-3 Steel Strength Distribution for Grade 60 Reinforcing Bars



MODIFIED LOG-NORMAL DISTRIBUTION

$$\text{PDF} = \frac{C}{y\sigma_x\sqrt{2\pi}} * \exp \left[-\frac{1}{2} \left(\frac{x-\bar{x}}{\sigma_x} \right)^2 \right]$$

$$\bar{x} = 1.19456, \sigma_x = 0.14112$$

$$c = 0.43429$$

$$y = (f_y - 55 \text{ ksi}), \quad x = \text{LOG}_{10} y$$

NORMAL DISTRIBUTION

$$\bar{x} = 71.8 \text{ ksi}, \sigma_x = 5.506 \text{ ksi}$$

$$x = f_y \text{ ksi}$$

Figure A-4 Probability Density Function for Grade 60 Bars

the cross-sectional area of reinforcing bars. The values of A_e/A_n are reproduced from available literature (4, 8, 43) in Table A-1. Table A-1 indicates that the data reported by Baker⁶ for Grade 60 steel demonstrates high mean value and coefficient of variation. Such values cannot be explained in definite terms. It is possible that the collected data contained a good percentage of values from mills with old rolls that increased the mean and coefficient of variation. Furthermore, British rolling practice may differ from Canadian practice. For these reasons, these values were not included in the analysis.

The ratios of A_e/A_n from tests on Grade 40 and 60 reinforcing bars, manufactured in Canada (Study No. 1 and 3 in Table A-1), were plotted on normal probability paper. These values exhibited close agreement in the range from the 5th to the 95th percentile for Grade 40 steel and from the 2nd to the 98th percentile for Grade 60 bars with a normal distribution. When the values for both studies were combined they resulted in a normal distribution in the range between the 4th and 99th percentile with a mean value of 0.988 and a coefficient of variation of 2.4%. The effect of such a small coefficient of variation is not large enough to have any significant effect on the coefficient of variation of $A_s f_y$. For this reason a single value for A_e/A_n seems to be more appropriate. Allen⁴ has suggested a value of 0.97 for A_e/A_n . This seems to be a conservative estimate of the average values of A_e/A_n shown in Table A-1, and close to ASTM

rolling tolerances that allow an average ratio as low as 0.965 and a minimum single value up to 0.940.

Effect of Rate of Loading

The apparent yield strength of a test specimen increases as the strain rate or the rate of loading increases. Since mill tests on steel specimens are generally carried out at much greater strain rates (approximately 1040 micro-in/in/sec) than encountered in a structure, they tend to overestimate the yield strength. A strain rate of 1 in/in/sec may increase the yield strength of Grade 40 steel as much as 50% over the static yield strength (34).

Tests conducted on steel coupons of A36, A441 and A514 steel (51) demonstrated a yield strength reduction more or less of the same value for all types of steel with decrease in the rate of strain. The equation developed by Fao⁵¹ on the basis of these tests gives values of static yield strength that are 4.8 ksi and 3.4 ksi less than the yield strengths obtained at cross-head speed of 1000 and 200 micro-in/in/sec respectively. NRC tests on Grade 40 bars (4) showed a reduction of approximately 3 ksi in the mean yield strength when speed of the testing machine was dropped from 208 micro-in/in/sec to static. This value correlates well with the one obtained from Rao's equation. Similarly, for Grade 40 bars, it has been shown at the University of Illinois (34) that the difference between the yield strength

at a strain rate of 1040 micro-in/in/sec and the strength at a strain rate of 20 micro-in/in/sec is about 9% or 4 ksi. ETH tests (36) for high strength reinforcement demonstrated a reduction of 3 ksi for static conditions.

For evaluation of the static yield strength from mill tests, Allen⁴ has suggested a decrease of 4 ksi. This value seems to be a reasonable estimate for the available test data.

Effect of Bar Diameter

The strength of steel tends to vary across the cross-section of a reinforcing bar with the highest strength near the outside of the bar. This is probably due to the cold-working of circumferential sections of bars during the rolling process. Thus the mean yield strength is expected to decrease with increasing diameter. The variation of the mean yield strength with size is plotted in Figures A-5 and A-6. The data shown in the figures were taken from several test series for Grade 40 and Grade 60 reinforcement (4,44,8,9,24). For bars with relatively small diameter the effect of this variation is small and not clearly established. For large diameter bars such as #14 and #18 this effect becomes more significant. In addition, the ASTM specifications allow the use of small specimens machined from samples of large diameter bars for testing purposes. A specimen machined to a smaller diameter from a quarter-piece

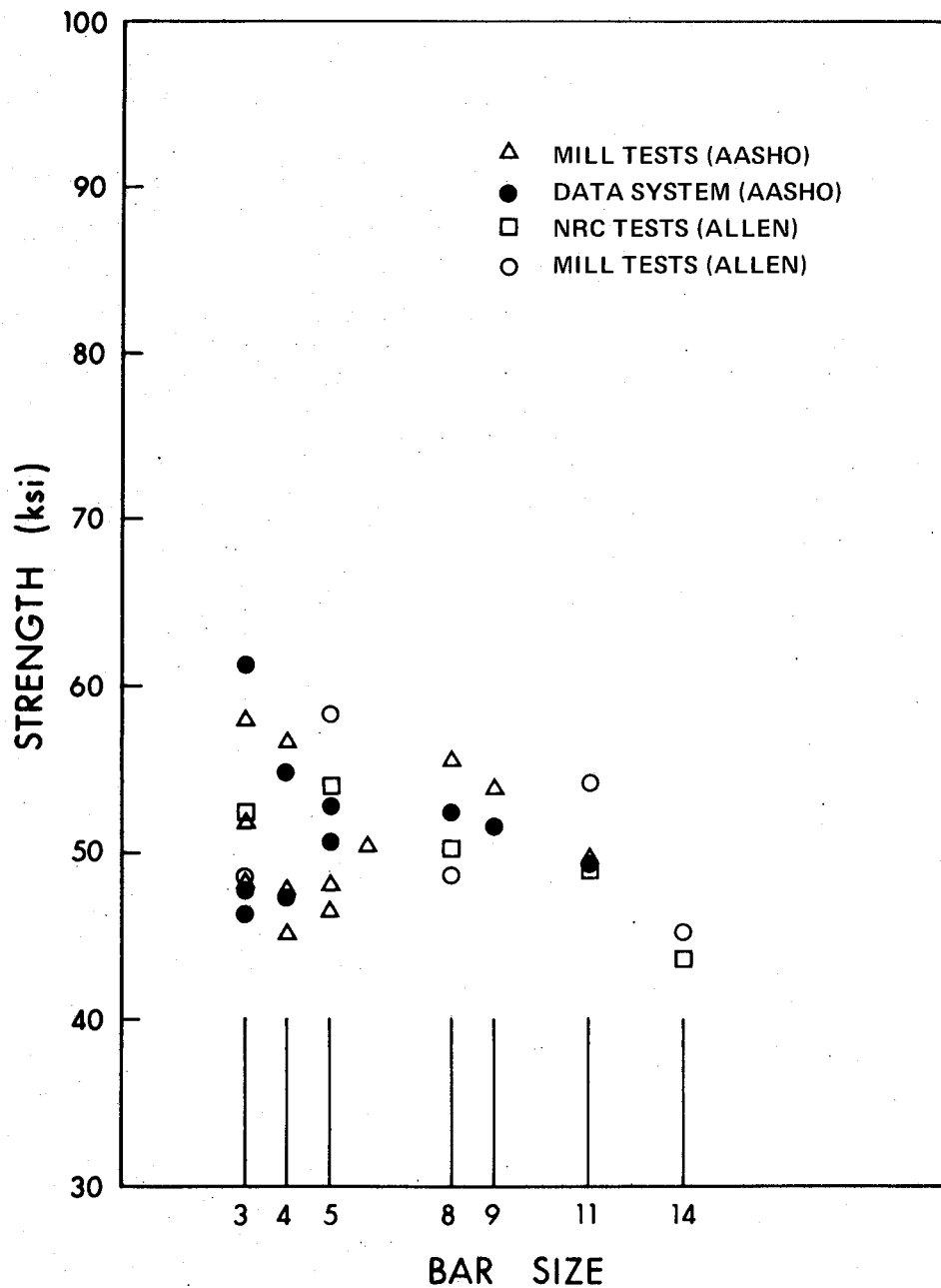


Figure A-5 Effect of Bar Diameter on Steel Strength, Grade 40

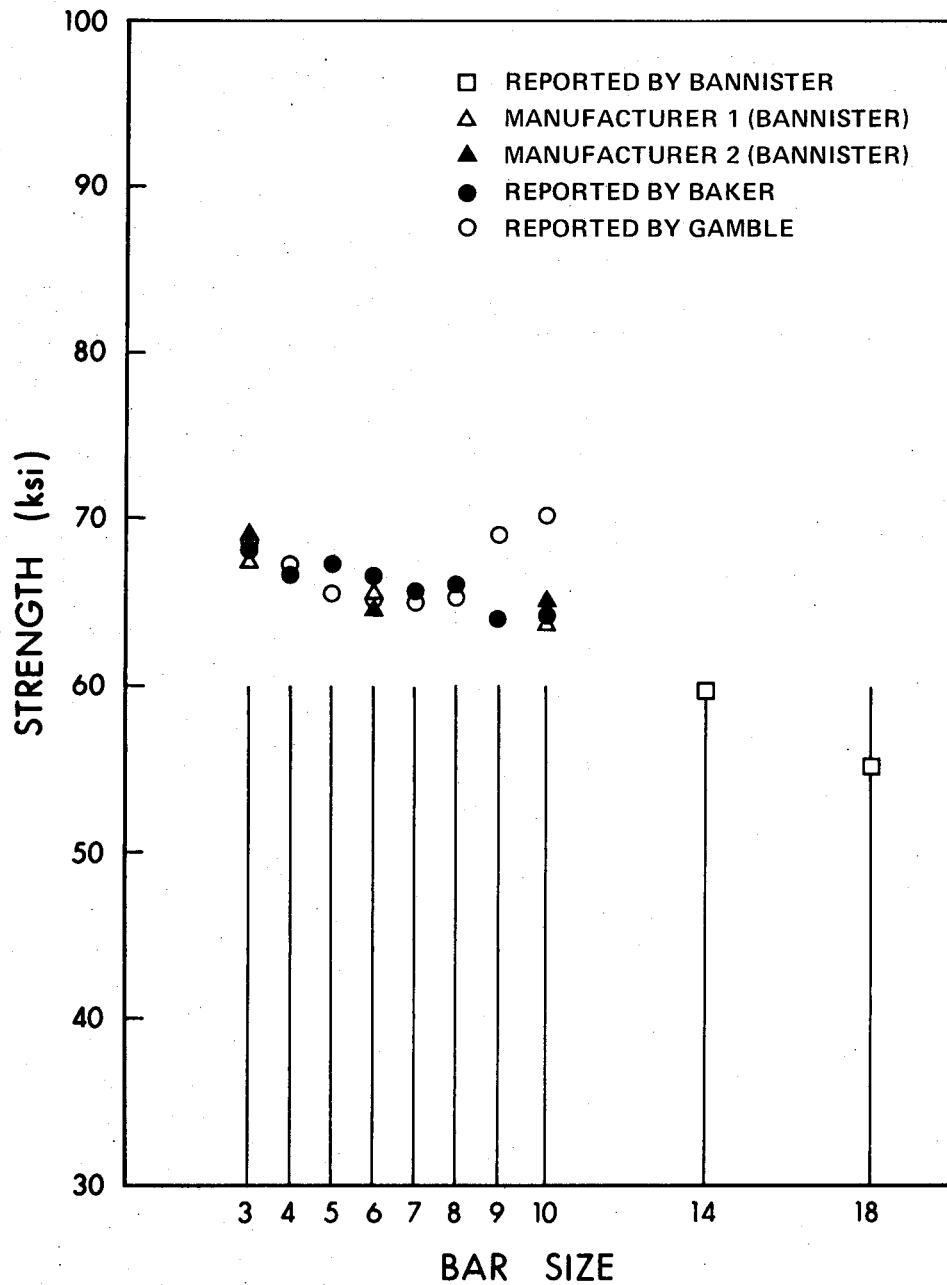


Figure A-6 Effect of Bar Diameter on Steel Strength, Grade 60

of a full size bar tends to show higher yield strength than the bar itself (24). Since some manufacturers may use these tests as a measure of quality control, the #14 and #18 bars tend towards a higher probability of passing through quality controls without developing the required strength.

An extremely limited amount of data is available for #14 and #18 bars. Tests on Grade 40, #14 bars carried out by Allen⁴ showed that the mean yield strength of #14 bars was 44 ksi, a 15% decrease from the strength of #3 to #11 bars produced by the same manufacturer. Some data has been reported by Gamble²⁴ for #14 and #18 bars of Grade 60 steel. The mean yield strengths were 60 ksi for #14 and 55 ksi for #18 bars. These strengths were referred to the nominal areas. Using the mean yield strength of Grade 60, #3 to #11 bars as 71.5 ksi (as per Study No. 3 in Table A-1) and a 3% adjustment for the deviation from the nominal area, the reduction in strength is approximately 13% for #14 bars and 21% for #18 bars. This comparison is, however, not truly justified since the data for both studies was not drawn from the same source. Nonetheless, it strongly indicates the understrength of #14 and #18 bars. Until more data is available, it seems reasonable that the yield strength of #14 and #18 bars should be reduced at least 15% below the yield strength of reinforcing bars with smaller diameter.

Summary

The modified log-normal distribution curves shown in Figures A-1 through A-4 seem to correlate well, particularly near the lower tails of the curves, with the available North American data for Grade 40 and Grade 60 reinforcing bars. The Probability Density Function for these curves can be calculated using the following equation:

$$PDF = \frac{c}{y\sigma_x\sqrt{2\pi}} \cdot \exp \left[-\frac{1}{2} \left(\frac{x-\bar{x}}{\sigma_x} \right)^2 \right]$$

where:

$$c = 0.43429$$

$$y = f_y - 34 \text{ ksi for Grade 40 bars}$$

$$y = f_y - 55 \text{ ksi for Grade 60 bars}$$

$$x = \text{Log}_{10} y$$

$$\bar{x} = 1.14482 \text{ for Grade 40 bars}$$

$$\bar{x} = 1.19456 \text{ for Grade 60 bars}$$

$$\sigma_x = 0.14866 \text{ for Grade 40 bars}$$

$$\sigma_x = 0.14112 \text{ for Grade 60 bars}$$

The mean yield strength of the selected data was found to be 48.8 ksi (c.o.v. = 10.7%) for Grade 40 bars and 71.5 ksi (c.o.v. = 7.7%) for Grade 60 bars. The modification constants were empirically established and found to be 34

ksi and 55 ksi for Grade 40 and Grade 60 steel respectively.

A value of 0.97 for the ratio A_e/A_n seems to be reasonable to account for deviations from the nominal areas. Similarly, for the evaluation of the static yield strength, at least 4 ksi should be deducted from the yield strength obtained in mill tests or at high strain rates allowed by ASTM specifications.

When calculating the yield strength of #14 and #18 reinforcing bars from the strength of bars of smaller sizes at least a 15% reduction should be used to account for the effect of the large diameter.

APPENDIX B

COLUMNS STUDIED

This appendix contains the details of the two major columns studied. Tables B-1 and B-2 are tables of the properties of the 12 in. and 24 in. columns respectively. Figures B-1 and B-2 are diagrams of each column showing the designer's properties and the mean values of the column properties used in the Monte Carlo calculations.

Table B-1

Properties of the 12 in. Column Assumed in the Calculations

	Specified	Mean In-	σ	C.O.V.
		situ		
<u>Material Strengths</u>				
Concrete Strength	3000 psi.	3712 psi.	---	0.176
Steel Yield Strength	40 ksi.	48.8 ksi.	1.41 ksi.	---

Dimensions

b, h	12.00 in.	12.06 in.	0.280 in.	---
d	9.75 in.	9.51 in.	0.166 in.	---
d'	2.25 in.	2.55 in.	0.166 in.	---
A _S	1.76 sq.in.	---	---	---
A _S '	0.88 sq.in.	---	---	---
s	12.00 in.	12.00 in.	---	---
b", d"	9.00 in.	8.47 in.	0.166 in.	---
A _S "	0.11 sq.in.	0.11 sq.in.	---	---

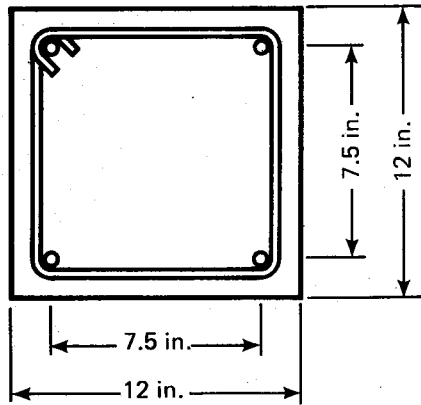
Individual Longitudinal Steel Bars

ASB(1) to ASB(4)	0.44 sq.in.	0.44 sq.in.	---	---
DS(1), DS(2)	2.25 in.	2.55 in.	0.166 in.	---
DS(3), DS(4)	9.75 in.	9.51 in.	0.166 in.	---

Table B-2

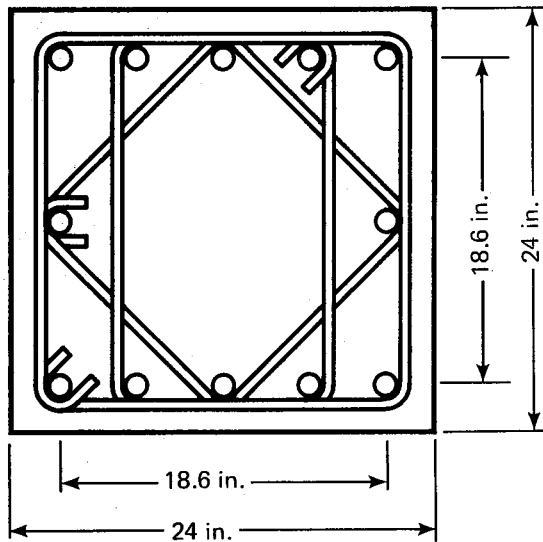
Properties of the 24 in. Column Assumed in the Calculations

	Specified	Mean In- situ	σ	C.O.V.
<u>Material Strengths</u>				
Concrete Strength	3000 psi.	3712 psi.	---	0.176
Steel Yield Strength	40 ksi.	48.8 ksi	1.41 ksi.	---
<u>Dimensions</u>				
b, h	24.00 in.	24.06 in.	0.280 in.	---
d	21.30 in.	21.01 in.	0.166 in.	---
d'	2.70 in.	3.05 in.	0.166 in.	---
A _S	18.72 sq.in.	---	---	---
A _S '	7.80 sq.in.	---	---	---
s	12.00 in.	12.00 in.	---	---
b", d"	20.50 in.	19.87 in.	0.166 in.	---
A _S "	0.20 sq.in.	0.20 sq.in.	---	---
<u>Individual Longitudinal Steel Bars</u>				
ASB(1) to ASB(12)	1.56 sq.in.	1.56 sq.in.	---	---
DS(1) to DS(5)	2.70 in.	3.05 in.	0.166 in.	---
DS(6), DS(7)	12.00 in.	12.07 in.	0.993 in.	---
DS(8) to DS(12)	21.30 in.	21.01 in.	0.166 in.	---



- $f_y = 40,000$ psi
- $f'_c = 3,000$ psi
- $A_s = 2\# 6$ bars
- $A'_s = 2\# 6$ bars
- $A''_s = \#3 @ 12$ in

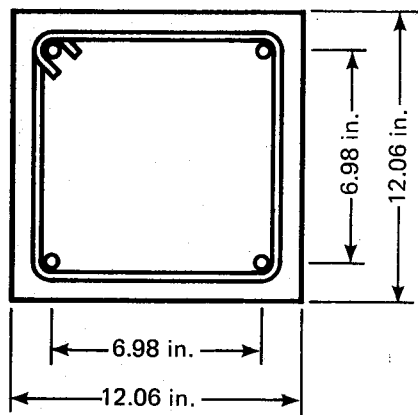
12 in. x 12 in. COLUMN



- $f_y = 40,000$
- $f_y = 40,000$ psi
- $f'_c = 3,000$ psi
- $A_s = 7\# 11$ bars
- $A'_s = 5\# 11$ bars
- $A''_s = \#4 @ 12$ in.
in sets of 3

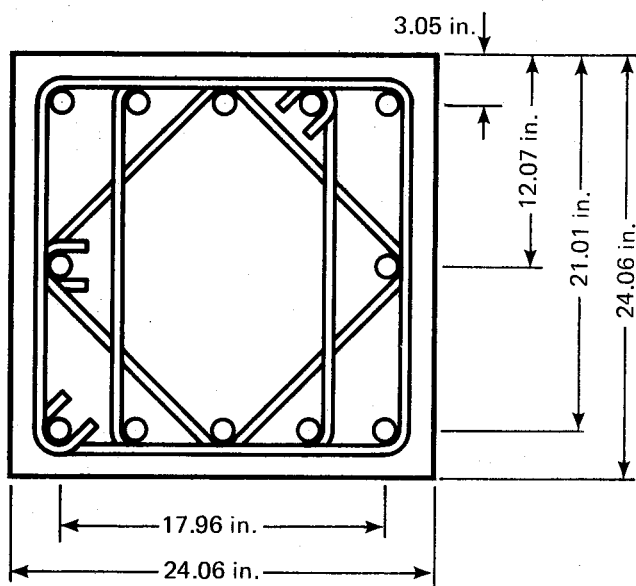
24 in. x 24 in. COLUMN

Figure B-1 Nominal or Designer's Properties of the 12 in. and 24 in Columns



$$\begin{aligned} \bar{f}_y &= 48,800 \text{ psi} \\ \bar{f}_c &= 3712 \text{ psi} \\ A_s &- 2\# 6 \text{ bars} \\ A'_s &- 2\# 6 \text{ bars} \\ A''_s &- \#3 @ 12 \text{ in} \end{aligned}$$

12 in. x 12 in. COLUMN



$$\begin{aligned} \bar{f}_y &= 48,800 \text{ psi} \\ \bar{f}_c &= 3712 \text{ psi} \\ A_s &- 7\# 11 \text{ bars} \\ A'_s &- 5\# 11 \text{ bars} \\ A''_s &- \#4 @ 12 \text{ in.} \\ &\text{in sets of 3} \end{aligned}$$

24 in. x 24 in. COLUMN

Figure B-2 Mean Values of the Properties of the 12 in. and 24 in Columns

APPENDIX C

FLOW DIAGRAMS OF THE MONTE CARLO PROGRAM

This appendix contains detailed flow diagrams of the complete Monte Carlo Program including:

The Main Program

Subroutine PROP

Subroutine ACI

Subroutine ASTEEL

Subroutine CURVE

Subroutine THMEAN

Subroutine THEORY

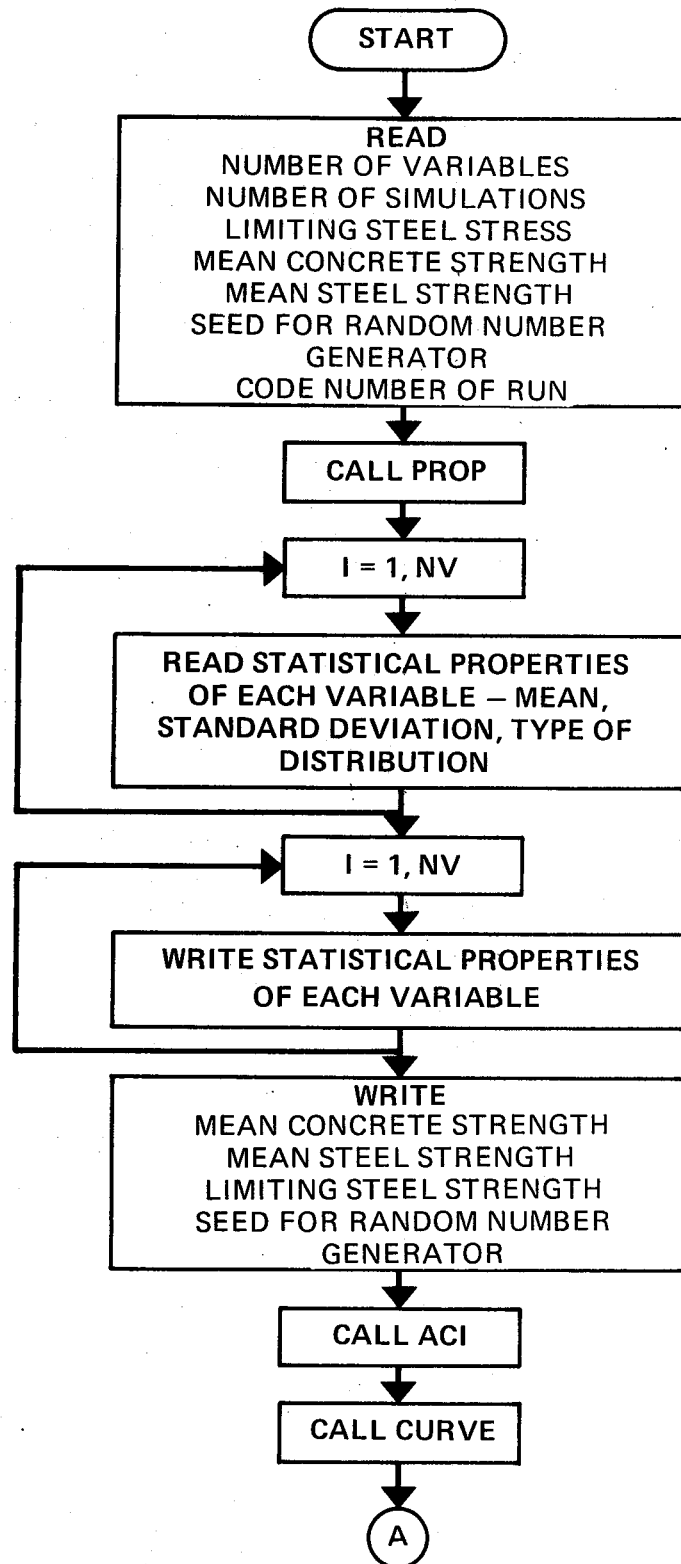
Subroutine AXIAL

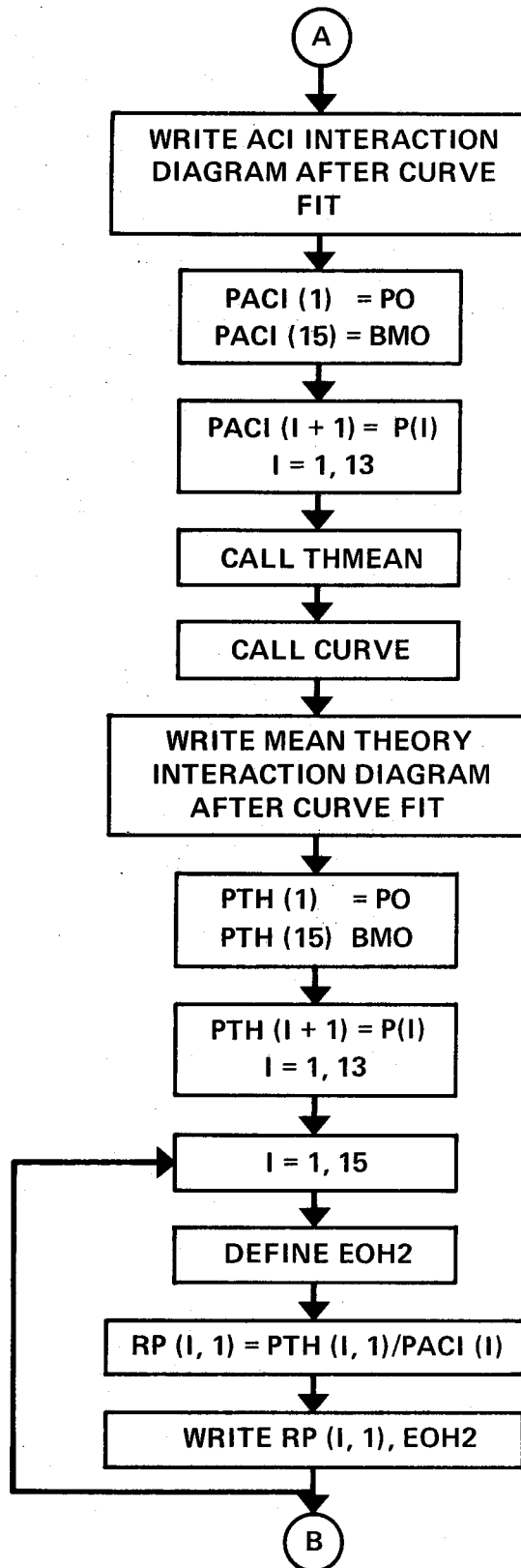
Subroutine FSTEEL

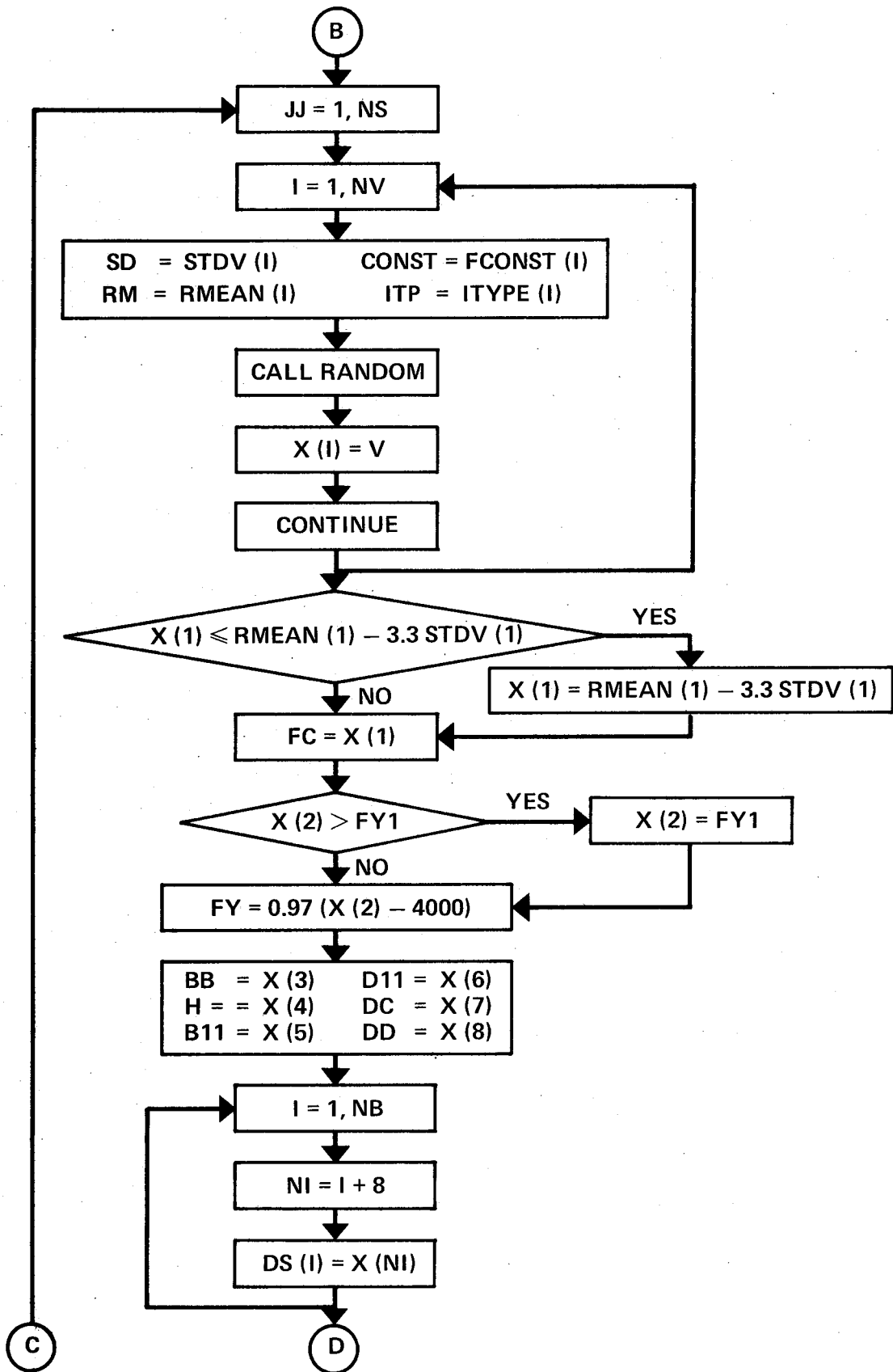
Subroutine RANDOM

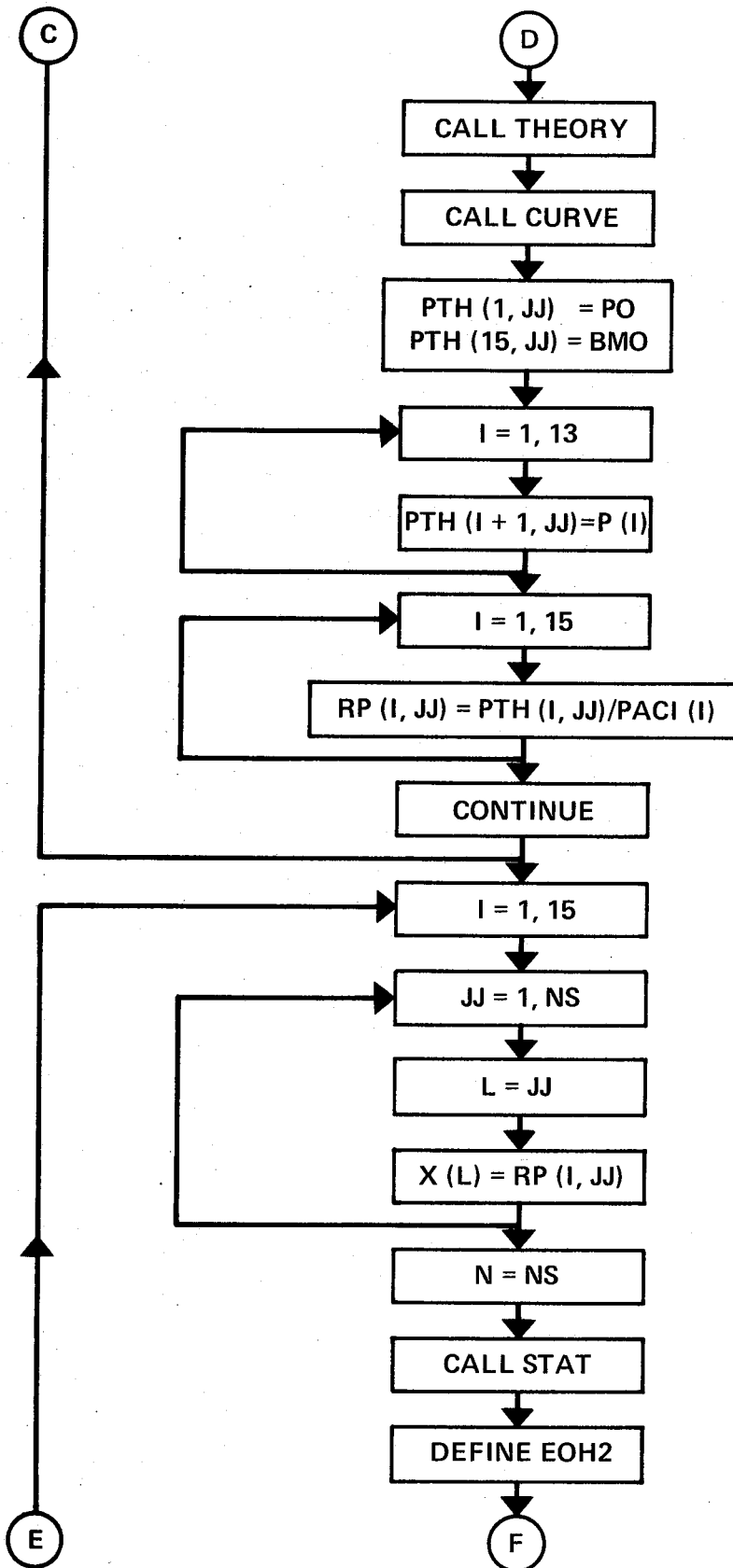
Subroutine STAT

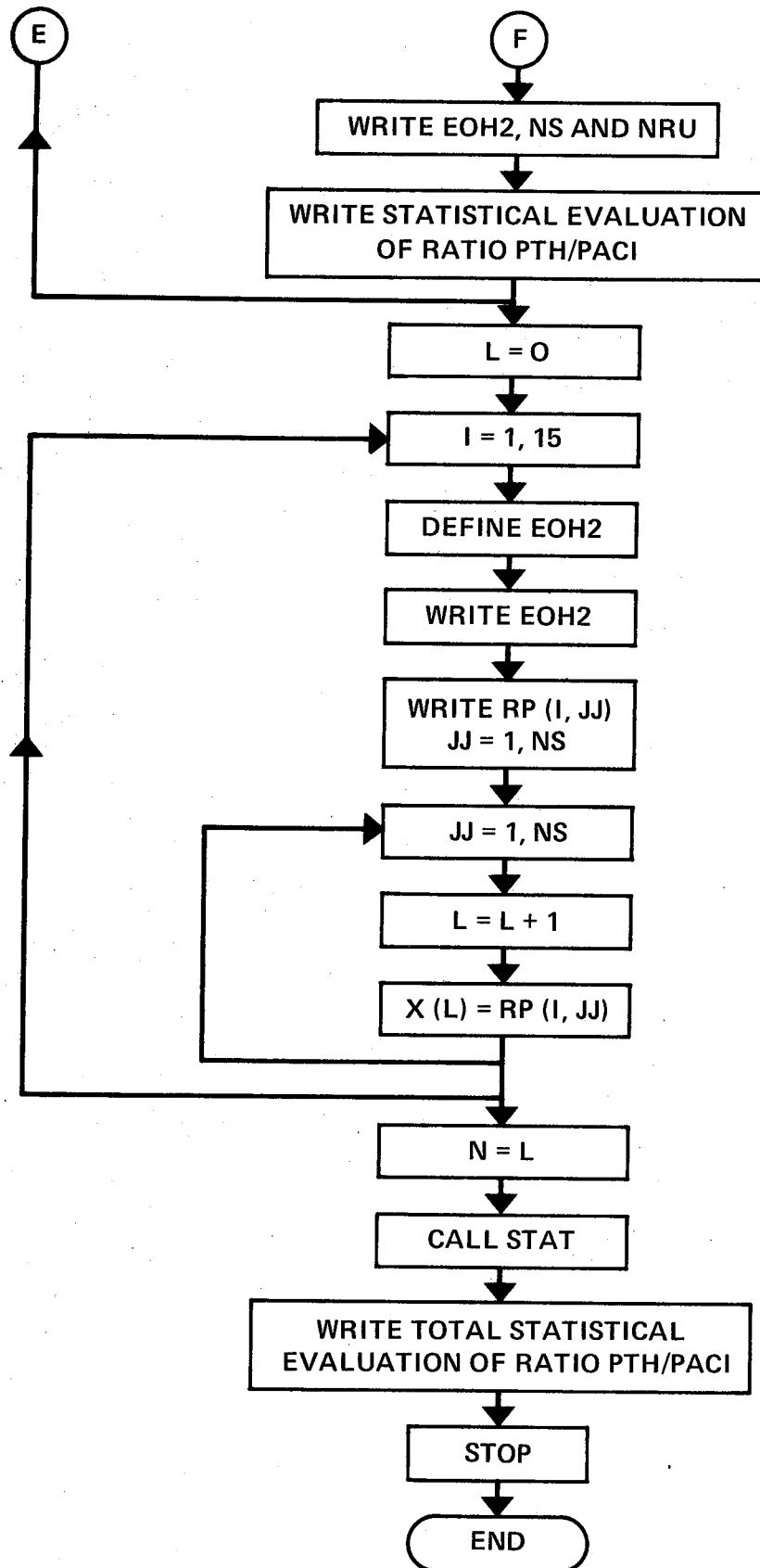
MONTE CARLO PROGRAM



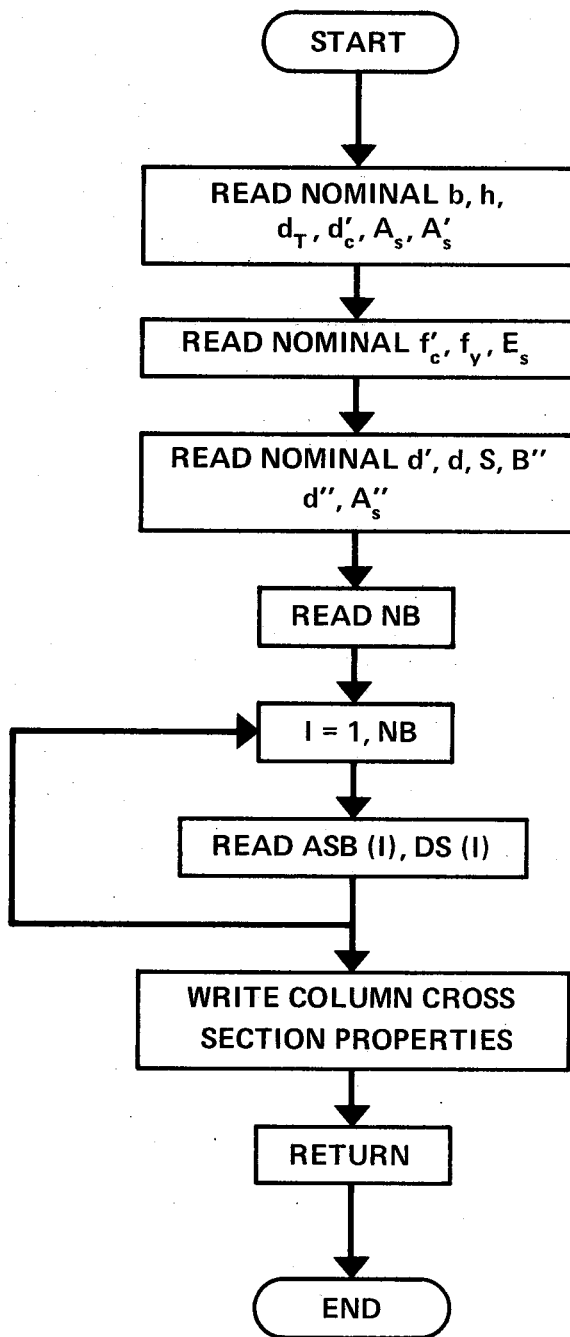




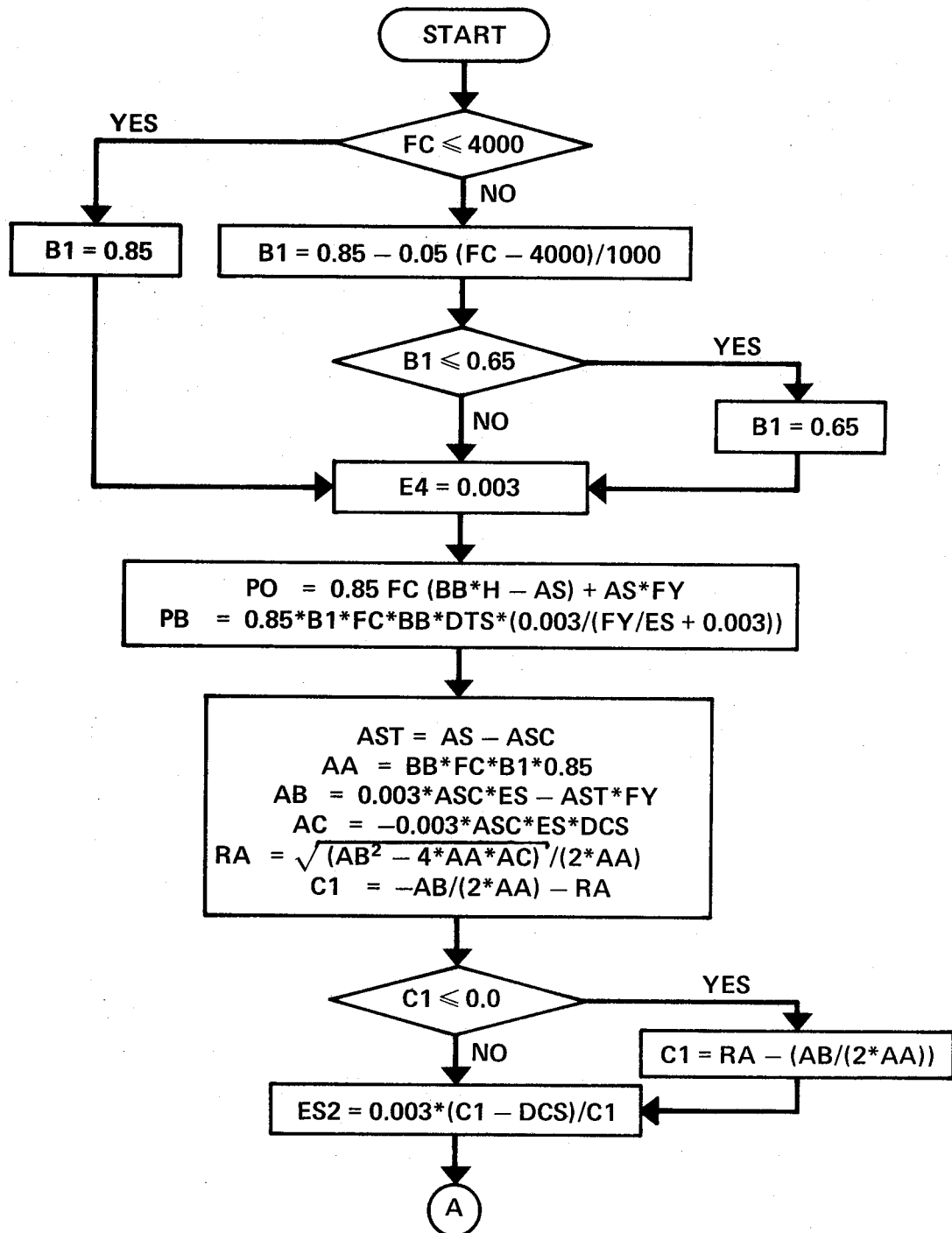


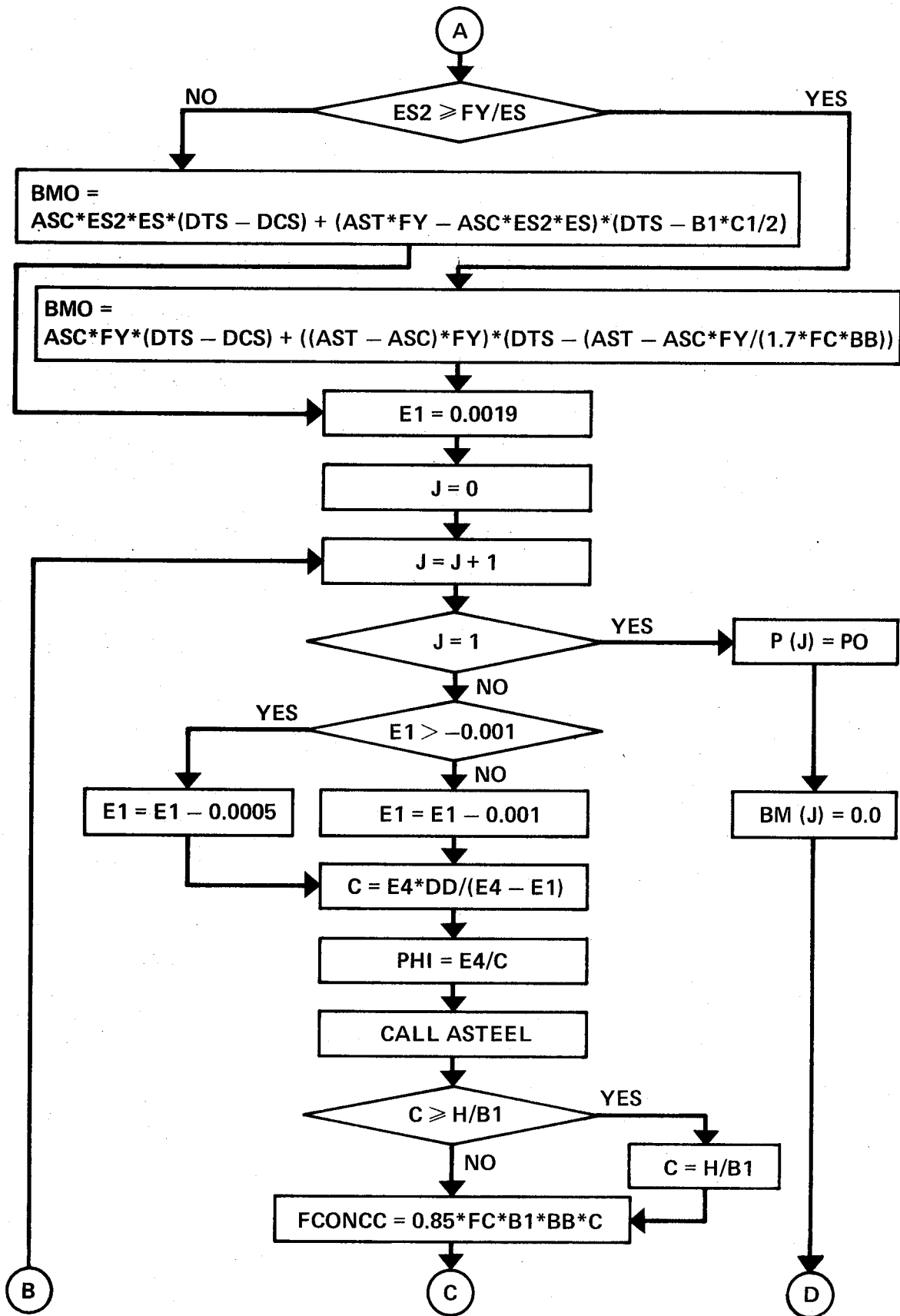


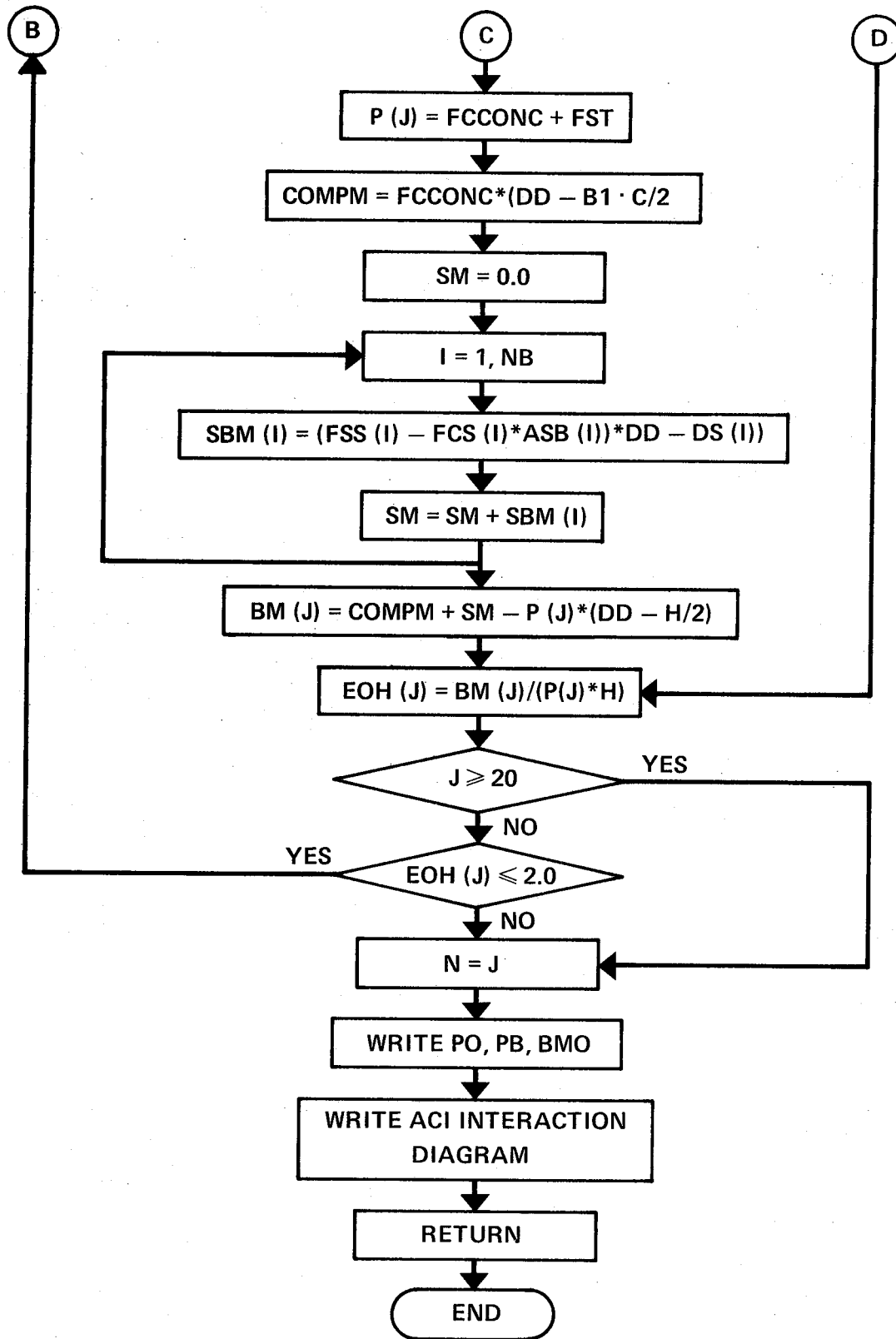
SUBROUTINE PROP



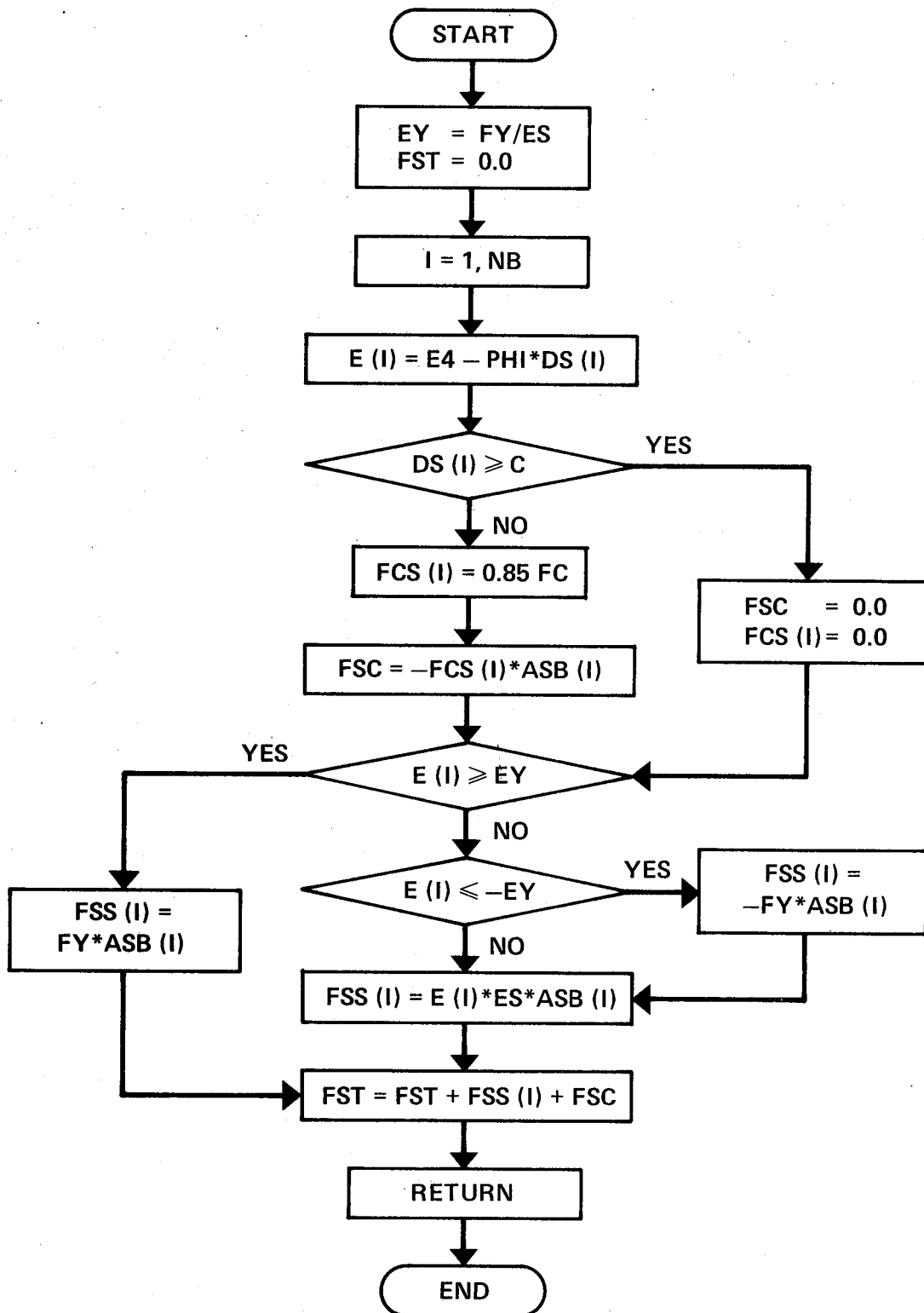
SUBROUTINE ACI



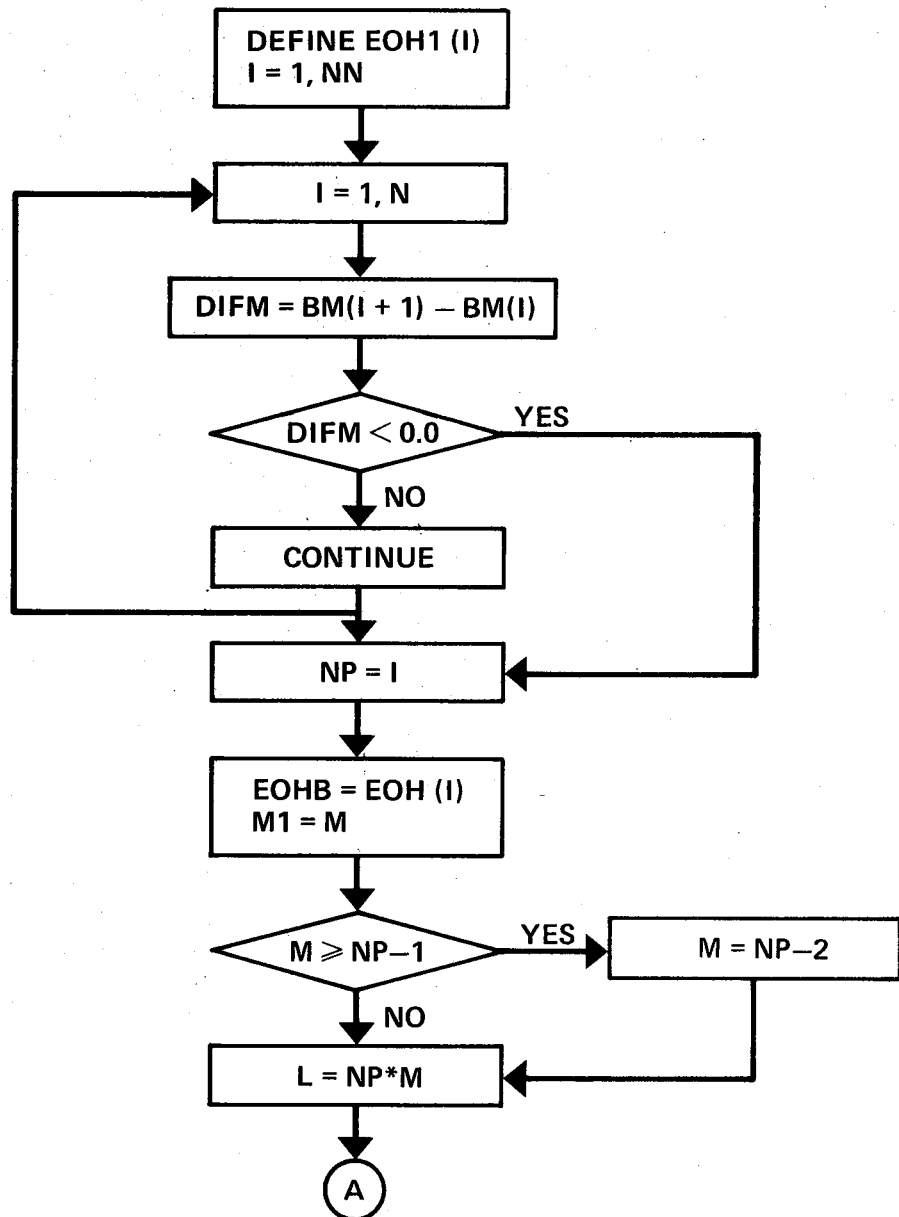


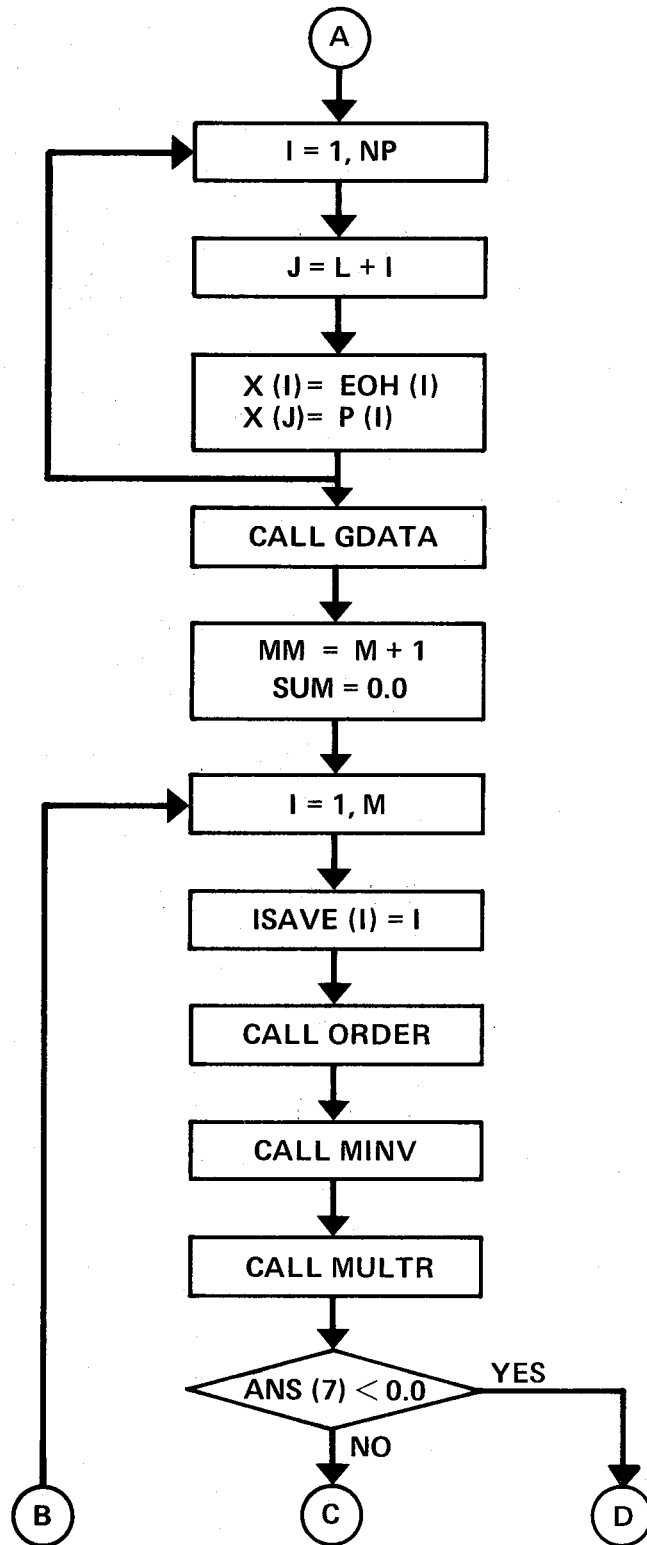


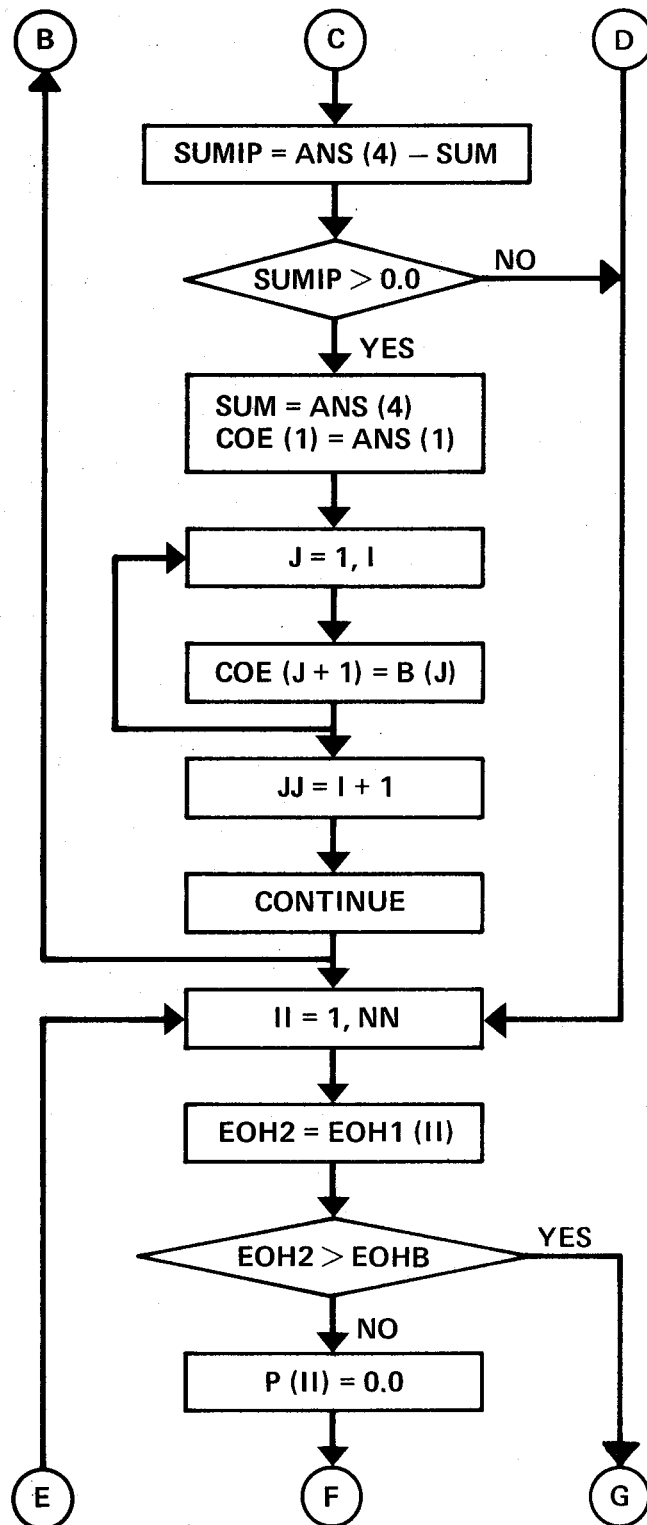
SUBROUTINE ASTEEL

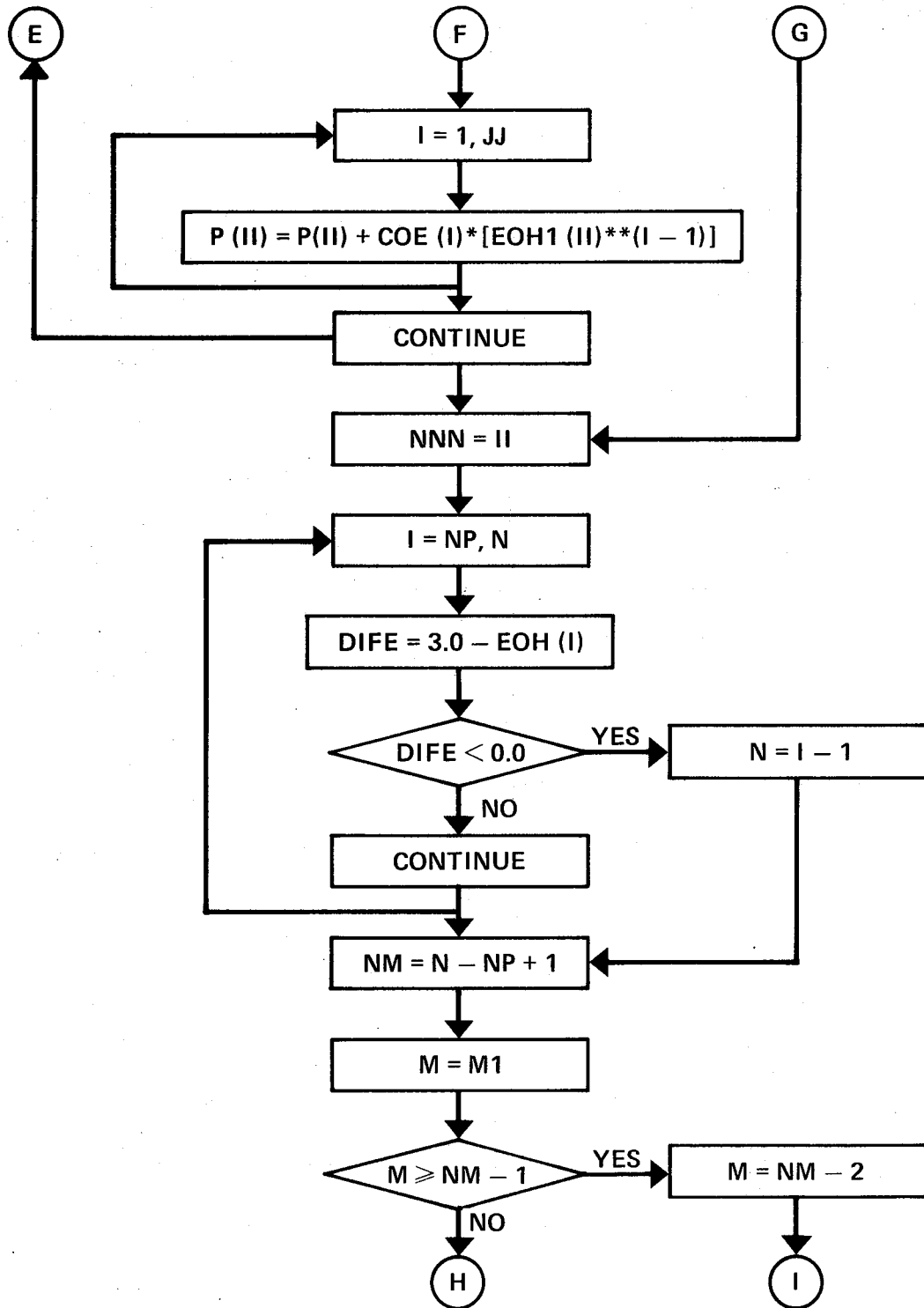


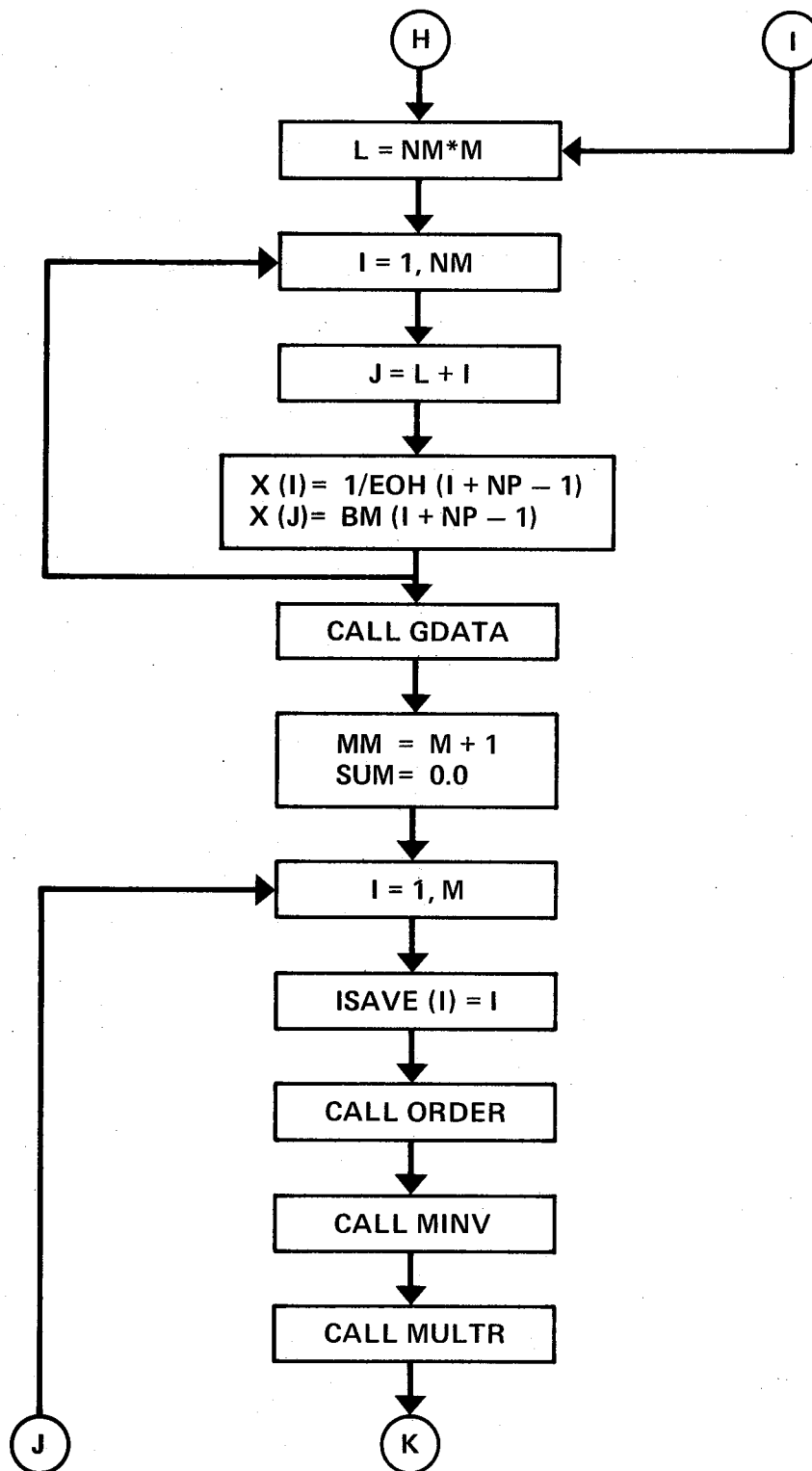
SUBROUTINE CURVE

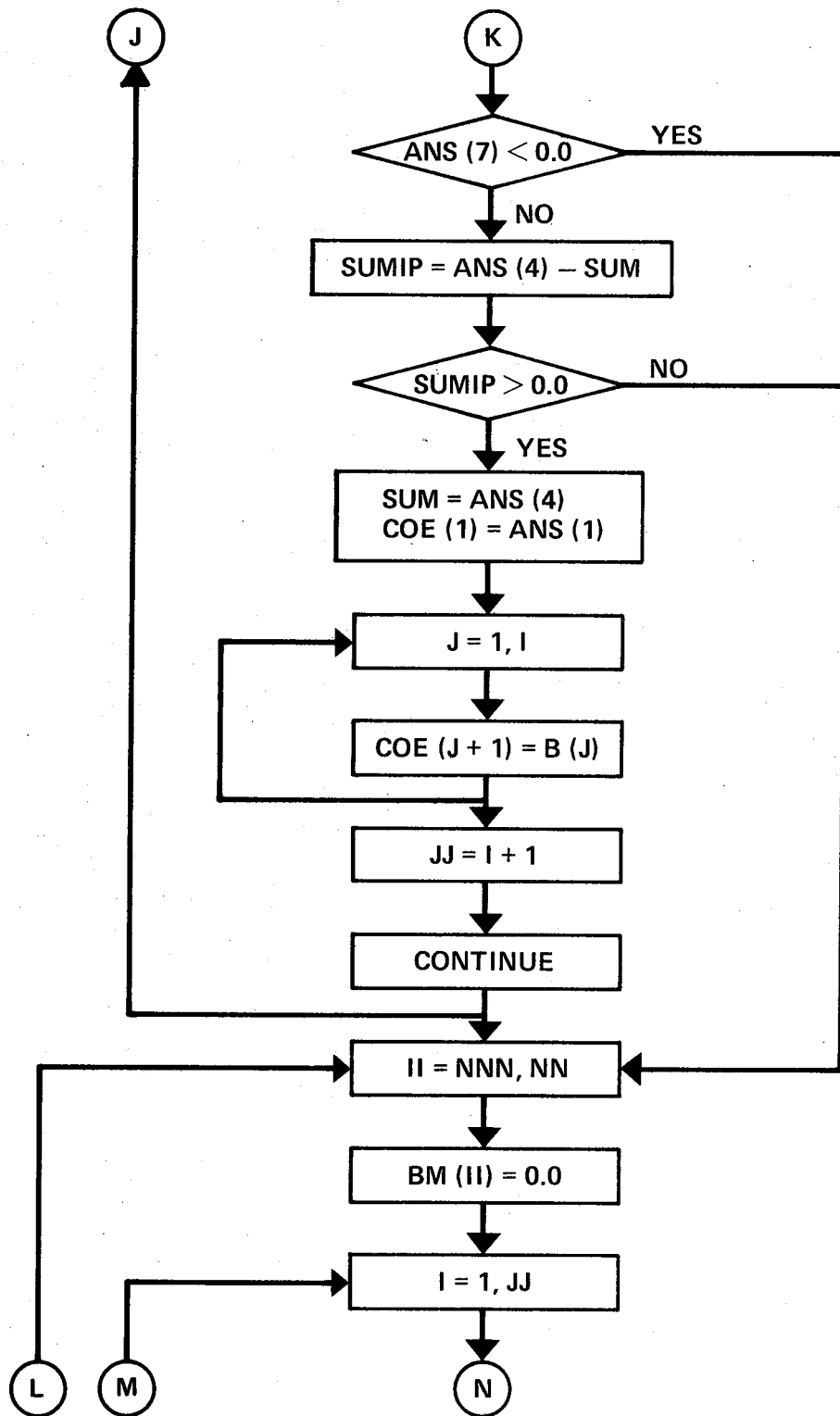


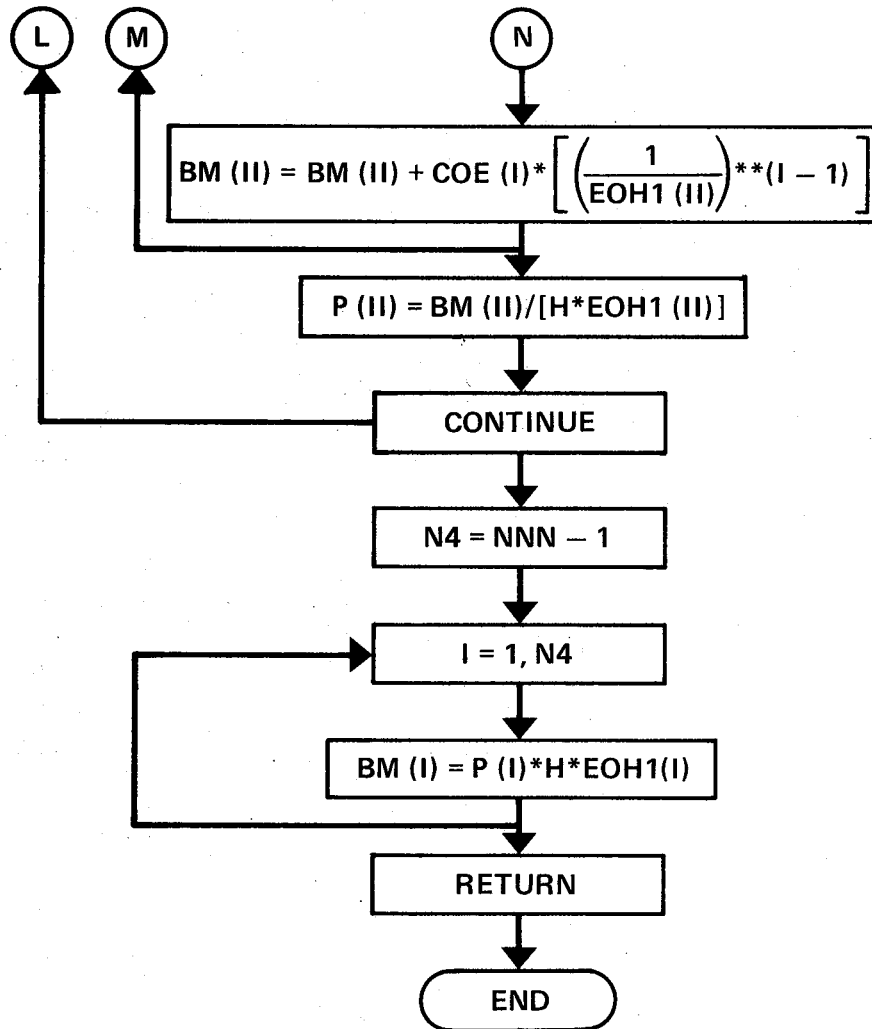




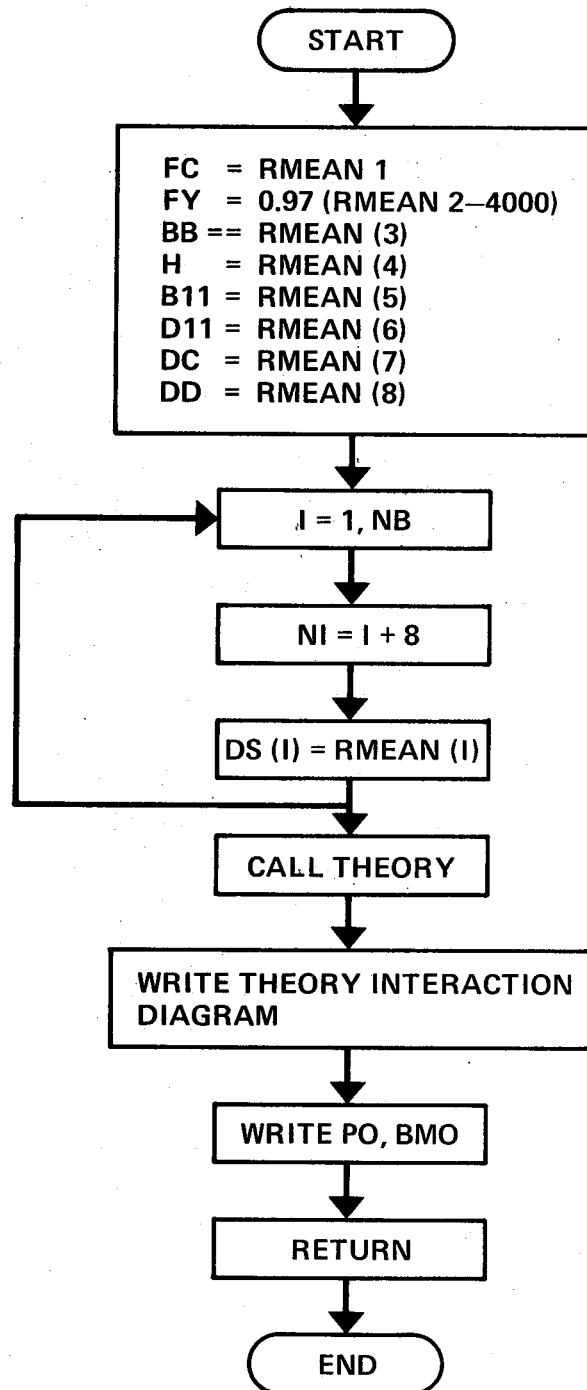




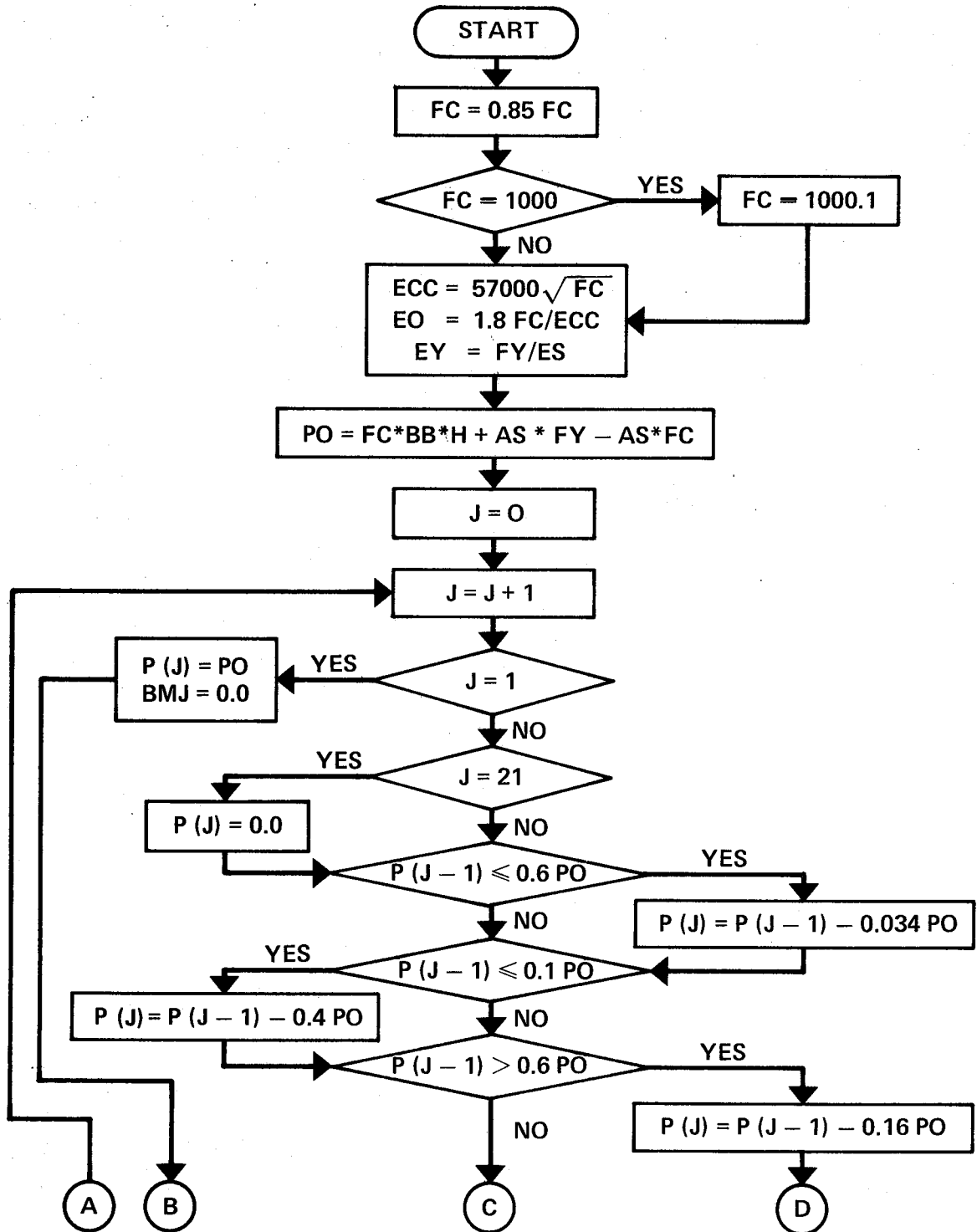


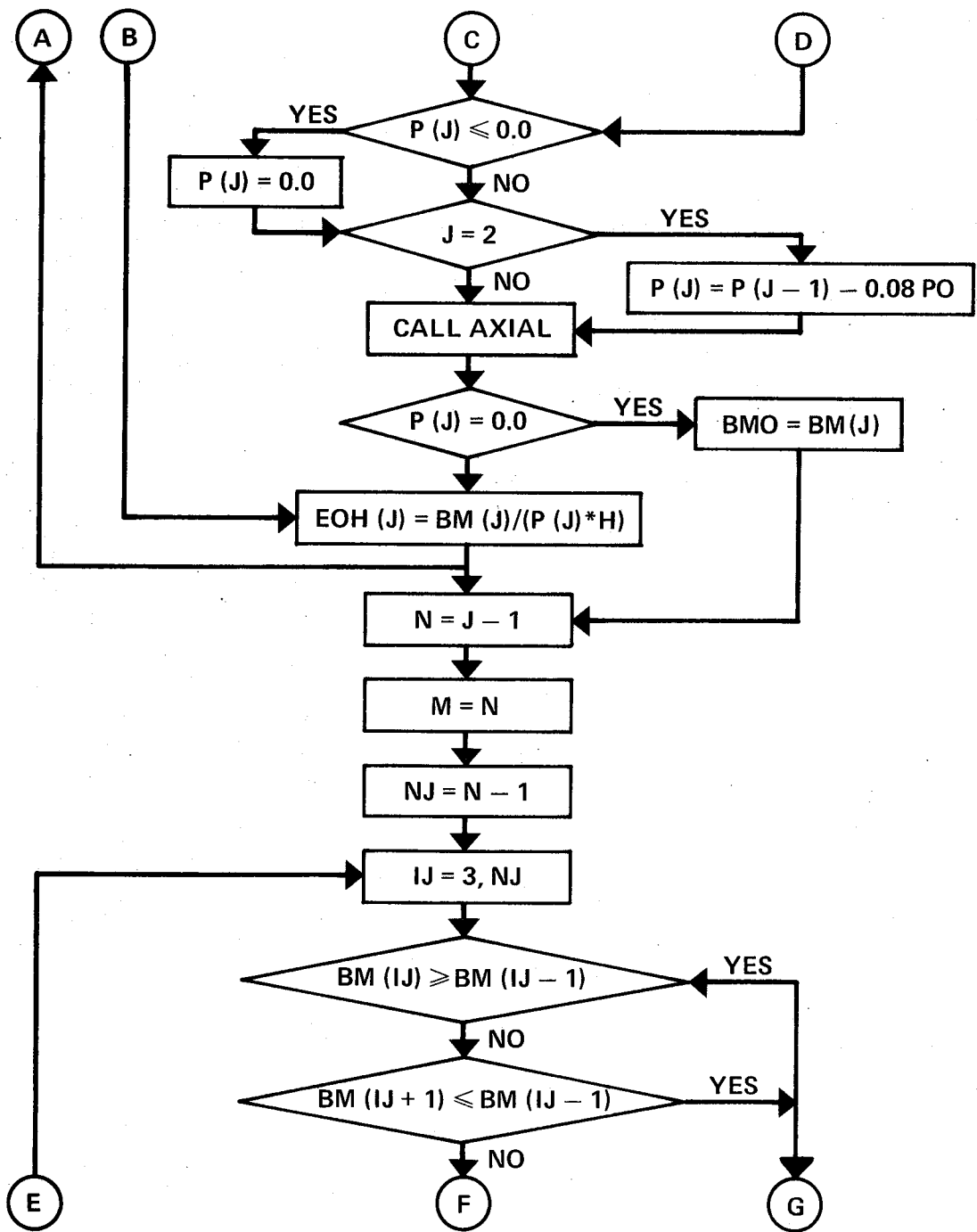


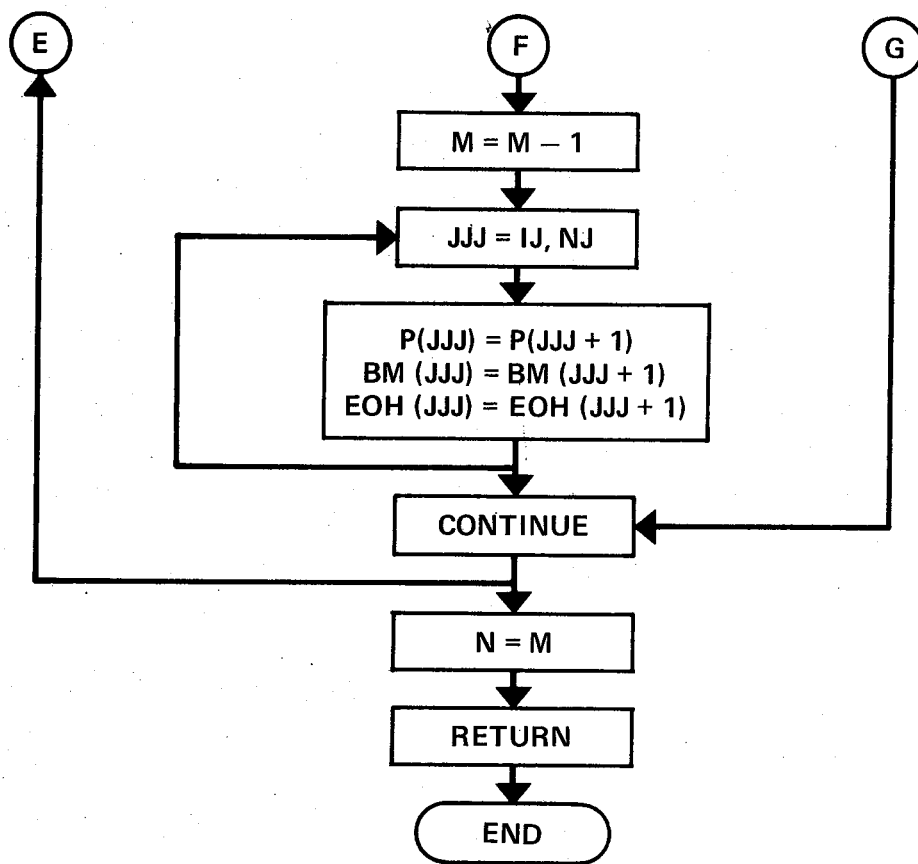
SUBROUTINE THMEAN



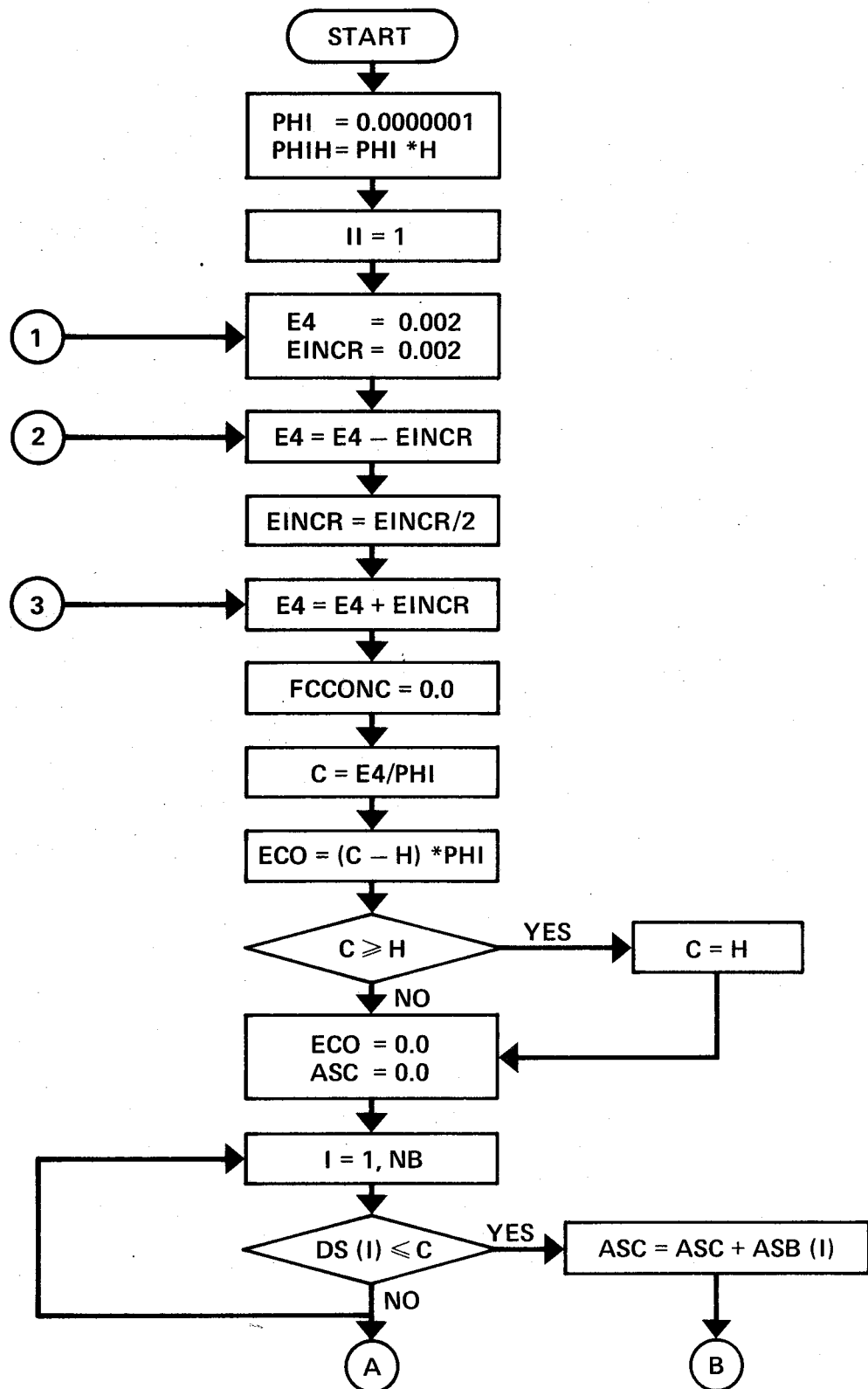
SUBROUTINE THEORY

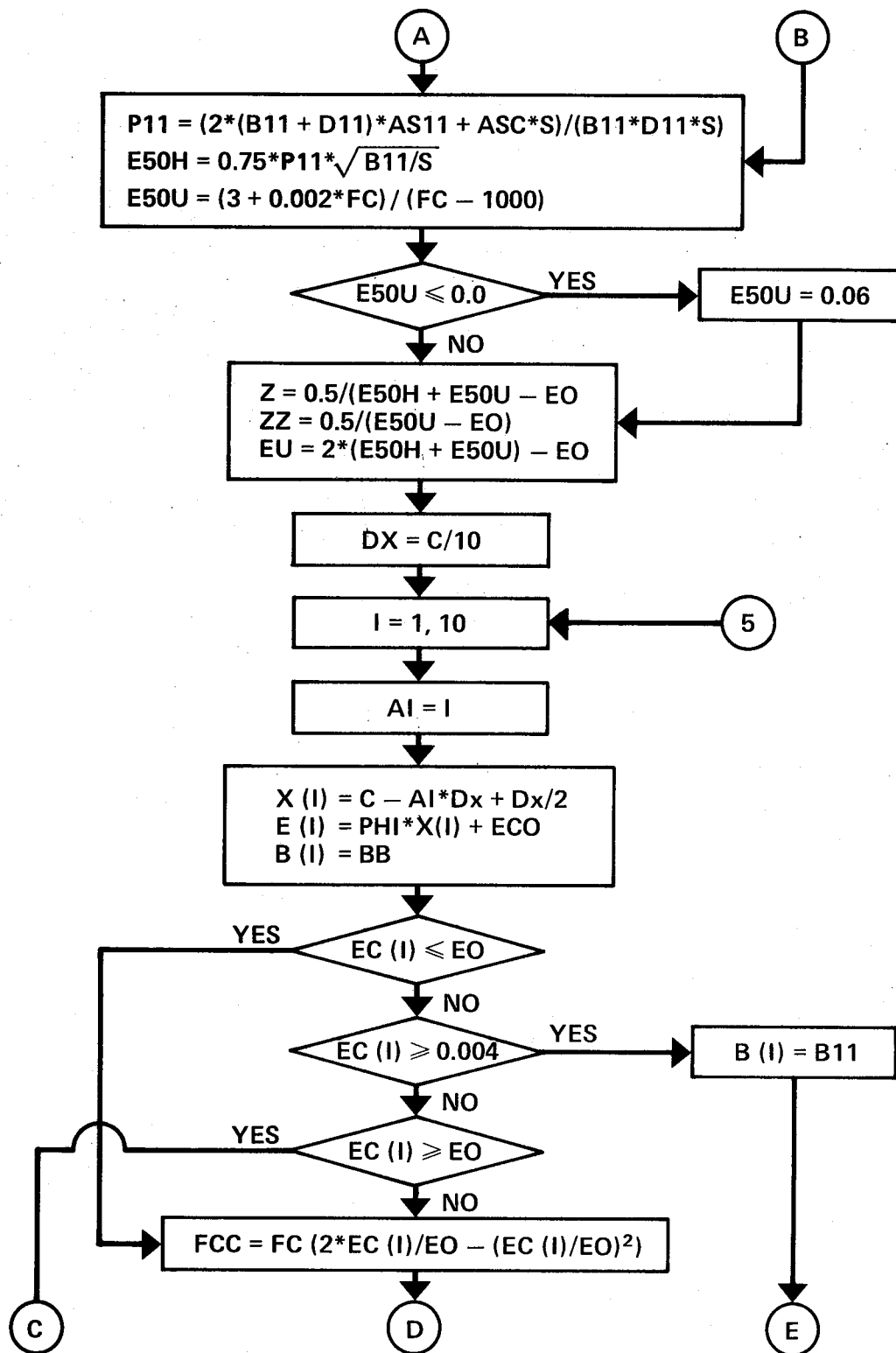


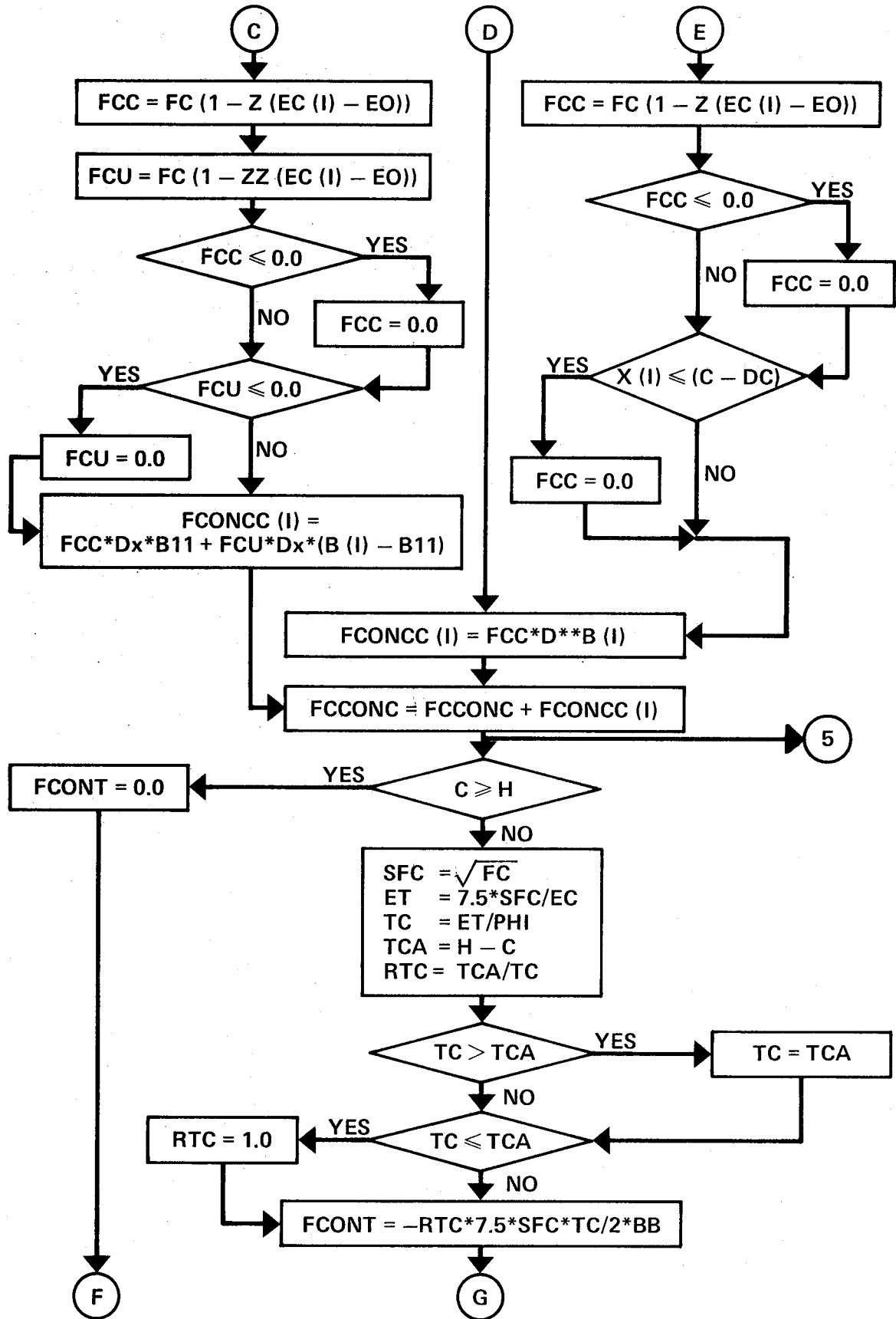


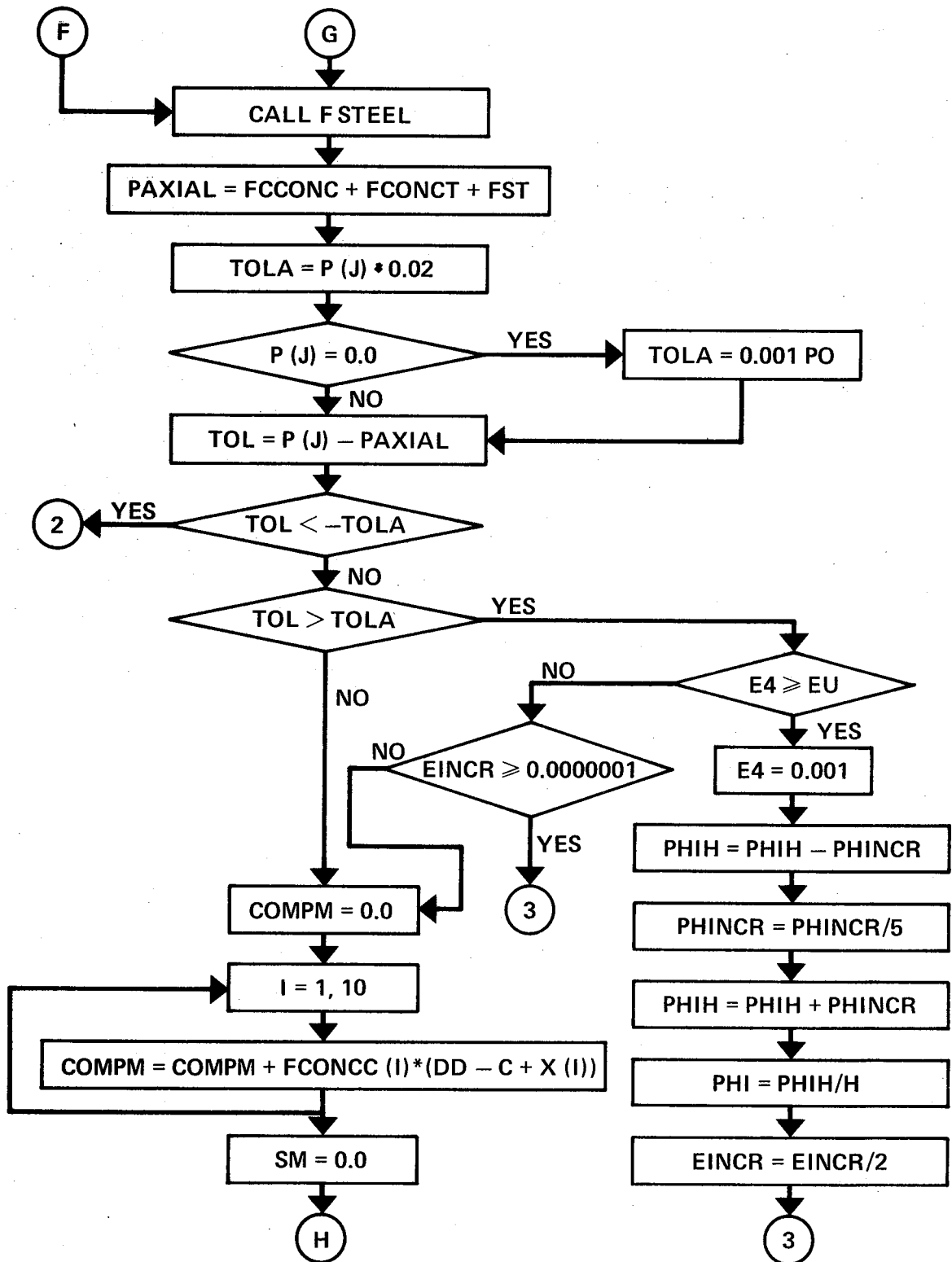


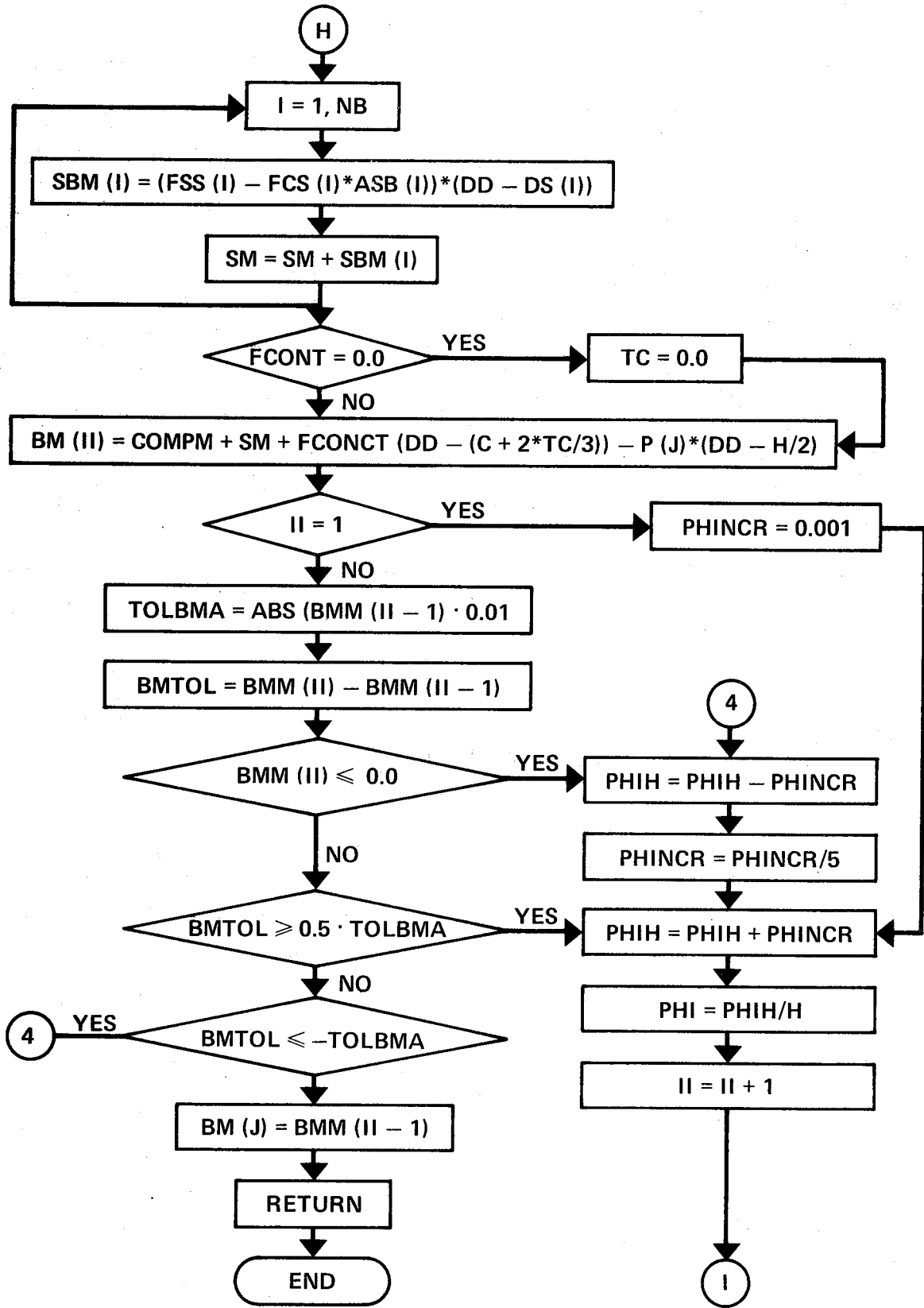
SUBROUTINE AXIAL



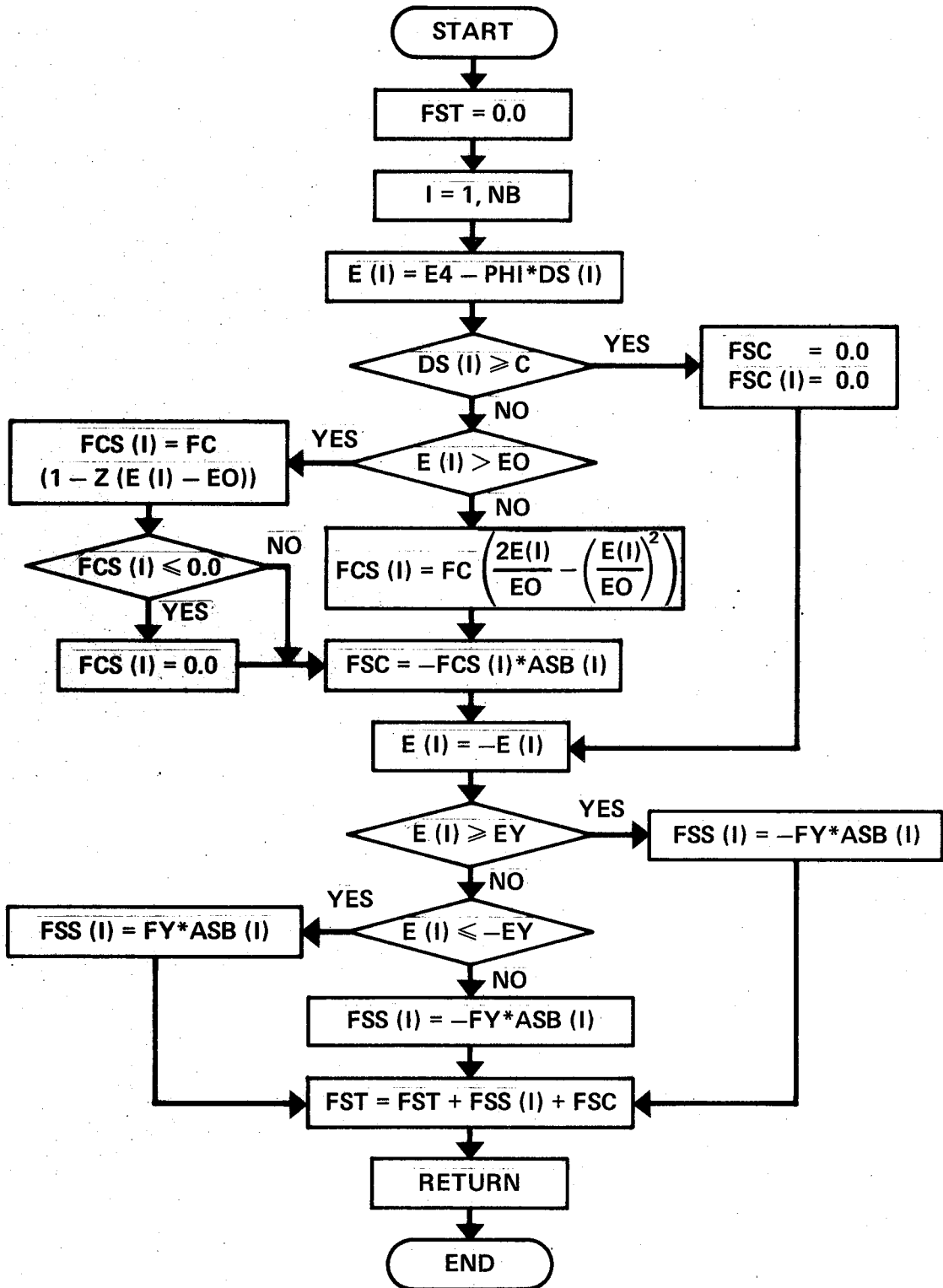




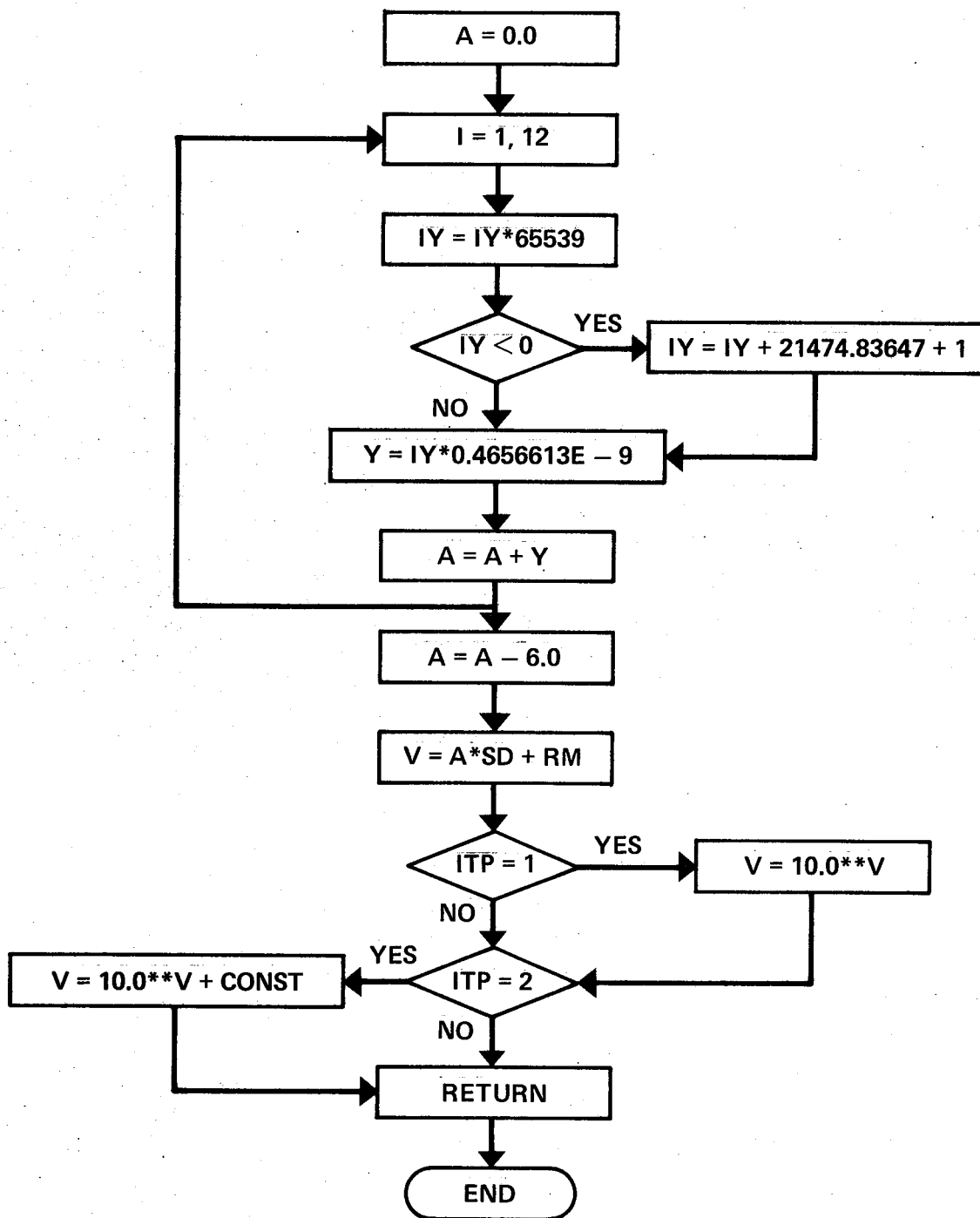




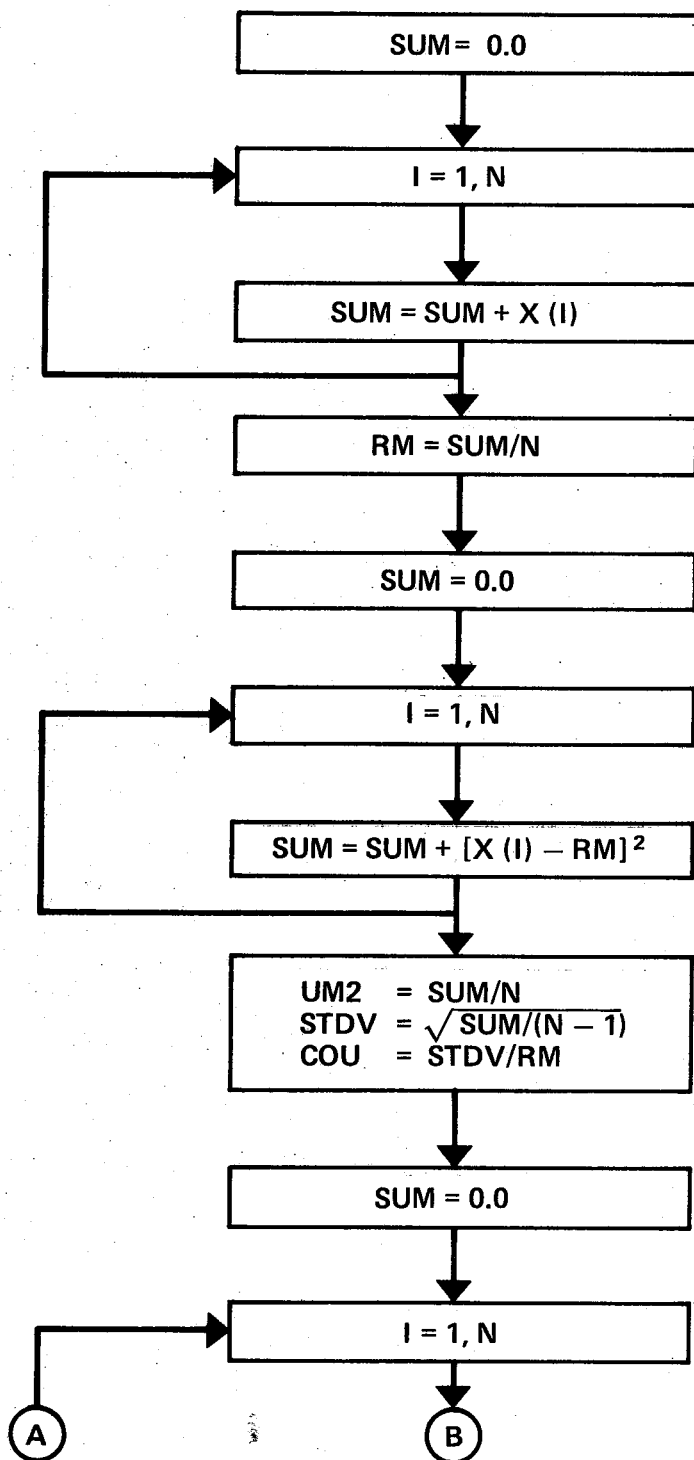
SUBROUTINE F STEEL

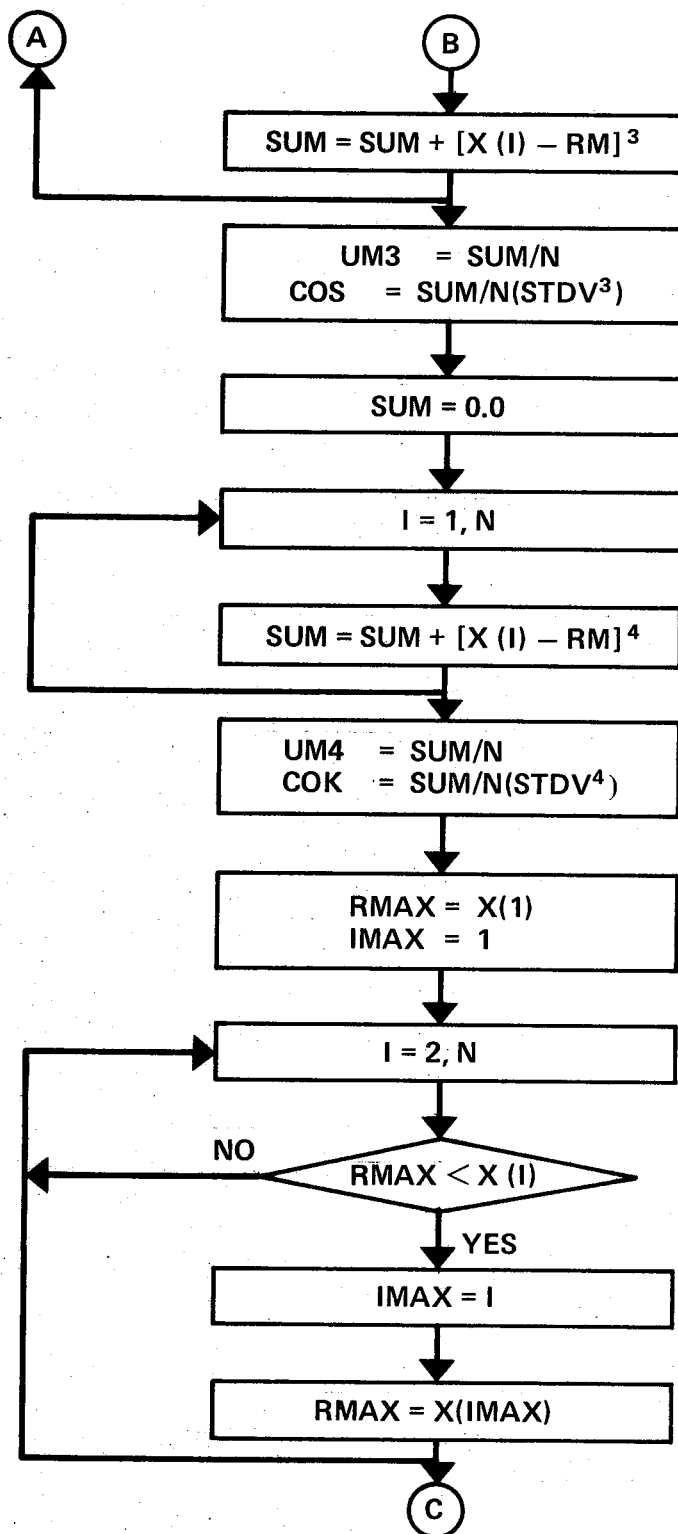


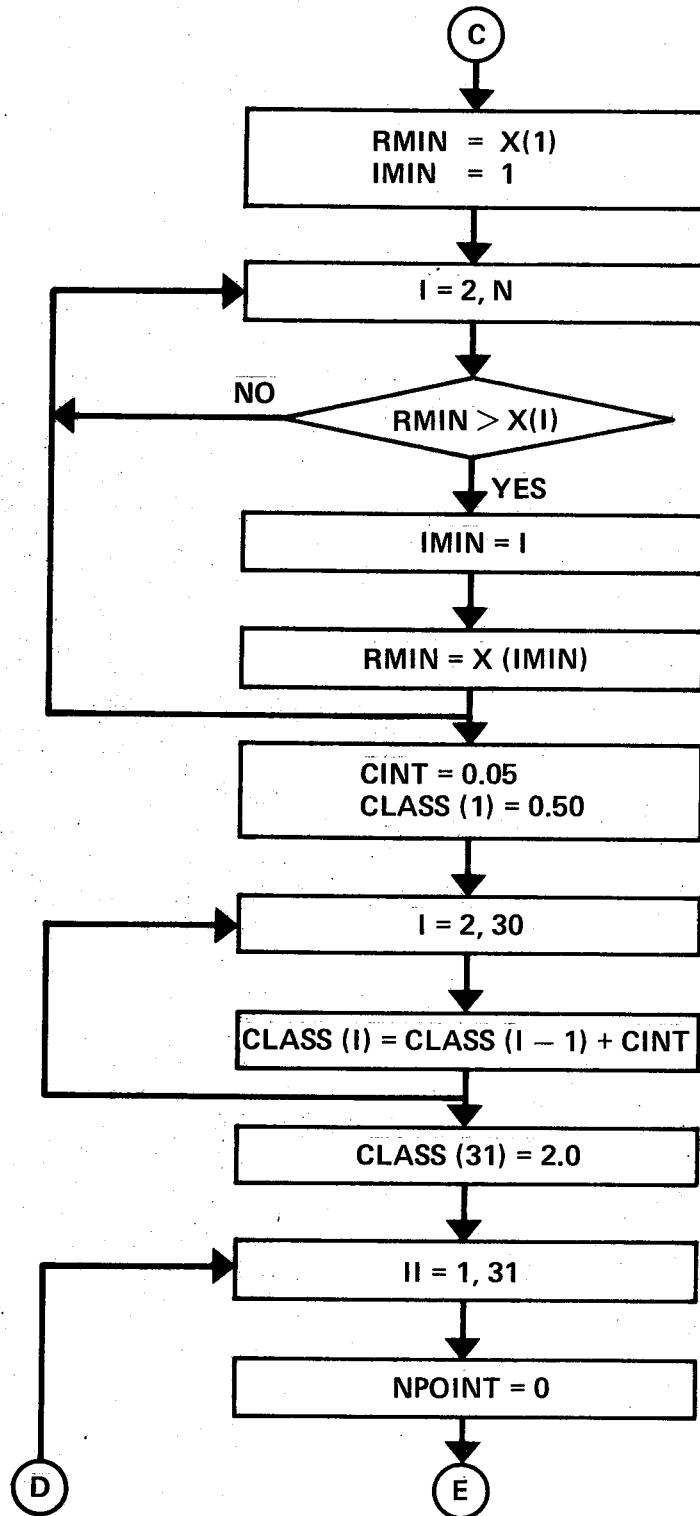
SUBROUTINE RANDOM

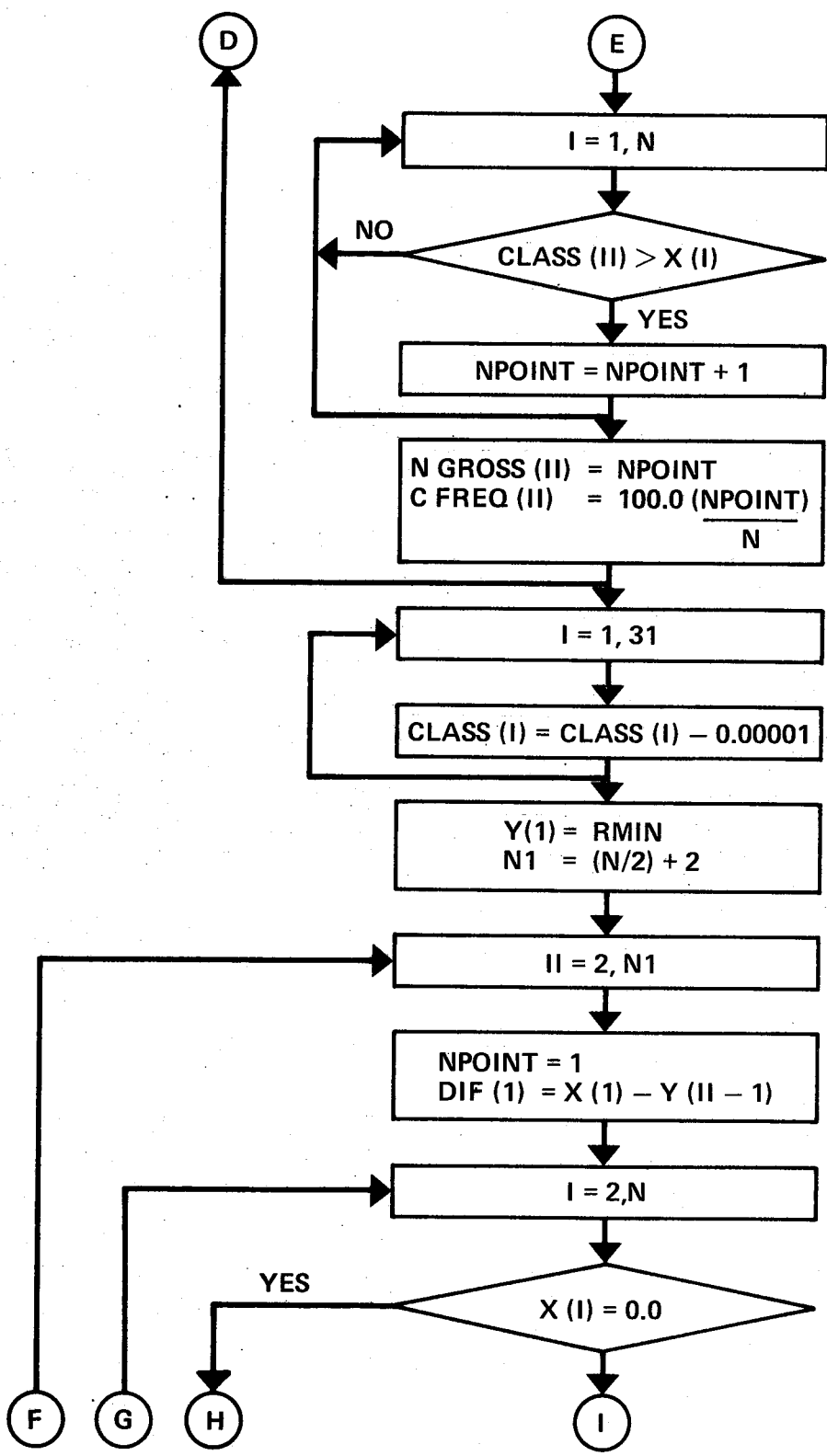


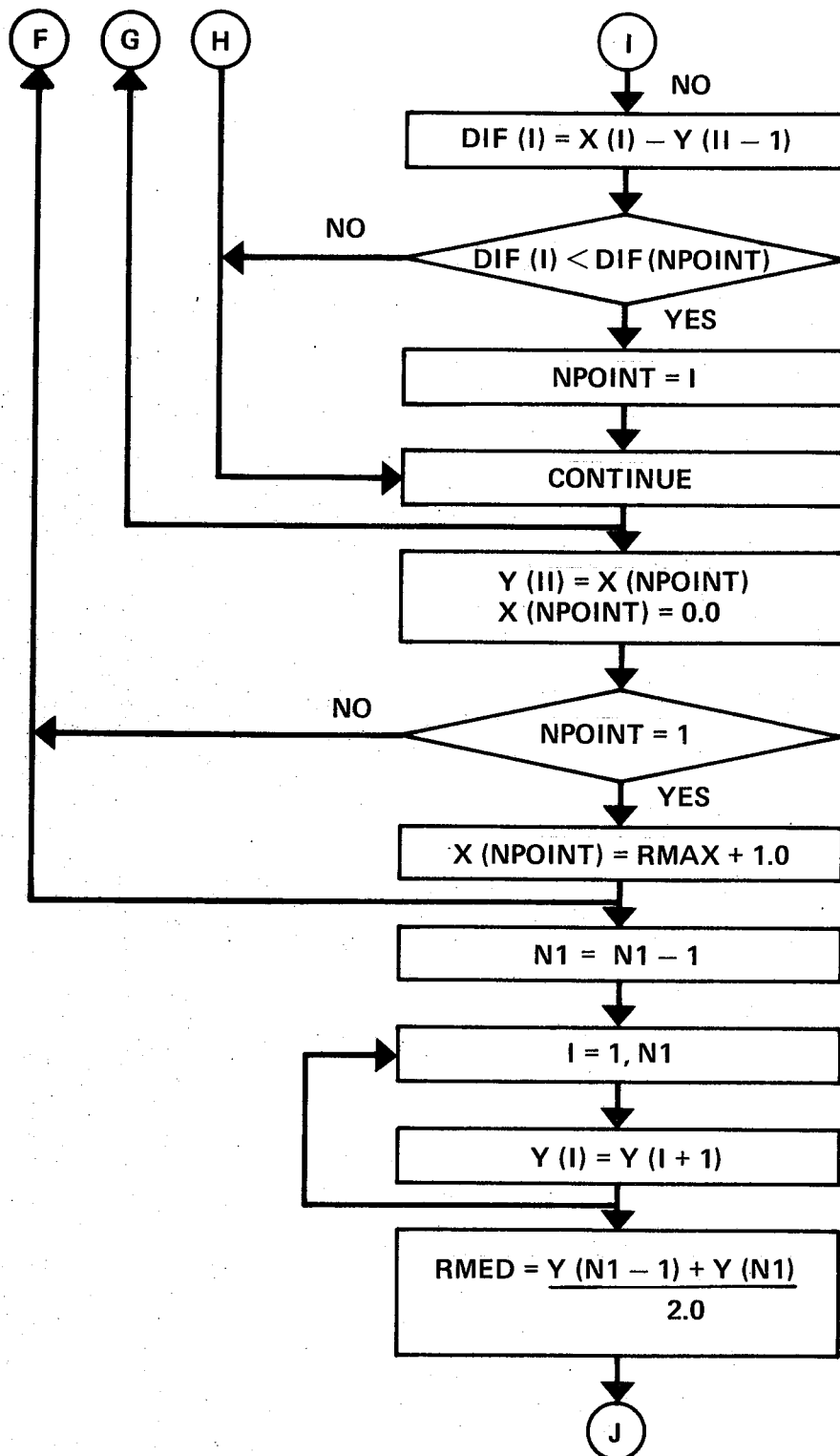
SUBROUTINE STAT

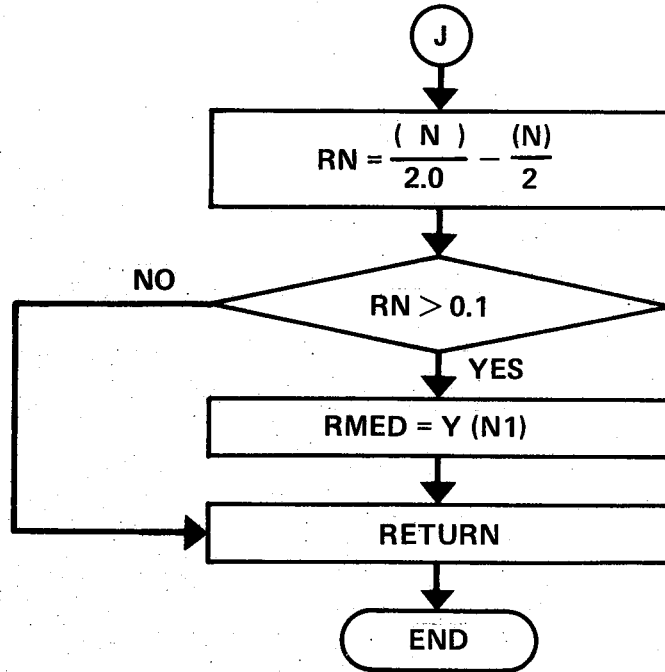












APPENDIX D

LISTING OF THE MONTE CARLO PROGRAM

This appendix contains a complete listing of the Monte Carlo Program. The modified IBM Subroutine MULT to MULTR is also listed. The listing includes:

The Main Program
Subroutine THMEAN
Subroutine ACI
Subroutine ASTEEL
Subroutine PROP
Subroutine CURVE
Subroutine RANDOM
Subroutine THEORY
Subroutine AXIAL
Subroutine FSTEEL
Subroutine STAT
Subroutine TMULTR

```

SLIST P2 ON *PRINT*
1
2 C*****
3 COMMON N,EOH1(13),PO,BMO,DCS,DTS
4 COMMON FC,FY,ES,BB,H,DC,DD,AS,AS11,B11,D11,S,C,ZZ,NRU
5 COMMON PHI,EO,J,Z,ECC,EY,FCONCC(20),ASC,EOH(40),FCONST(25)
6 COMMON X(16000),EC(20),B(20),P(40),BMM(1000),BM(40),FCS(20)
7 COMMON FST,E(20),NB,DS(20),ASB(20),FSS(20),SBM(20)
8 DIMENSION PACI(15),PTH(15,2000),RP(15,2000)
9 DIMENSION RMEAN(25),STDV(25),ITYPE(25)
10 DIMENSION CLASS(31),CFREQ(31),NGROSS(31)
11 C READ QUANTITIES NEEDED FOR MONTE CARLO SIMULATIONS
12 READ(5,500) NV,NS,FY1
13 500 FORMAT(2I5,F9.2)
14 READ(5,511) RMEAN1,RMEAN2,IY,NRU
15 511 FORMAT(2F15.5,2I10)
16 C READ NOMINAL PROPERTIES
17 CALL PROP(NS)
18 C READ STATISTICAL PROPERTIES OF VARIABLES
19 DO 5 I=1,NV
20 READ(5,510) RMEAN(I),STDV(I),FCONST(I),ITYPE(I)
21 510 FORMAT(3F15.5,I5)
22 5 CONTINUE
23 C WRITE STATISTICAL PROPERTIES OF VARIABLES
24 WRITE(6,512)
25 512 FORMAT('1',//////27X,'DISTRIBUTION PROPERTIES OF VARIABLES')
26 WRITE(6,519) NS,NRU
27 519 FORMAT(31X,'(,I4,'SIM',I5,')'//)
28 WRITE(6,513)
29 513 FORMAT(16X,'          MEAN-VALUE  STD-DEVIATION          FCONSTANT TYPE'//)
30 DO 1000 I=1,NV
31 1000 WRITE(6,514) RMEAN(I),STDV(I),FCONST(I),ITYPE(I)
32 514 FORMAT(16X,3F15.5,I5)
33 WRITE(6,515)
34 515 FORMAT(////20X,' FC(MEAN-VALUE) FY(MEAN-VALUE)'//)
35 WRITE(6,516) RMEAN1,RMEAN2
36 516 FORMAT(20X,2F15.5)
37 WRITE(6,522) FY1
38 522 FORMAT(////21X,'FY LIMIT=',F9.2)
39 WRITE(6,520) IY
40 520 FORMAT(////21X,'ISEED=',I10)
41 C CALCULATE THE ACI INTERACTION DIAGRAM
42 CALL ACI(NS)
43 C FIT A POLYNOMIAL TO THE ACI INTERACTION DIAGRAM
44 CALL CURVE
45 C WRITE THE ACI INTERACTION DIAGRAM AFTER THE CURVE FIT
46 WRITE(6,100)
47 100 FORMAT('1',//////23X,'****ACI INTERACTION DIAGRAM****')
48 WRITE(6,519) NS,NRU
49 WRITE(6,517)
50 517 FORMAT(30X,'(AFTER CURVE FIT)'//)
51 WRITE(6,103)
52 103 FORMAT(19X,'P(J) LBS',6X,'M(J) LB-IN',7X,'EOH(J)')
53 DO 6 J=1,13
54 6 WRITE(6,104) P(J),BM(J),EOH1(J)
55 104 FORMAT(/16X,3E15.7)
      PACI(1)=PO

```

```

56     PACI(15)=BMO
57     DO 1 I=1,13
58     1 PACI(I+1)=P(I)
59     C CALCULATE MEAN THEORY INTERACTION DIAGRAM
60     CALL THMEAN (RMEAN,RMEAN1,RMEAN2,NS)
61     C FIT A POLYNOMIAL TO THE THEORY INTERACTION DIAGRAM
62     CALL CURVE
63     C WRITE MEAN THEORY INTERACTION DIAGRAM AFTER CURVE FIT
64     WRITE (6,101)
65     101 FORMAT ('1',,//////19X,'*****MEAN THEORY INTERACTION DIAGRAM*****')
66     WRITE (6,519) NS,NRU
67     WRITE (6,517)
68     WRITE (6,103)
69     DO 3 J=1,13
70     3 WRITE (6,104) P(J),BM(J),EOH1(J)
71     PTH(1,1)=PO
72     PTH(15,1)=BMO
73     DO 15 I=1,13
74     15 PTH(I+1,1)=P(I)
75     WRITE (6,105)
76     105 FORMAT (//18X,'MEANTH/ACI',2X,'EOH')
77     C CALCULATE AND WRITE RATIO MEAN THEORY/ACI
78     DO 17 I=1,15
79     IF (I.EQ.1) EOH2=0.0
80     IF (I.GT.1) EOH2=EOH1(I-1)
81     IF (I.EQ.15) EOH2=99.99
82     RP(I,1)=PTH(I,1)/PACI(I)
83     17 WRITE (6,106) RP(I,1),EOH2
84     106 FORMAT (16X,2F10.5)
85     C MONTE CARLO CALCULATION OF THEORETICAL STRENGTH
86     DO 4 JJ=1,NS
87     DO 10 I=1,NV
88     SD=STDV(I)
89     RM=RMEAN(I)
90     CONST=FCONST(I)
91     ITP=ITYPE(I)
92     CALL RANDOM (IY,SD,RM,CONST,ITP,V)
93     X(I)=V
94     10 CONTINUE
95     IF (X(1).LE.(RMEAN(1)-3.3*STDV(1))) X(1)=RMEAN(1)-3.3*STDV(1)
96     FC=X(1)
97     IF (X(2).GT.FY1) X(2)=FY1
98     FY=(X(2)-4000.0)*0.97
99     BB=X(3)
100    H=X(4)
101    B11=X(5)
102    D11=X(6)
103    DC=X(7)
104    DD=X(8)
105    DO 2 I=1,NB
106    NI=I+8
107    2 DS(I)=X(NI)
108    C CALCULATE THEORETICAL INTERACTION DIAGRAM
109    CALL THEORY
110    C FIT A POLYNOMIAL TO THE THEORY INTERACTION DIAGRAM
111    CALL CURVE
112    PTH(1,JJ)=PO
113    PTH(15,JJ)=BMO
114    DO 9 I=1,13
115    9 PTH(I+1,JJ)=P(I)

```

```

176      L=L+1
177      7 X(L)=RP(I,JJ)
178      N=L
179      CALL STAT (RM,SD,COV,COS,COK,RMIN,RMAX,UM2,UM3,UM4,IMAX,IMIN,RMED,
180      1CLASS,CFREQ,NGROSS)
181      DO 11 I=1,15
182      IMAX=IMAX-NS
183      IF (IMAX.LE.0) GO TO 12
184      11 CONTINUE
185      12 IMAX=IMAX+NS
186      DO 13 I=1,15
187      IMIN=IMIN-NS
188      IF (IMIN.LE.0) GO TO 14
189      13 CONTINUE
190      14 IMIN=IMIN+NS
191      WRITE (6,21)
192      21 FORMAT ('1',//////26X,'<*> TOTAL STATISTICAL EVALUATION <*>')
193      WRITE (6,519) NS,NRU
194      WRITE (6,20)
195      WRITE (6,25) RM,SD,COV,COS,COK
196      WRITE (6,30)
197      WRITE (6,35) RMIN,IMIN,RMAX,IMAX,RMED
198      WRITE (6,36)
199      WRITE (6,37)
200      WRITE (6,38) UM2,UM3,UM4
201      WRITE (6,39)
202      WRITE (6,40)
203      DO 55 I=1,31
204      55 WRITE (6,50) I,CLASS(I),CFREQ(I),NGROSS(I)
205      1600 CONTINUE
206      WRITE (6,1900) JJ
207      1900 FORMAT ('1',/20X,'****',I5,'****')
208      STOP
209      END
210      C*****
211      C
212      C*****
213      SUBROUTINE THMEAN (RMEAN,RMEAN1,RMEAN2,NS)
214      COMMON N,EOH1(13),PO,BMO,DCS,DTS
215      COMMON FC,FY,ES,BB,H,DC,DD,AS,AS11,B11,D11,S,C,ZZ,NRU
216      COMMON PHI,EO,J,Z,ECC,EY,FCONCC(20),ASC,EOH(40),FCONST(25)
217      COMMON X(16000),EC(20),B(20),P(40),BHM(1000),BM(40),FCS(20)
218      COMMON FST,E(20),NB,DS(20),ASB(20),FSS(20),SBM(20)
219      DIMENSION RMEAN(25)
220      C SET EACH VARIABLE EQUAL TO ITS MEAN VALUE
221      FC=RMEAN1
222      FY=(RMEAN2-4000.0)*0.97
223      BB=RMEAN(3)
224      H=RMEAN(4)
225      B11=RMEAN(5)
226      D11=RMEAN(6)
227      DC=RMEAN(7)
228      DD=RMEAN(8)
229      DO 2 I=1,NB
230      NI=I+8
231      2 DS(I)=RMEAN(NI)
232      C CALCULATE THEORETICAL INTERACTION DIAGRAM
233      CALL THEORY
234      C WRITE MEAN THEORY INTERACTION DIAGRAM
235      WRITE (6,100)

```



```

236     100 FORMAT ('1',////////19X,'*****MEAN THEORY INTERACTION DIAGRAM*****')
237     WRITE (6,519) NS,NRU
238     519 FORMAT (31X,'(','I4','SIM',I5,')'//)
239     WRITE (6,101)
240     101 FORMAT (//19X,'P(J) LBS',6X,'M(J) LB-IN',7X,'EOH(J) ')
241     DO 4 J=1,N
242     WRITE (6,102) P(J),BM(J),EOH(J)
243     102 FORMAT (/16X,3E15.7)
244     4 CONTINUE
245     WRITE (6,103)
246     103 FORMAT (//20X,'PO LBS',7X,'BMO LB-IN')
247     WRITE (6,104) PO,BMO
248     104 FORMAT (16X,2E15.7)
249     RETURN
250     END
251 C*****
252 C
253 C*****
254 SUBROUTINE ACI (NS)
255 C
256 C THIS SUBROUTINE CALCULATES THE ACI INTERACTION DIAGRAM
257 C
258 COMMON N,EOH1(13),PO,BMO,DCS,DTS
259 COMMON FC,FY,ES,BB,H,DC,DD,AS,AS11,B11,D11,S,C,ZZ,NEU
260 COMMON PHI,EO,J,Z,ECC,EY,FCONCC(20),ASC,FOH(40),PCONST(25)
261 COMMON X(16000),EC(20),E(20),P(40),BMM(1000),BM(40),FCS(20)
262 COMMON FST,E(20),NB,DS(20),ASB(20),FSS(20),SBM(20)
263 IF (FC.LE.4000.0) GO TO 1
264 B1=0.85-0.05*(FC-4000.0)/1000.0
265 IF (B1.LE.0.65) B1=0.65
266 GO TO 4
267 1 B1=0.85
268 4 E4=0.003
269 C CALCULATE PURE AXIAL LOAD CAPACITY
270 PO=0.85*FC*(BB*H-AS)+AS*FY
271 C CALCULATE AXIAL LOAD CAPACITY AT BALANCED CONDITIONS
272 PB=0.85*E1*FC*BB*DTS*(0.003/(FY/ES+0.003))
273 C CALCULATE PURE MOMENT CAPACITY
274 AST=AS-ASC
275 AA=BB*FC*B1*0.85
276 AB=0.003*ASC*ES-AST*FY
277 AC=-0.003*ASC*ES*DCS
278 RA=SQRT(AB**2-4.0*AA*AC)/(2.0*AA)
279 C1=(-AB/(2.0*AA))-RA
280 IF (C1.LE.0.0) C1=RA-(AB/(2.0*AA))
281 ES2=0.003*(C1-DCS)/C1
282 IF (ES2.GE.(FY/ES)) GO TO 9
283 BMO=ASC*ES2*ES*(DTS-DCS)+(AST*FY-ASC*ES2*ES)*(DTS-B1*C1/2.0)
284 GO TO 8
285 9 BMO=ASC*FY*(DTS-DCS)+{(AST-ASC)*FY*(DTS-(AST-ASC)*FY/(1.7*FC*BB))}
286 C INITIALIZE STRAIN IN TENSION STEEL
287 8 E1=0.0019
288 J=0
289 2 J=J+1
290 IF (J.EQ.1) GO TO 5
291 C MODIFY TENSION STEEL STRAIN
292 IF (E1.GT.-0.001) E1=E1-0.0005
293 IF (E1.LE.-0.001) E1=E1-0.001
294 C CALCULATE NEUTRAL AXIS DEPTH
295 C=F4*DD/(E4-E1)

```

```

296          PHI=E4/C
297      C  CALCULATE FORCES IN STEEL BARS
298          CALL ASTEEL (E4)
299      C  CALCULATE CONCRETE COMPRESSIVE BLOCK FORCE
300          IF (C.GE.(H/B1)) C=H/B1
301          FCCONC=0.85*FC*B1*BB*C
302      C  CALCULATE AXIAL LOAD LEVEL
303          P(J)=FCCONC+FST
304      C  CALCULATE BENDING MOMENT DUE TO CONCRETE COMPRESSIVE FORCE
305          COMPM=FCCONC*(DD-B1*C/2.0)
306          SM=0.0
307      C  CALCULATE BENDING MOMENT DUE TO STEEL FORCES
308          DO 3 I=1,NP
309          SBM(I)=(FSS(I)-FCS(I)*ASB(I))*(DD-DS(I))
310          3 SM=SM+SBM(I)
311      C  CALCULATE TOTAL BENDING MOMENT CAPACITY
312          BM(J)=COMPM+SM-P(J)*(DD-H/2.0)
313          GO TO 6
314          5 P(J)=0.85*FC*((BB*H)-AS)+AS*FY
315          BM(J)=0.0
316      C  CALCULATE ECCENTRICITY E/H
317          6 EOH(J)=BM(J)/(P(J)*H)
318          IF (J.GE.20) GO TO 7
319          IF (EOH(J).LT.2.0) GO TO 2
320          7 N=J
321      C  WRITE THE ACI INTERACTION DIAGRAM
322          WRITE (6,100)
323          100 FORMAT ('1',//////23X,'*****ACI INTERACTION DIAGRAM*****')
324          WRITE (6,519) NS,NRU
325          519 FORMAT (31X,'(' ,I4,'SIM',I5,')'//)
326          WRITE (6,101)
327          101 FORMAT (/19X,'P(O) LBS',7X,'P(B) LBS',6X,'M(O) LB-IN')
328          WRITE (6,102) PO,PB,BMO
329          102 FORMAT (/16X,3E15.7)
330          WRITE (6,103)
331          103 FORMAT (/19X,'P(J) LBS',6X,'M(J) LB-IN',7X,'EOH(J)')
332          DO 20 J=1,N
333          WRITE (6,104) P(J),BM(J),EOH(J)
334          104 FORMAT (/16X,3E15.7)
335          20 CONTINUE
336          RETURN
337          END
338      C*****
339      C
340      C*****
341          SUBROUTINE ASTEEL (E4)
342      C
343      C  THIS SUBROUTINE CALCULATES THE ACI FORCES IN THE STEEL
344      C
345          COMMON N,EOH(13),PO,BMO,DCS,DTS
346          COMMON FC,FY,ES,BB,H,DC,DD,AS,AS11,B11,D11,S,C,ZZ,NRU
347          COMMON PHI,EO,J,Z,ECC,EY,FCONCC(20),ASC,EOH(40),FCONST(25)
348          COMMON X(16000),EC(20),B(20),P(40),BMM(1000),BM(40),FCS(20)
349          COMMON FST,E(20),NB,DS(20),ASB(20),FSS(20),SBM(20)
350          EY=FY/ES
351          FST=0.0
352          DO 4 I=1,NP
353          E(I)=E4-PHI*DS(I)
354          IF (DS(I).GE.C) GO TO 5
355          FCS(I)=0.85*FC

```

```

416      105 FORMAT (/16X,1F6.1,5X,1F7.1,4X,1F10.1)
417      WRITE (6,106)
418      106 FORMAT (//16X,'B (IN) ',5X,'H (IN) ',5X,'D (IN) ',4X,'DC (IN) '
419      1,4X,'AS (SQIN) ',3X,'ASC (SQIN) ')
420      WRITE (6,107) BB,H,DD,DC,AS,ASC
421      107 FORMAT (/12X,6F10.2)
422      WRITE (6,108)
423      108 FORMAT (//16X,'DCS (IN) ',2X,'DTS (IN) ',4X,'S (IN) ',4X,'B11 (IN) ',
424      14X,'D11 (IN) ',2X,'AS11 (SQIN) ')
425      WRITE (6,109) DCS,DTS,S,B11,D11,AS11
426      109 FORMAT (/12X,6F10.2)
427      WRITE (6,112)
428      112 FORMAT (//16X,'NB',4X,'ASB (I) ',5X,'DS (I) ')
429      DO 114 I=1,NP
430      WRITE (6,113) NB,ASB (I),DS (I)
431      113 FORMAT (15X,1I3,2F10.2)
432      114 CONTINUE
433      RETURN
434      END
435      C*****
436      C
437      C*****
438      SUBROUTINE CURVE
439      C
440      C THIS SUBROUTINE FITS A POLYNOMIAL TO THE INTERACTION
441      C DIAGRAM
442      C
443      COMMON N,EOH1(13),PO,BMO,DCS,DTS
444      COMMON FC,FY,ES,BB,H,DC,DD,AS,AS11,B11,D11,S,C,ZZ,NRU
445      COMMON PHI,EO,J,Z,ECC,EY,FCONCC(20),ASC,EOH(40),FCONST(25)
446      COMMON X(16000),EC(20),B(20),P(40),BMH(1000),BM(40),FCS(20)
447      COMMON FST,E(20),NB,DS(20),ASB(20),FSS(20),SEM(20)
448      DIMENSION DI(400),D(70),SB(10),T(10),COE(11)
449      DIMENSION XBAR(11),STD(11),SUMSQ(11),ISAVE(11),ANS(10)
450      DIMENSION XX(500),BBB(10),EE(10)
451      N=N-1
452      EOH1(1)=0.05
453      EOH1(2)=0.10
454      EOH1(3)=0.15
455      EOH1(4)=0.20
456      EOH1(5)=0.30
457      EOH1(6)=0.40
458      EOH1(7)=0.50
459      EOH1(8)=0.60
460      EOH1(9)=0.70
461      EOH1(10)=0.80
462      EOH1(11)=0.90
463      EOH1(12)=1.00
464      EOH1(13)=1.50
465      N=N-1
466      DO 2 J=1,N
467      P(J)=P(J+1)
468      BM(J)=BM(J+1)
469      2 EOH(J)=EOH(J+1)
470      DO 100 I=1,N
471      DIPM=BM(I+1)-BM(I)
472      IF (DIPM) 105,100,100
473      100 CONTINUE
474      105 NP=I
475      EOH=EOH(I)

```

```

476      M1=M
477      IF (M.GE. (NP-1)) M=NP-2
478      L=NP*M
479      DO 110 I=1, NP
480      J=L+I
481      XX(I)=EOH(I)
482      110 XX(J)=P(I)
483      LL=L+NP
484      CALL GDATA (NP,M,XX,XBAR,STD,D,SUMSQ)
485      MM=M+1
486      SUM=0.0
487      DO 200 I=1, M
488      ISAVE(I)=I
489      CALL ORDER (MM,D,MM,I,ISAVE,DI,EE)
490      CALL MINV (DI,I,DET,BBB,T)
491      CALL TMULTR (NP,I,XBAR,STD,SUMSQ,DI,EE,ISAVE,BBB,SB,T,ANS)
492      IF (ANS(7)) 220,130,130
493      130 SUMIP=ANS(4)-SUM
494      IF (SUMIP) 220,220,150
495      150 SUM=ANS(4)
496      COE(1)=ANS(1)
497      DO 160 J=1,I
498      160 COE(J+1)=BBB(J)
499      II=I+1
500      JJ=I+1
501      200 CONTINUE
502      220 NN=13
503      DO 240 II=1, NN
504      EOH2=EOH1(II)
505      IF (EOH2.GT.EOHB) GO TO 250
506      P(II)=0.0
507      DO 245 I=1, JJ
508      245 P(II)=P(II)+COE(I)*(EOH1(II)**(I-1))
509      240 CONTINUE
510      250 NNN=II
511      DO 101 I=NP, N
512      DIFE=3.0-EOH(I)
513      IF (DIFE) 102,101,101
514      101 CONTINUE
515      GO TO 103
516      102 N=I-1
517      103 NM=N-NP+1
518      M=M1
519      IF (M.GE. (NM-1)) M=NM-2
520      L=NM*M
521      DO 310 I=1, NM
522      J=L+I
523      XX(I)=1.0/EOH(I+NP-1)
524      310 XX(J)=BM(I+NP-1)
525      CALL GDATA (NM,M,XX,XBAR,STD,D,SUMSQ)
526      MM=M+1
527      SUM=0.0
528      DO 300 I=1, M
529      ISAVE(I)=I
530      CALL ORDER (MM,D,MM,I,ISAVE,DI,EE)
531      CALL MINV (DI,I,DET,BBB,T)
532      CALL TMULTR (NM,I,XBAR,STD,SUMSQ,DI,EE,ISAVE,BBB,SB,T,ANS)
533      IF (ANS(7)) 320,330,330
534      330 SUMIP=ANS(4)-SUM
535      IF (SUMIP) 320,320,350

```

```

536     350 SUM=ANS(4)
537       COE(1)=ANS(1)
538       DO 360 J=1,I
539     360 COE(J+1)=BBB(J)
540       JJ=I+1
541     300 CONTINUE
542     320 DO 340 II=NNN,NN
543       BM(II)=0.0
544       DO 345 I=1,JJ
545     345 BM(II)=BM(II)+COE(I)*((1.0/EOH1(II))**(I-1))
546       P(II)=BM(II)/(H*EOH1(II))
547     340 CONTINUE
548       N4=NNN-1
549       DO 370 I=1,N4
550     370 BM(I)=P(I)*H*EOH1(I)
551       RETURN
552     END
553 C*****
554 C
555 C*****
556     SUBROUTINE RANDOM (IY,SD,RM,CONST,ITP,V)
557 C
558 C THIS SUBROUTINE GENERATES VALUE OF THE VARIABLES WITH
559 C THE MEAN, STANDARD DEVIATION, AND DISTRIBUTION GIVEN
560 C
561     COMMON N,EOH1(13),PO,BMO,DCS,DTS
562     COMMON FC,FY,ES,BB,H,DC,DD,AS,AS11,B11,D11,S,C,ZZ,NRU
563     COMMON PHI,EO,J,Z,ECC,EY,FCONCC(20),ASC,EOH(40),FCONST(25)
564     COMMON X(16000),EC(20),B(20),P(40),BMM(1000),BM(40),FCS(20)
565     COMMON FST,E(20),NB,DS(20),ASB(20),FSS(20),SBM(20)
566     A=C.0
567     DO 50 I=1,12
568     IY=IY*65539
569     IF (IY.LT.0) IY=IY+2147483647+1
570     Y=IY*0.4656613E-9
571     50 A=A+Y
572     A=A-6.0
573     V=A*SD+RM
574     IF (ITP.EQ.1) V=10.0**V
575     IF (ITP.EQ.2) V=10.0**V+CONST
576     RETURN
577     END
578 C*****
579 C
580 C*****
581     SUBROUTINE THEORY
582 C
583 C THIS SUBROUTINE CALCULATES THE THEORETICAL P-M DIAGRAM
584 C
585     COMMON N,EOH1(13),PO,BMO,DCS,DTS
586     COMMON FC,FY,ES,BB,H,DC,DD,AS,AS11,B11,D11,S,C,ZZ,NRU
587     COMMON PHI,EO,J,Z,ECC,EY,FCONCC(20),ASC,EOH(40),FCONST(25)
588     COMMON X(16000),EC(20),B(20),P(40),BMM(1000),BM(40),FCS(20)
589     COMMON FST,E(20),NB,DS(20),ASB(20),FSS(20),SBM(20)
590     FC=FC*0.85
591     IF (FC.EQ.1000.0) FC=1000.1
592     ECC=57000.0*SQRT(FC)
593     EO=1.8*FC/ECC
594     EY=FY/ES
595 C CALCULATE PURE AXIAL LOAD CAPACITY

```

```

596         PO=FC*BB*H+AS*FY-AS*FC
597         J=0
598         1 J=J+1
599     C   SET AXIAL LOAD LEVEL
600         IF (J.EQ.1) GO TO 5
601         IF (J.EQ.2) P(J)=0.0
602         IF (P(J-1).LE.(0.6*PO)) P(J)=P(J-1)-0.034*PO
603         IF (P(J-1).LE.(0.1*PO)) P(J)=P(J-1)-0.04*PO
604         IF (P(J-1).GT.(0.6*PO)) P(J)=P(J-1)-0.16*PO
605         IF (P(J).LE.0.0) P(J)=0.0
606         IF (J.EQ.2) P(J)=P(J-1)-0.08*PO
607     C   CALCULATE MOMENT CAPACITY AT SPECIFIED AXIAL LOAD
608         CALL AXIAL
609         IF (P(J).EQ.0.0) BMO=BM(J)
610         IF (P(J).EQ.0.0) GO TO 7
611         GO TO 6
612     5   P(J)=PO
613         BM(J)=0.0
614     6   EOH(J)=BM(J)/(P(J)*H)
615         GO TO 1
616     7   N=J-1
617     C   ELIMINATE ERRATIC POINTS ON THE INTERACTION CURVE
618         M=N
619         NJ=N-1
620         DO 8 IJ=3,NJ
621         IF (BM(IJ).GE.BM(IJ-1)) GO TO 8
622         IF (BM(IJ+1).LE.BM(IJ-1)) GO TO 8
623         M=M-1
624         DO 9 JJJ=IJ,NJ
625         P(JJJ)=P(JJJ+1)
626         BM(JJJ)=BM(JJJ+1)
627     9   EOH(JJJ)=EOH(JJJ+1)
628     8   CONTINUE
629         N=M
630         RETURN
631         END
632     C*****
633     C
634     C*****
635     SUBROUTINE AXIAL
636     C
637     C   THIS SUBROUTINE CALCULATES THE MOMENT AFTER BALANCING P
638     C
639         COMMON N,EOH1(13),PO,BMO,DCS,DTS
640         COMMON FC,FY,ES,BE,H,DC,DD,AS,AS11,B11,D11,S,C,ZZ,NRU
641         COMMON PHI,EO,J,Z,ECC,EY,FCONCC(20),ASC,EOH(40),PCONST(25)
642         COMMON X(16000),EC(20),B(20),P(40),BMM(1000),BM(40),FCS(20)
643         COMMON PST,E(20),NB,DS(20),ASB(20),FSS(20),SBM(20)
644         PHI=0.000001
645         PHIH=PHI*H
646         II=1
647     14  E4=0.002
648         EINCR=0.002
649     33  E4=E4-EINCR
650         EINCR=EINCR/2.0
651     32  E4=E4+EINCR
652         FCONC=0.0
653         C=F4/PHI
654         ECO=(C-H)*PHI
655         IF (C.GE.H) C=H

```

```

656         IF (C.LT.H) ECO=0.0
657         ASC=0.0
658         DO 34 I=1,NB
659         IF (DS(I).LE.C) ASC=ASC+ASB(I)
660     34 CONTINUE
661     C  CALCULATE PARAMETERS OF THE CONCRETE STRESS STRAIN CURVE
662         P11=(2.0*(B11+D11)*AS11+ASC*S)/(B11*D11*S)
663         E5CH=0.75*P11*SQRT(B11/S)
664         E5OU=(3.0+0.002*FC)/(FC-1000.0)
665         IF (E5OU.LE.0.0) E5OU=0.06
666         Z=0.5/(E5OH+E5OU-EO)
667         ZZ=0.5/(E5OU-EO)
668         EU=2.0*(E5OH+E5OU)-EO
669         DX=C/10
670     C  CALCULATE THE CONCRETE COMPRESSION BLOCK FORCE
671         DO 23 I=1,10
672         AI=I
673         I(I)=C-AI*DX+DX/2
674         EC(I)=PHI*X(I)+ECO
675         B(I)=BB
676     C  MAXIMUM STRAIN FOR UNCONFINED COMPRESSION 0.004
677         IF (EC(I).LE.EO) GO TO 3
678         IF (EC(I).GE.0.004) GO TO 21
679         IF (EC(I).GT.EO) GO TO 4
680     3  FCC=FC*(2.0*EC(I)/EO-(EC(I)/EO)**2)
681         GO TO 22
682     4  FCC=FC*(1.0-Z*(EC(I)-EO))
683         FCU=FC*(1.0-ZZ*(EC(I)-EO))
684         IF (FCC.LE.0.0) FCC=0.0
685         IF (FCU.LE.0.0) FCU=0.0
686         FCONCC(I)=FCC*DX*B11+FCU*DX*(B(I)-B11)
687         GO TO 23
688     21 B(I)=B11
689         FCC=FC*(1.0-Z*(EC(I)-EO))
690         IF (FCC.LE.0.0) FCC=0.0
691         IF (X(I).GE.(C-DC)) FCC=0.0
692     22 FCONCC(I)=FCC*DX*B(I)
693     23 PCCONC=FCCONC+FCONCC(I)
694     C  CALCULATE THE CONCRETE TENSION BLOCK FORCE
695         IF (C.GE.H) GO TO 25
696         SFC=SQRT(FC)
697         ET=7.5*SFC/ECC
698         TC=ET/PHI
699         TCA=H-C
700         RTC=TCA/TC
701         IF (TC.GT.TCA) TC=TCA
702         IF (TC.LE.TCA) RTC=1.0
703         FCONCT=-RTC*7.5*SFC*TC/2.0*BB
704         GO TO 18
705     25 FCONCT=0.0
706     18 CALL FSTEEL (E4)
707     C  CHECK FORCE COMPATIBILITY
708         PAXIAL=FCCONC+FCONCT+FS1
709         TOLA=P(J)*0.02
710         IF (P(J).EQ.0.0) TOLA=0.001*PO
711         TOL=P(J)-PAXIAL
712         IF (TOL.LT.-TOLA) GO TO 33
713         IF (TOL.GT.TOLA) GO TO 35
714         GO TO 36
715     35 IF (E4.GE.EU) GO TO 44

```

```

716         IF(EINCR.GE.0.0000001) GO TO 32
717         36 COMPM=0.0
718     C     CALCULATE THE MOMENT DUE TO THE CONCRETE COMPRESSION FORCE
719         DO 24 I=1,10
720         24 COMPM=COMPM+FCONCC(I)*(DD-C+X(I))
721         SM=0.0
722     C     CALCULATE THE MOMENT DUE TO THE STEEL FORCES
723         DO 13 I=1,NB
724         SBM(I)=(FSS(I)-FCS(I)*ASB(I))*(DD-DS(I))
725         13 SM=SM+SBM(I)
726         IF(FCONCT.EQ.0.0) TC=0.0
727     C     SUM THE MOMENTS ABOUT THE TENSION STEEL
728         BMM(II)=COMPM+SM+FCONCT*(DD-(C+2.0*TC/3.0))-P(J)*(DD-H/2.0)
729         IF(II.EQ.1) GO TO 17
730         TOLBMA=ARS(BMM(II-1)*0.01)
731         BMTOL=BMM(II)-BMM(II-1)
732         IF(BMM(II).LE.0.0) GO TO 42
733         IF(BMTOL.GE.(0.5*TOLBMA)) GO TO 41
734         IF(BMTOL.LE.-TOLBMA) GO TO 42
735         GO TO 16
736     17 PHINCR=0.001
737         GO TO 41
738     44 E4=0.001
739         PHIH=PHIH-PHINCR
740         PHINCR=PHINCR/5.0
741         PHIH=PHIH+PHINCR
742         PHI=PHIH/H
743         EINCR=EINCR/2.0
744         GO TO 32
745     42 PHIH=PHIH-PHINCR
746         PHINCR=PHINCR/5.0
747     41 PHIH=PHIH+PHINCR
748         PHI=PHIH/H
749         II=II+1
750         GO TO 14
751     16 BM(J)=BMM(II-1)
752         CONTINUE
753         RETURN
754         END
755 C*****
756 C
757 C*****
758     SUBROUTINE FSTEEL (E4)
759 C
760 C     THIS SUBROUTINE CALCULATES THE THEORY FORCES IN THE STEEL
761 C
762     COMMON N,EOH1(13),PO,BMO,DCS,DTS
763     COMMON FC,FY,ES,BB,H,DC,DD,AS,AS11,B11,D11,S,C,ZZ,NRU
764     COMMON PHI,EO,J,Z,ECC,EY,FCONCC(20),ASC,EOH(40),FCONST(25)
765     COMMON X(16000),EC(20),B(20),P(40),BMM(1000),BM(40),FCS(20)
766     COMMON FST,E(20),NB,DS(20),ASB(20),FSS(20),SBM(20)
767     FST=0.0
768     DO 4 I=1,NB
769     E(I)=E4-PHI*DS(I)
770     IF(DS(I).GE.C) GO TO 5
771     IF(E(I).GT.EO) GO TO 6
772     FCS(I)=FC*(2.0*E(I)/EO-(E(I)/EO)**2)
773     GO TO 7
774     6 FCS(I)=FC*(1.0-Z*(E(I)-EO))
775     IF(FCS(I).LE.0.0) FCS(I)=0.0

```



```

776       7 FSC=-FCS(I)*ASB(I)
777       GO TO 8
778       5 FSC=0.0
779       FCS(I)=0.0
780       8 E(I)=-E(I)
781       IF (E(I).GE.EY) GO TO 2
782       IF (E(I).LE.-EY) GO TO 1
783       GO TO 3
784       1 FSS(I)=FY*ASB(I)
785       GO TO 4
786       2 FSS(I)=-FY*ASB(I)
787       GO TO 4
788       3 FSS(I)=-E(I)*ES*ASB(I)
789       4 FST=FST+FSS(I)+FSC
790       RETURN
791       END
792
793 C*****
794 C
795 C*****
796       SUBROUTINE STAT (RM,STDV,COV,COS,COK,RMIN,RMAX,UM2,UM3,UM4,IMAX,IM
797       1IN,RMED,CLASS,CFREQ,NGROSS)
798 C
799 C THIS SUBROUTINE CALCULATES THE MEAN, COEFFICIENT OF
800 C VARIATION, COEFFICIENT OF SKEWNESS, COEFFICIENT OF
801 C KURTOSIS, AND CUMULATIVE FREQUENCY TABLE
802 C
803       COMMON N,EOH1(13),PO,BMO,DCS,DTS
804       COMMON FC,FY,ES,BB,H,DC,DD,AS,AS11,B11,D11,S,C,ZZ,NRU
805       COMMON PHI,EO,J,Z,ECC,EY,FCONCC(20),ASC,EOH(40),FCONST(25)
806       COMMON X(16000),EC(20),B(20),P(40),BMM(1000),BM(40),FCS(20)
807       COMMON FST,E(20),NB,DS(20),ASB(20),FSS(20),SBM(20)
808       DIMENSION CLASS(31),CFREQ(31)
809       DIMENSION Y(8002),DIF(16000),NGROSS(31)
810       SUM=0.0
811       DO 10 I=1,N
812       10 SUM=SUM+X(I)
813       RM=SUM/N
814       SUM=0.0
815       DO 20 I=1,N
816       20 SUM=SUM+(X(I)-RM)**2
817       UM2=SUM/N
818       STDV=SQRT(SUM/(N-1))
819       COV=STDV/RM
820       SUM=0.0
821       DO 30 I=1,N
822       30 SUM=SUM+(X(I)-RM)**3
823       UM3=SUM/N
824       COS=SUM/(N*(STDV**3))
825       SUM=0.0
826       DO 40 I=1,N
827       40 SUM=SUM+(X(I)-RM)**4
828       UM4=SUM/N
829       COK=SUM/(N*(STDV**4))
830       RMAX=X(1)
831       IMAX=1
832       DO 50 I=2,N
833       IF (RMAX.LT.X(I)) IMAX=I
834       50 RMAX=X(IMAX)
835       RMIN=X(1)
836       IMIN=1

```

```

836      DO 60 I=2,N
837      IF (RMIN.GT.X(I)) IMIN=I
838      60 RMIN=X(IMIN)
839      CINT=0.05
840      CLASS(1)=0.50
841      DO 70 I=2,30
842      70 CLASS(I)=CLASS(I-1)+CINT
843      CLASS(31)=2.0
844      DO 90 II=1,31
845      NPOINT=0
846      DO 80 I=1,N
847      80 IF (CLASS(II).GT.X(I)) NPOINT=NPOINT+1
848      NGROSS(II)=NPOINT
849      90 CFREQ(II)=(100.0*NPOINT)/N
850      DO 100 I=1,31
851      100 CLASS(I)=CLASS(I)-0.00001
852      Y(1)=RMIN
853      N1=N/2+2
854      DO 66 II=2,N1
855      NPOINT=1
856      DIF(1)=X(1)-Y(II-1)
857      DO 65 I=2,N
858      IF (X(I).EQ.0.0) GO TO 65
859      DIF(I)=X(I)-Y(II-1)
860      IF (DIF(I).LT.DIF(NPOINT)) NPOINT=I
861      65 CONTINUE
862      Y(II)=X(NPOINT)
863      X(NPOINT)=0.0
864      66 IF (NPOINT.EQ.1) X(NPOINT)=RMAX+1.0
865      N1=N1-1
866      DO 67 I=1,N1
867      67 Y(I)=Y(I+1)
868      RMED=(Y(N1-1)+Y(N1))/2.0
869      RN=(N/2.0)-(N/2)
870      IF (RN.GT.0.1) RMED=Y(N1)
871      RETURN
872      END
873      C*****
874      C      SUBROUTINE MULTR
875      C*****
876      C
877      C      PURPOSE
878      C      PERFORM A MULTIPLE LINEAR REGRESSION ANALYSIS FOR A
879      C      DEPENDENT VARIABLE AND A SET OF INDEPENDENT VARIABLES. THIS
880      C      SUBROUTINE IS NORMALLY USED IN THE PERFORMANCE OF MULTIPLE
881      C      AND POLYNOMIAL REGRESSION ANALYSES.
882      C
883      C      USAGE
884      C      CALL MULTR (N,K,XBAR,STD,D,RX,RY,ISAVE,B,SB,T,ANS)
885      C
886      C      DESCRIPTION OF PARAMETERS
887      C      N      - NUMBER OF OBSERVATIONS.
888      C      K      - NUMBER OF INDEPENDENT VARIABLES IN THIS REGRESSION.
889      C      XBAR   - INPUT VECTOR OF LENGTH M CONTAINING MEANS OF ALL
890      C      VARIABLES. M IS NUMBER OF VARIABLES IN OBSERVATIONS.
891      C      STD   - INPUT VECTOR OF LENGTH M CONTAINING STANDARD DEVI-
892      C      ATIONS OF ALL VARIABLES.
893      C      D      - INPUT VECTOR OF LENGTH M CONTAINING THE DIAGONAL OF
894      C      THE MATRIX OF SUMS OF CROSS-PRODUCTS OF DEVIATIONS
895      C      FROM MEANS FOR ALL VARIABLES.
896      C

```

```

897      C
898      C
899      C
900      C
901      C
902      C
903      C
904      C
905      C
906      C
907      C
908      C
909      C
910      C
911      C
912      C
913      C
914      C
915      C
916      C
917      C
918      C
919      C
920      C
921      C
922      C
923      C
924      C
926      C
927      C
928      C
929      C
930      C
931      C
932      C
933      C
934      C
935      C
936      C
937      C
938      C
939      C
940      C
941      C
941.1    C
942      C
943      C
944      C
945      C
946      C
947      C
948      C
950      C
951      C
952      C
953      C
954      C
955      C
956      C
957      C

```

RX - INPUT MATRIX (K X K) CONTAINING THE INVERSE OF INTERCORRELATIONS AMONG INDEPENDENT VARIABLES.
RY - INPUT VECTOR OF LENGTH K CONTAINING INTERCORRELATIONS OF INDEPENDENT VARIABLES WITH DEPENDENT VARIABLE.
ISAVE - INPUT VECTOR OF LENGTH K+1 CONTAINING SUBSCRIPTS OF INDEPENDENT VARIABLES IN ASCENDING ORDER. THE SUBSCRIPT OF THE DEPENDENT VARIABLE IS STORED IN THE LAST, K+1, POSITION.
B - OUTPUT VECTOR OF LENGTH K CONTAINING REGRESSION COEFFICIENTS.
SB - OUTPUT VECTOR OF LENGTH K CONTAINING STANDARD DEVIATIONS OF REGRESSION COEFFICIENTS.
T - OUTPUT VECTOR OF LENGTH K CONTAINING T-VALUES.
ANS - OUTPUT VECTOR OF LENGTH 10 CONTAINING THE FOLLOWING INFORMATION..
ANS (1) INTERCEPT
ANS (2) MULTIPLE CORRELATION COEFFICIENT
ANS (3) STANDARD ERROR OF ESTIMATE
ANS (4) SUM OF SQUARES ATTRIBUTABLE TO REGRESSION (SSAR)
ANS (5) DEGREES OF FREEDOM ASSOCIATED WITH SSAR
ANS (6) MEAN SQUARE OF SSAR
ANS (7) SUM OF SQUARES OF DEVIATIONS FROM REGRESSION (SSDR)
ANS (8) DEGREES OF FREEDOM ASSOCIATED WITH SSDR
ANS (9) MEAN SQUARE OF SSDR
ANS (10) F-VALUE

REMARKS
N MUST BE GREATER THAN K+1.

SUBROUTINES AND FUNCTION SUBPROGRAMS REQUIRED
NONE

METHOD
THE GAUSS-JORDAN METHOD IS USED IN THE SOLUTION OF THE NORMAL EQUATIONS. REFER TO W. W. COOLEY AND P. R. LOHNES, 'MULTIVARIATE PROCEDURES FOR THE BEHAVIORAL SCIENCES', JOHN WILEY AND SONS, 1962, CHAPTER 3, AND B. OSTLE, 'STATISTICS IN RESEARCH', THE IOWA STATE COLLEGE PRESS, 1954, CHAPTER 8.

.....

SUBROUTINE TMULTR (NPN,K,XBAR,STD,D,RX,RY,ISAVE,BBB,SB,T,ANS)
COMMON N,EOH1(13),PO,BMO,DCS,DTS
COMMON FC,FY,ES,BB,H,DC,DD,AS,AS11,B11,D11,S,C,ZZ,NFU
COMMON PHI,EO,J,Z,ECC,EY,FCONCC(20),ASC,EOH(40),FCONST(25)
COMMON X(16000),EC(20),B(20),P(40),BMM(1000),BM(40),FCS(20)
COMMON FST,E(20),NB,DS(20),ASB(20),FSS(20),SBM(20)
DIMENSION XBAR(11),STD(11),D(11),RX(40),RY(10)
DIMENSION ISAVE(11),BBB(10),SB(10),T(10),ANS(10)

.....

IF A DOUBLE PRECISION VERSION OF THIS ROUTINE IS DESIRED, THE C IN COLUMN 1 SHOULD BE REMOVED FROM THE DOUBLE PRECISION STATEMENT WHICH FOLLOWS.

DOUBLE PRECISION XEAR,STD,D,RX,RY,B,SB,T,ANS,RM,BO,SSAR,SSDR,SY,
1 FN,PK,SSARM,SSDRM,F

```

958      C
959      C
960      C      THE C MUST ALSO BE REMOVED FROM DOUBLE PRECISION STATEMENTS
961      C      APPEARING IN OTHER ROUTINES USED IN CONJUNCTION WITH THIS
962      C      ROUTINE.
963      C
964      C      THE DOUBLE PRECISION VERSION OF THIS SUBROUTINE MUST ALSO
965      C      CONTAIN DOUBLE PRECISION FORTRAN FUNCTIONS.  SQRT AND ABS IN
966      C      STATEMENTS 122, 125, AND 135 MUST BE CHANGED TO DSQRT AND DABS.
967      C      .....
968      C
969      C      MM=K+1
970      C      BETA WEIGHTS
971      C
972      C
973      C      DO 100 J=1,K
974      C      100 BBB (J)=0.0
975      C      DO 110 J=1,K
976      C      L1=K*(J-1)
977      C      DO 110 I=1,K
978      C      L=L1+I
979      C      110 BBB (J)=BBB (J)+RY (I)*RX (L)
980      C      RM=0.0
981      C      BO=0.0
982      C      L1=ISAVE (MM)
983      C
984      C      COEFFICIENT OF DETERMINATION
985      C
986      C      DO 120 I=1,K
987      C      RM=RM+BBB (I)*RY (I)
988      C
989      C      REGRESSION COEFFICIENTS
990      C
991      C      L=ISAVE (I)
992      C      BBB (I)=BBB (I)*(STD (L1)/STD (L))
993      C
994      C      INTERCEPT
995      C
996      C      120 BO=BO+BBB (I)*XBAR (L)
997      C      BO=XBAR (L1)-BO
998      C
999      C      SUM OF SQUARES ATTRIBUTABLE TO REGRESSION
1000     C
1001     C      SSAR=RM*D (L1)
1002     C
1003     C      MULTIPLE CORRELATION COEFFICIENT
1004     C
1005     C      122 RM= SQRT ( ABS (RM) )
1006     C
1007     C      SUM OF SQUARES OF DEVIATIONS FROM REGRESSION
1008     C
1009     C      SSSD=D (L1)-SSAR
1010     C      IF (SSDR.EQ.0.0) SSSD=0.1
1011     C
1012     C      VARIANCE OF ESTIMATE
1013     C
1014     C      FN=NPN-K-1
1015     C      SY=SSDR/FN
1016     C
1017     C      STANDARD DEVIATIONS OF REGRESSION COEFFICIENTS
1018     C
1019     C      DO 130 J=1,K

```

```
1020      L1=K*(J-1)+J
1021      L=ISAVE(J)
1022      125 SB(J)=SQRT(ABS((RX(L1)/D(L))*SY))
1023      C
1024      C      COMPUTED T-VALUES
1025      C
1026      130 T(J)=BBB(J)/SB(J)
1028      C      STANDARD ERROR OF ESTIMATE
1030      135 SY=SQRT(ABS(SY))
1032      C      F VALUE
1034      FK=K
1035      SSARM=SSAR/FK
1036      SSDRM=SSDR/FN
1037      P=SSARM/SSDRM
1039      ANS(1)=BO
1040      ANS(2)=RM
1041      ANS(3)=SY
1042      ANS(4)=SSAR
1043      ANS(5)=FK
1044      ANS(6)=SSARM
1045      ANS(7)=SSDR
1046      ANS(8)=FN
1047      ANS(9)=SSDRM
1048      ANS(10)=F
1049      RETURN
1050      END
END OF FILE
$SIGNOFF
```

APPENDIX E

DATA INPUT FOR THE MONTE CARLO PROGRAM

Note: All units are in inches and pounds.

Card	Columns	Data Description	Format
1	1- 5	Number of Variables (NV)	I5
	6-10	Number of Simulations (NS)	I5
	11-19	Limiting Steel Strength (FY1)	F9.2

Note: The limiting steel strength is a maximum value of steel strength which could reasonably be expected. This is required so that extremely high values of steel strength are not used for the theoretical calculations.

2	1-15	Mean Concrete Strength (RMEAN1)	F15.5
	15-30	Mean Steel Strength (RMEAN2)	F15.5
	31-40	Initial Seed (IY)	I10
	41-50	Number of Run (NRU)	I10

Note: The initial seed is any integer. This number is required to initiate the random number generating subroutine. The number of run is any identifying number for the specific run.

3	1- 5	Width of Column (BB)	F5.2
	6-10	Depth of Column (H)	F5.2
	11-15	Distance From the Compression Face to Longitudinal Steel Closest to the Tension Face (DD)	F5.2
	16-20	Distance From Compression Face to Nearest Longitudinal Steel (DC)	F5.2

DATA INPUT CONTINUED

Card	Columns	Data Description	Format
	21-25	Total Longitudinal Steel Area (AS)	F5.2
	26-30	Longitudinal Compression Steel Area (ASC)	F5.2
4	1-10	Concrete Design Strength (FC)	F10.0
	11-20	Steel Yield Strength (FY)	F10.0
	21-30	Steel Modulus of Elasticity (ES)	F10.0
5	1- 5	Depth From Compression Face to the Centroid of Compression Steel (DCS)	F5.2
	6-10	Depth From Compression Face to the Centroid of Tension Steel (DTS)	F5.2
	11-15	Spacing of Steel Ties (S)	F5.2
	16-20	Width of Ties (B11)	F5.2
	21-25	Depth of Ties (D11)	F5.2
	26-30	Area of Steel Tie (AS11)	F5.2
6	1- 3	Number of Longitudinal Bars (NB)	I3
7	1- 5	Area of Individual Steel Bars (ASB(I))	F5.2
	6-11	Distance From Compression Face to the Individual Steel Bars (DS(I))	F5.2
Note: This card is repeated for each longitudinal bar.			
8	1-15	Variable Mean Value (RMEAN(I))	F15.5
T4		Variable Standard Deviation (STDV(I))	F15.5
	31-45	Variable Constant (FCONST(I))	F15.5
	46-50	Variable Distribution Type (ITYPE(I))	I5
Note: This card is repeated for each variable. In this			

DATA INPUT CONTINUED

Card	Columns	Data Description	Format
------	---------	------------------	--------

program the order of variables is as follows:

Concrete Strength

Steel Strength

Cross Section Width

Cross Section Depth

Core Width

Core Depth

Distance From Compression Face to Nearest

Longitudinal Steel

Distance From Compression Face to the

Longitudinal Steel Furthest From the

Compression Face

Distance From the Compression Face to

Each Longitudinal Bar

APPENDIX F

NOMENCLATURE

A''_S	Cross sectional area of tie steel, one side of column
b''	Width of column core
c_a	Actual cover of exterior steel layers
c_{sp}	Specified cover of exterior steel layers
d''	Depth of column core
D	Dead load
e/h	Eccentricity of axial load divided by the column dimension perpendicular to the neutral axis
e_n	Error in placement of interior steel layers
E_c	Modulus of elasticity of concrete in compression
E_{ct}	Modulus of elasticity of concrete in tension
E_s	Modulus of elasticity of steel
f_c	Concrete stress
f'_c	Concrete design strength
\bar{f}_c	Mean in-situ concrete strength
f_{cr}	Average concrete cylinder strength
h	Depth of cross section
L	Live load
$M_{(R-S)}$	Mean value of (R-S)
PACI	ACI calculated axial load
Ptheory	Axial load calculated from Subroutine theory
Ptest	Axial load from Hognestad's tests
R	Nominal resistance or strength
s	Spacing of ties

NOMENCLATURE CONTINUED

V_R	Coefficient of variation of γ_R
α	Separation function, 0.75
β	Safety index
γ_D	Dead load factor
γ_L	Live load factor
ϵ_c	Concrete strain
ϵ_{50h}	Increase in strain at 50% of maximum stress due to confinement of concrete by tie steel
ϵ_o	Concrete strain at maximum stress
ϵ_t	Concrete tensile strain
ϵ_{tr}	Concrete strain at rupture in tension
ϵ_u	Crushing strain of unconfined concrete
ϵ_{50u}	Concrete strain at 50% of maximum stress of unconfined concrete
ρ	Steel percentage
ρ''	Tie steel volumetric ratio
σ	Standard deviation
$\sigma_{(R-S)}$	Standard deviation of (R-S)
σ_t	Stress in tension
σ_{tr}	Rupture strength of concrete
ϕ	Understrength factor